5-6-2014 12:00 AM

The Methodological and Diagnostic Applications of Micro-CT to Palaeopathology: A Quantitative Study of Porotic Hyperostosis

Jennifer A. Morgan, *The University of Western Ontario*

Supervisor: Dr. Andrew Nelson, *The University of Western Ontario*
Joint Supervisor: Dr. Joseph Eldon Molto, *The University of Western Ontario*
A thesis submitted in partial fulfillment of the requirements for the Doctor of Philosophy degree in Anthropology
© Jennifer A. Morgan 2014

THE METHODOLOGICAL AND DIAGNOSTIC APPLICATIONS OF MICRO-CT TO
PALAEOPATHOLOGY: A QUANTITATIVE STUDY OF POROTIC HYPEROSTOSIS

(Thesis format: Monograph)

by

Jennifer A <u>Morgan</u>

Graduate Program in Anthropology

A thesis submitted in partial fulfillment
of the requirements for the degree of
Doctor of Philosophy

The School of Graduate and Postdoctoral Studies
The University of Western Ontario
London, Ontario, Canada

Abstract

The purpose of this dissertation was to assess the value of micro-CT to palaeopathology for the non-destructive analysis of orbital and cranial porotic hyperostosis, common lesions observed in many archaeological skeletal collections. The objectives of this study were to: 1) identify palaeoepidemiological trends in the prevalence of porotic hyperostosis that may support differential diagnoses, 2) evaluate the reproducibility and reliability of two-dimensional (2D) and three-dimensional (3D) methods of micro-CT data collection for the quantitative analysis of bone microarchitecture, and 3) quantitatively evaluate orbital and cranial porotic hyperostosis to determine the value of micro-CT methods for understanding disease pathogenesis and improving the differential diagnosis of these lesions.

Sixty-six individuals obtained from four skeletal collections were assessed macroscopically using published methods of visual analysis as well as quantitatively using micro-CT methods. Structural indices used to quantify bone microarchitecture included bone volume density (BV/TV), specific bone surface (BS/BV), trabecular thickness (Tb.Th.), trabecular number (Tb.N.), and trabecular spacing (Tb.Sp.) (Hildebrand et al. 1999). The results of the visual analysis demonstrated an age-related trend in the prevalence of porotic hyperostosis, supporting previous hypotheses that this condition has an onset in childhood (e.g. Stuart-Macadam 1985).

The micro-CT results illustrated that the most reliable and reproducible method for quantifying bone microarchitecture was a 3D volume of interest (VOI) method that maximized VOI size. Three-dimensional methods using VOIs of a uniform size were recommended with caution, and 2D VOI methods did not provide consistent observer agreement.

The analysis of orbital porotic hyperostosis demonstrated significant changes ($p < 0.05$) to bone microarchitecture in the advanced stages of disease pathogenesis, but not in the early or healing stages. The results for cranial porotic hyperostosis demonstrated significant changes only in the light stage. These results suggest that orbits are differentially and more significantly affected than the cranial vault likely due to structural differences between the bones of the skull. Changes to bone microarchitecture included an overall loss of trabecular

bone and an increase in thinned, gracile trabeculae. Considering these findings within the clinical literature a differential diagnosis that includes anaemic conditions was supported. The identified palaeoepidemiological context also supported this differential diagnosis. Overall, the application of 3D micro-CT methods is of significant value for elucidating the process of disease pathogenesis and supporting current differential diagnoses of porotic hyperostosis in archaeological skeletal remains.

Keywords

Acknowledgments

First and foremost, I extend my deepest gratitude to Dr. Andrew Nelson for his guidance, patience, and encouragement throughout this long, and often difficult, process. Not only has he guided me through the process of completing this dissertation, he has also been a significant personal support over the last five years. If it were not for his constant understanding and encouragement, this dissertation would not be where it is today. I would also like to thank Dr. El Molto for significantly contributing to this dissertation as a joint supervisor. His expertise and guidance have helped me to make sense of my data and to develop this research into a significant contribution to the palaeopathological literature. He has been an amazing support and I could not have finished this dissertation without him.

I would also like to thank Dr. Anne Keenleyside from Trent University and Dr. Chris White, Dr. Alexis Dolphin, and Dr. David Holdsworth from Western University for taking part in my doctoral examination. Their suggestions and advice have both informed and improved this work. It is because of their knowledge and valuable input that I have emerged from my graduate studies as a better writer and researcher.

Thank you to Jay Maxwell for providing me with a starting point for this dissertation research and for giving me his blessing to continue the research that he had started several years ago. Thank you to Diane Belleville, without whom I would be lost in the logistical mess of graduate school paperwork. Their involvement in the completion of this dissertation has been essential and is very much appreciated.

Additional thanks are due to Dr. Anne Keenleyside and Dr. Chris White for graciously allowing me access to the Apollonia and Maya skeletal collections and to Dr. Andrew Nelson, Dr. Rhonda Bathurst, Dr. Neal Ferris, and all of the folks at Sustainable Archaeology for providing me with access to the micro-CT equipment that was necessary to conduct this research project. I would also like to thank Jose Sanchez not only for his support, but for also participating in the data collection process. All of these contributions to this dissertation research are immeasurable, and I could not have completed it without such generosity.

Table of Contents

List of Tables

List of Figures

List of Appendices

Chapter 1

1   Introduction

1.1   Research Context

Palaeopathology has come to be defined as the study of diseases in antiquity whose existence can be demonstrated from the analysis of archaeological human and animal remains (Roberts and Manchester 2005). As a discipline, its objectives are to accurately reconstruct the chronology, geography, and evolution of diseases through time from a clinical perspective while emphasizing the interaction of disease and cultural processes from an anthropological, or biocultural, perspective (Miller et al. 1996; Lovell 2000; Armelagos 2003; Mays 2012). Knowledge of the pathology and epidemiology of diseases through time contributes greatly to our knowledge and understanding of modern diseases (Bosch 2000; Rühli et al. 2007). Therefore, the accuracy of diagnosis in ancient human skeletal remains is fundamental not only for the work of palaeopathologists and palaeoepidemiologists, but also for clinical researchers.

To effectively meet the objectives of palaeopathology, it is essential that researchers develop methods that are capable of improving the reliability of differential diagnoses. With the aid of more accurate diagnoses, palaeopathologists will be able to expand their knowledge of the causes, distribution, and prevalence of diseases, the evolution and history of diseases (Schultz, 2001), and the social and cultural aspects of health. The purpose of this dissertation research is to assess the value of micro-computed tomography (micro-CT), a relatively new digital method for the evaluation of archaeological bone, to research in palaeopathology. The aim of this research is two-fold: 1) to provide a standardized, reliable micro-CT method for investigating disease processes in the assessment of porotic lesions of the skull, and 2) to determine whether or not micro-CT is capable of contributing to the differential diagnosis of porotic hyperostosis in archaeological human remains. Not only does this method have the potential for contributing to the increased reliability of differential diagnosis, it will also provide a method which will eliminate the need for destructive sampling of valuable archaeological materials.

Porotic hyperostosis is a descriptive term characterizing pitting and porosity on the external and internal surfaces of the cranial vault, as well as the external surface of the orbital roofs of the skull. These porotic lesions are some of the most commonly reported pathological observations in archaeological human skeletal remains (Lallo et al. 1977; Schultz 2001; Wapler et al. 2004; Walker et al. 2009). Explanations for the presence of these lesions have been debated since the first description of orbital porosity in an early work done by Welcker in 1885. Since then, many researchers have agreed with the suggestion that these skeletal lesions are osseous reactions to an anaemic condition of either acquired or genetic origin with a specific focus on acquired iron-deficiency anaemia (e.g. Aksoy et al. 1966; El-Najjar et al. 1976; Lallo et al. 1977; Stuart-Macadam 1987; Tayles 1996; Wapler et al. 2004; Walker et al. 2009). It is important to keep in mind, however, that porotic hyperostosis of the cranial vault and orbital roofs is not characteristic of a specific disease, but rather it is the morphologic expression of various diseases (Schultz 2001).

In a review of the literature, support for the anaemia hypothesis comes from several clinical studies which have revealed that the macroscopic structural alterations of the skull that result in porotic lesions have been commonly observed in radiographic and post-mortem examinations of individuals with diagnosed genetic (Cooley et al. 1927; Caffey 1937; Walker et al. 2009) or acquired anaemias (Askoy et al. 1966; Lanzkowsky 1968). In addition to radiological similarities, epidemiological data including age- and sex- specific prevalence of iron-deficiency anaemia in modern pre-industrial populations are often similar to patterns identified in bioarchaeological studies of past populations (e.g. Lallo et al. 1977; Kent 1986; Palkovich 1987; Reinhard 1990; Stuart-Macadam 1992; Larsen 1995; Holland and O'Brien 1997; Roberts and Manchester 2005; Sullivan 2005; Beňuš et al. 2010). However, the etiology of porotic hyperostosis has received a significant amount of attention in palaeoepidemiology, and relatively recent publications have addressed a range of etiological factors and co-factors for the presence of these lesions (Fairgrieve and Molto 2000; Wapler et al. 2004; Walker et al. 2009).

Fairgrieve and Molto (2000) were the first to suggest additional factors for the presence of anaemia in two skeletal populations from the Dakleh Oasis, Egypt based on the presence of orbital porotic hyperostosis in some infants prior to the expected minimum age for the development of iron-deficiency anaemia. Upon considering the epidemiological profile of orbital porotic hyperostosis in the Dakleh population, it appears that megaloblastic anaemia, rather than iron-deficiency anaemia, is a more likely explanation for the presence of porotic orbital lesions. In addition to megaloblastic anaemia, caused by deficiencies in folic acid, the epidemiological profile of orbital porotic hyperostosis in the Dakleh populations also suggests that gastroenteritis, malaria, and botulism infection cannot be eliminated as contributing sources of anaemic stress (Fairgrieve and Molto 2000). In 2009, Walker and colleagues echoed the earlier views of Fairgrieve and Molto (2000), questioning the etiology of porotic hyperostosis in a reappraisal of the iron-deficiency hypothesis. In this publication, Walker et al. (2009) suggested that iron-deficiency anaemia does not provide a sufficient physiological explanation for the bony changes observed in porotic hyperostosis and that these lesions are more likely the result of a synergistic relationship between megaloblastic anaemia acquired through infant weaning practices and gastrointestinal infections. In addition to reconsiderations of the iron-deficiency hypothesis, other anthropological investigations have suggested that, in some cases, the microscopic structural features of bone in lesions of porotic hyperostosis do not support a diagnosis of an anaemic condition at all (Schultz 2001; Wapler et al. 2004).

Microscopic analyses of thin-ground sections of individuals with porotic hyperostosis have indicated the presence of several pathological conditions which can produce similar morphological changes to the cranial vault and orbits that cannot be differentiated by gross visual inspection (Schultz 2001; Wapler et al 2004). These conditions include rickets, scurvy, localized or systemic infections (e.g. osteomyelitis), and post-mortem erosion (Schultz 2001; Wapler et al. 2004; Sullivan 2005). Therefore, current interpretations of the presence of porotic hyperostosis may need to be reconsidered in a number of archaeological skeletal collections. The reconsideration of the etiology of porotic hyperostosis has important implications for current interpretations of past

population health and the presence of disease. For example, the high prevalence of porotic hyperostosis among Maya populations has played an important role in the development of the nutritional argument of the ecological model of Maya collapse (Saul 1972; Willey and Shimkin 1973; Wright and White 1996). Several researchers have attributed the prevalence of these lesions among the Maya to iron-deficiency anaemia, scurvy, and infectious disease (Saul 1972; Wright and White 1996; White et al. 2006). However, considering a combination of paleoecological and stable isotope studies, the presence of scurvy among the ancient Maya is highly unlikely (Wright and White 1996). Palaeoecological studies indicate that despite an increase in maize consumption, many Maya populations lived in environments that were diverse and rich in sources of vitamin C originating from various fruits and vegetables including zapote, nance, ciruela, hackberry, wild grape, avocado, and chile peppers (Wright and White 1996). Among coastal Maya populations, marine resources were readily available and, based on evidence from stable isotopic analyses, were readily consumed, providing these populations with sufficient sources of iron and vitamin C (Sizer and Whitney 2000; White et al. 2006). These data suggest that dietary deficiencies alone are unlikely etiological factors contributing to the prevalence of porotic hyperostosis among many Maya populations and that etiological factors likely varied both geographically and temporally (Wright and White 1996). These findings may have significant implications for the current health arguments of ecological models of the Classic Maya collapse. For health arguments to be upheld, evidence must support the proposition that the Maya disease burden was greater than that for other societies and that the burden increased until the time of collapse (Wright and White 1996). Evidence that etiological factors may have varied across populations and over time suggests that the health burden likely fluctuated throughout Maya occupation and, therefore, reconsiderations of contributing factors to the collapse of Maya civilizations may be necessary.

The presence of porotic hyperostosis in Greek skeletal collections has also raised questions regarding the etiology of porotic hyperostosis among Mediterranean populations (Angel 1966, 1971; Keenleyside and Panayotova 2006). Typically attributed to thalassemia, a genetic anaemia due to the presence of endemic malaria in the

Mediterranean region, alternative etiologies continue to be proposed by many researchers. This is because in some cases skeletal evidence does not appear to be consistent with a diagnosis of thalassemia, leaving many researchers to question the potential etiological factors contributing to the presence of these lesions in Mediterranean populations (Musgrave 1980; Stravopodi 2004; Keenleyside and Panayotova 2006; Walker et al. 2009). The difficulties in establishing a reliable differential diagnosis and etiological explanation have been attributed not only to issues with the assumption that malaria was endemic in Mediterranean populations, but also to the reliability of observations and diagnoses based only on the macroscopic examination of skeletal remains (Musgrave 1980). Multifactorial approaches to the analysis and interpretation of porotic hyperostosis are necessary and the use of multiple methods should be emphasized. In addition to macroscopic methodologies, research done by Schultz (2001) and Wapler et al. (2004) suggests that a detailed microscopic analysis of bone structure may have the potential to reveal important information regarding the etiology and pathogenesis of porotic hyperostosis in this geographic region.

Over the last several decades, microscopic research has suggested that porotic hyperostosis has a much more complicated etiology than the early literature suggests and that the complex processes of lesion development and healing require further exploration beyond the limitations of macroscopic research (Schultz 2001; Wapler et al. 2004). Based on these findings, current assumptions and understandings of the causes and pathogenesis of porotic hyperostosis in palaeopathology should be carefully reconsidered. As has been illustrated using examples from Egyptian, Maya, and Mediterranean collections, reconsidering the etiology of porotic hyperostosis can have important implications for our current interpretations of health and the prevalence of disease in early human populations (Wapler et al. 2004; Walker et al. 2009). As such, in order to establish a reliable differential diagnosis in palaeopathology, it is clear that it may be necessary to not only assess macroscopic features, but to also evaluate the changes to the microscopic structures of affected bone (Schultz 2001; Rühli et al. 2007). By providing simple descriptions of the types of bone processes occurring at the microscopic level, important information can be combined with other lines of evidence (e.g. macroscopic, radiological, palaeoecological, archaeological) to improve differential diagnosis. The

classic tool for the high-resolution examination of bone microstructure is histology, which is considered to be the gold standard. Histological analyses can reveal alterations to, and patterns of features in, bone microstructures which may provide valuable information regarding the pathogenesis and potential causes of disease, leading to more reliable diagnoses. As a result, pathological conditions with similar macroscopic osteological manifestations can be better differentiated and more reliably diagnosed using microscopic methods of analysis.

1.2   Research Purpose and Objectives

The purpose of this dissertation research is to assess the value of micro-CT, a high-resolution, non-destructive alternative to histology, to palaeopathology for the objective, quantitative analysis of porotic hyperostosis. The use of micro-CT in palaeopathology to date has been limited and mainly focused on subjective qualitative assessments of bone lesions with little exploration into the value of objective quantitative data to the process of differential diagnosis (e.g. Kuhn et al. 2007; Rühli et al. 2007). Currently, palaeopathologists record the presence of porotic hyperostosis in a number of different ways (e.g. Nathan and Haas 1966; Steinbock 1976; Mensforth et al. 1978; Stuart-Macadam 1982, 1985; Buikstra and Ubelaker 1994). The most common method is to evaluate the lesions using an arbitrary and subjective scale of severity from light, scattered porosity to severe, large apertures radiating from one or more areas of the cranial vault or orbital roof (Nathan and Naas 1966; Stuart-Macadam 1982). Mensforth et al. (1978: 23) introduced the concept of evaluating disease pathogenesis by recording porotic hyperostosis as being "unremodelled" or "remodeled". This evaluation of lesion activity was done in order to assess age-related palaeoepidemiological patterns that may reveal important information regarding the development and etiology of porotic hyperostosis. Regardless of the refinement of these macroscopic methods over many years, each one has the same inherent flaw, subjectivity. Since these methods are subjective, there will always be specimens that do not fit into one single category, and different investigators may evaluate the same specimen differently (Fairgrieve 1993). Not only does micro-CT have the potential for an increased reliability of diagnosis due to its

ability to provide 3D quantitative data on internal bone structures, it also provides a non-destructive method for refining these subjective scales of assessment.

The objectives of this study are to: 1) evaluate the presence of any palaeoepidemiological trends in the prevalence of porotic hyperostosis that may support differential diagnoses in the study sample, 2) evaluate the reproducibility and reliability of 2D and 3D methods of data collection for the quantitative analysis of bone micro-architecture from micro-CT images of archaeological skeletal remains, and 3) apply reliable micro-CT image analysis methods in the evaluation of porotic hyperostosis to determine the value of such methods to understanding the processes of lesion development and to improving the differential diagnosis of these lesions in palaeopathology. These objectives are designed not only to examine the pathogenesis and possible etiological avenues of porotic hyperostosis, but to also attempt to link subjective visual scales of assessment with an objective and scientifically reproducible method of palaeopathological evaluation.

The major contribution of this research is to provide future researchers with a standardized, non-destructive method of micro-CT image analysis for improving the process of differential diagnosis of pathological skeletal lesions on archaeological human remains. Improving the reliability of differential diagnoses and better understanding the process of pathological structural changes to bone will in turn result in more accurate reconstructions of the presence and prevalence of disease in past populations. This, along with additional lines of modern clinical, archaeological, and palaeoecological evidence can be combined to achieve a better palaeoepidemiological understanding of the social, cultural, and environmental origins of disease throughout our human past (Armelagos and Van Gerven 2003; Zuckerman et al. 2012).

To assess the first objective of this research, the essential requirement for this dissertation is an archaeological skeletal sample from a population with an established archaeological context that also includes individuals exhibiting porotic hyperostosis. The skeletal sample should include males and females as well as individuals from different age cohorts so that a demographic profile can be determined. Several well-documented collections from the Maya skeletal series as well as a Greek colonial sample have been

compiled to make up the skeletal sample to be examined in this study. It will be necessary to first consider the overall palaeoepidemiological pattern of porotic hyperostosis in the populations represented by these skeletal collections in order to provide as accurate a differential diagnosis of porotic hyperostosis as possible. A synthesis of demographic information, macroscopic assessment, palaeopathological analyses, and the archaeological context of the skeletal remains will allow for the development of a palaeoepidemiological model. The micro-CT data that is collected in this study can then be evaluated within the context of this model to determine the value of this technology to the process of differential diagnosis. The identification of any palaeoepidemiological trends will be achieved through the testing of the following hypotheses:

$H1_o$ = No relationship exists between the age of the individual and the severity and activity of porotic hyperostosis.

$H2_o$ = No relationship exists between the sex of the individual and the severity and activity of porotic hyperostosis.

After identifying any palaeoepidemiological trends, the second objective of this dissertation is to assess the reproducibility and reliability of various methods of data collection used on micro-CT volumes of archaeological human skeletal remains. The assessment and recognition of the sources of measurement error in micro-CT volume analysis will contribute to an improved understanding of how to best utilize this technology in palaeopathological research in order to achieve accurate representations of bone microstructures. Standardized methods of quantitative micro-CT data collection can then be recommended and developed for use in palaeopathology to ensure that results are reliable, consistent, and comparable across research studies. There are typically two different methods that can be employed to obtain quantitative structural data from micro-CT volumes for the assessment of bone microstructures. First, data can be collected from regions of interest in two dimensions (2D) from a micro-CT cross-section in a single anatomical plane, which is analogous to a histological thin-ground section. Second, data can be collected from volumes of interest in all three anatomical planes and, therefore, in

three dimensions (3D). On the basis of achieving different research goals, clinical studies, as well as the limited number of palaeopathological research studies, using micro-CT for the structural analysis of bone, have employed 2D and 3D methods (e.g. Kuhn et al. 2007; Rühli et al. 2007; Particelli et al. 2011). However, the literature is lacking on research that specifically evaluates the reliability and reproducibility of different 2D and 3D methods of data collection, and additional research that explores which of these data collection methods provides the most accurate representation of structural properties of bone is needed. Therefore, the second objective of this dissertation research will be to determine which methods of micro-CT image analysis produce the most accurate and precise results for the investigation of bone microstructures in archaeological human remains. To address this second objective, the null hypothesis of interest is as follows:

H3$_o$ = There are no differences in the reproducibility or reliability of 2D and 3D quantitative methods for the analysis of trabecular bone microarchitecture.

The third objective of this research is to apply the micro-CT image analysis method that produces the most reliable and reproducible results to the evaluation of skeletal lesions in archaeological skeletal collections. The morphologic expression of several disease processes referred to as porotic hyperostosis will be investigated using micro-CT image analysis methods in an attempt to quantitatively assess potential changes to internal microstructures that may provide important information on the disease process. The purpose of this third objective is to determine if the quantification of bone microarchitecture using micro-CT image analysis methods reveals any important diagnostic information regarding the pathogenesis and/or etiology of pathological conditions that give rise to the general macroscopic appearance of porotic hyperostosis. This objective will be addressed through the following null hypothesis statements:

H4$_o$ = No significant differences exist in trabecular bone microarchitecture between unaffected individuals and affected individuals based on the visually observed categories of lesion *severity* (light, medium, severe).

H5$_o$ = No significant differences exist in trabecular bone microarchitecture between unaffected individuals and affected individuals based on the visually observed categories of lesion *activity* (active, healed, mixed).

Based on the applications of micro-CT for the high resolution assessment of bone microarchitecture in clinical histologic research (e.g. Müller et al. 1996; Müller et al. 1998; Balto et al. 2000; Kuhn et al. 2007; Rühli et al. 2007; Particelli et al. 2011) and in previous palaeopathological research (e.g. Kuhn et al. 2007; Rühli et al. 2007; Wade et al. 2009), it is anticipated that the results of this study will make a significant contribution to palaeopathology by providing reliable and reproducible methods of data collection, improving our understandings of disease processes in conditions with debatable and complex etiologies, as well as increase our epidemiological understandings of health and disease in ancient societies.

Overall, the role of this research within the broader discipline of anthropology is to provide a standardized, non-destructive method for collecting accurate primary evidence for the state of health of past human populations in order to allow for the reliable reconstruction of the dynamic interactions between the environment, culture, and disease in archaeological populations in future studies. Culture, as a component of an individual's environment, can significantly influence the prevalence and pattern of pathological conditions (Waldron 1994; Larsen 1997; Armelagos and Van Gerven 2003; Zuckerman et al. 2012). By reliably reconstructing cultural systems and behaviour, the palaeopathologist can evaluate a population's effectiveness for responding, or failing to respond, to disease processes and other environmental stressors (Norr 1984; Larsen 1997; Goodman and Armelagos 1989). In other words, we can understand the impact of cultural practices on human adaptation or maladaptation, and begin to establish links between disease, cultural practices and ecological settings. Reliable differential diagnoses are vital for establishing these links and for correctly interpreting disease prevalence, population health, and the biocultural factors that may have contributed to health, illness, and the spread of disease in the past. Understanding the biocultural and evolutionary factors that contributed to the presence and patterns of pathological conditions in the past can help us to understand the factors that generate patterns in

contemporary populations and global disease prevalence (Zuckerman et al. 2012). Therefore, rigorously testing and standardizing new palaeopathological methods, such as micro-CT, for improving our understandings of disease processes and, therefore, the reliability of differential diagnoses are necessary not only for answering important anthropological and biocultural questions about our human past, but also for contributing to our current understandings of disease etiology and epidemiology.

1.3　　Dissertation Outline

In order to address the hypotheses and objectives of the current research study it is important to first have an understanding of the history and development of palaeopathology and palaeoepidemiology, a basic knowledge of bone biology and the underlying mechanisms of pathological bone change, and a familiarity with the process and methods of differential diagnosis in palaeopathology. Chapter 2 explores the role and importance of modern medical epidemiological practice to palaeopathology and to the study of disease in archaeological skeletal populations through discussions of the history of palaeopathology, the introduction of new technologies in the study of skeletal disease, and the beginnings of a palaeoepidemiological approach. This chapter also details the limitations of incorporating epidemiological methods intended for the study of living populations in palaeopathological research on skeletal populations and addresses the limitations inherent in the study of skeletal samples through a discussion of Wood et al.'s (1992) debate known as the osteological paradox.

Chapter 3 provides a review of basic bone physiology, bone biochemistry, and the basic mechanisms of pathological or abnormal bone change. The final sections of this chapter provide detailed considerations of the physiological mechanisms and resultant bony responses that occur in the various conditions that contribute to the morphological appearance of porotic hyperostosis. This chapter attempts to facilitate a basic understanding of the physiological mechanisms that contribute to the osteological manifestations of external and internal stressors that are observed in archaeological skeletal remains and the differential diagnostic possibilities for the presence of the lesions of interest in the current study – orbital and cranial porotic hyperostosis.

The final background chapter addresses the process of differential diagnosis in palaeopathology. Chapter 4 describes the process of differential diagnosis in the clinical sciences and how this process relates to differential diagnosis in palaeopathology. The contributions of the clinical sciences, historical data, and archaeological data to the process of palaeopathological diagnosis are discussed and the different methodological approaches and recent advances to palaeopathological methods of diagnosis are reviewed in detail. Methods of palaeopathological diagnosis relevant to providing the background for the current study are included such as gross visual inspection, radiography, clinical computed tomography, and microscopy and histology. An introduction and review of the application of micro-CT to palaeopathology is provided and offers a foundation for the objectives of the current study.

Chapter 5 offers details on the specific skeletal collections used in this study to address the hypotheses outlined above and explanations as to why these collections were chosen. The proceeding methods section discusses the facilities and micro-CT equipment that made the current research study possible and describes the procedures used in the collection of macroscopic palaeopathological data as well as the process of micro-CT data acquisition, collection, and subsequent quantitative analyses.

Chapter 6 reviews the results of the macroscopic assessment of lesion severity and activity, the evaluation of observer reproducibility and reliability with 2D and 3D micro-CT methods, and the quantitative 3D micro-CT analysis of trabecular bone micro-structures. Tests for dependence on factors such as age or sex of the individual are presented to identify any palaeoepidemiological trends the sample used in this study may exhibit. An evaluation of observer reproducibility and reliability is provided to identify the most reliable methods of image analysis for the application of micro-CT methods to palaeopathological research. Finally, the quantitative analyses of the structural variables used to evaluate trabecular bone micro-structure and evidence of disease pathogenesis are presented and evaluated.

Finally, Chapter 7 discusses porotic hyperostosis in the context of the study and considers the palaeoepidemiological patterns demonstrated in the study sample within the context

of the published literature. After exploring the palaeoepidemiological patterns, the remaining objectives of the current research study are addressed through a thorough discussion of the results of the micro-CT evaluation of trabecular bone microarchitecture. Future research recommendations and directions are also provided.

Chapter 2

2 Palaeoepidemiology

The nature and the cause of disease and illness, both in modern and archaeological contexts, has been a subject of curiosity and scientific inquiry throughout human history. When it comes to understanding the processes and causes of disease, this inherent curiosity has encouraged research into questions such as who got what?, when?, and where? (Waldron 2007). Attempts at answering these questions in modern medical and archaeological contexts have led to the development of the disciplines of epidemiology and palaeoepidemiology. The first sections of this chapter will briefly introduce the discipline of epidemiology, the role of epidemiological methods in palaeopathology, and the history and development of palaeopathology and palaeoepidemiology. The latter sections will review and discuss the applications and limitations of epidemiological methods within palaeoepidemiology.

2.1   Introduction to Epidemiology

Epidemiology is the scientific study of the patterns, causes, and effects of disease in living human populations and aims to infer and/or identify the causal relationships between demographic, social, and cultural risk factors and disease (Pinhasi and Turner 2008). Epidemiological studies involve collecting data on exposure factors that are involved in producing a specific disease or group of diseases (Lilienfeld and Stolley 1994). These factors include host factors, such as age, sex, and heredity, and environmental factors, including climate, pollution, disease vectors, and living conditions (Waldron 2007; Pinhasi and Turner 2008). In order for researchers to evaluate different diseases and their associated risk factors, or exposure variables, a case-control study strategy is commonly used (Waldron 2007).

The first step in conducting a case-control study is defining the specific disease of interest and establishing diagnostic criteria. Epidemiological research, in this sense, is retrospective and the outcome, the disease, is identified first followed by the assessment of possible risk factors, or exposure variables, that produced the outcome (Merril and

Timmreck 2006; Waldron 2007). The next step is to identify the study population and to group those individuals as cases, those experiencing the disease or health related issue, and controls, individuals from the same general population who have the same possibility of being exposed, but do not have the disease (Gordis 2000; Merril and Timmreck 2006; Pinhasi and Turner 2008). Once the cases and controls have been identified, data on the exposure status and potential causal factors are collected using medical records, interviews, and/or questionnaires (Merril and Timmreck 2006; Waldron 2007). The use of this type of study design is well illustrated by the epidemiological research conducted during an outbreak of hantavirus pulmonary syndrome (e.g.. Zeitz et al. 1995).

In May 1993, an outbreak of illness in the south-western United States, characterized by fever and respiratory distress, was identified as hantavirus pulmonary syndrome (HPS). During the epidemic period, a case-control study was conducted by Zeitz et al. (1995) to identify the risk factors for HPS to assist in the development of prevention strategies. Case patients were identified through the solicitation of clinicians, medical examiners, and infection control practitioners and were diagnosed by laboratory confirmation of hantavirus infection. These case patients were matched with individuals from 3 groups of controls: non-infected members of case-patient households (household controls), members of neighbouring households, and individuals of randomly selected households greater than 24 km away. A standard questionnaire was used during interviews to collect data regarding activities performed during the 6 weeks before the onset of illness for cases and for the same period for matched controls. These data revealed that case-patients were more likely than controls to have an increased number of small rodents in the household, participate in agricultural activities involving hand plowing and planting domestic crops, and to clean animal sheds and areas used for food storage. These environmental factors were all related to an increased exposure to trapped live, or dead, rodents and the inhalation of aerosolized rodent excreta. In terms of host factors, cases were more likely than controls to report chronic autoimmmune or hyperimmune disorders, such as allergies or asthma, reflecting the potential role of immune response in the pathophysiology of HPS. The findings of this study suggest that eliminating rodents from human environments through prevention of rodent entry into buildings and the removal of potential rodent food sources was the basis for prevention (Zeitz et al. 1995).

This example is an illustration of the overarching goal of epidemiological research which is to use collected data to affect public health policies and to implement or inform medical interventions and treatments for a particular disease in a particular population (Waldron 2007; Pinhasi and Turner 2008). It is important to note that the key features of epidemiology are that the population, rather than the individual, is the unit of study and research is quantitative and observational, as opposed to qualitative and experimental (Pearce 2005, in Pinhasi and Turner 2008).

Modern epidemiology is concerned with identifying and understanding the determinants of disease in living populations, paying little to no attention to human remains or to the study of disease in past human populations (Waldron 2007). Palaeoepidemiology, on the other hand, can be broadly described as an interdisciplinary area of research which combines aspects of palaeopathology with epidemiology through the application of selected epidemiological methods to the study of disease in human skeletal remains from past populations (de Souza et al. 2003; Pinhasi and Turner, 2008). The role of palaeopathology is to provide data on the range of pathological conditions identifiable in bones and teeth from past human populations. Estimating how common these pathological conditions were in past populations is where epidemiological methods become pertinent (Pinhasi and Turner 2008; Boldsen and Milner 2012). Like modern epidemiology, palaeoepidemiology also integrates data on environmental change, geographic location, sociocultural disease risk factors and information from modern clinical diagnosis in order to contextualize and evaluate possible disease etiologies. In terms of the host, factors such as age, sex, and genetic relationships also have to be determined or, in the case of palaeoepidemiology, estimated (Waldron 2007; Pinhasi and Turner 2008).

Unlike epidemiology, palaeoepidemiologists are interested in skeletal populations and therefore do not have the luxury of collecting data from living populations using the case-control approach, nor do investigations begin with an identified outcome (Waldron 2007, 2009). Rather, palaeoepidemiological investigations are cross-sectional in nature and begin with the collection of various forms of biocultural and archaeological information, including evidence of disease from skeletal material, which are used to reconstruct

16

possible sociocultural and biological disease risk factors, or exposure variables. The reconstruction and contextualization of exposure variables in past populations is integrated with collected skeletal data and knowledge of modern clinical data on known diseases and an outcome variable is proposed (Buikstra and Cook 1980). The outcome variable will be either a specific or non-specific disease that is identified through the process of differential diagnosis (Waldron 2009). Although relevant to palaeopathological studies, analytical epidemiological methods have not always played a significant role in palaeopathology due to the nature of archaeological skeletal assemblages and limited sample sizes. As a result of such limitations, even today many researchers do not incorporate these types of methods into their analyses. However, with an understanding of the limitations of skeletal samples, the use of population level analyses may aid in the development of important inferences about the evolution, spread, and history of disease in past human populations (Pinhasi and Turner 2008). The gradual incorporation of a population based, or epidemiological, approach into the study of disease in the past is best understood through a brief review of the history and development of palaeopathology as a discipline.

2.2　The History and Development of Palaeopathology and Palaeoepidemiology

The field of palaeopathology is approximately two hundred years old and its development as a scientific discipline has been explored by a number of researchers. Reviews of its history describe a chronological succession of defined eras, each characterized by the evolution of scientific concepts and methods (i.e. Buikstra and Cook 1980; Aufderheide and Rodriguez Martín 1998; Roberts and Manchester 2005; Grauer 2008). Although there are some differences in the scope and definition of these eras, there appears to be a general recognition of an early period, prior to the mid-nineteenth century, devoted to the study of disease in fossilized animal bones. This was followed by a period during the latter half of the nineteenth and early twentieth centuries in which focus shifted to an interest in pathological changes in human remains and, finally, a period covering a large span of time in which the discipline matured through a recognition of the role of epidemiology, the standardization of diagnostic definitions and criteria, and the

development of new methodologies (Aufderheide and Rodriguez Martín 1998; Roberts and Manchester 2005).

Prior to the mid-nineteenth century, work devoted to the study of ancient disease was limited to the research of anatomists and naturalists interested in pathological lesions in prehistoric animal bones (Aufderheide and Rodriguez Martín 1998; Roberts and Manchester 2005). Though focused primarily on diseases of prehistoric animals, there was some recognition of the importance of understanding the antiquity of human disease. Reviews of the literature produced during the later nineteenth and early twentieth centuries highlight the trend that although there was increasing recognition that studying human disease could be beneficial to exploring past population histories, research concentrated mainly on case studies and isolated lesion descriptions with little scientific precision (Roberts and Manchester 2005; Grauer 2008; Pinhasi and Turner 2008). During this period, specimens with pathological lesions were viewed more so as curiosities or interesting anomalies and not as sources of valuable medical or historical knowledge (Lovell 2000; Roberts and Manchester 2005). The cultural context and broader views on the history and dynamics of disease in ancient human populations were not of any concern early on in the development of palaeopathology (Buikstra and Cook, 1980; Armelagos and Van Gerven, 2003). Skeletal biology and palaeopathology remained primarily descriptive sciences with little theoretical or anthropological foundation (Armelagos 2003). Researchers at this time, including Rudolf Virchow (1821-1902), Frederic Wood Jones (1879-1954), and Sir Marc Armand Ruffer (1859-1917), relied on their medical training as physicians and anatomists to identify pathological lesions in human bone and were strongly committed to a clinical approach with the basic goal of describing and diagnosing skeletal lesions in individual case studies (Lovell 2000; Armelagos 2003; Grauer 2008). Although their work contributed greatly to the development of macroscopic and microscopic analyses in palaeopathology, observations and descriptions were not objectively presented using standardized language and data collection procedures, and there was little to no interest in exploring epidemiological perspectives (Buikstra and Cook 1980; Aufderheide and Rodriguez-Martín 1998). As a result of a strictly clinical approach, the range of differential

diagnoses offered was limited and the lack of standardized observations made the testing of alternative diagnostic hypotheses difficult if not impossible (Buikstra and Cook 1980).

Perhaps one of the most significant medical advances to influence palaeopathological research during this early period was the discovery of x-rays by Roentgen in 1895, and the subsequent development of clinical radiography (Chhem 2008; Mays 2008; Conlogue and Beckett 2010). Archaeologists were quick to realize the possible applications of x-rays for the non-destructive examination of archaeological human remains and, in 1896, radiography was applied to the study of Egyptian human and cat mummies for the first time, mostly to reveal what lay beneath the wrappings (Böni et al. 2004; Mays 2008). In 1898, F.J. Clendinnen published one of the first papers dedicated solely to the radiographic analysis of skeletal abnormalities in human remains, reporting an abnormal number of bones in the hand of an Egyptian mummy (Mays, 2008). However, it was Sir Marc Armand Ruffer (1859–1917) who paved the way for the use of both radiographic and histological methods for the investigation of skeletal disease in Egyptian mummies (Sandison 1967; Aufderheide and Rodriguez-Martín 1998; Grauer 2012). His innovative approach relied on detailed observations, careful documentation, and comparisons of clinical manifestations of disease to lesions found on archaeological human remains (Sandison 1967; Grauer 2012). Soon after, radiography began to be applied not only to mummified remains, but also to the study of dry archaeological bones for the purpose of visualizing pathological changes (e.g. Eaton 1916; Means 1925; Williams, 1929), and rigorous methods beyond visual descriptions were introduced in attempts to improve the process of differential diagnosis (Buikstra and Cook 1980; Roberts and Manchester 2005). Though there was a rapid adoption of this innovative methodological approach, and an initial explosion of publications, radiology failed to become routine in palaeopathological research and was largely neglected as a diagnostic tool until as late as the 1960's (Wells 1963; Mays 2008).

In the mid-twentieth century, palaeopathology experienced an important theoretical advance with the introduction of a new analytical approach towards understanding the history and antiquity of disease. This new approach is demonstrated by the works of Earnest Hooton (1930) and Aleš Hrdlička (1941) (Aufderheide and Rodriguez-Martin

1998; Lovell 2000; Roberts and Manchester 2005). At Harvard University, using his detailed records and observations, Hooton applied a population based perspective to palaeopathology by using an ecological and cultural approach to better understand the determinants of disease in the Pecos Pueblo population (Aufderheide and Rodriguez-Martin 1998; Grauer 2008). Aleš Hrdlǐcka was also instrumental during this time, creating a Division of Anthropology at the Smithsonian Institution where he accumulated large skeletal collections from North and South America for palaeopathological study at the population level (Roberts and Manchester 2005).   Research in the field began to focus on the complex relationships between disease processes, ecological variables, culture, and human behaviour (Grauer 2008). Although three decades would pass before similar population-level methodologies became widely adopted, Hooton's work foreshadowed the value and future applications of an epidemiological approach to palaeopathology (Zuckerman et al. 2012).

While there was much excitement generated by Hooton's (1930) classic epidemiological report on Pecos Pueblo, this work, along with many publications from this period, should be considered critically (Waldron 1994, 2007; Buikstra and Cook 1980). Scholars optimistically applied newly developed medical technologies, such as radiology, to the study of ancient skeletal remains with little consideration of the potential limitations of the archaeological record (Buikstra and Cook 1980). Diagnoses were rarely questioned and the limitations of using new medical technologies for studying long dead individuals were not readily acknowledged. The criteria used for diagnosis were seldom explicitly stated, lesion descriptions continued to be limited, and differential diagnoses, where they did occur, did not include an appropriate range of pathological conditions (Buikstra and Cook 1980; Grauer 2008). In addition, normal and pathological variability across populations was either not considered or was infrequently discussed. As a result, conclusions made at the individual level were limited and these limitations were only multiplied as inferences about the health status of the broader population were attempted (Buikstra and Cook 1980).   Regardless of the critiques and limitations of many of the works of this era, the introduction of new interpretive analytical approaches and some attempts to standardize the collection of data slowly began to transform palaeopathology. By the end of this period palaeopathology would begin to emerge as a scientific

discipline with research gradually shifting from simple description and case study analysis to an interest in the ways in which biological, cultural, and behavioural determinants of disease change over time and across different geographic regions at the population level (Lovell 2000; Roberts and Manchester 2005; Waldron 2007).

After the publication of Hooton's work in the 1930s, the period from the late 1930s until the mid-1960s saw only sporadic efforts to advance the discipline by few individuals, and theoretical and methodological progress in palaeopathology began to stagnate (Jarcho 1966; Sandison 1967; Buikstra and Cook 1980). Case studies once again dominated the literature and the small remainder of publications that described larger skeletal collections presented raw biological data that were culturally, spatially, and ecologically decontextualized (Armelagos et al. 1982; Larsen 1997; Zuckerman et al. 2012). A lack of fundamental theoretical contributions and a failure to apply innovative diagnostic methodologies to the study of ancient skeletal remains were highlighted in Jarcho's 1966 volume *Human Palaeopathology* (Buikstra and Cook 1980; Grauer 2008). Jarcho (1966) called for a necessary organization and synthesis of research on the investigation of ancient disease in order to make large amounts of collected osteological data available to a wider research community. In addition, for progress to be made in the discipline, Jarcho (1966) voiced the need for the adoption of rigorous and standardized diagnostic methods as well as the application of previously neglected medical technologies to the study of ancient human bone.

In response to the mid-1960s evaluation of the state of palaeopathology, a number of efforts were put forward in attempts to resolve the lack of synthesis of information, to improve diagnostic rigour through the standardization of data collection, and to re-introduce population-based strategies for disease diagnosis (Buikstra and Cook 1980; Grauer 2008). In 1967, stemming from the need to pool collected osteological data, Brothwell and Sandison's seminal work, *Diseases in Antiquity*, provided a compilation of identified skeletal conditions observed in archaeological collections. This volume also provided insights into the geographical patterns and scope of different skeletal lesions and emphasized the importance of radiographic and histological techniques (Brothwell and Sandison 1967; Buikstra and Cook 1980; Grauer 2008). Later, in 1976, Steinbock

published a comprehensive textbook aimed at organizing and synthesizing diagnostic criteria for the purpose of the identification and diagnosis of disease in ancient skeletal remains. Steinbock (1976) led the way in efforts to provide a standardized and basic foundation for differential diagnosis and the interpretation of skeletal lesions by synthesizing both clinical and archaeological data (Grauer 2008). Comprehensive lists of differential diagnoses are provided, along with information on the pathogenesis of conditions and descriptions and images of the gross morphology and radiographic appearance of different diseases as they appear in archaeological samples. Since then, more recent efforts have been put forward in order to standardize data collection methods and to aid palaeopathologists in the accurate diagnosis and interpretation of skeletal lesions. Such efforts include: *Identification of Paleopathological Conditions in Human Skeletal Remains* (Ortner and Putschar 1981), *Human Paleopathology* (edited by Ortner and Aufderheide 1991), *The Cambridge Encyclopedia of Human Paleopathology* (Aufderheide and Rodriguez-Martín 1998), *The Archaeology of Disease* (Roberts and Manchester 2005), and *Palaeopathology* (Waldron 2009).

Throughout the 1970s and 1980s, research in palaeopathology continued to focus on developing new rigorous means of diagnosis, but also emphasized the value of blending biological, clinical, epidemiological, and archaeological methods with the goal of reconstructing and understanding the biocultural processes that occurred as populations adapted to their ecological and cultural environments (Armelagos and Van Gerven 2003; Roberts and Manchester 2005; Waldron 2007; Grauer 2012). This phase of development situated palaeopathology within the broader disciplines of anthropology and epidemiology by embracing the notion that a society's social organization, environment, and even its ideology could play a major role in influencing biological events such as patterns of disease in the past (Armelagos 2003; Armelagos and Van Gerven 2003). Livingstone's (1958) early seminal paper on sickle-cell anaemia pioneered the later development of this holistic biocultural approach, and with his theoretical contributions came a broader understanding of the nature and scope of human disease (Armelagos 2008; Zuckerman et al. 2012). In linking population growth, subsistence strategies, and areas with high densities of mosquito malarial vectors with the distribution and genetic frequency of the sickle cell trait in West Africa, Livingstone (1958) demonstrated the

importance of environmental context to the interpretation of health and disease. This integration of anthropological and epidemiological perspectives resulted in an increased focus on raising hypotheses regarding biocultural adaptation and thoroughly testing those hypotheses with both qualitative and quantitative skeletal data from large numbers of individuals (Armelagos and Van Gerven 2003; Roberts and Manchester 2005).

With this paradigmatic shift, researchers in the 1970s and 1980s began to acknowledge the importance of anthropologically oriented reconstructions of trends in past human population health, while at the same time recognizing the interpretive limitations imposed by a focus on case studies and the diagnosis of individual lesions and specific diseases (Ubleaker 1982; Larsen 1997; Cook and Powell 2006; Zuckerman et al. 2012). Through the integration of multiple sources of data palaeopathologists were able to interpret population level patterns of stress, nutrition, trauma, and disease within an epidemiologically, culturally, and ecologically contextualized framework (Larsen 1997).

In the last several decades, progress in palaeopathology can be attributed to improved methodological standardization leading to increased diagnostic accuracy, more realistic disease classifications, and the examination of disease in a biocultural context (Lovell 2000; Roberts and Buikstra 2003; Grauer 2008). The new biocultural theoretical approach initiated a need to incorporate previously ignored variables into osteological analyses and to standardize and improve the recording and diagnosis of disease. Important variables in recognizing and interpreting disease at the population level included the age at death and sex of the individual, the cultural and physical environments, and genetic and developmental factors (Armelagos and van Gerven 2003; Waldron 2007; Grauer 2008). The integration of multiple variables and the examination of the biocultural context of disease are exemplified by the work of Buikstra and Cook (2003). By successfully integrating archaeological, historical, and clinical data on tuberculosis with detailed descriptions of skeletal lesions and the incorporation of demographic data into the process of differential diagnosis, the authors provide a much broader, global perspective of disease in the past.

Also, to meet the needs for population-based approaches and cross-cultural comparisons, there was a growing need for the adoption of standardized recording measures (Grauer 2008). Efforts were made in the 1990s to improve the standardization of data collection and facilitate data sharing including one of the most well-known contributions out of North America, *Standards for Data Collection From Human Skeletal Remains* (Buikstra and Ubelaker 1994). This work provides stringent guidelines for the use of descriptive terminology, methods of data collection, and offers a detailed coding system for recording data that can be comparable between researchers. In addition, as palaeoepidemiological and biocultural approaches became better established within palaeopathology, new chemical, histological, biomolecular, and radiographic methods were rapidly emerging, improving not only diagnostic accuracy but also the ability to better contextualize interpretations of skeletal data (Grauer 2012; Zuckerman et al. 2012).

Methods for analyzing trace elements and stable isotopes from archaeological bone have been of significant value for the study of ancient diet, mobility, and life history processes such as weaning, growth, and health status (Zuckerman et al. 2012). Biochemical and histological techniques have been greatly developed and used to improve diagnoses for various diseases, including anaemia and syphilis (Zuckerman et al. 2012). The recent development of polymerase chain reaction (PCR)-related techniques (Saiki et al. 1988) for identifying ancient DNA (aDNA) from bone and mummified tissues has allowed for the mapping and identification of a number of ancient pathogens including leprosy (e.g. Haas et al. 2000; Donoghue et al. 2005), the trepanematoses (e.g. Kolman et al. 1999, Drancourt et al. 2007), and tuberculosis (e.g. Donoghue et al. 1998). Methodological developments of radiographic imaging in modern medicine have also offered new diagnostic possibilities in palaeopathology (Wanek et al. 2012). Although the first use of radiographic techniques in mummy research came only one year after the discovery of x-rays in 1895, more advanced methods of x-ray based examination came with the advent of computed tomography (CT) in 1967 (Lynnerup 2008).

Conventional x-ray is still a widely used non-invasive tool for the investigation of skeletal disease. However, the introduction of CT opened up many new possibilities for the diagnostic imaging of bone abnormalities not only for medicine, but also for

palaeopathology (Resnick and Pettersson 1992; Rühli et al 2007). Though expensive and often restricted to medical research, since the 1970s CT has become a well-established method in palaeopathology (Recheis et al. 1999; Spoor et al. 2000; Rühli et al. 2002). CT scanning of mummies was first carried out in 1976 by Lewin and Harwood-Nash (1977). Since this pioneering work, the applications of CT have expanded to not only include the analysis of mummies, but also the analysis and diagnosis of disease in dry archaeological bone (Rühli et al. 2007). This is the direct result of the increased commercial availability of various CT scanners over the last several decades, making the technology more accessible to anthropological and palaeopathological research (Rühli et al 2007).

More recently, Feldkamp and colleagues (1989) developed the first micro-computed tomography (micro-CT) scanner designed for the high resolution evaluation of the three-dimensional micro-structure of trabecular bone. The first commercially available bone micro-CT scanner was presented in 1994. Although this technology has shown great promise for the study of bone micro-structures in the field of biomedicine, its diagnostic value to palaeopathology has been evaluated by only a few researchers over the past several years (e.g. Rühli et al. 2002; Kuhn et al. 2007; Rühli et al. 2007; Wade et al. 2009). The current study seeks to further investigate the contributions that micro-CT can make to further advance the fields of palaeopathology and palaeoepidemiology both methodologically and theoretically. Micro-CT has the potential to increase the reliability of disease diagnoses from human remains by revealing information on the micro-structural changes that occur due to various pathological conditions. More reliable diagnoses allow for a better understanding of disease etiology and, therefore, the ability to answer important archaeological and biocultural questions regarding the interactions between diseases, cultural practices, the environment, and the effects of disease on past human populations (Waldron 1994; Grauer 2012; Zuckerman et al. 2012).

Although the individual is the unit of diagnosis, using the population as the unit of analysis has allowed palaeopathologists to make broad-scale anthropological interpretations about health and illness in the past. As a result of the contributions of many researchers throughout the history of palaeopathology, the analysis of skeletal data can now be approached using innovative methodological techniques and a

palaeoepidemiological perspective in order to reconstruct and understand the effects of different regions and local ecosystems, dietary choices, and changes to cultural systems (i.e. the development of agriculture, social and class differentiation, etc.) on the prevalence of disease in our human past (Waldron, 1994; Larsen, 1997; Armelagos, 2003; Boldsen and Milner 2012).

2.3   Palaeoepidemiology: Analytical Approaches

Although the focus of palaeopathology is on the analysis of archaeological human remains, a common interest in disease patterns and change over time, and a focus on processes that concern populations rather than individuals is shared with medical epidemiology (Pinhasi and Turner 2008). Therefore, an approach of clear value to the study of past populations in palaeopathology involves the application of epidemiological methods to the investigation of disease in archaeological skeletal samples (Waldron 1994, 2007; Pinhasi and Turner 2008).

In epidemiology, the most common methods used to measure the status of disease in living populations are incidence and prevalence (Rothman 2002; Waldron 2007; Pinhasi and Turner 2008). Simply defined, the incidence of disease is the number of new cases that occur in a population at risk over a certain unit or period of time (Waldron 1994, 2007). In epidemiological practice, determining incidence requires defining a study population and determining a period of observation, which may be short or long depending on the nature of the disease, and counting the number of individuals who develop the disease of interest (Rothman 2002; Waldron 1991, 2007; Pinhasi and Turner 2008). By contrast, prevalence is calculated as the number of individuals who have a specific disease within a specified time divided by the number of individuals in the study population (Rothman 2002; Waldron 1994, 2007). Whereas incidence can only be determined in a longitudinal, or follow-up, study, prevalence can be estimated by examining a population at one point in time, known as a cross-sectional approach (Waldon 1991). Due to the cross-sectional nature of palaeopathological studies, incidence cannot be measured in skeletal populations as neither the number of new cases nor the magnitude of the population at risk can be determined (Waldron 1994, 2007). Palaeoepidemiology must focus, instead, on the use of prevalence as a measure of disease

from skeletal populations and, more specifically, period or point prevalence where the period may be defined as tens, or even hundreds, of years (Baker and Pearson 2006; Waldron 1994, 2007).

Additional measures of population morbidity and mortality that are relevant in palaeoepidemiology include age- and sex-specific disease prevalence, age-at-death distributions/mortality tables, and the calculation of life tables (Waldron 1994, 2007). Mortality is calculated as the relative frequency of deaths in relation to population size, and the mortality, or age-at-death, distribution illustrates at what age people were dying and whether or not there are differences between male and female mortality (Roberts and Manchester 2005). Life tables are another means of presenting information on mortality and survivorship in a population and include calculations of the probability of dying in a certain age category and life expectancy (the average number of years an individual is expected to live once entering a specific age category) (Chamberlain 2001; Roberts and Manchester 2005). As such, knowledge about the demographic parameters of the population under study is necessary for obtaining these data and for making meaningful interpretations about the disease status of both individual skeletons and the once living population as a whole (Roberts and Manchester 2005).

Palaeodemography is a branch of biological anthropology that can provide palaeopathologists with data on the distribution of the skeletal sample by age-at-death and sex, which is then supplemented by individual-health level information from the analysis of skeletal lesions in order to reconstruct patterns of population morbidity and mortality. An increased understanding of the role of age and sex in disease processes has necessitated the incorporation of palaeodemographic information into palaeopathological skeletal analyses (Grauer and Stuart-Macadam 1998; Grauer 2012).

Estimations of age-at-death and the determination of sex are important for the calculation of both general and age-specific prevalence rates of a specific pathological condition as well as for reconstructions of mortality distributions. This is because different diseases strike different age groups with different frequencies and bony lesions tend to accumulate with increasing age (Pinhasi and Bourbou 2008). Understanding and accounting for the

27

relationship between a specific disease and how it differentially affects specific age cohorts and sex is necessary for comparing disease prevalence between two or more archaeological populations. Accounting for age eliminates the possibility that observed differences in disease prevalence between archaeological samples are the result of age differences in the populations (Gourdis 2000; Pinhasi and Bourbou 2008). In principle, then, palaeodemography allows for the reconstruction of demographic trends over time and the indices of morbidity and mortality appear to be readily attainable and interpretable (Wood 2005). Due to persistent methodological and conceptual problems, however, interpreting these indices can be difficult (i.e. Wood et al. 1992).

Through the application of the appropriate epidemiological and palaeodemographic tools, such as calculations of disease prevalence, age- and sex-specific prevalence, and age-at-death profiles, palaeopathologists can begin to reconstruct the spatial, temporal, and social distributions of disease in past human populations (Waldron 1994; De Souza et al. 2003). Palaeoepidemiology and palaeodemography offer a means to measure and compare population level variation in the disease status of prehistoric populations, facilitating research on broader questions regarding population morbidity, mortality, fertility, and fecundity (Baker and Pearson 2006; Waldron 2007). However, as indicated above, there are a number of limitations, sources of bias, and methodological and conceptual problems that are inherent in archaeological skeletal samples which must be taken into consideration when using a palaeoepidemiological approach.

2.4   Limitations of Archaeological Samples and 'The Osteological Paradox'

In order to achieve some understanding about the characteristics and health status of a population, the palaeopathologist must determine how representative a skeletal assemblage is for a population based analysis of disease (Bourbou and Pinhasi 2008). In other words, how well does a sample of skeletal remains represent the larger, once living population? (Waldron 2007). Under ideal conditions, the skeletal sample available for analysis will represent the total number of deaths in the population during a specific time period (Alesan et al. 1999; Pinhasi and Bourbou 2008). In reality, there are a number of various non-random taphonomic, cultural, and demographic factors which affect how

well the skeletal sample will represent the larger population (Waldron 1994, 2007; Hoppa 2002; Pinhasi and Turner 2008).

Almost everything about a skeletal sample is non-random, and its composition is beyond the control of the palaeoepidemiologist (Waldron 2007). Factors that may affect the skeletal sample available for population analysis include the proportion of a population buried at a site, the proportion of remains lost due to disturbance and poor preservation, the proportion of remains discovered, and the proportion excavated (Roberts and Manchester 2005; Waldron 1994, 2007, 2009). The proportion of individuals lost at each stage will vary, but it is important to recognize these factors as potential sources of bias when applying a palaeoepidemiological approach to the analysis of a skeletal sample (Wood et al. 1992; Roberts & Manchester 2005; Waldron 1994, 2009).

The proportion of a population buried at a site is affected by cultural factors, specifically burial practices, and can bias data in important ways (Buikstra and Cook 1980). In cemeteries, individuals are often buried in specific locations or spatial clusters according to age, sex, family relation, social status, or social exclusion (Donnelly et al. 1999; Pinhasi and Bourbou 2008). For example, studies such as those done by Donnelly et al. (1999) and Roberts et al. (2002) have noted that certain segments of a population, such as unbaptized infants, social outcasts (e.g. mentally handicapped, suicides), and the visibly deformed or diseased were often buried in alternative locations, separated from the rest of the buried population. These types of burial practices often make it impossible to determine whether the excavated sample is in fact a true random sample of the cemetery population and thus representative of the living population (Pinhasi and Bourbou 2008). Palaeopathologists must therefore be aware of the location of the excavated proportion of individuals in relation to the rest of the cemetery and how this may create bias in the sample, the analysis, and the estimates of disease prevalence.

Fundamental to the diagnosis of disease, and therefore to the assessment of disease prevalence, is the physical condition, or preservation, of bone (Pinhasi and Bourbou 2008; Turner-Walker 2008). The proportion of the remains lost will depend on the type of burial environment to which they are exposed over hundreds or even thousands of

years, and their ability to retain the strength to remain intact during excavation, transportation, and ultimately analysis. Since different components of the skeleton vary in their physical strength and structure, preservation patterns will vary and fragile skeletal elements can be underrepresented (Buikstra and Cook 1980; Lambert et al. 1982; Pinhasi and Bourbou 2008). The low mineralization and high fragility of sub-adult bones also contribute to poor preservation and therefore to the underrepresentation of young individuals in excavated skeletal samples (Gordon and Buikstra 1981; Nicholson 2001). It is also important to note that the survival of bones with pathological lesions will also vary depending on the severity and type of the specific condition and how it affected the mechanical strength and physical integrity of the bone. For example, in leprosy, damage to the peripheral nerves of the hands and feet results in a loss of sensation, eventually leading to ulceration of the skin and secondary infections to hand and foot bones (Steinbock 1976; Aufderheide and Rodríguez-Martín 1998). As a consequence, the hand and foot phalanges are more susceptible to decomposition and post-mortem damage and may be missing from affected individuals in the skeletal sample (Pinhasi and Bourbou 2008). Clearly, in many archaeological cases, skeletal elements can be damaged or missing resulting in the poor preservation or complete loss of pathognomonic features and/or non-specific skeletal indicators of disease (Buikstra and Cook 1980; Pinhasi and Bourbou 2008). As such, palaeopathologists must carefully assess the preservation and completeness of specimens as well as the possible presence of other surviving diagnostic criteria in order to decide whether differential preservation may bias diagnoses and/or disease prevalence estimates (Pinhasi and Turner 2008).

Finally, the representativeness of archaeological samples is also affected by the proportion of a buried population that is discovered and excavated (Waldron 1997, 2004). Budgetary, time, and logistical constraints will affect the extent of a cemetery excavation and will often limit archaeologists from excavating a cemetery in its entirety (Pinhasi and Bourbou 2008). In addition, the total extent of a cemetery may never be discovered if it has been obliterated or obscured by modern construction (Waldron 1994, 2007). Even in cases where the total extent of a cemetery is known, determining whether or not the proportion of the cemetery excavated truly represents a random sample of the total cemetery population is impossible (Waldron 2007; Hoppa 2002; Pinhasi and Bourbou

2008). As discussed earlier, certain cemetery locations may be specific to families, social classes, and/or specific age cohorts (Mays 1997; Donnelly et al. 1999; Parker-Pearson 1999). Palaeopathologists have no means of completely resolving these issues. However, careful note can be taken of the possible factors that may affect the representativeness of a skeletal sample in order to limit bias in interpretations and conclusions.

The limitations encountered by palaeopathologists as a result of the nature of skeletal samples illustrate the difficulties encountered in the interpretation of general disease prevalence rates in past populations. For palaeopathologists who wish to assess age- and sex-specific health profiles of a population (age- and sex-specific prevalence, age-at-death mortality profiles), this process becomes even more difficult due to methodological and conceptual limitations inherent in reconstructions of the demographic structure of the sample (Wood 2005; Grauer 2008). In modern epidemiology, the demographic structure of the sample of individuals chosen to represent the larger population is known and can be controlled. In palaeoepidemiology, however, the demographic structure of the sample can only be estimated through the application of bioarchaeological methods of skeletal aging and sexing (Wood 2005; Grauer 2008).

Information on age-at-death can be obtained from analyses of the growth and development of specific skeletal features including: dental development, closure of long bone epiphyses and cranial sutures, and changes in the articular surfaces of the pelvis (Buikstra and Ubelaker 1994; Ortner 2003; Roberts and Manchester 2005). Methods for obtaining palaeodemographic age estimates based on these skeletal changes, however, are subject to differing degrees of error which arise from individual variability in the process of maturation, and many methods are low in accuracy and high in error, particularly in cases of older adults when the processes of skeletal growth and development have ceased (Wood 2005; Pinhasi and Turner 2008). Error rates may be decreased if all available methods of skeletal age estimation are combined for each individual. However, in cases where the preservation of the skeleton is poor, and the number of available methods limited, error in age estimates increases. Finally, since accuracy for a number of age estimation methods is dependent upon variations in growth rates between the sexes,

problems with the accuracy of age estimation are confounded by an inability to determine sex in infant and juvenile skeletal remains (Saunders 2000; Ortner 2003; Roberts and Manchester 2005).

Since mortality distributions and each component of a life table are derived from data on estimated age-at-death for each individual, a lack of accuracy in age estimations and the inability to determine sex for infants and juveniles will result in inherent errors in the calculation of the number of deaths among individuals of each age category, calculations of the probability of dying in a certain age category, and the calculation of life expectancy (Roberts and Manchester 2005). Ongoing research in bioarchaeology and palaeopathology continues to improve upon existing techniques of skeletal age and sex estimation in attempts to overcome some of these methodological issues so that more reliable interpretations of the impact of disease on morbidity and mortality at the population level can be achieved (Wright and Yoder 2003).

The Osteological Paradox (Wood et al, 1992), a highly influential publication in palaeoepidemiology and bioarchaeology, also highlights some important conceptual problems regarding the interpretation of data from skeletal assemblages (Wood et al. 1992; Pinhasi and Bourbou 2008). Wood et al. (1992) point out three key issues with the evaluation of population health status using archaeological skeletal samples: 1) demographic nonstationarity, 2) selective mortality, and 3) hidden heterogeneity in risk. The first conceptual issue, demographic nonstationarity, refers to the departure of a population from a stationary state. Stationary populations are described as closed to migration, having zero growth rate, a constant age-specific fertility and mortality, and a stable age distribution (Wood et al. 1992; Wright and Yoder 2003). Unless a population is stationary, and most populations are not, estimated age-at-death distributions of the skeletal sample and summary statistics such as life expectancy and mean age at death will reflect measures of fertility rather than patterns of mortality. Small changes in fertility will have major effects on age-at-death distributions, while mortality has only minor effects (Wood et al. 1992).

The selective mortality problem addresses the fact that mortality is selective and that not all individuals are at equal risk of disease or death at a given age (Wood et al. 1992; Cohen et al. 1994). An archaeological skeletal sample represents only those individuals who died at a given age and will never represent all individuals in the population who were at risk of death at that age. This means that each age cohort will be highly selective for skeletal lesions that increase the risk of death in that age range. Therefore, the prevalence calculated for the skeletal sample will not directly reflect the true prevalence in the once living population but will, in fact be an overestimate (Wood et al. 1992).

The third issue, hidden heterogeneity in risks, articulates the observation that the population from which the skeletal sample is drawn is made up of an unpredictable and unknown mix of individuals who will vary in their susceptibility to disease and death, depending on multiple biological, environmental, and cultural factors (Wood et al., 1992; Roberts & Manchester, 2005). The clinical manifestations of some diseases will vary in severity, distribution, and infectivity due to differences in the immune status and susceptibility of each individual in a given population (Ridley and Jopling, 1966). At one extreme, the skeletal remains of an infected individual may show features pathognomonic of a disease whereas another individual with the same condition may show few observable skeletal changes. Factors that contribute to this variation in susceptibility, or frailty, are generally not identifiable and may confound the interpretation of skeletal disease prevalence (Wood et al. 1992; Roberts and Manchester 2005; Pinhasi and Bourbou 2008). Wood et al. (1992) also caution palaeopathologists against using the presence and/or absence of skeletal lesions in a sample as a direct indicator of health and disease in a population as this can also affect interpretations of disease prevalence in a once living population (Wood et al., 1992; Roberts and Manchester, 2005). To illustrate, a skeletal sample, or age cohort within that sample, showing a high prevalence of pathological lesions may not necessarily be reflective of an unhealthy population, but rather one in which there was low susceptibility and high disease survivability for long enough to result in bone changes. Alternatively, a low prevalence of skeletal lesions within a sample may indicate a highly susceptible group of individuals whose ability to resist disease was insufficient for survival long enough for bone lesions to develop, rather

than reflecting a generally healthy population (Wood et al. 1992; Pinhasi and Bourbou 2008).

2.5   Summary

Currently, debates regarding the interpretation of prevalence data in palaeoepidemiology have yet to be resolved. However, if palaeopathologists are conscious of the notion that different interpretations of prevalence data are possible, and that additional demographic, biological, cultural, and environmental data are needed to support prevalence data, reconstructions of health and disease in past populations can still be made (Wright and Yoder 2003; Pinhasi and Bourbou 2008). Recent research on improving age and sex estimation, palaeodemography, biodistance and ancient DNA, and palaeodiet may help palaeopathologists address some of the methodological and conceptual issues encountered in studies of heath and disease in past populations. In addition, improvements in the reliability and accuracy of differential diagnosis of skeletal lesions are also essential for providing a foundation for a palaeoepidemiological approach (Waldron 1994, 2007).

The purpose of this chapter was to introduce palaeoepidemiology and the role of epidemiological methods in palaeopathology. Approaches to the palaeoepidemiological study of past populations were briefly discussed along with the limitations that are encountered in any population based analysis of archaeological skeletal assemblages. The nature of an archaeological skeletal sample can make applying palaeoepidemiological methods challenging, but palaeopathologists should not be discouraged by the biases and limitations discussed here. As is evident in the history of the discipline, in order to better understand the complex relationships between the environment, culture, and disease in past populations, a paradigmatic shift towards a population-based approach in palaeopathology is necessary (Waldron 2007; Pinhasi and Bourbou 2008). Future research in palaeopathology must therefore recognize and acknowledge any potential biases inherent in skeletal samples while incorporating palaeodemographic and contextual biocultural factors into the process of differential disease diagnosis and the interpretation of disease prevalence estimates. In addition, methodological improvements and advances in technology, such as µCT, must also be

applied where available and appropriate to improve the palaeopathologist's ability to reliably diagnose, contextualize, and interpret disease in our human past.

Chapter 3

3 Bone Biology and the Biological Basis of Pathological Change

Although bone is one of the hardest substances in the body, it is a living, dynamic tissue that is constantly changing shape in response to different stresses that are placed upon it. Bones respond to physiological disruptions and disease just as other tissues and systems in the body. Bones atrophy if not used, they die if not supplied with blood and nutrients, they become infected, and they heal after trauma (Bloom and Fawcett 1994; Schwamm and Millward 1998). Pressure applied to bone leads to resorption, whereas tension applied leads to the development of new bone (Goodman & Armelagos, 1989; Gartner & Hiatt, 2007). The interpretation of these responses often reveals a great deal about the physiological stressors to which an individual was exposed during life. In palaeopathology, the first step in the process of differential diagnosis is to distinguish between what is a normal response and that which is abnormal (Ortner 2012). Although living bone is limited in its ability to react, the recognition of pathological changes from normal states may reveal the mechanisms of disease. Therefore, a basic understanding of bone biology and histology is vital to the interpretation of bone response and adaptation, as well as to differentiating between normal and abnormal bone responses to physiological stressors such as disease (Buikstra and Cook 1980). The following chapter explores the normal anatomy, histology, and physiology of bone, as well as the processes of abnormal bone changes in order to provide a baseline for the interpretation and differential diagnosis of abnormal pathological conditions that are encountered in the palaeopathological analysis of human skeletal remains (Ortner 2003; Brickley and Ives 2008).

3.1 Basic Bone Structure

Bone is a highly organized and specialized connective tissue made up of cells, vessels, and crystalized mineral compounds (Nather et al. 2005). The adult skeletal system is composed of both bone and cartilage and serves both structural and metabolic functions within the body. Structurally, bone both supports and protects the vital internal organs

and provides a space for the blood-forming marrow, while providing muscle attachment sites to allow for joint movement and locomotion (Weiner and Wagner 1998; Ortner 2003). Metabolically, bone functions as a reserve of calcium and phosphate needed for the maintenance of plasma homeostasis (Ortner 2003; Hadjidakis and Androulakis 2006).

The outermost solid layer of the skeleton is called cortical or compact bone and comprises 80% of the skeleton (Bartl and Frisch 2009). Cortical bone is dense, compact, has a slow metabolic rate, and provides mechanical strength and protection. This type of bone makes up the shafts of the long bones and forms a thin outer layer around the ends of the long bones as well as the irregular bones of the skeleton such as the inner and outer tables of the skull (Ortner 2003; Brickley and Ives 2008; Bartl and Frish 2009). Trabecular or cancellous bone represents 20% of the skeletal mass and is associated with the bone marrow (Nather et al. 2005; Bartl and Frish 2009). Trabecular bone is less dense, more elastic, and has a higher turnover rate than cortical bone. This type of bone consists of a complex honeycomb network of interconnecting plates of bone called trabeculae which provides a large surface area for the metabolic activities of bone as well as mechanical strength without adding excessive bone mass (Nather et al. 2005). In addition to these important functions, the haematopoietic bone marrow can also be found within the spaces of this trabecular network (Nather et al. 2005; Brickley and Ives 2008). The bone marrow tissue is the organ of haematopoiesis and fills the cylindrical cavities of the long bones and the spaces of trabecular bone. In mature long bones, the marrow is yellow and consists mainly of fat cells and some marrow cells. The marrow of flat and short bones, in contrast, is red and contains connective tissue, blood vessels and numerous marrow cells – myelocytes, erythroblasts, giant cells, and fat cells (Bloom and Fawcett 1994; Nather et al. 2005). The proportion of trabecular bone varies in different skeletal regions and is found mainly in the epiphyseal ends of the long bones, the bodies of the vertebrae, and the inner portions of the flat bones of the pelvis and skull (Ortner, 2003; Nather et al. 2005). It should be noted that in the case of the skull vault, these types of bone are given different anatomical designations. The cortical bone that makes up both the inner and outer tables is referred to as the internal and external lamina, respectively, and the trabecular network found between them is called the diplöe (Bloom & Fawcett 1994; Schultz 2001).

The outer and inner surfaces of bone are covered by layers of connective tissue and osteogenic cells. The outer surface of cortical bone is covered by the periosteal membrane or periosteum, a thin vascular membrane-like surface consisting of an outer layer of dense fibrous connective tissue and an inner layer containing flattened osteogenic cells. The interior surfaces and the central cavities of bone are lined with endosteum – a layer of osteogenic cells and a small amount of connective tissue (Schultz, 2001; Nather et al., 2005). The osteogenic cells found in both the periosteum and the endosteum provide a continuous supply of new bone-forming cells for the repair or growth of bone (Nather et al. 2005).

3.1.1   Histological Types of Bone Tissue

In the human skeleton, two types of bone can be differentiated in histological examinations: woven (primary, immature) bone and lamellar (secondary, mature) bone (Bloom and Fawcett 1994; Ortner 2003; Schultz 2001). When bone forms during fetal development, growth, bone repair, and in response to disease processes it will develop primarily as woven bone which is then later replaced by more organized lamellar bone. Woven bone is associated with rapid growth during the early growth phase, beginning with the fetus and continuing through early childhood. However, woven bone may be found in later adulthood in abnormal bone tissue, such as fracture callus, neoplasms, and beneath the periosteum in response to infection (Ortner 2003, 2012; Roberts and Manchester 2005). This type of bone tissue is porous, disorganized, and abundant in randomly scattered osteocytes and irregular bundles of collagen which do not show regular linear orientation (Schultz 2001; Roberts & Manchester 2005; Gartner & Hiatt, 2007). Lamellar bone is more mature, older, and the collagen fibres are organized, parallel with each other, and have a typical linear orientation. Lamellar bone is characterized by parallel or concentric bony lamellae and lacunae which are distinctly separated and dispersed at regular intervals. Canaliculi, the network of inter-communicating channels that facilitate the flow of nutrients, hormones, ions, and waste products to and from osteocytes, connect neighbouring lacunae and can be distinguished in mature bone – (Schultz, 2001; Gartner & Hiatt, 2007). Differentiating between these two types of bone can be essential for identifying mechanisms of pathological bone

change. Disease processes that were active at the time of death are identifiable by the presence of new woven bone, whereas healed lesions are characterized by lamellar bone and suggest that a disease process was overcome at the time of death (Roberts & Manchester, 2005).

3.1.2   Bone Matrix

The basic structural components of bone matrix include a specialized osseous cell system and extracellular matrix (Bartl and Frisch 2009). The extracellular matrix consists of a combination of organic matter, inorganic mineral material, and water (Gartner and Hiatt 2007; Brickley and Ives 2008; Turner-Walker 2008). First, approximately 90% of the organic matter is made up of Type I collagen fibres and 10% non-collagenous proteins such as osteocalcin, glycoprotein, and osteopontin. The role of non-collagenous proteins in bone matrix is not yet fully understood. However, the main non-collagenous protein produced is osteocalcin, which plays a role in the stabilization of the inorganic bone mineral within the matrix and the regulation of bone formation (Ducy et al. 1996; Hadjidakis and Androulakis 2006). The combination of collagen, non-collagenous proteins, and water provides living bones with elasticity and tensile strength (Turner-Walker 2008). Second, the inorganic mineral material of the extracellular matrix is made up of stiffening substances responsible for the rigidity and compressive strength of bone (Gartner and Hiatt 2007; Brickley and Ives 2008; Pinhasi and Mays 2008). Inorganic bone mineral is composed of crystals of calcium and phosphate, together known as hydroxyapatite $Ca_{10}(PO_4)_6(OH)_2$. These crystals are found in a complex arrangement both on the collagen fibres as well as interspersed between them. Together, this complex association of collagen with hydroxyapatite provides bone with its characteristic properties including: elasticity (flexibility), rigidity, and resistance to tension, bending, and compression (Nather et al. 2005; Pinhasi and Mays 2008).

3.1.3   Cellular Components of Bone

Living bone is a physiologically active tissue constantly adapting to mechanical stress, and repairing itself when damaged (Turner-Walker 2008). The cellular component of bone constitutes a specialized osseous system that is responsible for bone adaptation,

repair, and maintenance (Gartner and Hiatt 2007). The characteristic bone cells interspersed throughout the matrix are called osteoblasts and osteocytes. Osteoblasts, or bone forming cells, are derived from mesenchymal stem cells found in the bone marrow. These cells can be found embedded on the surface of bone in a sheet-like arrangement and are responsible for the production of the unmineralized organic component of bone. The main function of these cells is the synthesis of the bone matrix through the secretion of a substance called osteoid, which is rich in collagen fibers (Schultz, 2001; Gartner & Hiatt, 2007). Osteoblasts form bone by producing bone matrix through the increased secretion of osteoid, which is stimulated by the secretion of growth hormone by the pituitary, thyroid hormone (calcitonin), and the sex hormones. Once the bone formation process nears completion, approximately 15% of the mature osteoblasts become entrapped in the new bone matrix and differentiate into osteocytes, whereas those cells that remain on the bone surface become flattened bone lining cells (Hadjidakis and Androulakis 2006; Brickley and Ives, 2008).

Osteocytes are, essentially, modified osteoblasts that have become embedded within the bone matrix as a result of being surrounded by the matrix they produce. Although they are no longer involved in matrix formation, they communicate with other osteocytes, bone lining cells, and osteoblasts through a network of thread-like cytoplasmic extensions (Ortner 2003). Osteocytes reside in flat oval-shaped holes called lacunae and their cytoplasmic extensions pass through small channels in the bone matrix called canaliculi (Schultz 2001; Gartner & Hiatt 2007). This network of canaliculi also permits the transport of nutrients, waste products, and chemical signals between blood vessels and bone cells. There is growing evidence that osteocytes play an important role in bone response to mechanical stress, or loading. Increased mechanical loading forces extracellular fluid through the network of canaliculi. This increase in fluid is sensed by osteocytes which, in turn, send electro-chemical or hormonal signals to other cells involved in bone maintenance and remodeling, specifically osteoblasts and osteoclasts (Ortner 2003).

Osteoclasts differ significantly from osteoblasts in that they are not found embedded in the bone matrix, but are mobile, multinucleated, giant cells which play a major role in the

resorption and remodelling of bone tissue. These cells are derived from haematopoietic stem cells in bone marrow under the stimulation of vitamin D_3. They occupy shallow, sharply defined depressions called Howship's lacunae, which identify regions of bone resorption (Bloom & Fawcett, 1994; Schultz, 2001; Gartner & Hiatt, 2007). Osteoclasts adhere to bone surfaces at a determined site using its apical membrane, defining the extent of bone that is to be resorbed (Ortner 2003; Brickley and Ives 2008). Once adhered, the cell forms a ruffled border to increase the surface area in contact with the bone surface. Within the osteoclast, the enzyme carbonic anhydrase catalyzes the intracellular formation of carbonic acid from carbon dioxide and water. The carbonic acid dissociates into hydrogen and bicarbonate ions within the cell, and hydrogen ions are pumped into the sub-osteoclastic compartment at the ruffled border, reducing the pH of the microenvironment (Gartner and Hiatt 2007). As the environment becomes acidic, the inorganic component of the matrix is dissolved, exposing the organic matrix that is then digested by lysosomal enzymes, ultimately forming a resorption pit. Finally, following resorption, the osteoclast detaches from the resorbed surface, undergoes apoptosis and the exposed resorption pit then attracts osteoblasts that proceed to lay down new osteoid. This process is the basic underlying mechanism of bone growth, modelling, and remodelling (Ortner 2003; Gartner & Hiatt, 2007; Brickley and Ives 2008).

3.2   Mechanisms of Bone Growth

Osteogenesis, the physiological process that gives rise to the skeleton, involves the production of bone onto soft tissues. The basic pattern of skeletal structures is established during embryonic development in the form of either soft fibrous tissue or cartilage. It is also the manner in which bone is initially formed at the site of injury, such as during fracture healing (Hadjidakis and Androulakis 2006). The process of growth is not to be confused with the processes of bone modelling and remodelling discussed below. Although all three processes are active simultaneously, growth is the development and enlargement of skeletal tissues without changes to the shape of bone or the replacement of bone, which occur via modelling and remodelling, respectively (Burr and Martin 1989; Hadjidakis and Androulakis 2006).

Osteogenesis involves two main processes – intramembranous and endochondral ossification - depending on the mechanism of growth and the soft tissue base onto which bone forms (Ortner 2003; Hadjidakis and Androulakis 2006; Stout and Crowder 2012). Intramembranous ossification is the process by which flat bones such as parts of the skull, mandible, scapulae, and clavicles are formed (Ortner 2003; Brickley and Ives 2008). The human skull vault consists mainly of five flat bones, the paired frontals and parietals, and the unpaired occipital. The squamous portion of the paired temporal bones and the greater wings of the sphenoid bone contribute to the enclosure of the lateral walls. All of these bones are formed by intramembranous ossification within a layer of mesenchymal cells between the dermal mesenchyme and the meninges surrounding the brain (Morriss-Kay and Wikkie 2005). This process is regulated by genes which initiate the proliferation of mesenchymal cells within the embryonic connective tissue. These cells eventually differentiate into osteoblasts which then produce woven bone matrix using connective tissue membranes as a template (Ortner 2003). This woven bone is eventually replaced by more mature and organized lamellar bone (Brickley and Ives 2008).

Endochondral ossification involves the differentiation of mesenchymal cells into chondroblasts, or cartilage cells, which create the cartilage model forming the general shape of the bone (Brickley and Ives 2008). Following blood vessel invasion and the introduction of osteoprogenitor and haemopoietic cells into the model, bone matrix is laid down and the cartilage is subsequently replaced by bone. This process of osteogenesis is responsible for the formation of the long bones and vertebrae (Ortner 2003; Downey and Siegel 2006; Brickley and Ives 2008)

3.3   Bone Modelling

During growth, the cartilage model forms the general shape of the long bones. However, this process does not account for the need to increase the width of the bones (Stout and Crowder 2012). Bone modelling is principally responsible for the major morphological changes to bone size, shape, and position during growth, and functions to adapt bones to their changing biomechanical environment by adjusting the amount and distribution of bone tissue throughout the body (Burr and Martin 1989; Ortner 2003; Stout and Crowder 2012). In order to meet these changing mechanical demands, it is necessary to remove

bone tissue from some locations and deposit new bone in other locations (Baron 1999; Ortner 2003; Brickley and Ives 2008). The modelling process involves the formation of new bone without prior resorption, or the resorption of bone without the need for subsequent formation (Burr and Martin 1989; Ortner 2003). This is in opposition to remodelling which refers to only the replacement of bone via a complex process of bone resorption and simultaneous bone formation (Burr and Martin 1989; Brickley and Ives 2008). The processes of bone resorption and bone formation that are involved in both the modelling and remodelling processes are described below. Although modelling does not include the same sequence of events as remodelling, the individual processes of bone resorption and bone formation are inherently the same.

3.4   Bone Remodelling

Both during growth and once growth has ceased, bones retain their general architectural shape, mechanical integrity, and respond to physiological stress via small scale changes that occur through a continuous process of bone remodelling (Gartner and Hiatt 2007; Brickley and Ives 2008). Remodelling also plays an important role in maintaining plasma calcium homeostasis. The regulation of bone remodelling takes place at both the systemic and local levels. The major systemic regulators include parathyroid hormone, calcitrol, and other hormones such as the growth, thyroid, and sex hormones. A large number of cytokines and growth factors that affect bone cell functions have been identified as local regulators (Hadjidakis and Androulakis 2006).

The process of normal bone remodelling involves a delicate balance of these systemic and local regulators acting on bone resorption with simultaneous bone formation (McCarthy and Frassica, 1998; Gartner and Hiatt, 2007; Feng and McDonald 2011). Cellular communication between osteocytes, osteoclasts, and osteoblasts stimulates the remodelling process to enable bone to respond to various physiological demands, such as the replacement of old osseous tissues, adaptation to weight bearing and differential loading, repair of damaged bone at the macroscopic and microscopic levels, and pathological conditions (Burr 2002; Brickley and Ives 2008; Bartl and Frisch 2009). The normal remodelling cycle takes approximately three to six months to complete, but may vary between bone tissue types and under pathological conditions (Brickley and Ives

2008). The process of remodelling can be divided into three distinct phases: activation, resorption, and formation (Ortner 2003; Bartl and Frisch 2009; Stout and Crowder 2012).

The activation phase of bone remodelling begins on a resting bone surface (quiescent), which is covered in bone lining cells (Brickley and Ives 2008). Stress-induced microdamage, or bone stimulating factors including parathyroid hormone, calcitrol, or other marrow-derived hormonal signals, are detected and transmitted to the bone lining cells via the osteocytic canalicular network (Ortner 2003; Bartl and Frisch 2009; Feng and McDonald 2011). The bone lining cells respond to these activation stimuli by swelling and withdrawing from the surface of bone, exposing the thin membranous layer of unmineralized collagenous osteoid and preparing the bone surface for resorption. Bone lining cells that have been activated then send chemical signals to osteoclast precursors within the bone marrow which then enter the peripheral blood via local blood supply and are recruited to the site of activation (Ortner 2003; Parfitt 2003; Stout and Crowder 2012). Once arrived at the activation site, these osteoclast precursor cells fuse to form differentiated, multinucleated osteoclasts and the next phase of bone remodelling is initiated. This process of activation is inhibited by the sex hormone estrogen (Ortner 2003).

The action of mature osteoclasts is responsible for resorption through a combination of acid dissolution of bone mineral and the digestion of the organic matrix by lysosomic enzymes (Ortner 2003). Osteoclasts resorb a pre-determined amount of bone and the resorption of bone leads to the formation of lacunae or resorption pits (Brickley and Ives 2008). As older cells undergo cell death, new osteoclasts are continuously activated as the cells migrate over the resorbing surface. This process of resorption is prolonged by vitamin A and cytokines, and is inhibited by estrogen, calcitonin, and the cytokine osteoprotegrin (OPG) (Ortner 2003; Stout and Crowder 2012).

As the resorption phase ends and formation begins, a brief process known as reversal, which is often considered a separate phase in the overall remodelling process, takes place. During reversal, osteoclasts withdraw from the bone surface, undergo cell death, and are replaced by bone lining cells that line the resorption pit (Ortner 2003; Brickley and Ives

2008; Bartl and Frisch 2009). These cells smooth the interior of the resorption pits by digesting any remaining collagen debris left by the osteoclasts. A thin mineral-deficient layer of fibrillar collagen is then excreted by these cells prior to osteoblastic bone formation and acts to cement newly deposited bone to the old surface (Stout and Crowder 2012). This initial layer of collagen forms what is called the reversal, or cement, line and can be identified histologically from adjacent bone tissue (Ortner 2003). Once reversal is complete, osteoblast progenitors are attracted to the resorbed area by growth hormones, parathyroid hormone, calcitrol, and possibly by chemical signals released by dead osteoclasts (Ortner 2003; Gartner and Hiatt 2007; Bartl and Frisch 2009). During the early stages of the formation phase, osteoblasts begin to secrete successive layers of the organic matrix, osteoid, in order to fill in the resorption pit. The proper production of osteoid is dependent on a number of elements including vitamin C, which is essential for effective collagen formation (Ortner and Eriksen 1997; Brickley and Ives 2002; Sakamoto and Takano 2002; Gartner and Hiatt 2007). Once the osteoid layers reach a thickness of about 6 μm, the process of osteoid mineralization is initiated and osteoblasts begin to deposit calcium phosphate crystals within the organic matrix through a complex and incompletely understood process of inhibition and regulation of calcium and phosphate crystallization (Ortner 2003; Brickley and Ives 2008). This mineralization process is particularly affected by the presence of adequate amounts of vitamin D, without which osteoid will remain unmineralized (Brickley and Ives 2008). Following mineralization, osteoblasts enter a quiescence phase and undergo one of three changes: those cells that are trapped within the newly formed bone become osteocytes, other cells may die, while others will become flattened bone lining cells arranged across the new surface until the remodelling process is activated again (Ortner 2003; Stout and Crowder 2012).

3.5   The Role of Bone in Calcium Homeostasis

Simply stated, bone mineral homeostasis refers to the control of intra- and extra-cellular concentrations of two ions – calcium and phosphate – by a complex relationship between three hormones: parathyroid hormone, the pro-hormone vitamin D (1,25 dihydroxyvitamin D), and fibroblast growth factor 23 acting on bone, the intestines, and

the kidneys. Calcium and phosphate are two of the most important minerals for general cellular function during life and enter the blood via absorption through the intestines, are stored principally in bone, and are excreted by the kidneys. Approximately 98% of the calcium and 85% of the phosphorus in the human adult are stored in the inorganic mineralized component of bone. Plasma calcium and phosphate are necessary to maintain normal bone mineralization during remodelling, cellular communication, as well as to maintain the stability of soft tissue plasma membranes (Brickley and Ives 2008). Calcium in the extracellular fluid also influences many important physiological functions including aiding in blood clotting and initiating muscle contraction (Heaney 2002; Brickley and Ives 2008). In order to maintain homeostasis and regulate plasma calcium and phosphate levels in the body, the net absorption of calcium and phosphate by the intestines must be balanced with net excretion of these ions by the kidney (Heaney 2002).

The absorption of calcium and phosphorus by the gastrointestinal tract depends on adequate dietary intake. The efficiency with which absorption of these minerals occurs is regulated by the presence of vitamin D (Heaney 2002; Gartner and Hiatt 2007). Inactive vitamin D_3 is obtained from dietary intake and/or the exposure of skin to sunlight. This inactive form is converted in the liver and kidneys into active vitamin D that can then be used in the metabolism of calcium and phosphorus. If there is a deficiency in vitamin D, or if the intestines do not respond to this pro-hormone, the amount of dietary calcium and phosphate that can be absorbed by the gastrointestinal tract will decrease, thereby lowering the plasma concentrations of calcium and phosphorous (Lemann and Favus 1999; Gartner and Hiatt 2007; Brickley and Ives 2008).

Low plasma concentrations of calcium and phosphorus are detected by the parathyroid glands and will trigger the production of parathyroid hormone. Parathyroid hormone plays a complex role in maintaining calcium and phosphate homeostasis and in bone remodelling (Brickley and Ives 2008). The prolonged and continuous release of parathyroid hormone will result in decreased osteoblast proliferation, inhibiting bone formation, while simultaneously activating bone resorption (Gartner and Hiatt 2007). Parathyroid hormone activates bone resorption by inducing the release of a molecule produced by osteoblasts which in turn interacts with receptors on pre-osteoclasts and

osteoclasts. This interaction increases both osteoclast number and activity which then begin to resorb bone, thus liberating the inorganic bone mineral in an attempt to restore the balance of serum calcium and phosphorus levels (Stuart-Macadam 1989b; Roberts and Manchester 2005; Haduch et al. 2009).

Plasma calcium homeostasis therefore involves a complex network of communication between minerals and hormones that work to regulate healthy blood levels of calcium and phosphate (Ortner 2003; Brickley and Ives 2008). This regulation entails carefully balanced hormonal control of how much mineral content is absorbed into the body from the diet and how much is stored and released from bone (Brickley and Ives 2008). Disruptions to the normal absorption of minerals and/or to the release of specific hormones caused by dietary deficiencies or certain pathological conditions, respectively, can ultimately lead to abnormal variations in normal bone structure and morphology such as osteoporosis (Ortner 2003). As such, a basic knowledge of the processes of normal bone remodelling and mineral homeostasis provides the foundation for understanding the mechanisms of pathological bone change.

3.6   Mechanisms of Pathological Bone Change

Pathological bone lesions identifiable on the human skeleton are the direct result of aberrations of normal growth, development, and/or maintenance (Ragsdale and Lehmer 2012). Normal bone remodelling depends on the balanced coordination of bone formation with bone resorption to ensure that there is no net change in bone mass, strength, or quality after the completion of each remodelling cycle (Feng and McDonald 2011). Under certain physiological conditions, both systemic and local factors can abnormally alter bone mass, strength, and/or quality by creating conditions that stimulate or inhibit the normal differentiation, recruitment, function, and life span of osteoblasts and osteoclasts during the remodelling process (Ortner 2003; Waldron 2009; Feng and McDonald 2011). Since these cells are influenced by various signals from vitamins, minerals, and the endocrine, paracrine, circulatory, and immune systems, pathological disturbances to these systems ultimately affect bone structures by disrupting normal cell activities and the coordinated balance of bone formation and bone resorption (Burr and Martin 1989; Russel and Skjodt 1993; Waldron 2009; Ragsdale and Lehmer 2012). The

net effect of a disruption to this balance is that bone is either formed or lost, or both, in excess. The skeletal manifestations of various pathological conditions can therefore be placed into one or more of the following categories related to abnormal cell activity: 1) abnormal bone formation, 2) abnormal bone destruction or failure to form or replace bone, 3) abnormal bone size, and 4) abnormal bone shape (Ortner 2003, 2012). Abnormal changes to bone mass, strength, and/or quality can therefore be viewed as products of local or systemic errors in the process of remodelling with bone cells being the specific effectors of change (Burr and Martin 1989; Waldron 2009; Feng and McDonald 2011). The categories of abnormal cell activity of relevance to the current study include abnormal bone formation and abnormal bone destruction and are discussed in greater detail below.

3.6.1 Abnormal Bone Formation

Abnormal bone formation is the result of disruptions to the normal activity of osteoblasts during the remodelling process and is most often associated with chronic conditions (Steinbock 1976; Ortner 2003, 2012). The most common type of abnormal bone formed during the pathological process, and the first type of bone to appear during the initial stages of abnormal bone formation, is woven bone (Bloom and Fawcet 1994; Ortner 2012). This poorly organized tissue may gradually be remodelled into compact bone in the case of relatively chronic conditions where the individual survived for some time after the lesion was formed. Inflammatory processes and vascular conditions associated with inflammation are most often the stimuli for abnormal bone formation and the presence of woven bone (Ortner and Putschar 1981; Ortner 2012). Examples of this include conditions such as fracture callus formation, some cases of infection, rickets, and primary cancers of bone (Brickley and Ives 2008; Ortner 2012; Ragsdale and Lehmer 2012). Although many compact bone lesions are created as woven bone remodels through the process of healing, it should also be noted that the development of abnormal compact bone can also occur without an initial phase of woven bone (Ortner 2012). Benign tumours and trauma-induced activation of the periosteum can result in lumps of compact bone on the skull and long bones (e.g. ossified hematomas), respectively, and chronic

infectious diseases such as treponematosis can also stimulate compact bone formation (Hackett 1976; Cook and Powell 2012).

3.6.2   Abnormal Bone Destruction

The activity of osteoclasts is responsible for resorption and destruction of bone. Abnormal bone destruction occurs when normal existing bone is destroyed or fails to be formed or normally replaced during the processes of modelling and remodelling, respectively (Ortner 2003; Gartner and Hiatt 2007; Brickley and Ives 2008). The morphological features produced by destructive processes can range from fine porosity of cortical bone to large areas of poorly defined bone destruction. In addition, destructive lesions can appear as clearly demarcated singular or multi-focal areas of bone destruction, or there can be a generalized loss of bone throughout the skeleton, as is seen in osteopenia and osteoporosis (Resnick and Niwayama 1995; Ortner 2003, 2012).

On one end of the spectrum of destructive bone changes, small porotic lesions on the skeleton can be caused by several pathological conditions including rickets, scurvy, some types of anaemia, and during the initial stages of treponematosis. Lesions caused by these conditions are generally characterized by small holes, or pores, particularly in the skull and/or the growing ends of bone (Stuart-Macadam 1989; Schwamm and Millward 1995; Brickley et al. 2007; Cook and Powell 2012; Ortner 2012). Larger areas of bone destruction define the other end of the spectrum of abnormal bone destruction and are often the result of acute, aggressive conditions such as cancer, specifically the carcinomas. Acute, aggressively destructive conditions continue to destroy bone until the death of the individual and result in lesions where the margin – the border between the lesion and normal bone - is difficult to define (Anderson et al. 1992; Melikian 2006; Waldron 2009; Brothwell 2012). In some cases, however, large lesions can be caused by slower destructive processes such as multiple myeloma, a cancer that produces small lytic lesions that coalesce to form larger, rounded lesions. The margins of these types of lesions are more clearly defined as the bone has time to react to the destructive process (Steinbock 1976; Roberts and Manchester 2005; Ortner 2012). With abnormal destruction of bone, determining the pathogenesis of the lesion relies on careful attention

to lesion size, location, distribution, morphology, and margin (Lovell 2000; Roberts and Manchester 2005; Ortner 2003, 2012).

3.7 The Etiology of Porotic Hyperostosis

With some pathological conditions, bone changes may involve abnormal bone formation, abnormal bone destruction, or a combination of both depending on the disease process responsible. Lesions that result from a combination of bone changes will reflect both types of abnormal cell activity (Ortner 2003, 2012). Abnormal morphological changes to the cranial vault and orbital roofs, referred to as porotic hyperostosis, are examples of such lesions (Stuart Macadam 1987; Lallo et al. 1977; Ortner 2003). Orbital lesions are commonly differentiated from vault lesions using the term "cribra orbitalia" in the palaeopathological literature (e.g. Welcker 1885; Nathan and Haas 1966; Stuart-Macadam 1989; Exner et al. 2004). However, since lesions of the cranial vault and orbital roofs are morphologically identical, lesions will not be terminologically differentiated in the current study and "porotic hyperostosis" will encompass all porotic lesions noted on the cranium. Porotic hyperostosis can be due to various pathological conditions including the various anaemias, scurvy, rickets, and several non-specific inflammatory processes (Fairgrieve and Molto 2000; Schultz 2001; Ortner 2003; Wapler et al. 2004; Walker et al. 2009). Therefore, these morphological features are not uniquely characteristic of a single but of several pathological conditions. The current research explores the application and potential of recent technological advances – micro-CT - to the differential diagnosis of porotic hyperostosis and, thus, a detailed understanding of the potential contributing etiological factors and the pathogenesis of these lesions is provided here.

Porotic hyperostosis can be identified macroscopically as areas of pitting and porosity on the external surface of the cranial vault and/or orbital roofs (Stuart-Macadam 1987; Walker et al. 2009). Since, at the macroscopic level, a number of pathological conditions produce similar or almost the same morphological changes in the skull, it is important to understand the mechanisms of change that occur at the level of bone microstructure for each condition. Schultz (2001, 2012) has demonstrated that by using microscopic analyses, a pattern of features represented by the architectural elements of bone may be

identified and possibly associated with a particular pathological condition. Therefore, microscopic methods and techniques may be valuable for diagnosing diseases which affect gross morphology in a similar way, yet may differentially affect the microstructure of the cortical and cancellous bone of the skull. For illustrations depicting the microstructural level differences in trabecular morphology between each of the following disease processes, see Schultz (2001).

3.7.1 The Anaemias

Anaemia is a general term that is used to describe various deficiencies or abnormalities of either red blood cells or the haemoglobin they contain, affecting the ability of the circulatory system to normally transport and exchange oxygen (Caffey 1937; Ortner 2003; Sullivan 2005; Walker et al. 2009). In a healthy state of homeostasis, the rate of bone marrow red blood cell production is equal to the rate at which these cells are destroyed (Stuart-Macadam 1985, 1989; Fandrey 2004; Sullivan 2005). In cases of anaemia, there are three principal causes for the disruption of this homeostatic state, none of which are mutually exclusive: blood loss, impaired erythropoiesis (process of red blood cell production), and increased hemolysis (premature red blood cell destruction (Sullivan 2005; Walker et al. 2009). The anaemias fall into two categories: acquired and genetic. Blood loss, lymphocytic cancers, gastrointestinal malabsorption of nutrients, and nutritional deficiencies, especially deficiencies in folic acid and iron are the most common causes of acquired anaemia. Two genetic conditions, sickle cell anaemia and thalassemia, which appear in high frequencies in malarial areas of the world, are the main causes of genetic anaemia (Salvadei et al. 2001; Fandrey 2004; Roberts and Manchester 2005; Walker et al. 2009).

3.7.1.1 Acquired Anaemia: Iron and Folic Acid

The nutrients required for maintaining red blood cell homeostasis include essential amino acids, iron, and vitamins such as A, B_{12}, B_6, and folic acid (Martini and Ober 2001; Walker et al. 2009). When the intake and/or absorption of iron, or other essential nutrients such as folic acid are insufficient, red blood cell production is impaired and acquired anaemia ensues. Iron, a key component in the development of hemoglobin, is

necessary for normal red blood cell production (Sullivan 2005; Walker et al. 2009). The main function of hemoglobin in red blood cell production, and thus the function of iron, is to transport oxygen throughout the body (Roberts and Manchester 1995; Sullivan 2005). Deficiencies in iron can result from a number of conditions, including excessive blood loss from parasitism, inadequate intestinal absorption through various forms of diarrhea-inducing infection, the high iron demands of the body during growth and reproduction, or the prolonged consumption of iron-poor foods (Sullivan 2005; Walker et al. 2009). When a chronic deficiency in the intake or absorption of iron depletes circulating iron levels both the synthesis of hemoglobin and the production of mature erythrocytes with adequate levels of hemoglobin are greatly affected. Iron-deficient red blood cells that are produced are abnormally small and pale due to a lack of sufficient hemoglobin, are inefficient at transporting oxygen to dependent tissues, and are shorter lived than normal red blood cells (Roberts and Manchester 2005; Sullivan 2005). A chronic reduction in red blood cell production and the hemoglobin that they contain then contributes to the development of iron-deficiency anaemia (Kempe et al. 2006; Walker et al. 2009).

In addition to iron, normal erythropoiesis also requires that the body has an adequate supply of both vitamin B_{12} (cobalamine) and folic acid (Fairgrieve and Molto 2000; Sullivan 2005; Walker 2009). Megaloblastic anaemia, another form of acquired anaemia, is most commonly caused by chronic dietary deficiencies and malabsorption of vitamin B_{12} and/or folic acid (Chanarin et al. 1985; Beck 1991; Fairgrieve and Molto 2000; Koury et al. 2000; Walker et al. 2009). Inadequate dietary intake and inadequate intestinal absorption due to intestinal parasites and/or chronic diarrheal illnesses are the most common causes of this form of anaemia (Fairgrieve and Molto 2000; Chanarin et al. 1985; Sullivan 2005). A deficiency in these nutrients impairs the synthesis of the amino acid thymine, an essential component of DNA, and the normal synthesis of RNA (Passmore and Eastwood 1986; Davenport 1996). This defective DNA synthesis causes the bone marrow to produce enlarged abnormal red blood cells called megaloblasts (Passmore and Eastwood 1986; Chanarin et al 1989; Koury et al. 2000). These megaloblasts are oversized but internally underdeveloped red blood cells that cannot efficiently or adequately perform their main function of oxygen transport (Sullivan 2005;

Walker et al. 2009). Red blood cell production and life expectancy are reduced due to this abnormality and the body enters an anaemic state (Davenport 1996; Sullivan 2005). Although megaloblastic anaemia is etiologically distinct from iron-deficiency anaemia, the effects of these two forms of acquired anaemia on the skeletal system are the same.

3.7.1.2   Genetic Anaemias

The genetic anaemias are the result of mutations that are responsible for hereditary anaemic conditions caused by increased hemolysis and/or abnormal hemoglobin synthesis (Ortner 2003; Walker et al. 2009). The genes that cause these forms of anaemia are usually dominant and typically result in death in infancy or early childhood when they occur in their homozygous expressions (Angel 1966; Ortner 2003). However, the heterozygous expression of these genes can result in improved resistance to the malarial parasite (Steinbock 1976; Tayles 1996; Waldron 2009). This resistance is mainly due to the decreased life span of red blood cells in heterozygous individuals which prevent the parasites from establishing infection in the circulatory system. Both sickle cell anaemia and thalassemia are highly associated with geographical areas where malaria is prevalent (Angel 1966; Steinbock 1976; Ortner 2003; Waldron 2009).

Sickle cell anaemia is caused by an abnormal hemoglobin gene, hemoglobin S, and is present in the homozygous condition (SS) (Steinbock 1976; Resnick 1995; Ortner 2003). Individuals with one sickle cell gene and one normal hemoglobin A gene (SA) have the sickle cell trait, but do not exhibit the symptoms of sickle cell anaemia. The abnormality in the hemoglobin occurs when the amino acid, valine, is substituted for glutamic acid (Angel 1967; Resnick 1995; Tayles 1996; Ortner 2003). In homozygous individuals, hypoxemic stress occurs when more oxygen is needed by the bodily tissues than is available in the bloodstream. In this low oxygen environment, the abnormal hemoglobin S crystallizes within the cell and erythrocytes assume an abnormal sickle shape. These sickled red blood cells are significantly more fragile than normal red blood cells, have a reduced life span, and are less effective at oxygen transport (Serjeant et al. 1969; Resnick 1995; Ortner 2003). In order to compensate for premature hemolysis and decreased oxygen exchange, there is an increased demand for red blood cell production (Serjeant et al. 1969; Resnick 1995). In this situation, red blood cell destruction exceeds production

and the body is constantly left in an anaemic state. Heterozygous individuals (SA) rarely exhibit symptoms and only extreme hypoxemic stress can produce hemolysis (Ortner 2003; Waldron 2009).

Thalassemia is a general term applied to a number of pathological conditions in which there is a decrease in the rate of the synthesis of one or more hemoglobin polypeptide chains (Greenfield 1986). This condition differs from sickle cell anaemia wherein the abnormality occurs in the hemoglobin itself rather than in its synthesis. Genetically, thalassemia results when one of several mutated or deleted genes leads to an amino acid substitution in either the alpha or beta chain of the hemoglobin molecule (Steinbock 1976; Greenfield 1986; Resnick 1995; Ortner 2003). The homozygous expression of thalassemia is called thalassemia major and the heterozygous expression is thalassemia minor. In thalassemia major, the mortality rate in infancy and childhood is high as hemoglobin synthesis is severely impaired and the body is left in a constant hypoxemic state. Thalassemia minor occurs with little to no anaemic symptoms, no skeletal involvement, and presumably has a selective advantage against malaria given its geographical distribution (Ortner and Putschar 1985; Ortner 2003; Lagia et al. 2007). The bone lesions in both thalassemia and sickle cell anaemia are entirely due to increased demands for hyperplastic erythropoeitic marrow and cannot be distinguished from one another (Ortner 2003).

3.7.1.3   Bone Changes in Anaemia

Chronic anaemic stress results in a significant drop in haemoglobin levels and, as a result, the body becomes oxygen starved. This hypoxic state triggers the body to mount a physiological response that involves the release of erythropoietin, a hormone produced by the kidneys, that accelerates red blood cell production and maturation (Halvorsen and Bechensteen 2002; Fandrey 2004; Walker et al. 2009). If this hormonal response fails to reinstate red blood cell homeostasis, the body resorts to stimulating the expansion of the haemopoietic bone marrow in an attempt to increase the production of red blood cells, a process known as marrow hyperplasia (Ross and Logan 1969; Stuart-Macadam 1985; Fandrey 2004; Walker et al. 2009). The pressure on the bone surrounding the expanding marrow space initiates osteoblastic and osteoclastic activity and leads to several changes

including the expansion of the marrow cavity and, in more chronic cases, openings from the marrow cavity to the external surface of bone (Carli-Thiele and Schultz 1997; Wapler et al. 2004). These bony changes are classified as non-specific as they will occur with the same morphologic expression regardless of the specific form of anaemia.

During growth and development, the distribution of red blood cell production sites within the body changes (Halvorsen and Bechensteen 2002; Loevener et al. 2002; Walker et al. 2009). During childhood and adolescence, the diplöe of the cranial vault and medullary cavities of the long bones are the primary sites for erythropoiesis, which explains why skeletal changes associated with anaemia are most severe in the skull. In adults, erythropoiesis shifts from the cranial vault to the vertebrae, sternum, and costal regions of the axial skeleton as a result of marrow conversion (Loevner et al. 2002; Walker et al. 2009). Marrow conversion is a normal process in which yellow fatty marrow gradually replaces red marrow. By 25 years of age, most of the red marrow has undergone conversion. Based on the process of marrow conversion, it can be argued that porotic hyperostosis is reflective of a childhood, or developmental, anaemia (Stuart-Macadam 1985; Kent 1986; Stuart-Macadam 1992). This argument is further supported by the observation that active porotic lesions are almost entirely restricted to the skeletons of children and adolescents in archaeological skeletal collections, whereas healed lesions are typical in adults (Stuart-Macadam 1985; Walker et al. 2009). It is germane to note that, on the infrequent occasion, when active lesions are observed in adults, this may represent reconversions of yellow marrow to red marrow when there is prolonged, chronic anaemic stress (Loevner et al. 2002).

Cranial porotic hyperostosis tends to be situated on the parietal bones close to the lambdoid suture, the parietal bosses, and, less frequently, on the occipital bone and endocranial surfaces of the skull. Orbital porotic hyperostosis is, as the name suggests, located on the orbital roof. These phenomena are characterized by several gross morphological features. The bone changes that occur in anaemia involve a pathological process of bone formation and bone destruction (Ortner 2003; Waldron 2009). Expansion of the diplöe occurs at the expense of the external lamina, which is gradually resorbed (bone destruction). This resorption creates porosity because the cancellous bone

(diplöe) becomes visible as the external lamina disappears, giving the lesions their characteristic morphological "spongy" appearance. In addition, the enlargement of the cancellous bone by radial growth of the bone trabeculae (bone formation) causes thickening of the affected region and also contributes to the reduction of the external lamina. In extreme cases of anaemia, the diploë expands far beyond the original external surface to create a distinctive "hair-on-end" effect that is readily observed in radiographs and histological thin sections (Stuart-Macadam 1989a; Sullivan 2005; Schultz 2001; Walker et al. 2009). Many anaemias, including sickle cell, thalassemia, and megaloblastic anaemia, are reflected by changes in skeletal mass and, specifically, decreased bone mass relative to bone volume. Radiographs reveal that this decrease in bone mass is related to a loss of trabecular bone as well as a thinning of wider plate-like trabecular structures (Garn 1970). During the early stages of this process, porosities of the cranial vault are very slight and can easily be confused with porosities caused by other pathological conditions. This is because, at this stage, only the external lamina becomes porotic, and the growth and expansion of the diplöe, which is diagnostic of marrow expansion, cannot yet be observed through macroscopic analysis (Schultz 2001).

The manifestation of bone changes in the thalassemias follows the same general pattern as for any other anaemia. However, in the case of thalassemia major, the bone changes are most severe and the skeleton as a whole is affected in various ways. The axial skeleton and the long bones are all affected by marrow hyperplasia (Moseley 1974; Steinbock 1976; Ortner 2003). The most severe changes occur in the skull. The earliest changes occur in the frontal bone and other characteristic changes occur within the maxillary, sphenoidal, and temporal bones. Expansion of the marrow in these bones inhibits, delays, and, in some cases, completely prevents the normal development of the paranasal sinuses and mastoid air cells (Greenfield 1986; Steinbock 1976; Ortner 2003). The external dimensions of the facial bones, particularly the maxilla and zygomatic bones, are also enlarged by the process of marrow hyperplasia resulting in prominent cheek bones and protrusion of the incisors (Moseley 1974; Greenfield 1986; Ortner 2003). Changes in the paranasal sinuses, mastoids and facial bones are seldom found in sickle cell or the acquired anaemias (Steinbock 1976).

The long bones of the appendicular skeleton show marked expansion of the marrow cavity accompanied by thinning of the cortex and an overall loss of the normal bone contour (Steinbock 1976; Greenfield 1986; Ortner 2003). In children, the metacarpals, metatarsals, and phalanges show enlargement and thin cortices. Delayed epiphyseal closure may also be observed in this disease. In some cases the long bones may be affected by premature fusion of the epiphyses resulting in skeletal dwarfism and abnormal angulation of the bones, particularly of the humerus, which becomes evident after the age of 8-10 years (Greenfield 1986; Ortner 2003). In addition, the vertebral column and pelvic bones of the axial skeleton share the same basic changes associated with marrow hyperplasia; altered trabeculae, thinned cortices, and an overall loss of density (Greenfield 1986; Ortner 2003). Overall, the cranial changes of thalassemia generally resemble those in sickle cell anaemia, but the extensive lesions of the rest of the skeleton do not. The bone changes are also less severe in sickle cell and iron-deficiency anaemia and changes to the facial bones are not found (Greenfield 1986; Ortner 2003). These differences in bone changes are important to note when making a differential diagnosis.

Although porotic lesions due to anaemic conditions are very similar to other diseases in their macroscopic morphology, the process of marrow hyperplasia causes several characteristic architectural changes that can be identified using microscopic techniques (Schultz 2001). Histological thin ground sections examined microscopically show that in the early stages of pathological change, the external lamina begins to be resorbed and shows only few slightly enlarged spaces of the cancellous bone which open onto the surface of the external lamina. This stage corresponds with the macroscopic appearance of slight porosity (Stuart-Macadam 1989; Schultz 2001). As the anaemic condition becomes increasingly severe, the external lamina appears to disintegrate, either partially or completely, as the diplöe expands and the trabeculae in the affected areas are thinned and take on a parallel orientation relative to the original external surface (Schultz 2001, 2012). The growth and parallel orientation of the trabeculae produce the typical "hair-on-end" phenomenon characteristic of anaemic changes to bone (Steinbock 1976). Macroscopically, this corresponds with a thickened and coarsely porotic skull with confluent apertures, or short clefts, which sometimes gives the affected region a star-like

appearance (Nathan & Haas 1966; Schultz 2001). Thus, the classic features of hypertrophy of the bone marrow that distinguish cases of anaemia from other pathological conditions include a reduced or completely destroyed external lamina, enlargement of the spaces of cancellous bone, thickening of the skull vault and/or the orbital roof, and longitudinally enlarged, thinned, and parallel-oriented bone trabeculae (Stuart-Macadam 1989; Schultz 2001). It is important to note that although different pathological conditions may be distinguished from anaemia by bone histology, the various forms of acquired and genetic anaemias cause similar changes in bone, particularly in the cranial bones and the specific type of anaemia responsible for porotic cranial lesions can often not be determined (Wapler et al. 2004; Sullivan 2005).

3.7.2   Scurvy

Scurvy is a pathological condition that develops due to an inadequate amount, or complete absence of vitamin C (ascorbic acid) in the diet. It is a condition that is almost unique to the human species as most animals that require vitamin C are capable of synthesizing their own. Humans, however, cannot produce the enzyme necessary to synthesize vitamin C due to a gene mutation that prevents the final step in vitamin C biosynthesis (Stuart-Macadam 1989; Ortner and Eriksen 1997; Ortner et al. 1999). Vitamin C protects, regulates, and facilitates a number of biological processes in the human body. Its most important function is in the formation of connective tissues, particularly collagen, which is the main protein component of bone (Ortner & Eriksen 1997; Gartner & Hiatt 2007). Collagen is the basic structure of osteoid, thus a deficiency in vitamin C will lead to a reduction in the formation of osteoid, resulting in defective connective tissue as well as a defective cement substance which binds the endothelial layer in blood vessels (Jaffe 1972; Stuart-Macadam 1989; Schwamm and Millward 1995; Waldron 2009). A defect in this cement material causes increased susceptibility to blood vessel rupture and subsequent hemorrhage that can result from trauma or even normal movement or muscle activity such as chewing or eye motion (Ortner and Eriksen 1997).

3.7.2.1 Bone Changes in Scurvy

Both adults and children are susceptible to developing bone lesions during a scorbutic episode. In infants and small children, rapid growth is accompanied by rapid bone remodelling and the growth of body tissues, including blood vessels. Defective connective tissues and blood vessels that are formed during bouts of scurvy mean that scorbutic infants and children are particularly susceptible to hemorrhage and the subsequent bone response that can occur. The rapid process of growth and remodelling also creates conditions in which the periosteum is less tightly attached to the underlying cortical bone. Hemorrhaging that occurs between the periosteum and bone may lift the periosteum away from bone, stimulating bone formation (Ortner and Eriksen 1997; Roberts and Manchester 2005).

The morphological features central to scorbutic lesions of bone are areas of abnormal porosity of the cortical bone in the major long bones of the lower limb and the scapula (Jaffe 1972; Ortner and Putschar 1981; Ortner and Eriksen 1997). Porous lesions associated with scurvy have also been noted on the skull vault and the orbital roof and may also be responsible for the gross morphological features of porotic hyperostosis (Ortner et al. 1999; Walker et al. 2009). Chronic bleeding, caused by minor trauma to defective blood vessels, evokes a vascular inflammatory response that includes increased blood vessel formation at the affected site and an activation of the periosteum, which rapidly forms new bone. The new blood vessels formed often penetrate the underlying cortex, creating small holes which result in bone porosity. In addition, rapidly formed woven bone is laid down on the surface of the original bone and is due to the stimulation of the periosteum due to increased vascularity and inflammation associated with the removal of blood from the affected area (Ortner et al. 1999, 2001; Schultz 2001).

Porous lesions of the greater wing of the sphenoid and adjacent bones of the cranial vault appear to be the most common expression of scurvy (Ortner and Eriksen 1997; Ortner et al. 1997). These lesions are related to the association of this location with trauma to the branches of the maxillary artery that supply the temporalis muscle, a major muscle of mastication (Stuart-Macadam 1989; Ortner et al. 2001). These porous lesions are also associated with manifestations of chronic bleeding and inflammation at other sites in the

skull including the roof and lateral margins of the orbit, the posterior maxilla, the interior surface of the zygomatic bone, the infraorbital foramen, and the palate (Ortner and Eriksen 1997). Although a diagnosis of anaemia for the porous lesions of the greater wing of the sphenoid makes little biological sense, porous lesions on other aspects of the skull, particularly the orbit, do resemble the abnormal bone changes seen in anaemic conditions and inflammatory processes caused by infection (Ortner and Eriksen 1997; Schultz 2001; Walker et al. 2009). It is possible that early expressions of the lesions could overlap to the extent that differentiating these pathological conditions based on macroscopic observations would be difficult or impossible (Ortner and Eriksen 1997; Schultz 2001, 2012). Thus, a better understanding of the microscopic changes associated with scurvy will be valuable for differential diagnosis.

Microscopic changes due to hemorrhagic processes such as scurvy are restricted to the external surface of the skull vault. Histological thin sections show a thin, slip-like layer of newly built bone on the surface of the external lamina. This layer of newly built bone can range from a thin layer to several layers consisting of short, bulky bone trabeculae with extensive bridging. Both the external lamina and the diploë remain intact, maintain a normal structure, and there are no changes observed within the marrow cavity (Schwamm and Millward 1995; Schultz 2001). Therefore, the typical "hair-on-end" phenomenon and resorbed external lamina observed with marrow expansion are not observed in cases of scurvy (Schultz 2001). These architectural changes demonstrate that the bony response due to haemorrhagic processes is considerably different from that caused by anaemic conditions. An important distinction is whether or not porotic hyperostosis is the result of marrow hyperplasia or a superficial enlargement on the surface of the skull vault and/or orbits.

3.7.3   Rickets

Chronic rickets is also able to produce porotic hyperostosis (Schultz 2001, 2012; Wapler et al. 2004). Rickets is characterized by the failure of bone mineralization in children during growth and development due to a deficiency in vitamin D (Stuart-Macadam 1989; Schwamm and Millward 1995; Brickley et al. 2007). Vitamin D is essential for the adequate mineralization of osteoid in newly formed bone. The most common cause of

vitamin D deficiency is the combination of a lack of UV radiation (sunlight), which is responsible for vitamin D production in the skin, and a lack of appropriate vitamin D content in the diet (Berry et al. 2002; Holick 2006; Waldron 2009). Dietary deficiencies lead to the malabsorption of calcium and phosphorus in the intestines. This diminished absorption and transport of calcium and phosphorus in the body triggers the parathyroid glands to increase the production of parathormone. Parathormone activates osteoclasts to destroy bone, thus liberating bone mineral in an attempt to restore the balance of serum calcium and phosphorus levels, creating a negative feedback (Stuart-Macadam 1989b; Roberts & Manchester 2005; Haduch et al. 2009). Bone formation is increased as a response to the destroyed bone; however, the osteoid produced by the osteoblasts to replace the bone is not properly mineralized due to insufficient vitamin D (Stuart-Macadam 1989; Schwamm and Millward 1995; Holick 2006; Haduch et al. 2009). In adults, bone removed during normal remodelling is replaced by the unmineralized osteoid and, as a result, the organic matrix remains soft, eventually resulting in a considerable weakening of the skeleton (Stuart-Macadam 1989b; Brickley et al. 2007). When these changes are observed in adults, the condition is referred to as osteomalacia (Brickley et al. 2007).

3.7.3.1 Bone Changes in Rickets

In children, the morphological features of rickets can be observed in areas of the skeleton that are active in growth and development. Characteristic rachitic changes to the infracranial skeleton include swelling of long bone metaphyses and costal rib ends, flaring of epiphyses, and bending of the long bones (Brickley et al. 2007; Waldron 2009). Once a child begins to stand and walk the pressure of gravity on the lower limbs results in inward or outward tibial and femoral bowing due to the softening of the skeleton. This bowing of the lower limbs is an important diagnostic feature in the skeletal presentation of rickets (Stuart-Macadam 1989; Brickley et al. 2007; Waldron 2009).

In the flat bones of the skull, softening of the occipital area, enlarged sutures and fontanelles, and occipital or parietal flattening can be observed (Holick 2006). Porotic hyperostosis can develop as a result of the excessive resorption of bone which causes the cortex to become porous, the cancellous bone to become weakened and altered, and the

skull vault to be susceptible to deformity under even the slightest pressure - a condition known as craniotabes (Schwamm and Millward 1995; Holick 2006; Brickley et al. 2007). This porosity often resembles lesions associated with anaemia and scurvy (Schultz 2001, 2012).

The results of microscopic investigation may exclude both anaemia and scurvy as contributors to porotic hyperostosis in individuals affected by rickets (Schultz 2001). Investigations of the histological appearance of poorly mineralized bone identify large amounts of rapidly formed bone and enlarged lacunae with imperfectly mineralized walls. Incomplete and near-transparent regions in histological thin sections identify areas of bone weakening (Brickley et al. 2007). In the skull, the external lamina no longer appears as a continuous compact structure and is built up of layers of squamous plates of defective new bone, taking on a splintered appearance. This splintering effect is caused by the failure of new layers of bone to completely mineralize, leaving small fragments of new bone left unconnected to pre-existing bone (Schultz 2001; Brickley et al. 2007). The internal lamina retains its basic form, but is also splintered in affected areas. In addition, the diploic trabeculae are irregularly shaped within the marrow cavity. Unlike anaemia, there is no evidence of marrow hyperplasia or cranial thickening. Evidence of new bone formation due to subperiosteal hemorrhaging is also absent. In cases of rickets, or other such metabolic diseases, the presence of characteristic splintering and unmineralized osteoid rule out both anaemic and hemorrhagic conditions as potential etiologies of porotic hyperostosis (Schultz 2001).

3.7.4   Inflammatory Processes

Inflammation of bone is expressed in many ways and is frequently associated with infection of one or all of the different layers of bone (Ortner 2003; Roberts and Manchester 2005). Inflammatory processes can be divided into three categories based on the bone layer involved: periostitis, osteitis, and ostemyelitis. These categories are applied to infection of the periosteum, cortex, and medullary cavity, respectively. It is possible for these phenomena to lead to one another, and all three may be present together (Sandison and Tapp 1998; Roberts and Manchester 2005). Inflammation leading to periosteal reaction is most often caused by local or systemic infections that can be

brought about by various types of bacterial agents such as staphylococci, streptococci, and pneumococci (Roberts and Manchester 2005; Waldron 2009).

3.7.4.1   Bone Changes in Inflammatory Processes

Periostitis represents a basic inflammatory response and can be defined as peripheral bone inflammation. It can be caused by local infection, such as a break in the skin, or from a systemic infection originating from a focus elsewhere in the body that is spread via the bloodstream (Ortner 2003). Bone responds to inflammation caused by infection or injury by stimulating osteoblasts lining the periosteum to form new bone. This inflammatory process manifests morphologically as fine porosity, longitudinal striation, and, in the later stages, osseous plaques of new bone on the original cortical surface (Larsen 1997; Roberts and Manchester 2005).

Osteitis is an inflammatory process that primarily affects the internal vascular and medullary surfaces of bone (Ortner 2003; Roberts and Manchester 2005; Waldron 2009). Although this is also considered an inflammatory process of bone, osteitis does not present as porosity on periosteal surfaces and, therefore, does not contribute to the morphological appearance of porotic hyperostosis. For these reasons, osteitis will not be considered in detail.

Osteomyelitis is a term that can be used to encompass any form of infection of bone and bone marrow which results in an inflammatory bone response. The infection of bone can result from one of three sources: haemotogenous spread (bloodstream), direct spread from an infection of the overlying skin or adjacent organs, or by direct implantation by penetrating injuries, such as a compound fracture (Waldron 2009). Osteomyelitis is a pathological process involving bone destruction, pus formation, and simultaneous bone repair (Roberts and Manchester 2005; Waldron 2009). Bone destruction is indicated by porosity and irregularity of the bone surface. In addition, the production of pus within the bone interior increases the volume of material within the medullary cavity and raises the intra-medullary pressure. This pressure may be relieved through the destruction of cancellous bone and the gradual penetration of the compact bone through which pus is discharged into surrounding body tissues. If this condition remains untreated, large

passages called cloacae will form between the bone surface and the internal cavity to allow for the release of pus (Roberts and Manchester 2005; Waldron 2009). The bone repairing process in osteomyelitis is identified by the development of porous, plaque-like new bone on the cortical surface, much like that observed with periostitis (Larsen 1997; Roberts & Manchester 2005).

Inflammatory processes which affect different areas of the head can lead to both vault and orbital bone involvement. Infections such as sinusitis, conjunctivitis, tooth abscesses and other oral infections, nasopharyngeal infections, and pus forming skin inflammations can be transmitted into the periosteum and potentially deeper layers of bone, leading to periostitis and/or osteomyelitis. It is possible that a considerable proportion of the prevalence of porotic hyperostosis in archaeological collections may be caused by inflammatory processes as both periostitis and osteomyelitis involve the development of porous lesions on the skull vault and orbital roof (Wapler et al. 2004). Several researchers have noted that the gross morphological appearance of porotic lesions caused by inflammatory processes is often mistaken for the initial stages of marrow hyperplasia caused by anaemia (e.g. Schultz 2001; Wapler et al. 2004; Walker et al. 2009).

At the histological level, non-specific inflammatory processes always affect the bone surface and, in cases of osteomyelitis, the deeper structures of bone (i.e. medullary cavity). The newly built bone deposited on the original cortical surface appears as a layer of relatively long and thin bony trabeculae which are irregularly oriented and branch frequently (bone apposition). In the skull, periostitis is characterized by bone apposition on the external lamina. In cases of osteomyelitis, the skull vault is severely destroyed and bone apposition is apparent on both the external and internal lamina. In addition, the diplöe is either partially or completely resorbed by osteoclastic response to inflammation and most of the diploic trabeculae are damaged or completely resorbed (Schultz 2001). There is no evidence of marrow expansion or unmineralized bone deposition which are suggestive of anaemia and metabolic disorders, respectively. In addition, the destruction of the diplöic trabeculae observed with inflammatory processes also rules out hemorrhagic processes such as scurvy as differential diagnoses for porotic hyperostosis as scorbutic bone changes do not involve the diplöic space.

3.8 Summary

Bone is a metabolically active organ that undergoes continuous changes throughout an individual's lifespan. These changes can be either adaptive or maladaptive depending on the ability of skeletal tissues to normally respond to physiological and mechanical stressors (Burr and Martin 1989; Hadjidakis and Androulakis 2006). The purpose of this chapter was to provide a basic review of bone biology and the mechanisms of abnormal bone change in order to provide the necessary background for the understanding of the process of differential diagnosis in palaeopathology. This chapter also provided a review of the multiple etiological possibilities for cranial and orbital porotic hyperostosis, the skeletal lesions of interest in the current study. The etiological complexity of these lesions makes them ideal for research focused on the complexity of differential diagnosis and the need for the development of new and reliable methods for improving the accuracy of diagnoses in palaeopathological research.

The basis of any analysis of bone tissue for the purpose of differentially diagnosing the underlying causes of observable pathological lesions is a good working knowledge of bone physiology, histology, and the mechanisms of bone modelling, remodelling, and mineral homeostasis (Brickley and Ives 2008; Stout and Crowder 2012). Accurate interpretations of pathologic bone morphology are enhanced by a detailed understanding of the processes evident at the underlying bone cell level and the complex relationship between bone structure and the physiological function of bone (Brickley and Ives 2008).

Chapter 4

4   The Process and Methodology of Differential Diagnosis

The aims of palaeopathological research range from reconstructing the history and evolution of disease in human populations to addressing broader anthropological questions about the cultural and environmental variables that may have contributed to patterns of disease in the past. Much, if not all, of this research depends on the diagnosis of abnormal and/or pathological changes found in human skeletal remains obtained in an archaeological context (Miller et al. 1996; Mays 2012). The accurate identification and diagnosis of pathological processes from archaeological skeletal remains is one of the most challenging issues facing researchers working in palaeopathology today (Schultz, 2001; Byers and Roberts, 2003; Mays 2012).

Although the identification of specific disease processes is easily achieved for some conditions, such as fractures and a few classic infections (i.e. caries sicca with treponematoses), other conditions may lead to more ambiguous skeletal changes because of the limited number of ways in which bone can respond to disease (Buikstra and Cook 1980; Schultz 2001; Ortner 2012; Mays 2012). Unfortunately, for the palaeopathologist, similar abnormal changes to normal bone morphology can appear in association with several different disease processes, and a particular disease may produce more than one morphologic expression (Schultz 2001; Wapler et al. 2004; Ortner 2012; Ragsdale and Lehmer 2012). In addition, although not a common occurrence, an individual may have had more than one disease process contributing to the presence of lesions on the skeleton (e.g. co-morbidity) (Ortner 2008). Therefore, difficulties with determining a diagnosis in the field of palaeopathology most often arise from an inability to identify skeletal abnormalities or patterns of abnormalities that are specific to individual disease processes, which is referred to as non-specificity (Schultz, 2001; Byers and Roberts, 2003; Von Hunnius 2009; Walker et al. 2009). The limitation of bony responses to disease can often lead to misdiagnoses and, since the presence or absence of ancient disease processes on bone have been used to infer aspects of life and health in archaeological populations, misdiagnoses can have significant implications for our

understanding of disease etiology and epidemiology in the past (Steinbock, 1976; Ortner, 1991; Buikstra and Ubelaker, 1994). It is important for researchers to recognize that distinguishing between the options of pathological conditions responsible for a particular skeletal lesion(s) is rarely possible on the basis of skeletal evidence alone. For example, Hackett (1976) demonstrated that there are only two types of lesions pathognomonic of treponemal disease: *caries sicca*, unique bone changes to the cranial vault, and expansions and superficial cavitations on long bones. Although neither of these features are present in a case studied by Mays et al. (2003), systemic non-specific periosteal lesions throughout the skeleton were diagnosed as indicative of treponemal disease and used to establish an Old World case of treponematosis. Harper et al. (2011) argue that the non-specific lesions present in this particular case are not consistent with Hackett's (1976) pathognomonic features and, therefore, do not provide sufficient evidence to make the conclusion that treponemal infection was present during the pre-Columbian period in the Old World. This example demonstrates that palaeopathologists must be careful to avoid the temptation of overextending data and ascribing specific diagnoses where skeletal criteria may be ambiguous, increasing the potential for diagnostic and interpretative errors (Harper et al. 2011; Ortner 2012).

These challenges do not preclude, however, achieving some form of diagnosis. Careful attention to the type, distribution, and morphological characteristics of lesions will permit diagnoses to at least a general category of disease in most cases (Waldron 1994; Miller et al. 1996; Ragsdale and Miller 1996; Ortner 2003, 2012; Ragsdale and Lehmer 2012). Therefore, rather than focusing on the overwhelming and often troublesome task of diagnosing a specific disease, a more rational approach to diagnosis in palaeopathology is to focus on the process of differential diagnosis. This process involves the consideration of general disease categories rather than specific diseases in situations where pathognomonic diagnostic criteria are absent. A differential diagnosis in palaeopathology is developed by stating the most likely disease category into which skeletal lesions fit based on a detailed skeletal analysis and a consideration of the archaeological, palaeoenvironmental, and palaeoepidemiological contexts of the remains. In addition, a list of possible diagnostic alternatives in order of decreasing likelihood is also typically included and considered (Miller et al. 1996; Waldron 2009; Ortner 2008; Mays 2012).

This broad-based, non-specific approach not only enhances the comparability of data within palaeopathology, but also reduces the possibility for error in diagnosis and later interpretations of ancient health (Waldron 1994; Miller et al. 1996).

The purpose of this chapter is to discuss how differential diagnoses are conducted in palaeopathology through a review of the process of differential diagnosis in the clinical sciences and the relationship between clinical and palaeopathological data. The process of differential diagnosis from archaeological bone logically starts with understanding how disease affects the body in the clinical sense and, more specifically, the skeleton since most of the material that palaeopathologists work with is skeletonized (Schultz 2001; Roberts and Manchester 2005).   A brief overview of the secondary forms of diagnostic evidence, including historical, palaeoecological, and archaeological contextual evidence, used in the field of palaeopathology is also provided. Finally, this chapter will review the various methodological approaches used in the process of differential diagnosis, as well as explore recent advances in clinical diagnostic techniques that are relevant to the current palaeopathological study.

4.1   The Process of Differential Diagnosis in the Clinical Sciences

The purpose of a differential diagnosis in modern medicine is to evaluate observable symptoms in living patients, assess a reasonable prognosis, and plan the treatment and/or intervention of identified pathological conditions. Diagnosis, prognosis, and treatment are the three bases of clinical practice (Schwamm and Millward 1995; McCarthy and Frassica 1998; Waldron 2007, 2009. The process of differential diagnosis allows the clinician to more clearly understand the signs and symptoms of different types of conditions, eliminate immediately life-threatening complications, and enable patients to integrate chronic illnesses into their lives until they can be resolved, if possible (Waldron 2009). If the patient's health does not improve as anticipated when a treatment or therapy has been applied, the differential diagnosis must be reassessed and alternative diagnoses must be considered.

In living patients, physicians have many sources of data at their disposal to aid in diagnosing and treating pathological conditions. These include patient medical histories, eliciting signs and symptoms presented by the patient during clinical examination, and supplementary biochemical testing of soft tissues, organs, cells and body fluids (Ortner 2003; Waldron 2007). Once the physician has gathered as much information as possible, a differential diagnosis can be constructed in which all of the conditions that may give rise to the observable signs and symptoms are considered. The goal of this process is to determine the condition most likely responsible for the patient's condition through a rigorous process of elimination (Waldron 2007, 2009). Arriving at a correct diagnosis in clinical practice is of utmost importance as this is the primary step in the treatment of any condition in living patients. An incorrect diagnosis can lead to the wrong methods of treatment and can, in some cases, mean the difference between life and death (Caillé 1906; Waldron 1994, 2007).

4.1.1 The Clinical Diagnosis of Skeletal Disease

The approach to differential diagnosis in living patients with suspected skeletal disease, specifically, follows the same process of elimination as soft tissue and organ diseases. The initial approach to diagnosis is to place the skeletal lesion within one of seven general bone disease categories. These disease categories include: congenital, metabolic, traumatic, circulatory, infectious, neoplastic, and changes due to systemic disease (Schwamm and Millward 1995; McCarthy and Frassica 1998; Roberts and Manchester 2005). Choosing the correct category is an essential first step towards making a more specific diagnosis. Assigning a category, and ultimately establishing a correct diagnosis, depends on a thorough consideration of a bone lesion's clinical presentation, radiographic characteristics, and histological features (Schwamm and Millward 1995; McCarthy and Frassica 1998).

The clinical presentation of a lesion refers to the collection of important diagnostic information including: the age of the patient, the location and distribution of the lesion, the presence of swelling and/or deformity, and the presence of other diseases and systemic symptoms (Caillé 1906; McCarthy and Frassica 1998). The age of the patient is

relevant to diagnosis since some bone lesions are more prevalent in certain age groups than in others. For instance, many of the metabolic bone diseases that affect growth and development are rarely found in an active form in adult bones (Buikstra and Cook 1980; Stuart-Macadam 1985; Roberts and Manchester 2005). The location and distribution of the lesion(s) provide another diagnostic clue as disease processes often preferentially affect groups of bones, specific bones, and/or specific locations on bones (McCarthy and Frassica 1998; Ortner 2003; Roberts and Manchester 2005). For example, bone changes caused by leprosy occur most commonly in the hands and feet as the result of secondary infection and inflammation due to a loss of sensation from nerve damage. Thus, deformity and bone resorption in the toes and fingers are characteristic of leprosy (Manchester 2002). Infection with tuberculosis presents with a different clinical pattern and most commonly involves extensive bone destruction of the hip, femoral head, and the thoracic and lumbar vertebrae (Resnick and Niwayama 1995). Finally, knowledge of the presence of other diseases and systemic symptoms in the patient are also of value for diagnosis as the skeleton is sensitive to many systemic factors. The presence of disease in the renal, endocrine, hematologic, and/or pulmonary systems can influence the skeleton in different ways and may explain the presence of particular types of bone lesions (McCarthy and Frassica 1998). One such example is marrow expansion in the skull due to chronic anaemia (Stuart-Macadam 1985, 1987, 1989).

Once the clinical presentation is considered, the next, and most important, step in the clinical differential diagnosis of skeletal disease is the standard plain-film radiograph (McCarthy and Frassica 1998). For a reliable diagnosis to be achieved, it is important that the clinical pathologist be familiar with radiological imaging techniques and the identification of the specific radiographic characteristics of different skeletal diseases (Burgener and Kormano 1996; McCarthy and Frassica 1998). Plain-film radiographs allow the pathologist to assess the presence/absence of suspected bone lesions, delineate the extent of a lesion and the involvement of surrounding soft tissues, and assess the specific characteristics of a lesion. In addition to plain-film radiographs, there are several ancillary radiologic modalities that are available for more detailed studies of skeletal disease. The most commonly used modality is computed axial tomography (CT) (Genant et al. 1980; Moon et al. 1983; Seeram 1994; McCarthy and Frassica 1998; Lovell 2000).

However, as was previously mentioned, an accurate diagnosis can generally be established using conventional radiography. Therefore, unless there are specific questions regarding the characteristics of a bone lesion that can only be answered using these alternative modalities, it may be redundant and cost inefficient to apply them for diagnosis in clinical research. In attempting to answer the question of diagnosis using radiographic images, a bone lesion is defined by answering several key questions including: what does the lesion look like? Is the lesion formed by proliferation or resorption? How fast is the lesion forming/growing (Ortner 2003)? These questions can be answered by the clinical pathologist on the basis of three distinct patterns: 1) abnormal bone destruction (osteolysis), 2) abnormal bone formation (osteoblastic), and 3) a mixed reaction including both osteolysis and osteoblastic responses (McCarthy and Frassica 1998; Ortner 2003).

Just as radiographic techniques contribute greatly to the diagnosis of skeletal disease, special histological techniques can aid with determining a specific diagnosis and are most often the means by which diagnoses are refuted or confirmed. This is usually the final step in the process of clinical diagnosis (Schwamm and Millward 1995). Diagnostic tissue is obtained from a lesion using either an open (incision) or needle biopsy. This tissue can then be prepared as a histological thin section from which the immunohistochemistry and histomorphometry of a lesion can be analyzed. Immunohistochemistry identifies proteins specific to various types of tissues and is useful for the differentiation and identification of abnormal cells (Schwamm and Millward 1995; McCarthy and Frassica 1998). This technique is used to diagnose neoplastic disease such as metastatic carcinoma and malignant lymphoma (Kindblom et al. 1986). Histomorphometry is a computer-assisted microscopic analysis that is used to quantify the amount of bone present in a lesion (measured by cortical thickness and trabecular volume), the rate of bone turnover, and the efficiency of bone mineralization. This technique is generally used to diagnose metabolic diseases of bone, such as rickets and osteomalacia (McCarthy and Frassica 1998; Brickley et al. 2005). The results of these histological analyses are then correlated with data obtained from the clinical presentation and the observations made from the radiographs. Once all of this information is assessed together, a diagnosis can generally be suggested.

There are several examples of the process of differential diagnosis in the clinical literature. Anaemia, categorized as a systemic disease and, specifically, a disorder of the hematopoietic system, involves a pathological process that includes both bone destruction and bone formation. The body responds to chronic anaemic stress by stimulating the expansion of the hemopoietic bone marrow in an attempt to further increase the production of red blood cells (Halvorsen and Bechensteen 2002; Fandrey 2004; Walker et al. 2009). In the clinical presentation, mild effects of anaemia include lethargy, general weakness, cognitive development problems, and gastrointestinal disturbances. Patients with severe and chronic anaemia will often report additional pathological changes including: cardiac arrest, inflammation of the tongue, spoon-shaped brittle nails (koilonychias), gastritis, and a reduction in cell-mediated immunity (Stuart-Macadam 1989; Sullivan 2005; Roberts and Manchester 2005).

Abnormal bone changes have also been found to occur in children and are thought to be related to the hyperactive bone marrow. Since anaemia is a condition which affects bone during growth and development, skeletal changes are not typically observed in adults. However, healing or healed lesions resulting from childhood anaemia may be present in adulthood (Lallo et al. 1977; Stuart-Macadam 1987, 1989; Roberts and Manchester 2005). Considering these signs and symptoms, an individual's overall iron status is evaluated through blood testing by summing the amount of functional iron circulating in the haemoglobin of red blood cells, the amount of iron bound to the transport protein transferrin, and the amount of stored iron bound to the protein ferritin located in the cells of the bone marrow, liver, and spleen (Wadsworth 1975; Sullivan 2005).

The radiographic appearance of the bone changes associated with anaemia and marrow expansion are most notable in the skull and include the thinning of the outer table of compact bone, abnormal thickening of the diplöe and the orbital roof, and the presence of "hair-on-end" trabeculation (Aksoy et al. 1966; Stuart Macadam 1985, 1989; Larsen 1997; Ortner 2003). Infracranial changes also occur, but with less severity than the changes observed in the skull. Aksoy et al. (1966) and McCarthy and Frassica (1998) reported a thinning of the subchondral plates of the lumbar vertebral bodies and the cortices of the bones of the hand. Histological analyses reveal a cellular marrow,

enlarged marrow spaces, and a thinned or absent outer table in the skull. A pattern of cancellous bone with enlarged spaces open through to the outer table corresponded with porotic type lesions on the skull vault and the roof of the eye orbit (Whipple and Bradford 1932; Caffey 1937). These patterns are indicative of hypertrophic marrow as a result of a physiological response to anaemia. With a combination of the clinical presentation and the radiographic characteristics, the clinician can easily provide a diagnosis of anaemia and an appropriate course of treatment can be recommended (McCarthy and Frassica 1998).

In modern medicine, there are few physicians who are willing to admit that diagnosis is not an exact science and that not every combination of signs and symptoms fit into one, and only one, diagnostic category (Cambell et al. 1979; Waldron 2007). Realistically, despite the large amounts of data available to the physician, diagnosis is more art than it is science and the process of diagnosis is actually quite prone to error (Shojana et al. 2003). The boundaries between different disease categories are not discrete, but are frequently blurred and may overlap. Pathological processes are dynamic, progressing, and relapsing and, in a substantial number of cases, a diagnosis may take months, years, or may never actually be realized. In addition, even in those cases where a diagnosis is made, the chances of it being correct are, unfortunately, not very high (Shojana et al. 2003; Waldron 2007, 2009). Several studies have been done to assess the accuracy of diagnosis in clinical medicine by comparing a clinical diagnosis with findings recorded at autopsy. In a review of 53 published reports in which antemortem diagnoses were compared with autopsy findings, Shojania et al. (2003) found that up to half of diagnoses were in error and that the median error rate for the diagnosis of primary cause of death was 23.5% and 9.0% for errors that were made by the clinician that might have affected patient outcome. These rates of error in clinical diagnostics should raise caution for the palaeopathologist, who is armed with significantly fewer diagnostic clues. Soft tissues, organs, and cells play a significant role in clinical pathological investigations and can be studied to establish reliable diagnoses. Palaeopathologists can only examine the remnants of ancient disease in dry bone and in most cases soft tissues and cells have long since decomposed.

The factors contributing to error and misdiagnoses in the field of palaeopathology are complex and it is, therefore, essential that palaeopathologists develop standardized protocols for the analysis of pathological conditions on skeletal remains which are capable of providing a reliable differential diagnosis. Like any research, the quality of palaeopathological data depends upon the use of multiple lines of evidence and the application of as many appropriate, available, and rigorously tested methods as is possible (Miller et al. 1996; Ortner 2008; Mays 2012) The quality of data and the rigour in the methods used in collecting data are major factors contributing not only to the accuracy of diagnoses, but also to the legitimacy of the subsequent interpretations made regarding the prevalence of disease and the health of the population represented by a given skeletal sample (Ortner 2008). With the aid of increasingly reliable and reproducible methods of data collection, greater accuracy in diagnoses may be achieved, resulting in more informed conclusions regarding the causes, distribution, and frequency of disease, the evolution and history of disease, and the biocultural factors contributing to the presence of disease in ancient populations (Larsen 1997; Schultz 2001).

4.2 The Relationship between the Clinical Sciences and Palaeopathology

The relationship between the clinical sciences and palaeopathology is rooted in the history of the development of palaeopathology as a discipline. To many, the origins of palaeopathology can be traced to 19th century medicine with clinical anatomists and physicians such as Rudolf Virchow (1821-1902), Frederic Wood-Jones (1879-1954), Grafton Elliot Smith (1871-1937), and Sir Marc Armand Ruffer (1859-1917). Sir Marc Armand Ruffer, in particular, published numerous papers focused on comparisons of clinical manifestations of disease to lesions found in ancient remains. Over time, the recognition and diagnosis of skeletal lesions became more firmly based on known clinical manifestations of diseases and potential diagnoses were increasingly corroborated by histological and radiographic evidence (Grauer 2008). This approach paved the way for histological and radiographic investigation into ancient disease within paleopathology today (Sandison 1967; Aufderheide and Rodriguez-Martin 1998; Grauer 2012).

With the exception of mummies, the human-derived material available to the palaeopathologist is completely skeletonized. As such, understanding how disease affects the body, and particularly the skeleton, in modern clinical contexts is essential (Roberts and Manchester 2005). In order to achieve accuracy in palaeopathological diagnoses, it is vital that the diagnostic criteria that are used to assess skeletal lesions have a secure foundation derived from the clinical sciences (Aufderheide and Rodriguez-Martin 1998; Ortner 2003; 2012). The diagnosis of disease in archaeological skeletal remains relies upon the careful assessment and comparison of macroscopic, microscopic, and radiologic details of observed skeletal lesions with disease models based on clinical data (Buikstra and Cook 1980). In addition, a familiarity with bone biology, physiology, history, and human culture, are necessary in order to provide parallels between the epidemiology and skeletal expressions of clinically diagnosed diseases and lesions present in archaeological human remains (Stuart-Macadam 1987; Rogers et al. 1990; Roberts and Manchester 2005; Waldron 2009).

The history of the interpretation of porotic hyperostosis of the cranial vault and orbital roofs illustrates the importance of the collaborative relationship between palaeopathology and the clinical sciences. Given that porotic hyperostosis is one of the most commonly reported pathological conditions in archaeological collections of human skeletal remains, explanations for its occurrence have been noted in the palaeopathology and physical anthropology literature since the late 19th century (e.g. Welcker 1888) (Stuart-Macadam 1985; Walker et al. 2009; Mays 2012). While Rudolph Virchow was first to note the orbital lesions of porotic hyperostosis, Aufderheide and Rodriguez-Martin (1998) attribute the identification and description of porotic orbital and vault lesions to Welcker (1888).

Early interpretations, including racial and cultural explanations, were rather speculative. However, in the 1920s, reports of the macroscopic and radiographic changes in the cranial bones of individuals diagnosed with congenital anaemia, including thalassemia and sickle cell anaemia, began to appear in the clinical literature. Although clinical studies rarely describe the macroscopic appearance of bone in patients, Cooley et al. (1927), Witwer and Lee (1927), Whipple and Bradford (1937), and Caffey (1937)

described observations of porotic lesions of the cranial vault made from autopsy examinations of individuals with diagnosed hemolytic anaemia. Porotic hyperostosis of the orbital roofs was initially noted by Cooley et al. (1927) who described significant thickening of the horizontal plates of the frontal bone accompanied by the same sponge-like appearance as vault lesions. During this time, those clinicians who were aware of archaeological cases of porotic hyperostosis noted a resemblance between the radiographic changes observed in patients with congenital anaemia and radiographs of archaeological crania with visible porotic lesions (Moore 1929; Vogt and Diamond 1930; Feingold 1933). As a result, these early clinicians and subsequent anthropological researchers (e.g. Angel 1964, 1966, 1978) interpreted the changes observed in archaeological crania as representative of the congenital anaemias (Mays 2012). Perhaps the most well-known application of these clinical observations to palaeopathological research comes from the work of Angel (1978) who used the presence of porotic hyperostosis as a marker for thalassemia (Aufderheide and Rodriguez-Martin 1998).

Reports of cranial changes in chronic iron-deficiency anaemia in children also began to appear in the clinical literature in the 1950's and these changes were similar to those reported earlier in individuals with congenital anaemia (Britton et al. 1960; Moseley 1961; Aksoy et al. 1966; Reiman et al. 1976). Given that iron deficiency anaemia is the most geographically widespread type of anaemia, these clinical findings offered palaeopathologists a more plausible explanation for the high prevalence of porotic hyperostosis in populations in geographic regions where congenital anaemias were not likely a contributing cause (Bothwell 1995; Brugnara 2003; Walker et al. 2009; Mays 2012). This explanation was quickly and eagerly adopted and, until relatively recently, porotic hyperostosis became synonymous with iron-deficiency in the palaeopathological and bioarchaeological literature (Stuart-Macadam 1985, 1987 a,b; Walker et al. 2009; Stodder 2006; Mays 2012).

Over time, a divergence in the literature on the etiology of cranial bone changes in anaemia began to develop between palaeopathology and the clinical sciences. The clinical literature placed diagnostic emphasis on marrow hyperplasia, whereas palaeopathologists increasingly began focusing on the macroscopically observable

porosity and pitting on the orbital roof and cranial vault surfaces. This drift away from clinical evidence became problematic for diagnosis and interpretation in palaeopathology as porosity of the orbital roofs and cranial vault can occur in conditions other than anaemia including rickets, scurvy, and/or infectious processes (Schultz 2001; Wapler et al. 2004; Ortner 2003; 2012).

Over the last decade, palaeopathology has begun refocusing on clinical diagnostic criteria, including the presence of marrow hyperplasia as a requirement for a diagnosis of anaemia (Schultz 2001; Wapler et al. 2004). In order to shed further light on the issues of accuracy in diagnosis in palaeopathology, further clinical studies on large numbers of patients may be necessary, and more sophisticated and innovative methods for studying cranial bone changes in archaeological human remains are needed (Schultz 2001; Mays 2012). The preceding example demonstrates the important contributions that the clinical sciences have made, and continue to make, to further the efforts of diagnostic accuracy in palaeopathology, and also highlights the problems that can arise in interpretations of lesions if palaeopathologists fail to consider clinical evidence.

Although palaeopathologists have the advantage of being able to directly study the remains of diseased individuals, the major disadvantage is that their study is restricted to the dry bone of "patients" who can never describe their symptoms and, thus, the majority of diseases that can be studied are those that affect the skeleton (Roberts and Manchester 2005; Waldron 2009). As such, even though a collaborative relationship between the clinical sciences and palaeopathology is important, it must be recognized that clinical data cannot always be directly and uncritically applied to human skeletal remains derived from an archaeological context (Roberts and Manchester 2005). In addition to the theoretical and interpretive issues faced by skeletal researchers, as outlined by Wood et al. (1992) in the "Osteological Paradox" detailed in Chapter 2, there are several limitations that must be considered as palaeopathologists develop clinically based models for the differential diagnosis of disease in archaeological skeletal remains.

Unlike clinical pathologists, the data available to the palaeopathologist for diagnosis are limited to the analysis of archaeological materials and the remnants of ancient disease in

skeletonized human remains. Information that can be obtained from living patients, such as patient medical histories, the recognition of symptoms, and soft tissue and living cell analyses, is missing in dry archaeological bone (McCarthy and Frassica 1998; Waldron 1994, 2009; Schultz 2001). Palaeopathologists have had to adapt diagnostic criteria developed from clinical studies to their own research by compiling dry bone criteria for disease diagnosis from a combination of data obtained from medical pathology museum specimens and medical imaging data on living patients (Mays 2012). A number of published texts detailing the pathological skeletal changes caused by various diseases have been produced using these dry bone criteria with the aim of enabling diagnoses in archaeological specimens (e.g. Steinbock 1976; Zimmerman and Kelley 1982; Ortner and Putschar 1985; Aufderheide and Rodriguez-Martin 1998; Ortner 2003; Mann and Hunt 2005; Waldron 2009).

A second restriction faced by palaeopathologists is that disease processes in archaeological remains are static, meaning that there is no possibility of observing how the disease might develop, which often aids significantly in clinical diagnosis. The appearance of skeletal abnormalities is limited to one moment in time, the time of death (Waldron 2007, 2009). Finally, the skeletal manifestations of certain diseases, as described in clinical research, may not always fit what we see in an archaeologically derived skeleton – some features of a lesion may be similar to those described in the clinical data, some may be different. This is because diseases that may have affected the skeleton in the past may not have the same effect today due to changes in physical and sociocultural environments, as well as the introduction of medical interventions (Lovell 2000; Roberts and Manchester, 2005; Waldron, 2009). The disease processes observed in archaeological bone reflect chronic, longstanding conditions without any influence from drug therapy, which is why reference to the pre-antibiotic literature is so important in palaeopathology. There may be no exact clinical equivalent for a diagnostic comparison (Roberts and Manchester 2005). Diagnoses based exclusively on comparisons to modern clinical data may, therefore, be incorrect and introduce significant error into palaeopathological analysis and interpretation (Buikstra and Cook, 1980). Therefore, in addition to comparative clinical references, additional data must be compiled from

historical and archaeological sources of evidence where possible (Buikstra and Cook 1981; Ortner 2001; Roberts and Manchester 2005).

4.3　　The Role of Historical and Archaeological Data

Similar to the diagnosis of disease in clinical settings, where a variety of data are accumulated and multiple tests are conducted prior to diagnosis, palaeopathological studies must also rely on multiple lines of inquiry whenever possible. The accumulation of data from clinical, biological, historical and archaeological sources will have a substantial influence on the reliability of differential diagnoses as these data will narrow the likelihood of the presence of various types of pathological conditions in past human populations (Ortner 2003; Grauer 2008).

Primary sources of data on past disease processes are obtained from the direct analysis of skeletal and mummified human remains using a wide spectrum of analytical methods including macroscopic, microscopic, radiological, and histological observations, as well as biochemical and DNA studies (Lovell, 2000; Ortner 2003). In addition to skeletal remains, there are alternative sources of palaeopathological data available for analysis. Secondary sources of information may include documentary evidence of disease such as early medical texts, non-literary art forms (e.g. paintings, ceramics, sculpture), and artifacts such as splints and other medical devices, when available (Lovell, 2000; Roberts and Manchester, 2005). However, for those parts of our human history where there are no written or illustrative records, the only source of evidence that is available for studying disease is human skeletal remains (Roberts and Manchester 2005).

Additionally, archaeological data on the physical and social/cultural context for archaeological skeletal remains provide a tertiary source of evidence which aids enormously in the interpretation of the history and evolution of disease. These contexts provide important palaeoepidemiological information about past living conditions such as climate, geography, cultural practices, and settlement patterns which may have contributed to the presence and prevalence of certain diseases in ancient populations (Holland and O'Brien 1997; Lovell, 2000; Roberts and Manchester 2005). In addition to human skeletal remains, the archaeological record, which includes artifacts, features, and

plant and animal remains, provides information necessary to reconstruct the physical and social contexts of past populations (Dettwyler 1992; Lovell 2000; Zuckerman et al 2012). An understanding of the underlying environmental influences and social practices of past populations provides palaeopathologists with possible explanations for observed population level patterns of disease such as unequal distributions of disease, malnutrition, and trauma. These forms of evidence provide the necessary background for palaeoepidemiological reconstructions wherein researchers can establish links between social processes and their biological effects on past populations (Pinhasi and Turner 2008; Zuckerman et al. 2012). To gain an enriched understanding of the past, it is germane to collect data from all available forms of historical and/or archaeological evidence, including medical texts, ancient art forms, artifacts, structures, environmental evidence, and human remains. All of these sources of information are important for structuring research questions and informing interpretations in palaeopathology.

4.4 Methods for Achieving Differential Diagnoses in Palaeopathology

Just as in clinical research, there is no single method by which differential diagnosis is accomplished in palaeopathological studies. The palaeopathological analysis of skeletal lesions should involve as many appropriate methods as possible whenever possible (Grauer 2008). Several factors must be considered when determining the appropriateness and, particularly, the feasibility of various methodological approaches for achieving a differential diagnosis. First, the adequacy of skeletal preservation in some archaeological collections will determine which methods will be appropriate and available for analysis. Post-mortem damage, diagenesis, and contamination may compromise the application of a number of methods, such as imaging and biochemical methods, and can render them both impractical and unusable (Grauer 2008; Schultz 2001; Ortner 2003; Wanek et al. 2012).

Second, the types of data and the level of analysis that are required to answer the relevant research questions being asked will dictate which methods are necessary. Macroscopic visual observation is the first and primary method employed when examining and assessing archaeological skeletal remains for pathological lesions (Mays and Pinhasi

2008; Ortner 2012). In many cases, it is the only method that is required for a differential diagnosis and in others it may be the only method available (Miller et al. 1996; Lovell 2000; Ortner 2003; Grauer 2008). However, certain disease processes may only be reliably diagnosed by radiologic and microscopic techniques that can provide essential internal skeletal data that are needed to improve the reliability of differential diagnoses (Schultz 2001). Thus, the inclusion of additional methods should be considered when those methods are capable of providing important supplemental data that will make a significant contribution to the diagnostic process, and are worth the additional logistical and financial costs. Technologically complex methods, including histology, biochemistry, and radiologic imaging, should be applied sensibly as they can be expensive and, in some cases, destructive or invasive (Ortner 2003; Turner-Walker and Mays 2008). In summary, when selecting from the methods available for the palaeopathological analysis of skeletal remains, there must be careful consideration of the nature of the skeletal material being analyzed, the specific questions that are being asked, and the answers that are sought.

The following section focuses on the methods used for the proper description, documentation, and differential diagnosis of skeletal lesions in palaeopathology. As mentioned previously, the general methods of study necessary for properly describing the appearance of pathological lesions and achieving a reliable differential diagnosis rely, primarily, on macroscopic visual observations of the skeleton itself. However, additional methods of analysis that are often used to supplement these observations include conventional radiography (e.g. Stuart Macadam, 1989), clinical computed tomography (e.g. Harwood-Nash 1979; Lewin et al 1990), microscopy and histology (e.g. Schultz, 2001), and more recent technological advances relevant to the current research study - micro-computed tomography (e.g. Kuhn et al., 2007; Rühli et al., 2007). Additional methods including biomolecular (DNA, antigen detection) and biochemical techniques (stable isotopes, trace elements) have also made significant contributions to the field of palaeopathology and to the process of differential diagnosis. However, as these techniques are not directly relevant to the current study, detailed discussions of their applications and contributions to palaeopathological research can be found elsewhere (e.g. Aufderheide 1989; Ambrose 1993; Katzenberg et al. 1996; Wright and White 1996;

Dittman and Grupe 2000; Katzenberg 2000; Drancourt and Raoult 2005; Donoghue 2008).

4.4.1 Macroscopic Visual Analysis

Once all of the available sources of palaeopathological data are identified and collected, the process of differential diagnosis begins with the thorough macroscopic visual examination, description, and documentation of the skeletal remains (Buikstra and Cook 1980; Buikstra and Ubelaker 1994; Grauer 2008). Detailed lesion description and documentation are essential not only for achieving reliable diagnoses, but also for allowing the testing of alternative diagnostic hypotheses and for the comparability and consistency of data between studies and between populations for future research (Steinbock 1976; Buikstra and Cook 1980; Ortner 1991, 1992, 1994, 2003; Buikstra and Ubelaker 1994; Lovell 2000; Robb 2000; Grauer 2008). Although there is no universal list of objective descriptive terminology for documenting observations, several established publications in palaeopathology have been provided, as well as lists of recommended descriptive terms and operational definitions (e.g. Ortner 1991, 1992, 1994, 2003; Buikstra and Ubelaker, 1994; Brickley and McKinley 2004). These contributions are attempts to provide researchers with standardized guidelines for the use of unambiguous terminology and coding systems for documenting lesion variables (i.e. location, activity, severity) in order to ensure that documented descriptive data are more comparable between researchers. Therefore, the first step of palaeopathological investigation, description, and documentation must involve the careful selection of standardized terminology from the established literature.

Once a standardized method of description is chosen, the next step in the process of differential diagnosis involves providing descriptive summaries of the morphology of abnormal bone changes using macroscopic visual evaluation (Lovell 2000; Ortner 2003). There are several diagnostic criteria that are essential to a macroscopic descriptive system for recording abnormal bone changes and have been developed based on clinical models. These criteria include: 1) the appearance of the lesion, 2) the location of the lesion(s) within a skeletal element, 3) the skeletal distribution of the lesion(s) within an individual,

and 4) the distribution of lesions within a population (Ortner and Putschar 1981; Lovell, 2000; Ortner 2003). Visualizing and distinguishing these key criteria in the patterning of lesions can be crucial for accurately determining a diagnosis. The precise documentation of the appearance, anatomical location, and distribution of lesions is integral as different pathogens, combined with physiological changes in body functions and abilities, will differentially affect areas and/or groups of bones (Buikstra and Ubelaker 1994; Lovell 2000; Ortner 2003; Grauer 2008). Details that are vital for a differential diagnosis include recording the exact bone affected, the specific component(s) of the bone involved (e.g. epiphysis, diaphysis, etc), the aspect of the bone (e.g. anterior/lateral, posterior/medial), and any affected features of the bone (e.g. vascular channels, foramina, sutures) (Buikstra and Ubelaker 1994; Lovell 2000; Ortner 2003; Grauer 2008). The photographic documentation of abnormal bone changes is also considered crucial, particularly in cases where diagnoses may be ambiguous or questionable (Ortner and Putschar 1981; Ortner 2003).

On the basis of clinical data derived from autopsy examinations of individuals with anaemia, specific criteria for the visual assessment and proper documentation of porotic hyperostosis in archaeological skeletal collections have been established and are well-known in the palaeopathological literature (Nathan and Haas 1966; Mensforth et al. 1978; Stuart-Macadam 1985, 1989; Buikstra and Ubelaker 1994; Ortner 2003; Roberts and Manchester 2005). These criteria include information regarding the distribution of lesions (e.g. Stuart-Macadam 1985, 1989; Buikstra and Ubelaker 1994), categories of lesion expression (e.g. Nathan and Haas 1966; Steinbock 1976; Stuart-Macadam 1985), and the status, or activity, of lesions at the time of death (e.g. Mensforth et al. 1978; Buikstra and Ubelaker 1994).

In distribution, porotic hyperostosis is most commonly found on the roof of the orbits and the frontal, parietal and occipital bones of the cranial vault. Of the cranial vault bones, the parietal area is the most often affected, with the orbits being more often affected than the vault bones (Stuart-Macadam 1987, 1989). Standards for the proper recording of the distribution of porotic lesions have been undertaken by Stuart-Macadam (1991) and Buikstra and Ubelaker (1994). The severity of porotic hyperostosis of the cranial vault

and orbital roofs varies in macroscopic appearance from lightly scattered, fine foramina that affect the compact bone to large, coalescing openings accompanied by an outgrowth of the trabecular structure, which destroys the integrity of the compact bone (Nathan and Haas 1966; Stuart-Macadam 1982, 1985, 1989). A number of researchers have attempted to provide standardized methods for scoring the various expressions of porotic hyperostosis (e.g. Nathan and Haas 1966; Steinbock 1976; Mensforth et al. 1978; Guidotti 1984; Stuart-Macadam 1982, 1985). For the purposes of consistency and comparability, the method most often applied in the literature is that outlined by Steinbock (1976) and Stuart-Macadam (1985), adopted and modified from Nathan and Haas (1966). Finally, documenting the status, or activity, of the lesions at time of death is also important for the visual assessment and diagnosis of porotic hyperostosis. These data allow researchers to make interpretations regarding the effects of the disease on population morbidity and mortality and the pathogenesis of disease, leading to a better understanding of the potential contributing etiological factors (Lallo et al., 1977; Stuart-Macadam, 1985; 1987, 1989; Mittler and Van Gerven 1994; Roberts & Manchester, 2005). Lesion activity is recorded based on standardized terminology provided by Buikstra and Ubelaker (1994) (e.g. active, healed, mixed), and activity can be further defined following Mensforth et al. (1978) and Mittler and Van Gerven (1994). The specific methods for recording the distribution, specific categories of lesion expression (light, medium, severe), and lesion activity used in the current study are detailed in Chapter 5 and will not be repeated here.

The key to developing a differential diagnosis from a descriptive analysis of porotic hyperostosis is in making the distinction between bilateral porosis caused by marrow hyperplasia (anaemia) and unilateral porosis caused by other pathological stimuli that either superficially affect the skull (i.e. scurvy) or destroy its structural integrity completely (i.e. infection) (Ortner 2003). However, this distinction often cannot be made at the macroscopic level as the pathological processes that contribute to hyperostosis of the skull produce lesions that are similar in their gross morphology. As such, a careful descriptive analysis must also be accompanied by additional diagnostic tools.

Methods of visual evaluation have been considered the most valid methods since they have been developed over a century or more, are equally accessible and amenable to use by non-technical personnel, are relatively inexpensive and easy to use, and require modest sample preparation (Grauer 2008; Mays and Pinhasi 2008). The ultimate goal of a descriptive macroscopic analysis is identification of the disease process. However, the specific cause or etiology of a pathological condition cannot always be derived from a specimen (Miller et al., 1996; Ortner, 2003). While a variety of processes are capable of affecting bone in patterned and specific manners, diagnostic identification of lesions becomes challenging when disease signatures overlap (Schultz 2001; Wapler et al. 2004). This issue is highlighted through the example of the complexities and pitfalls of differentially diagnosing the etiology of porotic hyperostosis. Therefore, accurate diagnoses of abnormal or pathological conditions observed in archaeological skeletons will not only rely on the macroscopic assessment of lesions, but also on the accurate radiologic and microscopic assessments of the nature of the architecture of cortical and trabecular bone structures (Schultz 2001, 2012; Wapler et al. 2004).

4.4.2 Conventional Radiography

Imaging of skeletal lesions using conventional radiography has been conducted on ancient human remains for over 100 years and it continues to be an important adjunct to visual evaluation in the description and diagnosis of disease in palaeopathology (Lovell 2000; Mays 2008a). Although the application of radiography to palaeopathology was largely neglected between 1930 and 1960, due in part to the Second World War, radiographic examination is one of the most valued and frequently applied methods in the process of differential diagnosis in palaeopathological research today (Mays 2008a; Beckett and Conlogue 2010; Wanek et al. 2012).

The gross visual and radiographic appearance of abnormal bone should be considered together as part of the descriptive analysis of pathological lesions whenever relevant and possible. Although archaeological bone is not surrounded by soft tissue and can be directly examined, radiographic imaging can provide important diagnostic information regarding internal changes and characteristics of a skeletal lesion that may not be visible

through gross examination alone (Ortner, 2003; Roberts & Manchester, 2005; Rühli et al., 2007; Mays 2008a; O'Brien et al., 2009). Radiography should be considered an indispensable method for palaeopathologists in the following contexts: 1) when there are obvious external signs of disease, but the nature of the lesion is unclear (non-specific) (Ortner 2003), 2) when conditions, such as osteoporosis, involve the loss of bone mineral without changing the normal anatomical shape of the bone (Mays 2008a), and 3) when it is suspected that lesions may be completely concealed within the internal structures of a bone (e.g. Harris lines) (Mays 1995; Ameen et al 2005). In addition, radiographic methods have the advantage over chemical or histological methods in that they are non-destructive and should, therefore, always be used before the application of any destructive methodological approaches.

In the years since Röentgen's discovery in 1895, the design of X-ray equipment has undergone a number of modifications. However, the basic components of the X-ray imaging system and the principles of X-ray production have remained unchanged. In its most basic form, an X-ray imaging system consists of three main components: a high-voltage electrical supply to produce the kilovoltage (kV) requirements of the imaging system, an X-ray tube containing a cathode (negative electrode) and an anode (positive electrode), and an image detector (Carlton and Adler 2001; Saab et al 2008; Beckett and Conlogue 2010). The cathode consists of a coil of tungsten filament, much like the filament of a light bulb, and the anode usually consists of a tungsten target mounted on either a stationary or rotating surface (Saab et al. 2008).

For the production of X-rays, a current is passed through the tungsten filament within the cathode. The high resistance of the filament causes it to heat until electrons are released from its constituent atoms, creating an electrical field, or tube current, expressed in milliamperes (mA). The quantity of electrons produced by the filament in the cathode is determined by the tube current (mA) and the exposure time (s), which are set by the radiographer. If the tube current (mA) is doubled, the quantity of electrons available to hit the target is also doubled. In addition, increasing the duration of exposure heats the filament longer and also increases the quantity of electrons that are released into the tube. Both mA and time have a direct effect on the quantity and intensity of X-rays that are

produced and, together, are known as the milliampere-seconds (mAs). Therefore, mAs is the variable that determines the quantity of X-rays that are produced (Bushong 2008; Saab et al. 2008; Stock 2009; Beckett and Conlogue 2010)

To produce X-rays from the released electrons, the electrons must be accelerated toward the target within the anode. The speed of the electrons is controlled by the kilovoltage (kV) set by the radiographer. When a numerical value for the kV is set, it indicates the maximum kV, or peak kV (kVp), that will be applied to the cathode. As the accelerated electrons strike the target, a small fraction of the energy produced is released in the form of X-rays and the remainder as heat (Carlton and Adler 1992; Bushong 2008; Lynnerup 2008; Saab et al. 2008; Beckett and Conlogue 2010). The area of the anode that is bombarded by the stream of electrons is called the focal spot, which is oriented to direct the resultant X-ray beam towards the object to be imaged (Saab et al. 2008).

The production of a radiographic image involves the passing of produced X-rays out of the tube and through an object of interest. As an X-ray interacts with, and travels through, an object, its intensity is reduced through processes of absorption and scatter, and a fraction of these X-rays will then emerge through the object. The combined effect of these processes is known as attenuation (Seeram 1994; Bushong 2008; Stock 2009). The higher energy X-rays will penetrate the object and will be captured by the image receptor. Lower energy X-rays do not contribute to the image and add only radiation to the object. These X-rays can be selectively filtered if necessary through a process called beam hardening. Since X-rays are attenuated differentially by different tissues and materials, the X-rays that emerge will be captured by the image detector at different intensities. This produces a pattern of transmitted X-rays that is then translated into a negative image of gray values on radiographic film, or in real time as direct pixel-based images (Carlton and Adler 2001; Bushong 2008; Lynnerup 2008). These gray values will range based on the attenuation values of the tissues and/or materials being radiographed. Gray values for tissues with high attenuation, such as bone, will absorb and/or scatter a large number of passing X-rays and will appear in white or near white, while air, with little to no X-ray attenuation will appear as black (Carlton and Adler 2001; Lynnerup 2008).

For each density and thickness of a material, there are optimal system settings for producing the best quality image (Stock 2009). High quality radiographic images precisely reproduce the structures and composition of the object being imaged. There are a number of factors that affect image quality and include, but are not limited to, spatial resolution, contrast resolution, and noise (Bushong 2008; Saab et al. 2008; Stock 2009). Spatial resolution refers to the ability to distinguish anatomic detail on a radiographic image (Bushong 2008; Saab et al. 2008; Stock 2009). Resolution is closely related to image sharpness, which describes the abruptness between borders of fine anatomical details within an image. Images with low resolution or geometric unsharpness are described as "hazy" or "blurry" as there is a loss of recorded detail along the edges of anatomical structures (Saab et al 2008: 25).

There are several different causes of image blur, including object motion and the geometric arrangement of the X-ray equipment. Blurriness caused by object motion can be particularly problematic in imaging bioarchaeological specimens if they are not properly secured and they roll or shift during exposure. Additional causes of blurriness include geometric magnification and the penumbra effect – an image penumbra is the area of blur at the edge of an image (Bushong 2008; Saab et al. 2008). The effects of geometric magnification and the penumbra can be minimized by using a small focal spot size, increasing the distance between the focal spot (source) and image detector (SID), and decreasing the distance between the object and the image detector (OID) (Saab et al. 2008). These factors are based on the physical principle that X-rays diverge from the source of production, and will continue to diverge until they strike the detector. Reducing the amount of X-ray divergence after passing through an object will improve image quality.

Contrast resolution is the ability to detect small differences in the density, or the degree of X-ray attenuation, between adjacent structures on an image, and is primarily controlled by manipulating the kVp setting (Bushong 2008; Saab et al. 2008; Stock 2009; Beckett and Conlogue 2010). X-rays do not penetrate an object equally because of differences in the density of different tissues, structures, and/or materials that make up a given object. The kVp directly affects the penetrating ability of the X-ray beam, or the beam quality,

and will determine whether a tissue or material is adequately penetrated on the radiographic film. This is because the penetrating ability of the X-ray beam is controlled by the acceleration of electrons across the tube and, as kVp is increased, more of the high energy X-rays are produced, decreasing the differences in X-ray penetration throughout the object (Bushong 2008; Beckett and Conlogue 2010). For example, when viewing a processed radiograph of bone, it should be possible to not only see through the bone, but to also be able to discern internal structures such as trabeculae. If it is not possible to see through the bone, the radiographic film is considered underpenetrated. In this case, the kVp setting is inadequate for producing X-ray energies high enough to penetrate the bone, resulting in an image with high contrast – fewer shades of gray and more black and white. If it is possible to see through the bone, but anatomical features appear as shades of gray instead of white and internal structures are not discernible, the radiographic film is considered overpenetrated and the kVp setting is too high for adequate penetration. Higher kVp settings will increase the penetrating power of the X-ray beam and lower the contrast, resulting in more shades of gray and fewer areas of white (Beckett and Conlogue 2010). The kVp should be set at a minimal level that is adequate for object penetration, but still provides a level of contrast that allows for the differentiation of anatomical features and internal structures of interest (Saab et al. 2008).

Noise is a characteristic of radiographic imaging which reduces image quality by causing an image to appear grainy. Noise can be the result of properties inherent to the image detector itself, or from random interactions between X-rays and the image detector (Bushong 2008). Noise that is caused by random X-ray interactions (scatter) can be controlled by the radiographer by increasing the mAs to increase the quantity of X-rays that produce the image and decreasing the kVp. All of these factors must be considered and adjusted accordingly by the radiographer based on the image quality required to address the specific research questions of interest. More detailed discussions on the physics and principles of X-ray production and radiographic imaging can be found in Bushong (2008) and Carlton and Adler (1992).

For decades now, conventional radiography has been widely used in a number of anthropological applications and, specifically, as a non-destructive diagnostic tool in

palaeopathological research. Radiography is of value to palaeopathological investigations not only because it allows for a non-destructive approach to the analysis of internal bone changes caused by disease, but also because it provides a direct link between the appearance of lesions seen in archaeological skeletons and lesion morphology in living patients with known diseases (Resnick and Pettersson 1992; Rühli et al 2007; Wade et al. 2009; Beckett and Conlogue 2010). Comparisons of diagnostic criteria from clinical radiographs and archaeological radiographs provide a more rigorous, repeatable, and standardized method upon which to base a diagnosis (Stuart-Macadam 1987). As such clinical and archaeological radiographic data have been synthesized in several seminal palaeopathological works in attempts to provide a basic foundation for the differential diagnosis of disease from radiographic images (e.g. Brothwell and Sandison 1967; Steinbock 1976; Ortner and Putschar 1981; Aufderheide and Rodriguez-Martín 1998).

The process of developing an accurate differential diagnosis in palaeopathology using radiographic techniques relies first on obtaining the best possible X-ray image of the specimen (Chhem et al. 2008). This can be achieved by adjusting X-ray technical factors such as kVp and mAs, as discussed previously, and manipulating the positioning of remains in order to achieve the required projections. As such, palaeopathologists applying radiographic methods must be familiar with basic imaging principles in order to be successful in producing diagnostic images (Beckett and Conlogue 2010). Once an adequate image, or set of images, is obtained, the next important step is to identify all observable bony abnormalities. These abnormalities must then be carefully assessed to determine whether they are the result of a true pathological process, a normal anatomical variant, or a taphonomic alteration that has simulated a disease process (pseudopathology) (Steinbock 1976; Rühli et al. 2004; Chhem et al. 2008; Mays 2008a). The proper radiographic identification and differentiation of bone abnormalities requires additional training and/or collaboration with radiologists (Chhem et al. 2008; Mays 2008a; Beckett and Conlogue 2010). Basic radiographic training and collaboration are often necessary to ensure that important diagnostic clues are not overlooked or missed by palaeopathologists who may be unfamiliar with diagnostic radiographic image analysis.

Once pathological lesions have been identified, both macroscopic visual and radiographic observations should be considered together and used to answer the same important diagnostic questions asked by the clinical pathologist: What does the lesion look like? Was the lesion formed by a proliferative or resorptive process, or both? Was the process aggressive and rapid, or chronic and slow? Was the lesion active, healing, or healed? (Lovell 2000; Ortner 2003). These questions are addressed by systematically documenting diagnostic information including the location(s), shape, size, number, and distribution of all observable bony abnormalities using standardized terminology. Additional diagnostic information that can be obtained from radiographic images includes all patterns of observable internal bone changes. The main radiographic patterns that are identified and assessed follow those used in clinical diagnostic research and include radio-density (abnormal bone formation), radiolucency (abnormal bone destruction), or mixed (both formation and destruction) (Chhem et al. 2008). Any observable gross alterations to cortical bone and marrow cavities within pathological lesions are equally relevant for differential diagnosis and should also be documented and described (Brothwell and Sandison 1967; Steinbock 1976; Ortner and Putschar 1981; Stuart-Macadam 1987; Aufderheide and Rodriguez-Martín 1998). A differential diagnosis, including two or more possibilities, is then suggested once these patterns are compared to data from clinical radiographs of known diseases, and the archaeological and palaeoenvironmental contexts of the remains is considered (Ortner 2003; Chhem et al. 2008).

Although radiography plays a significant role in establishing a diagnosis in living patients, and clearly contributes to the process of differential diagnosis in palaeopathology, its role in dry bone analysis is not without technical limitations (Beckett and Conlogue 2010). First, although some bioarchaeologists have become increasingly competent in interpreting radiographic images, researchers without sufficient experience and/or training may not only be unable to identify abnormal structures on radiographic images, but may also misuse the technology. Consequentially, not only can large amounts of diagnostic information be missed through images being rendered useless by under- or overexposure, but insufficient equipment training can also result in a loss of

time, funds, and even damage to equipment through improper use and settings (Chhem and Brothwell 2008; Beckett and Conlogue 2010).

Second, and perhaps the most troublesome issue with radiography, a plain film radiographic image is essentially a two-dimensional visualization of three-dimensional anatomy. As a consequence, overlying and underlying tissues and bone structures are superimposed on the resultant image, making the analysis and interpretation of pathological structural changes challenging. Small changes to bone structures that may be important to the process of differential diagnosis may be missed or obscured by extraneous structures, even with the use of multiple projections (Rühli et al. 2007; Saab et al. 2008; Wu and Hochman 2009; Wade et al. 2009).

Conventional radiography has frequently been used in palaeopathology to contribute to the diagnosis and interpretation of a number of pathological conditions such as carcinomas, Paget's disease, treponematosis, fractures, rickets, anaemia, and scurvy, to name a few (e.g. Stuart-Macadam 1987; Andersen and Manchester 1992; Aufderheide and Rodríguez-Martín 1998; Ortner 2003; Mays et al. 2006; Stark and Garvie-Lok 2011). For example, radiographic studies of severe porotic hyperostosis in archaeological skeletal remains have established a set of criteria for the diagnosis of anaemic conditions (e.g. Ponec and Resnick 1984; Stuart Macadam 1987a,b, 1989). These radiographic studies illustrate a pattern of bone changes to the skull and orbits that include a thickening or widening of the diploic space, a "hair-on-end" trabecular pattern, texture changes to trabeculae, erosion or thinning of the outer lamina, and altered development of the frontal sinuses (e.g. Aksoy et al. 1966; Reimann et al. 1975; Steinbock 1976; Sebes and Diggs 1979; Stuart-Macadam 1987a). This radiographic pattern of bone changes resembles the pattern of bone changes observed on clinical radiographs of patients with chronic acquired or genetic anaemias associated with moderate to severe marrow hyperplasia (Stuart-Macadam 1987a) and, as such, have been applied in a number of research studies for diagnosing anaemia in archaeological skeletal collections (e.g. Stuart-Macadam 1989, 1992; Wright and Chew 1998; Lagia et al. 2007; Vercellotti et al. 2010).

With some pathological conditions, such as Paget's disease, treponematosis, fractures, and severe anaemia radiographic features may be uniquely characteristic and are easily identified and reliably diagnosed in archaeological bone. This is because clinically, the diagnosis of these conditions is heavily based on radiographic features which are well documented in the clinical literature (e.g. Stuart-Macadam 1987; Cushing 2002). In these cases, the issue of superimposition of bone structures in two-dimensional radiographic images is often irrelevant. However, care is required in the differential diagnosis of conditions including mild anaemia, rickets, and scurvy as each can cause porotic lesions of the cranial vault and orbital roofs that have only subtle differences in gross morphology, particularly in the early stages of pathogenesis (Schultz 2001; Wapler et al. 2004). In cases where morphological differences in bone structural changes may be subtle, two-dimensional radiographic images may not be sufficient for a reliable diagnosis and three-dimensional structural data become vital to the process of differential diagnosis (Wanek et al. 2012).

With three-dimensional visualization, skeletal structures can be assessed morphologically, as well as measured quantitatively for the detection of subtle differences caused by pathological changes, resulting in more reliable differential diagnoses and a better understanding of the pathogenesis of non-specific skeletal lesions (Wu and Schepartz 2009). With the advent and increasingly widespread use of new radiological technologies and methods in the clinical sciences, such as computed tomography, options for more detailed and efficient three-dimensional visualization and analyses of internal bone structures have become available for palaeopathological research (e.g. Melcher et al. 1997; Spoor et al. 2000; Rühli et al. 2002a,b; van Kaick and Delorme 2005; Lynnerup 2008; Wade et al. 2009).

4.4.3   Clinical Computed Tomography

In the early 1970's, British engineer Godfrey Hounsfield and medical physicist Allan Cormack independently described an innovative medical technology to overcome the superimposition limitation of conventional radiography (Hounsfield 1973; Goldman 2007; Lynnerup 2008; Saab et al. 2008; Conlogue et al. 2010). In 1979, Hounsfield and Cormack shared the Nobel Prize in Physiology and Medicine for the development of

computed tomography (CT) (Lynnerup 2008; Saab et al. 2008; Conlogue et al. 2010). The introduction of this technology not only advanced diagnostic medicine, but also opened up new possibilities for the diagnostic imaging of skeletal disease. Since its development, CT and its post-processing applications have become highly valued non-destructive methods in anthropological research (Recheis et al. 1999; Spoor et al. 2000; Rühli et al. 2002). However, access to CT technology by palaeopathologists has been difficult due to the lack of availability of equipment for non-medical research and the limited budgets of many researchers. Fortunately, these limitations are gradually being overcome for some researchers as more facilities become equipped with CT imaging systems, including some non-medical research facilities. With the increasing availability and affordability of CT scanning equipment, CT methods should be considered in the following research contexts: 1) when additional diagnostic information on the internal three-dimensional morphology of bone is desired and there is a need to preserve the archaeological material under investigation; and 2) when qualitative and quantitative data on internal pathological bone changes that are not obtainable from gross visual or radiographic methods may contribute to a more reliable differential diagnosis (Wanek et al. 2012).

A detailed history of the development of the various early and modern CT scanners will not be included here, but can be found in Seeram (1994) or Bushong (2008). The basic principles of CT image production and analysis will be discussed in limited detail below. Regardless of their design, all CT scanners share the same basic elements: an X-ray source, an image detector, and a computer. With CT scanners, X-rays are produced, emitted, and interact with matter in the same way as in conventional radiography. Unlike radiography, however, CT incorporates a coordinated motion between the X-ray source and the image detector (Goldman 2007; Conlogue et al. 2010). With traditional medical CT scanners, a configuration of rotating X-ray beams and detectors revolve 360º in a helical or step-wise progression around the sample being analyzed within a doughnut-shaped structure called the gantry, where the X-ray tube and detector are housed. The sample is positioned on a table that moves through the gantry as the X-ray tube and detector revolve. Instead of capturing a single projected image on film, the image receptor in a CT scanner is replaced by a detector that captures and stores collected X-ray

attenuation data to a computer that translates those data into an image (Bushong 2008; Saab et al. 2008; Scarfe and Farman 2008; Conlogue et al. 2010). For each angle, or direction, of the X-ray beam, the scanner records the X-ray attenuation of the different tissues or materials that make up a section of the sample. The computer then analyzes the various X-ray attenuation profiles collected from each projection angle around the sample, superimposes those profiles mathematically, and reconstructs individual image slices through the sample. In contrast to radiography, hundreds or thousands of slices are produced and can be viewed as serial, two-dimensional (2D) cross-sectional images (Bushong 2008; Goldman 2007; Lynnerup 2008). These 2D cross-sectional images can then be stacked using post-processing software programs to obtain a three-dimensional (3D) representation of the scanned sample and its internal structures (Scarfe and Farman 2008). Since CT images are essentially "cuts" through a sample, the sample is presented in cross-section without the issue of superimposition of adjacent and nearby structures (Goldman 2007; Saab et al. 2008).

Although a CT image appears as a continuous display of slices of tissue, it is actually made up of an array of 2D pixels, each of which represents a 3D volume of tissue within the slice (voxel). In other words, the X and Y dimensions in the plane of the slice are the same for a voxel and its representative pixel. However, the voxel also has a third dimension, Z, which corresponds to the thickness of the CT image slice. Each pixel is displayed as a level of brightness on a gray scale that represents the attenuation coefficient of the tissue contained within the voxel (Carlton and Adler 2001; Goldman 2007; Bushong 2008). Since each type of tissue or material attenuates X-rays differently, specific tissue types can be characterized by the reconstruction computer as a numerical value known as a CT number. CT numbers are measured in Hounsfield units (HU) which are scaled and calibrated arbitrarily using the attenuation of water and air as standards. Water will have an HU value of 0 and air will have an HU of -1000. Tissues or other materials that are more dense than water are represented by positive CT numbers and include bone (+3000) and muscle (+50). Negative CT numbers represent materials that are less dense than water, including fat (-100) and lung tissue (-200) (Gedgaudas-McClees and Torres 1990; Seeram 1994; Bushong 2008). During the final stage of image reconstruction, the CT numbers are converted into a gray-scale which is then used to

differentially shade the pixels that make up the 2D CT image (Hseih 2003; Bushong 2008; Lynnerup 2008). This gray scale can be manually adjusted in CT image visualization software so that tissues with only slight attenuation differences can be perceived as separate and that gray levels for the structure of interest are optimized. Adjusting the gray scale in this way is referred to as windowing (Seeram 1994; Bushong 2008).

As with conventional radiography, the quality of a CT image is determined by several factors including radiation dose, spatial resolution, contrast resolution, noise, and image artifacts (Bushong 2008). Radiation dose is a significant factor that must be considered when scanning living subjects, but is less of a concern with skeletal remains. While the dose to archaeological dry bone can theoretically be higher, ancient DNA may be damaged by very high dose radiation and it is wise to use as low a radiation dose as necessary to achieve adequate spatial resolution (Wanek et al. 2012). Knowledge of the remaining factors is also essential for setting up and optimizing a CT examination and in making a reliable diagnosis from the resulting images (Gedgaudas-McClees and Torres 1990; Seeram 1994).

Spatial resolution is one of the most important characteristics of a CT image and, similar to conventional radiography, refers to the ability to differentiate tissues, materials, or objects of varying density a small distance apart against a uniform background (Robb and Morin 1991; Seeram 1994; Stock 2009). Owing to certain limitations of the CT imaging system, image blurring is an inevitable aspect of CT images and a loss of detail along sharp edges of anatomical structures is to be expected (Gedgaudas-McClees and Torres 1990; Seeram 1994; Bushong 2008). Spatial resolution in CT imaging systems depends on several factors including the capabilities and limitations of the X-ray detector, focal spot size, and geometric magnification (Holdsworth and Thornton 2002; Stauber and Müller 2008; Stock 2009). The effects of focal spot size and geometric magnification have been discussed in the previous section; therefore, the following discussion will focus on the capabilities of the X-ray detector.

Since spatial resolution is a function of pixel size, the degree of blurring in a given set of CT images can be controlled by making adjustments to the pixel size as well as the slice thickness (voxel) (Bushong 2008). As a general rule, the smaller the pixel size, the better the spatial resolution. This is because structures that are smaller than a given pixel size will not be resolved. Since each pixel in a CT image is represented by a single gray-scale value, individual structures within a pixel will be blurred together. It may be possible to detect high-contrast structures that are smaller than the pixel size if their attenuation values are large enough to significantly affect the gray scale value of an individual pixel, but the specific structure itself will not be resolved (Seeram 1994; Bushong 2008; Bushberg et al. 2011). This must be kept in mind when determining the pixel size needed to resolve structures of interest in the resultant CT images. Depending on the capabilities and set up of the CT scanner and detector and the dimensions of the sample being scanned, the pixel size should be adjusted so that it is smaller than the specific structures of research interest. Adjustments to pixel size can be accomplished by making changes to the size of the scan field of view and/or the size of the image matrix. The scan field of view, also referred to as the reconstruction circle, refers to the circular region from which the attenuation measurements are recorded during a scan. The scan field of view contains the sample to be scanned and should exceed the dimensions of the sample. Therefore, larger samples may limit adjustments to pixel size (Stauber and Müller 2008). The image matrix is the two-dimensional grid of pixels that is used to display images on a computer monitor. The matrix determines the number of rows and columns of pixels that make up the image and can range from 64 x 64 to 2048 x 2048 and varies based on the maximum size of the detector in a given imaging system (Gedgaudas-McClees and Torres 1990; Seeram 1994). Most clinical scanner detectors can provide matrices of 512 x 512, resulting in a total of 262,144 pixels (Bushong 2008). To adjust the pixel size in a system with a fixed matrix size, the scan field of view can be increased or decreased. A decrease in the field of view will decrease the size of each pixel proportionately. When the field of view is fixed, pixel size may be decreased by increasing the size of the image matrix that is placed over the field of view if the detector size can be manipulated (Seeram 1994; Bushong 2008).

Thinner slice thicknesses also allow better spatial resolution. When CT numbers are computed for each pixel, the calculations are based on the linear attenuation coefficients for the voxel of tissue. If the voxel contains only one tissue type, then the calculated CT number will accurately represent that tissue. However, if the voxel contains two or more tissues or materials with different CT numbers, the final calculated CT number will be based on an average of the included tissues. This is known as partial volume averaging. For example, if a voxel partially contains both dense bone with a CT number of 1000 and white matter with a CT number of 46, the CT number that will be calculated for the voxel in the displayed image would be 523, which represents neither tissue actually present in the voxel. This partial volume averaging results in an image artifact called the partial volume effect (Seeram 1994; Bushong 2008; Stock 2009). Scanning samples at thinner slice increments will reduce the potential for including several tissues in a single voxel, thereby minimizing partial volume artifacts and improving the spatial resolution of CT images (Bushong 2008). Modern clinical CT scanners can provide X and Y voxel dimensions that vary from 100 microns (μm) to over 2mm, with slice thicknesses that can be adjusted from 0.5 to 10mm (Gedgaudas-McClees and Torres 1990; Seeram 1994; Bushong 2008). As with pixel size, determining an appropriate slice thickness requires a detailed consideration of the research questions being asked and the minimum spatial resolution requirements that are needed to answer those questions. If structures of specific interest are resolved in enough detail to achieve outlined research goals with a nominal spatial resolution of 1mm and a slice thickness of 2mm, then setting up a CT examination for higher resolution images (e.g.100μm with a slice thickness of 1mm) will only contribute to increased time and financial costs without contributing additional data.

The definition of contrast resolution in conventional radiography can also be used to describe contrast resolution in CT. However, the contrast resolution provided by CT is considerably higher than that available in conventional radiography and is affected not only by kVp and mAs, but also by slice thickness, detector sensitivity, image reconstruction algorithms, and noise. In conventional radiography, although image contrast between soft tissue and bone is easily detected, it is limited in its ability to produce contrast between the various soft tissues. Small differences in tissue density are obscured as a result of anatomy superimposition and a maximum density difference of

about 10% can be discriminated (Curry et al. 1990; Gedgaudas-McClees and Torres 1990; Seeram 1994). CT, on the other hand, can detect density differences ranging from 0.25 to 0.5%, since all of the tissues within a slice are viewed directly and because gray scale ranges can be manipulated through the process of windowing (Gedgaudas-McClees and Torres 1990). In palaeopathological investigations of dry bone, selecting appropriate CT and image settings for achieving optimal contrast resolution can be important for the investigation of pathological conditions, such as osteoporosis, infectious disease, and vitamin D deficiency, wherein small density changes to bone structures can aid in understanding the pathogenesis of disease (e.g. Cesarani et al. 2003; Kuhn et al. 2007). Contrast resolution, like spatial resolution, can also be enhanced by maximizing the number of pixels in the image (Farr and Allisy-Roberts 2004; Wanek et al. 2012).

Noise in CT is defined simply as the presence of graininess or a mottled appearance that is visible in CT images. If a homogenous material such as water is imaged, each pixel should have a CT number of 0. Since no imaging system is perfect, the CT numbers may average 0, but a range of values above or below zero will exist. This fluctuation in CT numbers from pixel to pixel is the noise of the system (Seeram 1994; Bushong 2008). CT scans with low noise levels will produce smooth images whereas scans with high noise produce grainy or spotty images. The presence of image noise reduces contrast resolution and image quality. The amount of image noise can be changed by manipulating the quantity of X-rays that are absorbed by each voxel. This can be done by increasing the kVp and/or mAs, or by increasing voxel size by manipulating slice thickness and pixel size. However, changes to these factors, particularly voxel size, involve a trade-off as these solutions will reduce the spatial resolution (Gedgaudas-McClees and Torres 1990; Bushong 2008; Wanek et al. 2012).

In addition to noise, a number of different image artifacts such as motion, metal, and beam hardening can also degrade CT image quality and affect image detail. Motion artifacts occur when the individual projections taken during the scan do not fit together properly at the later reconstruction stage, resulting in distortion or streak artifacts (Gedgaudas-McClees and Torres 1990; Stauber and Müller 2008). Distortion and/or streaking can significantly affect the ability to observe and analyze structures of interest

from obtained CT images. In addition to movement, the presence of metallic materials will also give rise to streak artifacts. With archaeological samples, metal materials may be encountered in collections where metal tape or wires have been used as part of restorative or preservation efforts. If metal materials cannot be removed from fragile samples, some post-processing software programs may be available to reduce metal streak artifacts (Seeram 1994). Finally, the most commonly encountered artifact in CT scanning is beam hardening. Beam hardening is the result of a "hardening" of the X-ray beam where low energy X-rays are absorbed as the beam passes through the object, increasing the mean energy of the beam after it passes through the object. This means that the effective attenuation coefficient of the sample material is altered and the resultant CT numbers will change. The change in CT numbers will cause the edges of an object to appear brighter than the centre, even if the material is the same throughout (Seeram 1994; Ketcham et al. 2001). Beam hardening artifacts can be reduced or eliminated by the use of beam hardening correction options during the image reconstruction stage. Another method for reducing beam hardening artifacts is by "pre-hardening" the X-ray beam by passing it through an attenuating filter before it passes through the scanned sample. Filters are commonly flat or shaped pieces of metal such as copper, brass or aluminum (Ketcham et al. 2001).

Once a set of CT projections is acquired, they are stored in the computer's memory. The set of 2D cross-sectional images are then reconstructed from these projections by a mathematical process called filtered back projection. Back projection is the process in which the computer takes the data collected for each scan view and back projects them over a plane to create an image. The images are then imported into CT reconstruction software programs where they can be automatically or manually corrected for beam hardening artifacts and improving image sharpness. Reconstruction algorithms can also be applied to reduce additional noise (Seeram 1994). Once the selection of reconstruction options is completed, the reconstruction and acquisition of the CT volume can be initiated and volume files are created.   These CT volumes can then be imported into 3D visualization software, for instance, Amira (http://www.amiravis.com), Mimics (http://www.materialise.com), or VGStudio MAX (http://www.volumegraphics.com), where they can be qualitatively analyzed as serial 2D cross sections in the axial plane, or

can be reformatted to view sections from all three anatomical planes: axial, sagittal, coronal. CT volumes can also be reconstructed into 3D virtual objects that can be manipulated using a variety of 3D graphic tools (Elliott and Dover 1982; Rühli et al 2007; Conlogue et al. 2010). Specific structures can also be manually delineated and extracted from the larger sample and viewed separately as 3D virtual objects. These programs also include measurement options for obtaining quantitative data such as linear, angle, and density measurements directly from the 2D cross-sections, as well as 3D graphic measuring tools that can be used to accurately determine size, angles, areas, and volumes from the virtual representation of a sample or object (Lynnerup 2008; Wu and Schepartz 2009). As such, this digital technology has allowed palaeopathologists to explore archaeological human remains in non-invasive ways and has shifted research questions to not only include diagnostic criteria based on qualitative observations, but to also consider what quantitative data have to offer for improving the reliability of diagnoses from archaeological human remains and for our understandings of disease processes in the past.

The most common application of CT in bioarchaeology has been in the analysis of mummies (e.g. Harwood-Nash 1979; Lewin et al. 1990; Cesarini et al. 2003; Gardner et al. 2004; Shafik et al. 2006; McErlain et al. 2007). The first CT scan of Egyptian mummy material was performed on September 27, 1976 on the preserved and desiccated brain of Nakht (Lewin and Harwood-Nash 1977). Using 3D imaging software, scanned mummies can be unwrapped and dissected non-invasively in a virtual environment, allowing for the accurate and detailed documentation of preserved skin, the skeleton, and the process of Egyptian mummification procedures (Chan et al. 2008). This can be done through the process of manually delineating and extracting soft tissue from bone so that both can be visualized and manipulated separately as 3D objects (Lynnerup 2008). The application of CT methods also allows researchers to assess sex, determine age, estimate stature, identify artifacts and foreign objects, and to identify anatomical abnormalities or pathological changes without having to destroy the integrity of the mummy (Gardner et al. 2004; Wu and Schepartz 2009).

Due to the success of CT based research on mummies throughout the 20th century, it became clear to researchers in bioarchaeology and palaeopathology that CT may be a valuable tool for investigating ancient health and patterns of disease in the past (van Kaick and Delorme 2005; Wu and Schepartz 2009). In 2002, the first CT-guided biopsy of an Egyptian child mummy was performed by Rühli and colleagues to demonstrate the value of CT methods to palaeopathological research. Based on initial radiographs, previous researchers had suggested a diagnosis of spinal tuberculosis in this individual. The use of CT-guided biopsy allowed Rühli and colleagues to refute this initial diagnosis and suggest that the changes observed in previous radiographs were, in fact, the result of the post-mortem disintegration of the thoraco-lumbar junction (Rühli et al. 2002a). CT methods have also been used to scan and evaluate pathological changes in hominin fossils, since destructive research is impossible due to the rare nature of these fossils (e.g. Spoor et al. 2000; Zollikofer et al. 2002). In CT scans of the Singa fossil calvaria from the Sudan, newly deposited pathological bone was noted in the inner ear, obliterating the inner air spaces. In addition, diploic expansion at the parietal bosses which is suggestive of hemolytic anaemia was also documented, indicating that the Singa individual experienced considerable impairment during life (Spoor et al. 1998). CT has also informed the investigation of non-specific and specific infectious diseases such as osteomyelitis (e.g. Alt and Buitrago-Téllez 2004) and leprosy (Haas et al. 2000) in archaeological skeletal remains outside of the context of mummy research. In 2004, a study by Exner and colleagues reported the value of the use of CT in the 3D visualization of porotic hyperostosis of the orbital roof. However, this research focused on qualitative visualization and failed to address the issue of assessing the pathogenesis of the bony changes (Exner et al. 2004). Although the literature abounds with research on the gross visual and radiographic appearance of porotic hyperostosis, to date there appears to have been only one micro-CT-based exploration into the pathogenesis of orbital porotic hyperostosis, but small sample size limited the findings of this research (e.g. Galea 2013).

The process of establishing an accurate differential diagnosis in palaeopathology using CT scanning techniques is similar to that of conventional radiography and relies first on obtaining the best possible set of CT images of the specimen (Chhem et al. 2008). Again, this requires at least some basic knowledge and training on the principles of CT scanning

and an understanding of the proper settings and operation of CT equipment. Palaeopathologists and bioarchaeologists interested in using CT techniques must also familiarize themselves with the process of CT image analysis and must be able to recognize the appearance of abnormal and pathological bone changes on CT cross-sections including abnormal thickening of cortical and/or trabecular bone, newly deposited bone structures, resorption of cortical and/or trabecular bone, changes in bone density, and evidence of taphonomic changes. Finally, researchers must also be trained on the use of 3D visualization programs and the types of analytical tools that are available for the qualitative and quantitative assessment of 2D images and 3D virtual reconstructions. A thorough knowledge of the applications available in these programs is necessary to ensure the extraction of as much information as possible from CT data (Lynnerup 2008).

Since the role of CT in the identification and analysis of disease in archaeological dry bone is still being established in the literature, standard protocols and techniques for collecting data from CT scan images continue to be refined and new methods for the morphometric analysis of bone structures continue to be developed. Although several relatively recent publications on the development of standardized protocols for diagnostic palaeoradiology have become available (e.g. Chhem and Brothwell 2008; Beckett and Conlogue 2010; Grauer 2012), there is still no single standardized protocol or terminology for the collection of data from CT scans in palaeopathology. Therefore future palaeopathological research should focus on improving diagnostic precision and the comparability of data through the standardization of CT scan and image analysis protocols as well as descriptive terminology. As protocols and standards designed to study skeletal disease using CT are developed and refined, the role of this method in the differential diagnosis of skeletal lesions in palaeopathology can be further explored.

In addition to providing non-destructive high-resolution images of internal structures of mummified tissues and bone, there are several other advantages to the use of CT techniques in bioarchaeology and palaeopathology. First, because clinical CT scanners are designed for rapid full body scanning of patients, no sample preparation is needed and image data can be acquired within several hours or less depending on CT settings and

sample size (Seeram 1994; Stauber and Müller 2008). Sample sizes fit for CT scanning can range from a single skeletal element to a complete, wrapped mummy, including the sarcophagus in some cases. This means that for palaeopathological research questions, a complete skeleton can be CT scanned for abnormalities and pathological changes, or scans can be limited to individual bones or bone fragments with suspected or confirmed pathological lesions. Second, since CT image data are created and stored digitally, permanent digital records of scanned samples are created which can be assessed, re-assessed, and shared or exchanged between researchers across the globe while still preserving the original condition of archaeological remains for future studies (Seeram 1994; Lynnerup 2008; Wanek et al. 2012).

Perhaps the greatest disadvantages of CT scanning techniques in palaeopathology are the accessibility and cost of using the equipment (Lynnerup 2008; Conlogue et al. 2010; Wanek et al. 2012). CT scanners have been designed for diagnosing disease and injury in living patients and this takes precedence over imaging individuals who have been long dead. This means that gaining access to a scanner often involves negotiating with clinical imaging facilities for times when patients are not scheduled (Conlogue et al. 2010). There are also significant operating costs that may limit the use of CT scanning techniques in palaeopathology (Ortner 2008; Conlogue et al. 2010). Living patients can be scanned in 5-10 minutes as the region to be scanned is known and pre-set patient protocols eliminate the amount of time needed to determine the technical factors required to scan a specific region. Without specific target regions and pre-set protocols for mummified and dry skeletal tissues, CT examinations can take up to several hours for one sample. Because the average cost of a clinical CT scanner can range from $850,000 to $950,000 with yearly maintenance and software updates that can cost up to $120,000, longer CT examination times can be extremely costly. In recent years, several facilities dedicated to research outside of medicine have been equipped with CT scanners and have improved the overall availability and accessibility of this equipment for anthropological research, but these facilities are currently the exception (Conlogue et al. 2010).

The misuse or misapplication of CT settings by improperly trained individuals or radiologists unfamiliar with CT protocols necessary for achieving optimal diagnostic

images from dry bone can also be a major disadvantage. Unfortunately, since CT scanners are designed with built-in protocols for scanning living people, it can be time consuming and costly to manipulate pre-set protocols for mummified and skeletal tissue. Several hours of trial and error are often necessary to determine the correct settings that will result in high quality CT images of dehydrated soft tissues and dry bone (Conlogue et al. 2010).

Finally the evaluation of bone micro-architecture which, in some cases, is necessary for achieving a reliable differential diagnosis in palaeopathological research is limited by the resolution achievable by most clinical CT scanners (Stauber and Müller 2008). Most modern clinical CT scanners can reach a spatial resolution of about 0.3 mm and a slice thickness around 0.5 mm which is ideal for the diagnostic assessment of larger soft tissue structures and bone morphology, but does not meet the resolution requirements for clearly displaying internal skeletal micro-anatomical structures such as the thickness, shape, and orientation of trabeculae (Kuhn et al. 2007; Stauber and Müller 2008; Wu and Schepartz 2009). The spatial resolution and slice thickness limitations of clinical CT scanners may result in substantial partial volume effects when the assessment of smaller structures is desired. Partial volume artifacts will degrade the quality of the CT images for smaller structures making the three-dimensional qualification and quantification of structures such as trabeculae difficult if not impossible (Zollikofer and Ponce de León 2005; Lynnerup 2008). Additionally, due to the nature of conventional CT images, spatial resolution will be maximized in slices viewed in the axial plane. This is because the voxels that make up individual CT images with most CT scanners are anisotropic. Anisotropic voxels are non-cubic rectangular voxels where the longest dimension is in the plane of the slice thickness (Z-plane). The effects of anisotropy mean that spatial resolution will be lower and the partial volume effect will be greater in the reformatted sagittal and coronal slices produced from the reconstructed CT volume (Scarfe et al. 2006). Therefore, CT images from the axial plane will be the most accurate for visualizing internal structures for diagnostic purposes. In cases where lesions are better visualized in the coronal or sagittal planes, the decrease in resolution and increase in partial volume artifacts can affect the accuracy of both qualitative and quantitative observations (Salvolini et al. 2000; Scarfe et al. 2006).

Overall, clinical CT techniques have proven to be of great value to anthropological research and, particularly, to the study of mummified human remains. The value of non-destructive CT imaging to palaeopathological research is significant and its role in the process of differential diagnosis continues to be explored (Lynnerup 2008). With the advent of research facilities dedicated to archaeological and geological research, CT equipment is becoming increasingly accessible for non-medical research. It is hoped that with the increase in availability and accessibility of this technology that research in palaeopathology using CT techniques will increase and will result in improved comparability of research data, the continued development of standardized CT protocols and methods of image analysis, and more reliable differential diagnoses from archaeological skeletal remains. It is important, however, to note that as a result of several limitations, clinical CT techniques may not be appropriate in all palaeopathological research contexts for which data on internal skeletal structures are desired. In some cases, improving the reliability of a differential diagnosis may require the examination of skeletal micro-architectures (Schultz 2001, 2012; Wapler et al. 2004), which is beyond the imaging capabilities of traditional clinical CT scanners. In these cases, bone micro-architecture is traditionally assessed using standard microscopic and histological procedures (Schultz 2001, 2012). Although CT is often valued over histology for its non-destructive applications, methods of microscopy and histology are considered to be the gold standard for the analysis of skeletal micro-architecture (Müller et al. 1998; Schultz 2001; Particelli et al 2011).

4.4.4   Microscopy and Histology

The history of histology goes back to as early as the 18th century soon after the invention of the microscope and the discovery of the cell by Robert Hooke in 1665 (Turner-Walker and Mays 2008). By the end of the 19th century, various microscopic techniques had been developed and the microscopic structures of bone had been described in medical contexts. At the same time, the first publication of microscopic structures of fossil bones appeared in the literature (Schaffer 1889). Later, significant work on the palaeohistology of modern and fossil animal bones was published by Enlow and Brown (1957, 1958). However, these works focused primarily on the evolution of bone as a tissue rather than

how bone microstructures may be affected by pathological or taphonomic processes. It was not until the 1920s that microscopy was applied to the analysis of pathological human bone with Weber's (1927) microscopic investigations of treponemal diseases in long bones (Schultz 2001). In the second half of the 20th century, important research was carried out on the palaeohistology of human skeletal remains using mainly thin-ground section techniques (e.g. Acsenzi 1969; Hackett 1976; Stout 1978). Today, over 3000 articles focused on the palaeohistopathology of human dry bone have been published and much anthropological work has been done on the histological determination of age at death and the study of diagenesis (De Boer et al. 2013). Regardless of the amount of research that has been done to date, the application of histology to the elucidation of palaeopathological conditions is limited. This is because microscopic examination requires destructive procedures and its potential use requires careful consideration. Museum curators are increasingly reluctant to allow irreversible damage or destruction to archaeological specimens and in many places institutional policies prevent destructive sampling (Ortner 2003; Turner-Walker and Mays 2008). As such, more than any other method used in palaeopathology, researchers must consider if microscopic methods are necessary for answering the research questions being asked. It is recommended that these methods only be applied in palaeopathological research when other non-destructive methods have been considered and when the end justifies the means. In other words, the expected microscopic findings must be of significant enough value to the advancement of our knowledge of pathological features and their relationship to the etiology of a disease that it justifies damage to, or the complete destruction of, archaeological bone (Turner-Walker and Mays 2008; Schultz 2001, 2012). Similar considerations must be made when applying chemical, DNA, and other destructive analyses (e.g. White 1993; Katzenberg et al. 1996;; Katzenberg 2000; Drancourt and Raoult 2005; Barnes and Thomas 2006; Cerutti et al. 2007; Donoghue 2008).

During a palaeopathological investigation, the situation often arises that no reliable diagnoses can be established by macroscopic or radiological techniques. Frequently, diagnoses established using these techniques can be doubtful as gross morphological changes caused by several diseases are often similar in their appearance. In addition, skeletal remains are often altered by diagenetic processes which may imitate true

pathological changes (Wapler et al. 2004; Schultz 2012). However, many diagenetic changes occur at the micro-level and are not visible on conventional radiographs and are difficult to differentiate at the maximum nominal resolution available with conventional CT images (Schultz 2001, 2012). In these cases, if it is likely that microscopic data would be valuable to the process of differential diagnosis, further investigation using these techniques should be considered (Schultz 2001, 2012). An immediate, reliable diagnosis may only be possible in a few cases. However, the inclusion of histological based observations can provide information on the different growth and resorption behaviours of pathological bone, and the differentiation of normal and pathological structural changes to microscopic cortical and trabecular components of bone. Accordingly, diagnosing pathological conditions at the micro-level has led to an increased understanding of the mechanisms of pathological bone change and disease processes in the past (Schultz 2001, 2012; Turner-Walker and Mays 2008).

The most common microscopic technique applied to dry archaeological bone is light microscopy, which is relatively inexpensive but somewhat time consuming (Schultz 2012). A brief history of light microscopy and the basic features and mechanics of the microscope are provided in Cho (2012) and will not be detailed here. Other techniques including scanning electron, confocal laser scanning, and transmission electron microscopy are much more elaborate and expensive microscopic methods that may be useful with regard to specific research aims, but often do not contribute any additional information to palaeopathological research when compared to light microscopy using transmission or polarized light (Schultz 2001, 2012). A number of techniques for the preparation of archaeological bone for microscopy have been derived from standard histological methodologies developed for the analysis of soft and mineralized modern tissues. Detailed descriptions of these techniques can be found in Caropreso et al. (2000), Schultz (2001), and Maat et al. (2001, 2006).

Essentially, there are two methods for preparing dry bone for light microscopy: 1) decalcified, cut with a microtome, stained, and viewed using transmitted light, or 2) prepared and examined as thin-ground sections using transmitted or polarized light (Schultz 2012). Since archaeological bone is dry, brittle, and collagen is often poorly

preserved, histological examination requires the standardized thin-ground section procedure. This is because in order to maintain the structural integrity of archaeological bone during the cutting, grinding, and polishing process, samples must first be embedded in plastic resin (Caropreso et al. 2000; Cho 2012; Schultz 2012). Detailed protocols on the embedding process and on cutting, grinding, polishing, and mounting procedures have been published in Caropreso et al. (2000), Schultz (2001), Turner-Walker and Mays (2008), and Cho (2012). This process can take several days to several weeks and results in a mounted thin section of bone that has been ground to a final thickness of 15-100 microns (μm), thin enough to allow the penetration of light so that bone microstructures can be viewed under the microscope (Schultz 2001; Cho 2012).

The reliable palaeopathological diagnosis of disease from histological sections rests on two factors: the quality of the thin-section produced and a sufficient background knowledge of bone micro-architecture and the physiology of pathological bone change (Turner-Walker and Mays 2008; Schultz 2012). By directly viewing a high quality thin-ground section using light microscopy, pathological changes to microscopic bone structures arising from imbalances in bone remodelling caused by mechanical and hormonal disturbances can be identified (Turner-Walker and Mays 2008). These changes can be identified by assessing the nature of the architecture of cortical and trabecular bone structures (Schultz 1993, 2001, 2012). To determine whether cortical and/or trabecular structures have been pathologically altered, morphological features such as the orientation and organization of collagen fibres (lamellar versus woven bone), the presence and thickness of circumferential lamellae, the size, thickness, and orientation of trabeculae, the distribution and number of Howship's lacunae, and the development of special cement lines should all be assessed (Schultz 2012). In order to obtain the maximum amount of information for a reliable differential diagnosis, all possible microscopic observations should be documented from the thin-ground section and described using standardized terminology.

As has been mentioned previously porotic hyperostosis of the cranial vault and orbital roofs is not a term that is used to refer to a disease or condition but rather to describe the morphological expression of several different conditions including anaemia, scurvy,

rickets, and inflammatory conditions (e.g. osteitis/osteomyelitis). Further complicating the issue of the differential diagnosis of these lesions is that several of these conditions can often co-occur in the same individual. Since these different conditions result in the same morphological expression, reliable differential diagnoses can often not be made using macroscopic investigation alone. Using techniques of histology and microscopy, Schultz (2001, 2012) has suggested that a particular disease process may be identified by diagnostic patterns of bone changes that are represented by the micro-architectural elements of bone. According to Schultz (2001, 2012) these patterns of changes are not found in their exact form in any other disease process and are, therefore, an efficient key to accurate diagnosis.

In lesions characteristic of anaemia, bone trabeculae will be abnormally thinned and oriented vertically. These microscopic changes will also be accompanied by the thinning of the cortical bone of the external lamina (Wapler et al. 2004; Schultz 2001, 2012). In scurvy, micro-morphological changes should reflect an organized hematoma and will only be found as newly built bone formations on the external surface of the cortical bone lamina below the periosteum. The original cortical and trabecular bone structures should remain pathologically unchanged (Schultz 2001, 2012). Rickets will affect bone micro-architecture as a whole because vitamin D deficiency is a systemic condition (Schultz 2012). The external cortical bone lamina will appear as layers of squamous plates, the internal cortical lamina will appear splintered, and trabecular structures will take on an irregular pattern rather than being oriented tangentially (Schultz 2001). Finally, in an inflammatory process, such as periostitis or ostemomyelitis, osteoclastic and osteoblastic reactions will significantly or completely destroy the normal physiological structure of both cortical and trabecular bone (Schultz 2001). An increased number of Howship's lacunae will be visible as a result of increased osteoclast activity (Wapler et al. 2004; Schultz 2012). Newly built bone may also be present if stages of healing had taken place and will be represented by gracile and irregularly oriented trabeculae and cement lines between lamellar and new woven bone (Wapler et al. 2004; Schultz 2001, 2012). These research findings suggest that by using the sum of all of the microscopic morphological features observed on the thin-section, a relationship can generally be established between

the nature of bone changes and general or specific pathological conditions (Schultz 2001, 2003, 2012).

In most cases, identified pathological micro-architectural changes can be allocated to general categories of disease and perhaps even to more specific categories such as hematological disorders, metabolic disorders, or inflammatory conditions. Although Schultz (2001, 2012) has optimistically stressed that specific diagnoses can be made to explain the presence of porotic hyperostosis, it is important to keep in mind that microscopic evidence may also not be sufficient for achieving a reliable differential diagnosis in all cases (Boer et al. 2013). For example, the presence of an isolated ossified hematoma on the cranial vault is not pathognomonic of scurvy, but rather indicates the presence of a non-specific hemorrhagic process (Van der Merwe et al., 2010). A diagnosis of scurvy can only be achieved in combination with gross visual methods that include the location and distribution of lesions, as well as a thorough consideration of the sociocultural and environmental contexts of the remains, and even then a definitive diagnosis may not be possible. This is not to say that the diagnosis of specific diseases using methods of microscopy is impossible. A recent review of the literature by De Boer et al. (2013) reveals that a few pathological conditions demonstrate specific histological features including Paget's disease, osteoporosis, hyperparathyroidism, and possibly osteomalacia. In all other cases, microscopic and histological methods may aid the process of differential diagnosis, but are unable to confirm a definitive diagnosis (Boer et al. 2013). As such, although promising, the research done by Schultz (2001, 2012) should be considered carefully and critically. Not only does this research appear to lack the inclusion of supportive and comparative clinical data on microscopic changes that different diseases show in dry bone, there is also the issue of diagnostic bias since these observations were not made using blind data collection methods. This does not preclude the use or value of microscopic and histological methods in palaeopathology, but rather stresses the need for future research in which histopathological diagnoses from archaeological bone are supported by experimental and comparative research or research with the use of clinically documented dry bone reference specimens (e.g. Assis 2013; De Boer et al. 2013).

In addition to qualitative observations, skeletal researchers have increasingly applied quantitative techniques in order to analyze the amount, size, and shape of various microscopic features of archaeological bone from thin sections (Ericksen 1976; Martin and Armelagos 1985; Cook et al. 1988). These quantitative techniques are known as histomorphometry and are often used in the clinical diagnosis of skeletal disease. The histomorphometric analysis of bone provides quantitative information on bone remodelling and three-dimensional micro-architecture and has been an important clinical diagnostic tool for assessing pathological changes to microscopic cortical and trabecular structures (Parfitt et al. 1983; Odgaard et al. 1994; Barbier et al. 1999). In anthropology, age-at-death estimation and the determination of human from non-human bone have been the most widely explored areas of histomorphometric research (Stout and Crowder 2012). However, the diagnostic value of histomorphometry for archaeological bone samples has not been overlooked in palaeopathological investigations. Several researchers have explored the applications of these techniques in an attempt to establish relationships between the patterns of cortical and trabecular architecture and bone dynamics both in normal and pathological states (e.g. Frost and Wu 1967; Cook et al 1988; Goldstein et al. 1993; Arlot et al. 2008).

The morphometric parameters most often assessed from thin sections of bone include bone volume density, specific bone surface density, trabecular thickness, trabecular number, trabecular spacing, trabecular connectivity, and the degree of trabecular anisotropy (Goldstein et al. 1993; Müller et al. 1998; Barbier et al. 1999; Stauber and Müller 2008). These morphometric parameters, also referred to as structural indices, are detected and measured from histologic thin sections and changes to cortical and trabecular structures are, therefore, observed only in two dimensions. In order to transform two-dimensional quantitative data into three dimensional structural data for analysis, stereological techniques must be applied using innovative computer software (Feldkamp et al. 1989; Barbier et al. 1999; Ulrich et al 1999). Therefore, the third dimension is added on the basis of mathematical theorems used in stereology (Müller et al. 1998). However, since stereological analyses are capable only of indirectly inferring 3D micro-architectural morphology, these analyses do not produce true 3D data (Barbier et al. 1999; Jiang et al. 2000). In clinical studies, several researchers have tried to

establish predictive relationships between histomorphometric structural data and the mechanical and cellular properties of bone (e.g. Cowin et al. 1985; Goulet et al. 1994). Unfortunately, unexplained variation in the predictive value of these relationships was found between different studies and has been attributed not only to systematic errors, but also to the inadequacy of inferred 3D structural data to accurately reflect the true morphological structures of bone (Ulrich et al. 1999). In attempts to overcome the limitations of the quantitative analysis of 2D histological sections, the method of serial sectioning – the preparation of at least two or more serial thin sections from different levels of the same bone – has also been employed to explore the third dimension of micro-architectural structures (Feldkamp et al. 1989; Müller et al. 1998; Schultz 2012). Although this approach enables the measurement of several structural indices based on a truly three-dimensional approach, it requires the sectioning of a larger sample of bone and, once sectioned, these samples are no longer available for subsequent research and analysis, particularly in different anatomical planes (Müller et al. 1998). Additionally, being truly destructive, once a bone sample has been sectioned, there is no going back to an original, unaltered state. If a sample is embedded, sectioned, or mounted improperly or in the wrong location, information can be permanently lost in current and for future research.

Overall, the use of microscopic and histological methods in palaeopathology are of value in cases where differential diagnoses based on gross visual and radiographic features can be improved through the assessment of micro-architectural features. However, the identification of micro-anatomical processes in human skeletal remains and their interpretation are considered challenging (Aufderheide and Rodríguez-Martín, 1998; Ortner, 2003; De Boer et al. 2013). Clinical pathologists have the advantage of the presence of soft tissue and bone tissue cells, and it is these components that provide the pathognomonic features that lead to reliable diagnoses in medicine and clinical research (e.g. Vigorita 1999; Rosai 2011). With the exception of mummified remains palaeopathologists are limited to dry bone, which is void of soft tissues and cells. Further complicating this issue is the nature of bone tissue, which only reacts to normal and abnormal stimuli in three ways visible on a microscopic level: bone formation (an osteoblastic bone response), bone resorption/destruction (an osteoclastic response), or a

combination of both (Ortner 2003, 2012; De Boer et al. 2013). Although Schultz (2001, 2012) appears optimistic that histological structural features can be linked to specific diseases, only a small subset of diseases can be associated with specific histological changes that can be regarded as pathognomonic (Stout and Simmons 1979; Waldron 2009). In other disease processes, microscopy and histology have significant potential for aiding in narrowing the list of potential disease categories and improving our current understandings of disease etiology and pathogenesis, but this will require continued research that includes clinical and comparative data.

Finally, although these methods are of value to palaeopathological research, microscopy and histology require time-consuming preparation procedures and the technique of thin-ground sections. This results in the significant destruction of valuable archaeological samples (Schultz, 2001; Rühli et al., 2007; Kuhn et al., 2007). Since the fragmentary and often sensitive nature of human remains often precludes the further destruction of archaeological bone, and since the preservation of skeletal collections for future research or repatriation remains a contemporary issue of ethical importance, the investigation of an alternative means of non-destructive high-resolution evaluation is critical (Rühli et al 2007; Wade et al. 2009).

4.4.5   New Technologies: Micro-Computed Tomography

With the ongoing development of clinical CT scanners, imaging technologies have evolved significantly over the last several decades and current CT systems have been developed to achieve higher levels of resolution while still employing the same physical working principles. In 1989, Feldkamp and colleagues were the first to build a micro-computed tomography (micro-CT) system for the non-destructive high-resolution imaging of three-dimensional bone micro-architecture in clinical investigations of osteoarthritis and osteoporosis in small animal models (Feldkamp et al. 1989; Kinney et al. 1995; Balto et al. 2000; Holdsworth and Thornton 2002). While the spatial resolution of clinical CT images can typically reach a maximum of 0.3 mm, micro-CT is able to achieve a spatial resolution between 10 to 100 times greater, ranging between 10 and 50 microns (μm), and structures traditionally visualized through microscopy and histology

can now be evaluated using imaging techniques (Feldkamp et al. 1989; Wanek et al. 2012).

The application of micro-CT techniques rather than conventional CT in any study of internal tissue and bone structures will depend on the maximum spatial resolution requirements needed to visualize specific structural features of interest, object shape and size, as well as whether or not quantitative structural data are required (Stock 2009). Since its development, this rapidly emerging technology has been used by a number of research groups to address the role of trabecular architecture on the mechanical properties of bone at the histological level both qualitatively and quantitatively (e.g. Goldstein et al. 1993; Rügsegger et al. 1996; Müller et al. 1998; Genant et al. 1999). For the investigation of diseases, Kurth and Müller (2001) examined the morphological features of osteolytic tumours, Tamada et al. (2005) examined metastases of prostate carcinoma, and micro-architectural changes to bone in osteoarthritis were investigated by Boyd et al. (2005). The application of this technology to clinical studies of the response of bone micro-architecture to disease processes such as those mentioned above, suggests that micro-CT may be of significant potential value to the process of differential diagnosis in palaeopathology (Rüegsegger et al. 1996; Rühli et al. 2007; Wanek et al. 2012). Qualitative and quantitative internal micro-structural data are not accessible by gross visual, radiographic, or conventional CT techniques. In cases where microscopic data have the potential to improve the reliability of differential diagnoses in palaeopathological research, and destructive 2D histological techniques are undesirable or inadequate, the application of micro-CT techniques may be of high value (Kuhn et al. 2007; Rühli et al. 2007).

The differences between conventional clinical CT and micro-CT are few and lie only in the size and design of equipment and the achievable spatial resolution. All micro-CT scanners follow the same general plan and operate under the same basic physical principles as conventional CT scanners. Detailed discussions of the different generations and components of micro-CT scanners can be found in Stauber and Müller (2008) and Stock (2009). In general, there are two types of micro-CT scanner setups. The first setup, which functions much like a conventional CT scanner, is gantry based and the

sample remains stationary while the x-ray tube and detector are rotated. These scanners are much smaller in design than their clinical counterparts and are typically used for small animals (in-vivo scanners), biomedical samples, microfossils, and other studies for which minute detail is desired. However, sample size is limited by the small size of the gantry, or by manufacturer provided sample holders in the form of cylindrical vials of different sizes, where the size of the sample holder reflects the maximum nominal resolution that can be achieved (Stauber and Müller 2008). This means that larger samples have to be prepared to fit through the gantry or into a sample holder matching the respective desired resolution (Stauber and Müller 2008; Stock 2009). This type of system is ideal for the analysis of small or fragmentary archaeological bones, but not for intact crania that are too large to be scanned without the need for destructive cross sectioning.

In the second setup, which is significantly different from conventional CT scanners, the X-ray source and large flat panel detector are stationary during the scan while the sample rotates on an open platform within a large X-ray cabinet (Stauber and Müller 2008; Stock 2009). Unlike the smaller micro-CT systems used for biomedical research, this setup is typically used for industrial applications and allows for high image resolution of larger samples. Micro-CT systems with these specifications are preferable for the high-resolution analysis of archaeological samples as the large cabinet and open platform obviate the need for destructive cross-sectioning of large samples such as complete skulls.

Micro-CT imaging systems offer several advantages over conventional CT and traditional histological methods for the evaluation and analysis of archaeological human bone. Unlike conventional CT scanners, not only does micro-CT offer higher resolution images in the micrometer range, the modified equipment set-up developed by Feldkamp et al. (1989) also allows micro-CT images to be reconstructed one to one in 3D, rather than as a series of two-dimensional slices (Feldkamp et al. 1989; Kuhn et al. 1990; Rühli et al. 2007). Instead of an array of linear detectors which rotate around a fixed sample and capture projection data as a series of 2D cross-sections, most micro-CT scanners are set-up with the source and detector in a fixed position and the object is rotated around its

long axis (Stauber and Müller 2008). The source is generally a microfocus X-ray tube with a focal spot diameter of 10-100 μm, and the detector is usually a large, flat, 2D panel which captures projections from hundreds or thousands of angles around the entire sample rather than around individual sections in sequence (Stauber and Müller 2008; Stock 2009). This particular setup results in micro-CT images that are made up of isotropic voxels (cubic voxels), which have the same dimensions in all three planes. Isotropic voxels overcome the image limitations of anisotropy encountered in conventional CT and allow for the visualization of 3D micro-architectural structures in all three anatomical planes with minimized partial volume effects (Feldkamp et al. 1989; Stauber and Müller 2008; Stock 2009).

One of the key advantages of micro-CT over histology is the ability to non-destructively qualify and quantify bone micro-structure in 3D. Evaluations of the morphological features and characteristics of cortical and trabecular bone based on 2D histologic sections are not necessarily representative of the entire 3D structure of the sample. Although the three-dimensional structure of cortical bone is relatively simple to characterize, trabecular bone structures are extremely complex and variable. Isolated 2D sections cannot provide a complete picture of the variation that occurs in trabecular micro-architecture whereas micro-CT imaging allows the true visualization of the 3D trabecular network of bone samples (Feldkamp et al. 1989; Guldberg et al. 2004; Rühli et al. 2007). Additionally, with the development of micro-CT, new image processing algorithms and quantitative analysis techniques have also evolved and post-processing tools for reliably measuring changes in bone micro-architecture and volume are available for the analysis of micro-CT image volumes (Feldkamp et al. 1989; Barbier et al. 1999; Holdsworth and Thornton 2002). Morphometric parameters traditionally collected from 2D histologic thin-sections and stereology can now be directly collected in three dimensions for non-destructive analysis (Barbier et al. 1999). Micro-CT post-processing computer programs, including Microview (www.parallax-innovations.com/microview) and VGStudio MAX (http://www.volumegraphics.com), offer 3D structure analysis tools that are capable of collecting data on the same morphometric parameters assessed from thin sections, including bone volume density, specific bone surface density, trabecular thickness, trabecular number, trabecular spacing, trabecular connectivity, and the degree

of trabecular anisotropy (Barbier et al. 1999; Ulrich et al. 1999; Stauber and Müller 2008). These data can be collected from specific regions of interest that can be placed across a small three-dimensional area, or from the entire scanned volume depending on the goals of a given research study.

Finally, the collection, reconstruction, and morphometric analysis of micro-CT images can typically be completed in several hours or less, depending on the sample size, scanning resolution, and efficiency of computer software and memory. A large number of bone samples can be scanned and analyzed efficiently and without the need for destructive sampling procedures. In comparison, the histological evaluation of archaeological bone samples, which includes cutting, embedding, sectioning, grinding, and polishing can take a week or more and causes irreversible damage and destruction to archaeological samples (Guldberg et al. 2004; Rühli et al. 2007).

In order to establish micro-CT as a reliable method for the 3D assessment and analysis of microscopic structures of bone, a number of studies have compared the capabilities of this technology with histological methods, the current gold standard, for its value as an alternative for the evaluation of bone micro-architecture (e.g. Müller et al. 1998; Balto et al. 2000; Kuhn et al. 2007; Rühli et al. 2007; Particelli et al. 2011). A review of these studies has demonstrated that there is a very high correlation between bone structural indices measured from 2D histological thin sections and from 3D analyses of micro-CT volumes, suggesting that micro-CT is an effective and efficient non-destructive alternative to histology. However, because micro-CT is a relatively new technology, its applications to the field of palaeopathology have not yet been fully explored. Micro-CT has mainly been used for clinical studies on altered mechanical properties of bone such as in osteoporosis (Müller 2003) or the influence of biomechanical stress on the development of trabecular structures (Fajardo and Müller 2001). To date, only a handful of palaeopathological studies have applied micro-CT techniques to the examination of historical and archaeological bone pathologies (e.g. McErlain et al. 2004; Kuhn et al. 2007; Rühli et al. 2007; Wade et al. 2009). Like conventional CT, micro-CT scanners and the specific software programs needed to reconstruct and visualize micro-CT images are expensive and the equipment is not yet readily available to the larger research

community, which may explain the lack of exploration into this method by palaeopathological researchers (Müller et al. 1998; Rühli et al. 2007). In recent years, various micro-CT scanners have become commercially available and researchers in a growing number of academic fields now own or have access to such scanners (Rühli et al. 2007). As such, the application of micro-CT imaging techniques to palaeopathological research is likely to become much more common in the future.

As with any other imaging modality, the key to obtaining reliable qualitative diagnostic data from micro-CT images lies with image quality. The manipulation of equipment and software settings during scan acquisition, reconstruction, and post-processing are no different than the procedures used in conventional CT and will similarly affect factors including spatial resolution, spatial contrast, noise, and artifacts (Stauber and Müller 2008; Stock 2009). However, since micro-CT is a relatively new technique, particularly for palaeopathology, the process and procedures for qualitatively and quantitatively analyzing pathological trabecular bone structures for diagnostic purposes have not yet been fully developed or standardized (Müller et al. 1998; Kuhn et al. 2007). As research into the applications of this technology in palaeopathology continues, standardized qualitative and quantitative diagnostic criteria of diseases and their differential diagnoses must be defined using clinical and comparative data from known diseases. Additionally, little is known regarding the effects of different methods of analysis on the results of structural quantification and how varying and unstandardized methods may affect the reliability and reproducibility of quantitative data (Müller et al. 1998). For these reasons, it is important that researchers investigate some of the basic effects and limitations with respect to methods of data acquisition in palaeopathological research that applies micro-CT techniques. This is particularly relevant if results for the quantitative evaluation of 3D structural properties are to be comparable across research studies in the future.

The methods of micro-CT scanning and three-dimensional visualization are powerful analytical tools for palaeopathological analyses of archaeological human remains. This technique allows the visualization and quantification of internal structures of bone at the micro-level (Kuhn et al. 2007; Rühli et al. 2007; Lynnerup 2008). With the continued development of micro-CT methods and the standardization of diagnostic criteria from

micro-CT images, the full potential of this technique to palaeopathological research can be explored. For example, these methods may be of particular value in the investigation of lesions with questionable etiology such as porotic hyperostosis, where micro-structural evaluation may contribute important data to the process of differential diagnoses. As suggested by Schultz (2001, 2012) micro-structural data on lesions of porotic hyperostosis may reveal distinct patterns of trabecular bone response to pathological processes. Although these data may not lead to specific diagnoses, they have the potential to increase our understanding of disease pathogenesis or, specifically, how bone micro-architecture adapts and changes throughout the different stages of a pathological process. To the best of my knowledge, microscopic research on porotic hyperostosis has so far been limited to the evaluation of qualitative diagnostic criteria with minimal exploration into quantitative analyses (e.g. Galea 2013). The application of micro-CT techniques offers a non-destructive means of not only validating current qualitative diagnostic criteria on porotic hyperostosis described by Schultz (2001, 2012), but also provides a means for supporting these subjective qualitative observations with objective quantitative data representative of 3D micro-architecture. Future palaeopathological research is needed to begin the process of standardizing methods of micro-CT analysis in palaeopathology so that the full potential of these methods to the process of differential diagnosis can be explored, and current gaps in the palaeopathological literature can be addressed.

4.5   Summary

The macroscopic study of skeletal lesions is likely to remain the foundation of palaeopathology not because it is inherently better than the available methodological alternatives, but because this method has been developed and standardized over a century or more and is the most readily available and commonly used method in palaeopathological research (Ortner 2003, 2012; Grauer 2008; Mays and Pinhasi 2008). Today, there remains a continued emphasis on the development and refinement of macroscopic diagnostic criteria (Steckel and Rose 2002; Ortner 2012). However, although there are some accessibility limitations as well as complications to the interpretation of data from radiological imaging and histological analyses of ancient

human remains, these techniques have recently played a significant role in palaeopathology and will continue to do so into the future.

A reliable differential diagnosis in palaeopathology should be achievable by using the sum of the results of all available and appropriate diagnostic methods including gross visual, radiological, microscopic, and biochemical techniques, as well as the inclusion of secondary sources of archaeological contextual evidence, and reference to clinical knowledge of bone pathology (Buikstra & Cook, 1980; Schultz, 2001; Roberts & Manchester, 2005). Over the last several decades, palaeopathology has embraced technology and the incorporation of advanced methods into the process of differential diagnosis together with the integration of palaeopathological data with archaeological data, and an understanding of the value of analytical models from epidemiology has improved our understandings of disease pathogenesis and etiology, providing researchers with new insights into individual and population health in the past. These technological and theoretical advances have only been possible as a result of collaboration with specialists such as radiologists, biochemists, clinicians, and epidemiologists (Mays and Pinhasi 2008). The continued development of palaeopathology as a discipline will therefore depend on the establishment and maintenance of collaborative relationships with other disciplines.

Although the process of diagnosis is similar, the importance of arriving at a correct diagnosis in palaeopathology is significantly different from that of clinical research. For the palaeopathologist, emphasis is not placed on the treatment of patients, but upon anthropological interpretations of health and disease in a biocultural context. Once a narrowed list of probable diagnoses has been identified, it is the population level distribution of the pathological condition according to time, space, and technology that becomes important for the interpretation of health and disease (Lovell 2000; Boldsen and Milner 2012; Buzon 2012; Katzenberg 2012). Reliable diagnoses are essential for the reconstruction of the history and geography of diseases, understanding the interaction between disease and cultural processes, documenting the evolution of diseases over time, and understanding the effect of disease processes not only on normal growth and development, but also on social interactions and the experience of disease in past

populations (Lovell, 2000; Boldsen and Milner 2012). The most important part of the process of differential diagnosis is to go beyond the descriptions and numbers and to also consider the archaeological context of the remains, the sociocultural context of a given ancient population, the epidemiological profile of the potential pathological condition(s), and the interpretive issues presented in Wood et al. (1992), as discussed in Chapter 2 of this dissertation. After the careful examination and differential diagnosis of pathological lesions, palaeopathologists should find themselves asking several important questions such as: How representative is the archaeological collection of the population as a whole? Were identified pathological lesions common throughout a population, or isolated to a single individual or sub-set of individuals (age, sex)? What are the possible reasons for any lesion patterning within a population? What does lesion patterning tell us about the presence of specific diseases and the possible impacts of those diseases on population dynamics? What do we know about the environmental, ecological, or geographical context of the population and how these factors may have affected the presence of disease? What does this tell us about sociocultural conditions such as settlement patterns, dietary choices, weaning practices, and social status? Do the differential diagnoses suggested from the palaeopathological data fit what we know about the environmental and sociocultural contexts of the population? Only after a careful consideration of these questions, should a confident diagnosis and interpretation of past population health be made (Lovell 2000; Pinhasi and Bourbou 2008; Boldsen and Milner 2012; Buzon 2012; Katzenberg 2012).

The purpose of this chapter was to explore the process of differential diagnosis in palaeopathology through a basic review of how diagnoses are achieved in the clinical sciences and the ways in which clinical science and palaeopathology are inherently and necessarily linked. This chapter also provided a review of several methodological approaches used in the process of differential diagnosis in order to lay the foundation for the current study which will explore the use of micro-CT as a relatively new palaeopathological diagnostic technique. Although relatively unexplored until recently, micro-CT has great potential for improving the reliability of differential diagnoses by providing objective quantitative methods of skeletal analysis (Rühli et al. 2007; Wanek et al. 2012). The advantage of providing reliable quantitative methods is that

palaeopathologists will be able to link current subjective qualitative observations with objective quantitative data in order to better support or refute differential diagnoses, achieve a better understanding of disease pathogenesis, and to arrive at more accurate interpretations of health and disease in past human populations. The aims of the current study are to 1) investigate the effects of different methods of micro-CT image data acquisition on the reliability and reproducibility of structural parameters in human trabecular bone from archaeological collections in an attempt to initiate standardized quantitative data collection; and 2) assess the diagnostic value of micro-CT methods for the quantitative evaluation of potentially pathogenic micro-structural changes occurring in the expression of porotic hyperostosis. It is anticipated that this research will be a first step toward the development of standardized methods of data collection as well as toward defining quantitative changes in bone micro-architecture for a pathological condition that is commonly observed in archaeological skeletal collections.

Chapter 5

5   Materials and Methods

5.1   Materials

The archaeological samples selected for this project were drawn from three Maya skeletal collections from San Pedro, Marco Gonzalez, and Lamanai, Belize and are currently housed at Western University, London, Ontario. An additional sample representative of a Greek colonial population from the Black Sea, Bulgaria was also provided by the Department of Anthropology at Trent University, Peterborough, Ontario. Each of these skeletal collections was selected because they have been well documented, and previous research has included isotopic, histological, and palaeoecological analyses, as well as detailed palaeopathological examinations. Additionally, crania from the Maya collections, specifically, represent a range of skeletal preservation from complete crania to small cranial fragments. This range in cranial preservation is ideal for illustrating the flexibility of the current research method to provide a standardized non-destructive high-resolution alternative to histological methods for skeletal samples of varying sizes. Finally, each of these collections includes a number of individuals with macroscopically identified and previously documented cases of orbital and cranial porotic hyperostosis.

Of the three Maya skeletal collections, two of the sites from which the collections originate, San Pedro and Marco Gonzalez, are neighboring coastal sites located on the southern tip of Ambergris Cay in Northern Belize and were populated during the Post-classic/Historic periods, which span from 1350-1650 AD (White et al. 2006). Lamanai is a much larger, inland site also located in Northern Belize along the shores of New River Lagoon, one of Belize's largest freshwater lakes. Lamanai was occupied from the Preclassic period until the arrival of the Spanish in the 1500's (Wright 1990; Graham 2000). Previous palaeopathological studies of the Maya series have indicated that the prevalence of porotic hyperostosis is quite high (77% in sub-adults, 65% in adults) when compared to other ancient maize-growing populations (Wright and White 1996). This high prevalence, of what is believed to be the skeletal manifestations of acquired iron-deficiency anaemia, has played an important role in the development of the nutritional

argument of the ecological model of Maya collapse (Saul 1972; Willey and Shimkin 1973; Wright and White 1996). As a result of this argument, a substantial amount of palaeodietary research has been done on Maya skeletal collections using stable isotope analyses (e.g. Wright and White 1996; White et al. 2006). These data provide a direct means of examining the relationship between diet and health, contributing significantly to the differential diagnosis of disease in Maya populations (Wright and White 1996). Second, in addition to anaemia, other conditions which can result in porotic hyperostosis, including scurvy and infectious disease, have also received substantial attention with respect to the Maya (Saul 1972; Wright and White 1996; White et al. 2006). However, a debate in the literature has emerged as a result of a combination of clinical data and paleobotanical studies which suggest that the presence of scurvy among the ancient Maya is highly unlikely (Wright and White 1996). Microscopic analyses of affected Maya crania may shed light on this debate by improving the reliability of differential diagnosis in human skeletal remains.

As with Maya populations, questions surrounding the etiology of porotic hyperostosis have also been particularly relevant among Mediterranean populations (Angel 1966, 1971; Musgrave 1980; Keenleyside and Panayotova 2006). The presence of these lesions in Greek skeletal remains has typically been attributed to thalassemia (e.g. Angel 1966, 1971), a genetic anaemia due to the presence of endemic malaria in the Mediterranean region. However, this view has been questioned and alternative etiologies have been proposed (Musgrave 1980; Stravopodi 2004; Walker et al. 2009). The Greek colonial population site of Apollonia is located on the Black Sea coast of Bulgaria and is dated from the 5th to 3rd centuries BC. In previous research on the Greek Black Sea population, skeletal evidence was not consistent with a diagnosis of thalassemia, leaving researchers to question the etiology of these lesions in Mediterranean populations (Keenleyside and Panayotova 2006). In fact, in earlier literature Musgrave (1980) not only criticized the assumption that malaria was endemic in Mediterranean populations, but also the reliability of observations and diagnoses based only on the macroscopic examination of skeletal remains. Multifactorial approaches to the analysis and interpretation of porotic hyperostosis were deemed to be necessary and the use of multiple methods should be emphasized. In addition to macroscopic methodologies, a detailed microscopic analysis

125

of bone structure may have the potential to reveal important information regarding the etiology and pathogenesis of porotic hyperostosis in this geographic region. Pending the results of this research, if µCT methods are found to be of high reliability, reproducibility, and value to the process of differential diagnosis in palaeopathological studies, future research on Maya and Mediterranean populations may aid in clarifying current etiological issues. For these reasons, the Maya and Greek colonial collections are ideal for the current research study.

The sample used for analysis in the current study was comprised of sub-samples of individuals selected from each of the three Maya collections as well as the Greek colonial collection. These sub-samples were combined to create one single sample for analysis. Although the prevalence of these lesions varies between each of these four populations, the current study aims to evaluate the process and pathogenesis of bone change independent of population. As such, the overall sample size was increased by combining individuals from these four separate populations. To meet the objectives of the current research, the selected sample must include males and females, individuals from different age-cohorts, and individuals with and without evidence of orbital and/or cranial porotic hyperostosis. The individuals with evidence of orbital and/or cranial porotic hyperostosis were selected and identified based on the presence and macroscopic identification of porotic lesions of the orbital roof and/or cranial vault. The criteria for the selection of comparative individuals included the absence of both orbital and cranial porotic hyperostosis as well as the absence of any other observable pathological conditions and/or skeletal indicators of stress.

The age and sex of each selected individual had been previously documented by Dr. Christine White of Western University and Dr. Anne Keenleyside of Trent University for the Maya and Greek samples, respectively. Age estimations for sub-adults were estimated based on published standards for dental eruption, diaphyseal length, and epiphyseal union (following: Ubelaker 1989; Buikstra and Ubelaker 1994), and adult age estimation was based on pubic symphysis morphology (following: Phenice 1969; Suchey and Katz 1986; Brooks and Suchey 1990) and sternal rib ends (following: Krogman and Iscan 1986) (Keenleyside and Panayotova 2006; White et al. 2006). Finally, sex was

determined for all adults, where preservation allowed, based on observations of cranial (following: Buikstra and Ubelaker 1994) and pelvic morphology (following: Phenice 1969; Buikstra and Ubelaker 1994). No attempts were made to determine the sex of the sub-adults included in the samples due to the difficulty of accurately sexing such individuals (Ubelaker 1989; Keenleyside and Panayotova 2006).

Due to the moderate to poor preservation and the fragmentary conditions of much of the Maya collections, some individuals could not be assigned a specific age range and some adults could not be accurately sexed; thus, direct age and sex matching of the unaffected controls to each of the affected individuals was not possible. However, efforts were made to select as many matched unaffected controls as was possible. A total of 57 individuals were selected from the Maya collections, including 32 with visible pathological lesions (10 females, 9 males, 13 undetermined) with ages ranging from 3 years ± 12 months to 40+ years, and 25 unaffected controls with no evidence of pathological lesions (13 females, 8 males, 4 undetermined) with ages ranging from 1-2 years to 50+ years. Due to the fragmentary nature of many of the Maya individuals, 13 of the individuals with pathological lesions and 6 of the unaffected individuals were not assigned a specific age range and were designated as "adult (18+ years)". Likewise, 3 of the individuals with pathological lesions could only be designated as "sub-adult (<18 years)".

The Greek colonial sample (5th-3rd centuries BC) consisted only of left or right eye orbits and consisted of the complete supraorbital ridge and roof of the orbit. Several orbits were separated from the frontal bone due to preservation issues and others had been previously cut and removed from otherwise complete frontal bones for histological research on orbital porotic hyperostosis at Trent University. Twelve individuals, including 7 with visible pathological lesions (4 females, 1 male, 2 undetermined) with ages ranging from 8 years ± 24 months to 35-50 years, and 5 unaffected controls (2 females, 2 males, 1 undetermined) with ages ranging from 12 years ± 36 months and 35-50 years, were selected for use in the current study.

The final skeletal sample selected for macroscopic assessment and micro-CT analysis included a total of 69 individuals including 39 individuals with porotic hyperostosis (14 females, 10 males, 15 undetermined) with ages ranging from 1-2 years to 50+, and 30 normal controls (15 females, 10 males, 5 undetermined) with ages ranging from 3 years ± 12 months to 35-50 years. For more detailed breakdowns of age and sex data for all selected individuals organized by sample see Appendix A.

5.1.1   Facilities and Equipment

The equipment used for the current study included an industrial micro-CT scanner as well as acquisition, reconstruction, and volumetric analysis software. The Nikon Metrology XT H 225 all-purpose X-ray and CT inspection system for industrial applications is configured with a stationary X-ray tube and flat detector panel and a rotating platform for sample positioning and mounting (Figure 5.1). This versatile system covers a wide range of applications including the inspection of small castings, plastic parts, complex mechanisms, as well as researching different types of materials and natural specimens, such as bone (Nikon Metrology, Inc.). This industrial inspection scanner was used to obtain the raw micro-CT images for the current study. The key features in the selection of this system were the large X-ray cabinet with the open rotatable platform provided to mount large archaeological skeletal samples, specifically complete and intact crania, a micro-focus reflection target X-ray source with a focal spot size of 3 microns (μm), and a Perkin and Elmer (XRD 1621 N ES) silicon detector panel (40 x 40 cm) which offers a 200 micron pixel size and an image size of 2048 x 2048 pixels (www.optoelectronics. perkinelmer.com).

Access to the micro-CT scanner system as well as all of the required software was provided through the CFI funded Sustainable Archaeology facility located at the Museum of Ontario Archaeology in London, Ontario. The software package that accompanies the XT H 225 includes both the CT acquisition (Inspect-X) and reconstruction (CT-Pro 3D) software. In addition, the software package used for the later visualization and quantitative analysis of the micro-CT data was VGStudio MAX, version 2.1. These programs were accessed at Sustainable Archaeology on two reconstruction computers that include 2 GeForce GTX 570 graphic processing units, 96 gigabytes of RAM, 2 Intel

Xeon E5520 @2.27 GHz CPUs, running 64-bit Windows 7. This software is used in a variety of application areas such as industrial CT, medical research, life sciences, and animation for the manipulation, design, and analysis of volume data. The methods for data acquisition, reconstruction, and the quantitative analysis of the micro-CT data within these software packages are discussed in greater detail in the methods section of this chapter.

Figure 5-1: Nikon Metrology XT H 225 all-purpose X-ray and CT inspection system
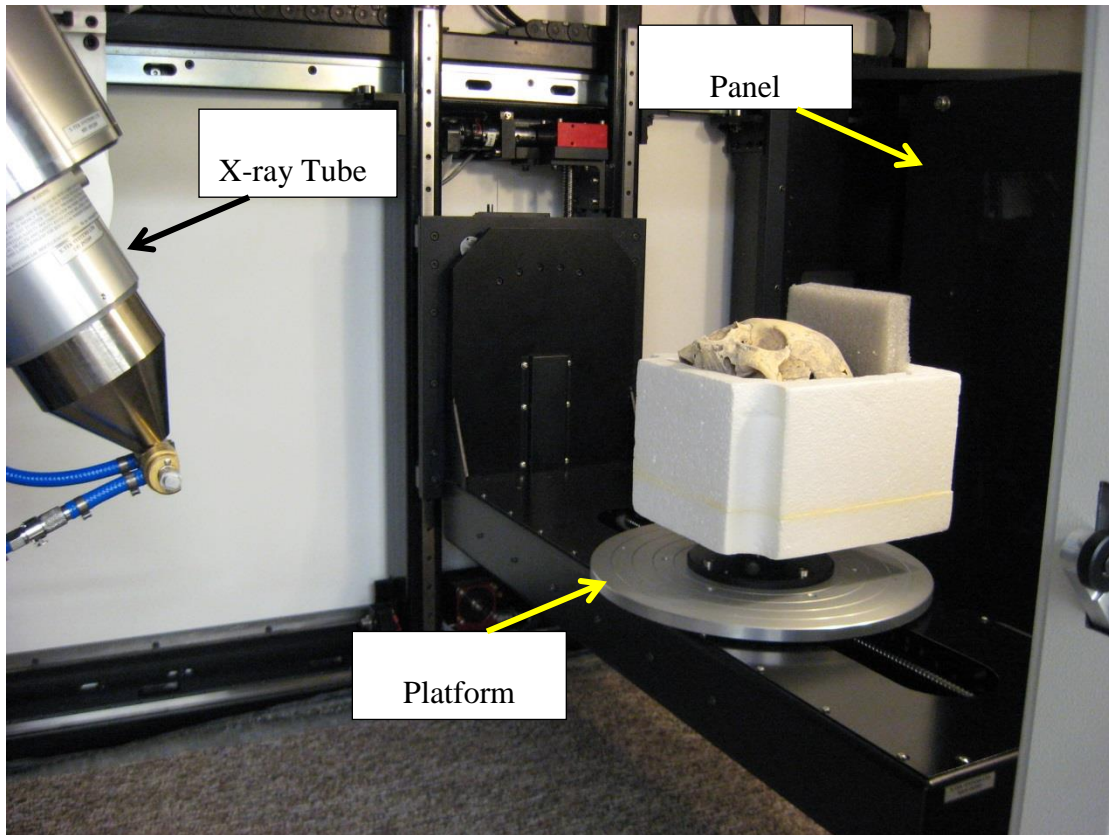
A view inside of the cabinet: stationary x-ray tube (left), detector panel (far right), and rotating sample platform (middle)

5.2　　Methods

Full skeletal inventories were completed for each of the selected individuals, including photographs of cranial elements with observable pathological lesions. Inventory forms based on standards outlined by Buikstra and Ubelaker (1994) were used for documenting the condition as well as the presence and/or absence of skeletal elements of each

individual. For example inventory forms, see Appendix B. Although skeletal inventories had previously been completed for these skeletal collections, the use of the Maya materials for other past and present studies, including those requiring destructive analyses, may have resulted in the removal of one or more skeletal elements, altering the original inventories. Since missing skeletal elements can limit the results of differential diagnosis (Lovell, 2000; Ortner, 2003), it was critical to re-inventory each individual selected for use in this study. Once the new skeletal inventories were completed, a full macroscopic palaeopathological analysis was conducted and included: a description of the appearance of all identified pathological lesions, the location of all identified lesions within the affected skeletal element, and the distribution of lesions within each individual (Example forms, see Appendix C). Evidence of artificial cranial modification was also recorded where applicable for the Maya populations. Modification was recorded as a potential confounding variable for later consideration as several studies have implicated cranial modification as a potential contributing factor to cranial porotic hyperostosis (e.g. Aufderheide and Rodriguez-Martin 1998; Blom et al. 2005; Mendonça de Souza et al. 2008).

For each of the 39 individuals with porotic hyperostosis, the next step was to macroscopically assess the severity of orbital and cranial porotic hyperostosis. This was completed using the modified Nathan and Hass (1966) scoring system proposed by Stuart-Macadam (1985):

> Light (Porotic Type): Scattered, isolated, fine foramina, or small openings, affecting the orbital roof and/or the skull vault (indistinct porosity) (Figure 5.2).

Figure 5-2: Light Porotic Hyperostosis

Left: light cranial porotic hyperostosis (Lamanai – YDL-1 85/6)
Right: light orbital porotic hyperostosis (San Pedro - SP11-8/2)

Medium (Cribrotic Type): Foramina are larger than Porotic Type, closer to one

another, and tend to conglomerate. Openings remain isolated and preserve

individuality. There may be a small amount of coalescing of foramina (no

expansive changes) (Figure 5.3).

Figure 5-3: Medium Porotic Hyperostosis

Left: medium cranial porotic hyperostosis (San Pedro – SP11-2/2)
Right: medium orbital porotic hyperostosis (Lamanai N12-11/3[3])

Severe (Trabecular Type): Outgrowth in trabecular structure from the normal

contour of the outer bone table (expansive changes). Foramina have lost all

individuality and are confluent. Appears as a network formed by bone trabeculae

of varying thickness, sometimes irregularly arranged in predominant directions

parallel to, or radiating from, one or various centres (Figure 5.4).

Figure 5-4: Severe Porotic Hyperostosis
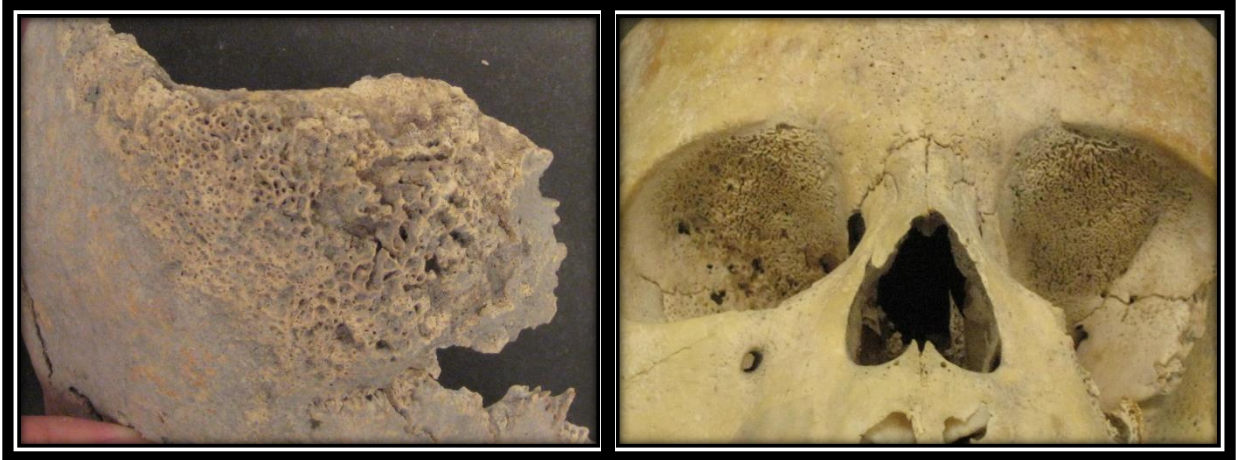
Left: severe cranial porotic hyperostosis (San Pedro - SP11-2/7b)
Right: severe orbital porotic hyperostosis (San Pedro – SP11-2/1)

Additional macroscopic observations included the location of each of the lesions (Table 5.1) as well as the activity (active vs. healing/healed) of all observed lesions (Table 5.2) as recommended by Buikstra and Ubelaker (1994). It should be noted that when intact crania were unavailable, the cranial fragments that were selected for analysis only included those fragments from the locations described by Buikstra and Ubelaker (1994; Table 5.1). Therefore, cranial fragments that could not be assigned to one or more of the locations included in Table 5.1 were not used in this study.

Table 5-1: Location of Porotic Hyperostosis (Buikstra and Ubelaker 1994)

   i) Orbits

   ii) Adjacent to sutures

   iii) Near bosses or within squamous portion of occipital

   iv) Both adjacent to sutures and within orbits

   v) Both adjacent to suture and near bosses/in squamous

Table 5-2: Lesion Activity at Time of Death (Buikstra and Ubelaker 1994)

   i) Active

   ii) Healed

   iii) Mixed reaction: evidence of healing + active lesions

Lesion activity was further defined following Mensforth et al. (1978) and Mittler and Van Gerven (1994). Active lesions were defined as having sharp and clearly defined margins in the cribiform structure of the affected area. Microporosity of the cribiform structure and increasingly thin bridges of bone were visible upon close examination, creating a sieve-like appearance - microporosity is characteristic of active lesions. Healed lesions were characterized by a "smooth lamellar texture with bone filling of peripheral pores" (Mensforth et al. 1978: 23). Unlike active lesions, microporosity is absent in healed lesions (Mensforth et al. 1978: 23; Mittler and Van Gerven 1994: 289).

To address the first objective of this study, which was to evaluate the presence of any palaeoepidemiological trends in the study sample, the data collected from the above described macroscopic assessment were combined with the recorded demographic information (Keenleyside and Panayotova; White et al. 2006), as well as the archaeological contextual evidence from the published literature on Maya and Greek archaeological populations. The evaluation of the existence of relationships between population demographics (age and sex) and lesion severity and activity will provide the necessary palaeoepidemiological context for evaluating the contribution of quantitative micro-CT data to the process of differential diagnosis. Without a full understanding of the palaeoepidemiological factors contributing to the prevalence of porotic hyperostosis, the micro-CT data cannot be properly interpreted or evaluated. The identification of palaeoepidemiological trends was achieved through an analysis of the collected macroscopic data on lesion severity and activity using 2 x 2 chi-square analyses to assess the possibility of the existence of relationships between disease pathogenesis and population demographics ($H1_o$ and $H2_o$, as outlined in Chapter 1, Section 1.2). The results of these analyses are detailed in Chapters 6 and 7.

5.2.1 Micro-computed tomography (micro-CT) Scanning Protocol

Prior to the acquisition of any micro-CT data, it was essential to properly fix the sample in an appropriate sample holder so as to prevent any movement from occurring for the duration of the scan. During their respective individual scans, each of the skeletal samples was fixed, without further preparation, in a styrofoam box measuring 212

millimetres (mm) in width, 234 mm in length, and 155 mm in height. This sample holder was designed to securely hold the largest of the 69 samples - an intact adult cranium. For smaller samples, additional pieces of rigid and soft styrofoam were positioned to surround and secure them in place within the box to prevent motion and maintain position (Figure 5.5). Styrofoam was selected for sample positioning and fixation as it is a radiolucent material that is nearly invisible to X-rays and does not impact the resultant images. Cardboard and other solid materials are radiopaque and impede the passage of X-rays, causing them to be visible on the processed images and were, therefore, not used in this study (e.g. Stauber and Müller 2008; Conlogue and Beckett 2010).

Figure 5-5: Styrofoam Sample Holder
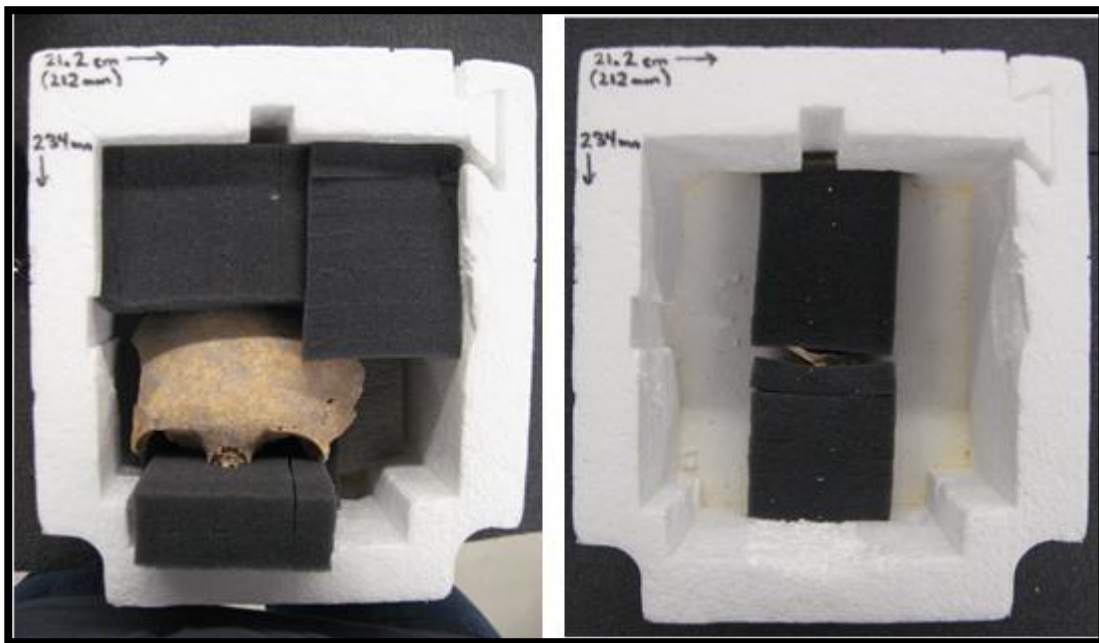
Left: partial frontal bone secured with foam
Right: small fragment of a left orbit secured with foam

Each sample was positioned in the sample holder so that the longest axis of the sample was aligned with the rotation axis of the scanner. Intact crania were scanned in a modified antero-posterior position to allow the X-rays to pass most easily through the orbits and parietal boss areas (Figure 5.6) (after Saab et al. 2008). Aligning the longest axis of a sample with the rotation axis of the scanner reduces the X-ray path length, or the

amount of material that the X-rays have to pass through (Saab et al. 2008; XTH225 CT User's Manual). This reduced the effects of beam hardening, described in Chapter 4, Section 4.4.3. Although beam hardening was corrected for during reconstruction, it was decided that reducing the X-ray path length during acquisition would be ideal to further control for this effect on image quality. Once samples were effectively positioned and secured within the sample holder, the holder was also secured to the scanning platform with double-sided tape to control for movement of the sample holder during scan acquisition.

Figure 5-6: Modified Antero-posterior Position for Intact Skull Scanning
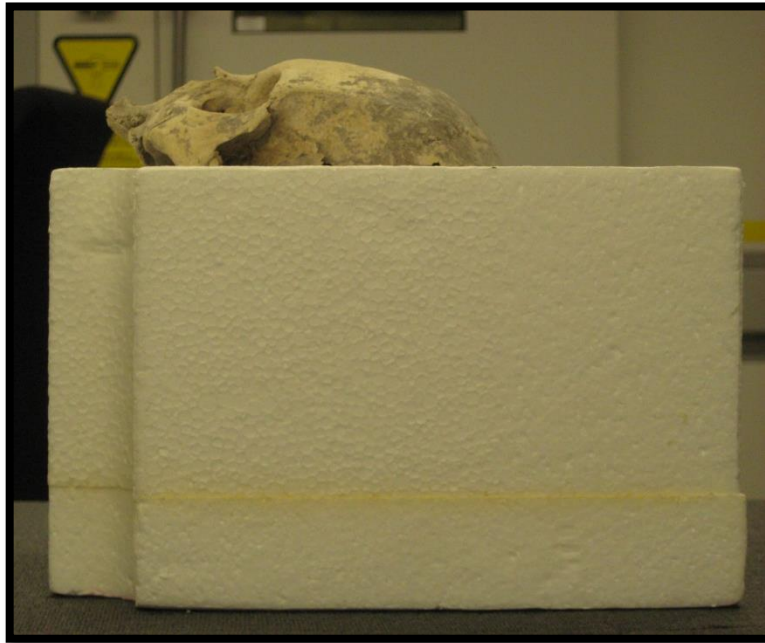
5.2.1.1   Maximum Nominal Spatial Resolution

The spatial resolution of micro-CT images is dependent upon several factors that should be considered in order to perform an optimal measurement. These factors include the resolution capabilities and limitations of the X-ray detector, focal spot size, geometric magnification, and the stability of the rotation mechanism (Holdsworth and Thornton

2002; Stauber and Müller 2008). The small focal spot size and large panel provided by the XT H 225 allow for increased geometric magnification of the image while retaining image quality. Therefore, this system was ideal for the high resolution, non-destructive analysis of archaeological bone microstructures.

Obtaining an optimal resolution also depends on the specific features that should be detected in the resultant images (Stauber and Müller 2008). For example, according to Stauber and Müller (2008), the ideal nominal resolution for detecting basic trabecular bone microstructure is between 50-100μm. However, the optimal resolution for detecting specific features of interest, such as trabecular microstructure, cannot simply be selected for and achieved for any sample. This is because the maximum nominal resolution that can be achieved also depends on the dimensions and size of the sample being scanned. The general rule for determining the maximum nominal resolution that can be achieved is to divide the approximate width of the sample by the number of pixels horizontally across the detector. So, if a sample has a maximum horizontal width of 200mm and the XT H 225 detector has 2000 pixels across it, then the resultant resolution will be approximately 100μm. Therefore, the higher the maximum nominal resolution desired, the smaller the sample must be to achieve that resolution (Stauber and Müller 2008). Thus, in many research studies using high resolution micro-CT methods, the first step often requires destructive preparation of the sample in order to achieve a desired maximum nominal resolution.

The goal of the current research study is to non-destructively analyze and quantify trabecular microstructures in archaeological human crania in order to improve differential diagnosis in palaeopathology. As such, the methods of micro-CT image acquisition had to be developed to achieve an ideal resolution for resolving trabecular structures without any destructive preparation of intact and fragmentary crania. Since the ideal resolution for detecting basic trabecular bone microstructure is between 50-100 μm (Stauber and Müller 2008), a non-destructive, standardized micro-CT scanning protocol needed to be developed to achieve a resolution within or as close to this range as possible. The maximum nominal resolution that was acquired in the current study was determined by the horizontal width of the largest sample. This sample was an intact cranium with an

approximate horizontal diameter of 185 mm. In order to determine the maximum nominal resolution for this study, the intact cranium, fixed in the sample holder, was adjusted in place on the scanner platform and, using the field of view and manual joysticks, the location and magnification of the sample within the scanner was adjusted until the sample filled approximately 90% of the width and length of the scan field of view. The sample was then rotated 360º to ensure that all parts remained in view at all rotation angles. The resultant maximum nominal resolution achieved for the largest intact crania was 102.1 µm. This result was slightly higher than the range suggested by Stauber and Müller (2008) for the analysis of trabecular structures. However, these structures were resolved with enough detail in the resultant images to successfully meet the goals of the current research project. The specific X,Y,Z coordinates corresponding to the location of the object in relation to the X-ray source and the detector was saved in the Inspect-X program to ensure standardized scan positioning and a nominal resolution of 102.1 µm for all subsequent samples.

Although local tomography can non-destructively achieve a higher nominal resolution for a specific magnified location on the cranium, image quality is reduced. Should any part of the sample leave the imaging window in the horizontal plane, image information about that part of the sample will not be obtained in those rotation angles. This results in artifacts in the reconstructed volume as the missing information is smeared over the image. Therefore, because it was necessary to identify and analyze small trabecular structures, a trade-off was made to achieve high image quality with a slightly lower nominal resolution than suggested by Stauber and Müller (2008), versus poor image quality with higher nominal resolution.

5.2.1.2   Micro-CT Scan Acquisition

Once the maximum nominal resolution was determined, a protocol for scanning each of the selected samples was developed. The energy (kVp), current (µAs), and number of projections varied, while the integration time and frame averaging remained consistent. Due to the inconsistencies in size, shape, and particularly thickness of the intact and fragmentary crania, the kVp was adjusted for each individual sample to ensure adequate penetration. As such, the optimal kVp was selected when all anatomical features were

discernible, trabeculae were visible, and the minimum gray level did not fall below 10,000. The current (µAs) was also adjusted for each sample to ensure that gray levels in the brightest areas were not above 60,000, avoiding saturation and overexposure.

Once fixed in the sample holder, and without further preparation, each sample was scanned between 130-145 kVp with a tube current of 25-50 µA. Exposure time was 500 ms, averaged over two frames. The number of projections was optimized for each sample and varied from 867 to 3142 projections depending on the width of the field of view, and scan time varied from 14 to 53 minutes. All scans were performed with a nominal isotropic resolution of 102.1 µm (See Appendix D for individual scan details).

When the scans were complete, the projection images were saved as a sequence of continuous TIFF files. The CT-Pro reconstruction software read the TIFF files for reconstruction and created the subsequent micro-CT volume. During reconstruction, a single centre of rotation was determined automatically to ensure the sharpest possible images. A beam hardening correction was applied and the image with minimal beam hardening effects was selected from the provided options during the reconstruction stage. No noise reduction algorithms were applied and the entire volume was selected for reconstruction. Once the selection of reconstruction options was complete the CT reconstruction was initiated and volume files containing the reconstructed volumes were created and saved in .VOL file format. Each of the reconstructed data sets was given a file name according to the original inventory numbers assigned to each individual used in this study. These data were then exported as 16 bit .VGI files (created from the reconstructed native 32-bit .VOL file), in order to reduce file size. In total, micro-CT scans for 69 individuals, represented by either intact crania or cranial fragments, were obtained for analysis.

5.2.2 Thresholding and Volume of Interest Methodology

After acquisition and reconstruction, the micro-CT data were analyzed using VGStudio MAX version 2.1 (VGStudio) in the Sustainable Archaeology facility at the Museum of Ontario Archaeology in London, Ontario, Canada. VGStudio provides a range of investigative tools for acquiring measurements and morphometric data for two-

dimensional (2D) and three-dimensional (3D) analyses, as well as options for the manipulation, rendering, editing, and segmentation of 3D data. After successfully importing the micro-CT volume data into the analytical software, the first step in the analysis was the application of automatic global thresholding, allowing for a correct separation between the object (bone) and the surrounding background (air), referred to in VGStudio as a surface determination. Before making any measurements or performing any analysis functions, the surface of each of the data sets has to be determined.

5.2.2.1   Thresholding and Image Segmentation

There are a number of different thresholding methods used in the process of segmenting objects in CT and micro-CT images (Sezgin and Sankur 2004; Hui-Fang 2006). Methods for thresholding, or image segmentation, work on the premise that the gray levels of pixels belonging to an object are different from the gray levels of pixels belonging to the surrounding background (Sezgin and Sankur 2004). VGStudio offers both automatic and manual tools for the separation of objects comprised of one or any number of different materials from the background. The automatic thresholding tool in VGStudio that was applied to the images in the current study uses the histogram shape-based method described by Otsu (1979) where the peaks, valleys, and curvature of the gray levels in the image histogram are analyzed to determine an optimal threshold value. The Otsu (1979) method works well when the gray levels of the images to be thresholded have clear peaks and valleys. In other words, it works best for images whose histograms show clear bimodal or multimodal distributions (Baveye et al. 2010), as is the case with bone scanned in air. The automatic threshold tool in VGStudio determines the mean gray level of the peak or peaks representing the object(s) and the mean gray level of the peak representing the background. Using these values, the valley in the histogram is located and represents the most adequate threshold of gray level values for extracting the object from its background.

The images for the current study represent a bimodal distribution of gray levels as there is a single peak for bone and a single peak for the background (air). Therefore, the automatic threshold tool in VGStudio was ideal for determining the most adequate

threshold values for the micro-CT images of each cranial sample. To ensure consistency in thresholding and comparability of the obtained data, automatic thresholding was chosen over the visual method of thresholding. Adjusting the threshold manually for perceived bone surfaces in each scan may have led to over- or under-representation of bony trabecular structures and, thus, the introduction of significant error to quantitative structural data across the sample. Although thresholding techniques are chosen by individual researchers, manual methods may be quite prone to error and in order to standardize quantitative data and ensure that data are comparable across research studies, automatic thresholding methods that use published algorithms are recommended (Baveye ey al. 2010). Automatic thresholding with no manual visual adjustments was applied to the micro-CT images for each of the scanned samples. Once automatic thresholding of the images was complete, a method for the analysis and collection of quantitative bone structural data was developed.

5.2.2.2   Creation and Placement of the Volumes of Interest

The second objective of this study was to test and compare the reliability and reproducibility of different data collection methods for the analysis and quantification of the trabecular structures of cranial diplöe. As such, 2D regions and 3D volumes of interest of varying sizes were determined for acquiring quantitative data. Although VGStudio refers to both 2D regions and 3D volumes of interest strictly as "Regions of Interest", for the purposes of the current study both the 2D regions of interest and the 3D volumes of interest will be referred to as volumes of interest (VOIs), since they each represent volumes of bone from each sample.

The key factors when selecting the various VOIs were their dimensions, size, and position. For each skeletal sample, three VOIs were defined: 2D standard, 3D standard, and 3D custom. The 2D standard VOI was a square measuring 2.5 mm^2, determined as the maximum VOI size with the same length and width, which would fit within the centre of the diplöic trabecular mass of the smallest sample without encroaching on the overlying cortical bone. Although this VOI was used to quantitatively represent the 2D architecture of trabecular bone, it should be noted that some data from the third dimension (Z) was included in this VOI. This is because the region of interest tool in

VGStudio MAX also included the Z-dimension of the image voxels which, in the current study measured 0.102 mm, or 102 μm. However, since measurements taken from 2D histological thin sections are often taken from sections ground to a thickness of approximately 100 μm, the inclusion of the slice thickness at 102 μm was considered to be an acceptable amount of additional data and this VOI was assigned to represent data collected from 2D micro-CT images. The 3D standard VOI was a cube measuring 2.5 mm^3, determined from the size of the 2D standard VOI and extended 2.5 mm into the third dimension (Z). The third VOI, 3D custom, was not created at a standard fixed size, but was determined by the maximum VOI size which included as much diplöic trabeculae as possible without encroaching on the outer cortical bone. This VOI was custom sized for each individual sample and varied in its X,Y,Z dimensions depending on the size of the sample and the specific section of bone into which the VOIs were placed. The purpose of the 3D custom VOI was to capture as much of the 3D trabecular architecture as possible for each individual sample without including cortical bone.

To create the 2D standard VOI, the "Distance" tool in VGStudio was used to draw a 2.5 x 2.5 mm square template onto the micro-CT cross section of interest in the X and Y planes. From the Region of Interest toolbar, the "Rectangle selection" tool was selected from the "create a new region of interest" option. The square region of interest was created using the 2.5 x 2.5 mm^2 square template as a guide to aid in correctly sizing the VOI. Once the VOI was sized to the pre-measured template, the option to "create ROI" was selected, creating and listing the new VOI in the scene tree of the workspace window for use in subsequent samples (Figure 5.7).

The 3D standard VOI was created from the 2D standard VOI which was extended into the Z direction by 2.5 mm, thereby creating a cube measuring 2.5 mm^3 (Figure 5.8). Once the 2D and 3D standard VOIs were created in the scene tree, they were exported and saved as standard 2D VOI and 3D VOI templates. These templates were later imported into all of the subsequent datasets so as to ensure that all of the VOIs used to collect the quantitative data from each sample were consistent and standardized.

Figure 5-7: Creating the 2D Standard VOI in VGStudio MAX
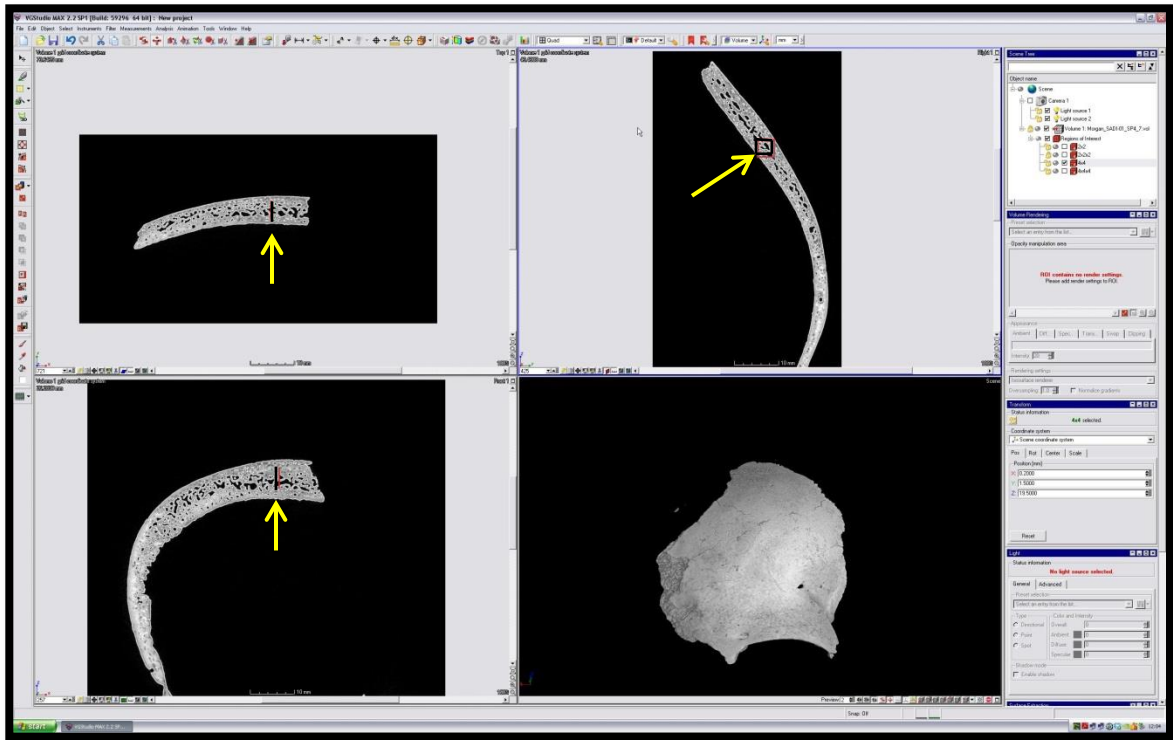
Top right: X-plane illustrating the cubic 2.5 x 2.5 mm^2 2D VOI; Top left: Y-plane illustrating the placement of the 2D VOI; Bottom left: Z-plane illustrating the placement of the 2D VOI; Bottom right: 3D reconstruction

The 3D custom VOI, unrestricted by a standardized shape or size, was created on the same cross-section as the 2D and 3D standard VOIs and sized to encompass both of these standard VOIs. Using the "Polyline Lasso selection" tool, a new custom drawn region of interest was created by tracing the outer edges of the cortical bone of the inner and outer laminae to include as many trabeculae as possible in the X and Y planes while keeping a sufficient distance from the cortical edge so as not to include it in the 3D custom VOI. Once the maximum size in the X and Y planes was determined, the 3D custom VOI was then extended in the Z direction until the edges of the cortical bone began to encroach on the outline of the VOI (Figure 5.9). Since not all individuals were represented by the same cranial elements, unlike the 2D and 3D standard VOIs, a single 3D custom VOI was not saved and imported into each data set; rather a new 3D custom VOI was created for each data set based on the unique shape and size of each sample. Therefore, the size of the 3D custom VOI varied for each individual depending upon the maximum volume of

trabeculae that could be captured from each cranial fragment. For individuals with pathological lesions, the location and extent of a given lesion was also a factor in determining the size and shape of the maximum 3D VOI. In these cases the 3D custom VOI was restricted to the maximum size of the lesion so that the trabecular architecture captured by the 3D custom VOI included only that affected by the pathological process.

Figure 5-8: Creating the 3D standard VOI in VGStudio Max
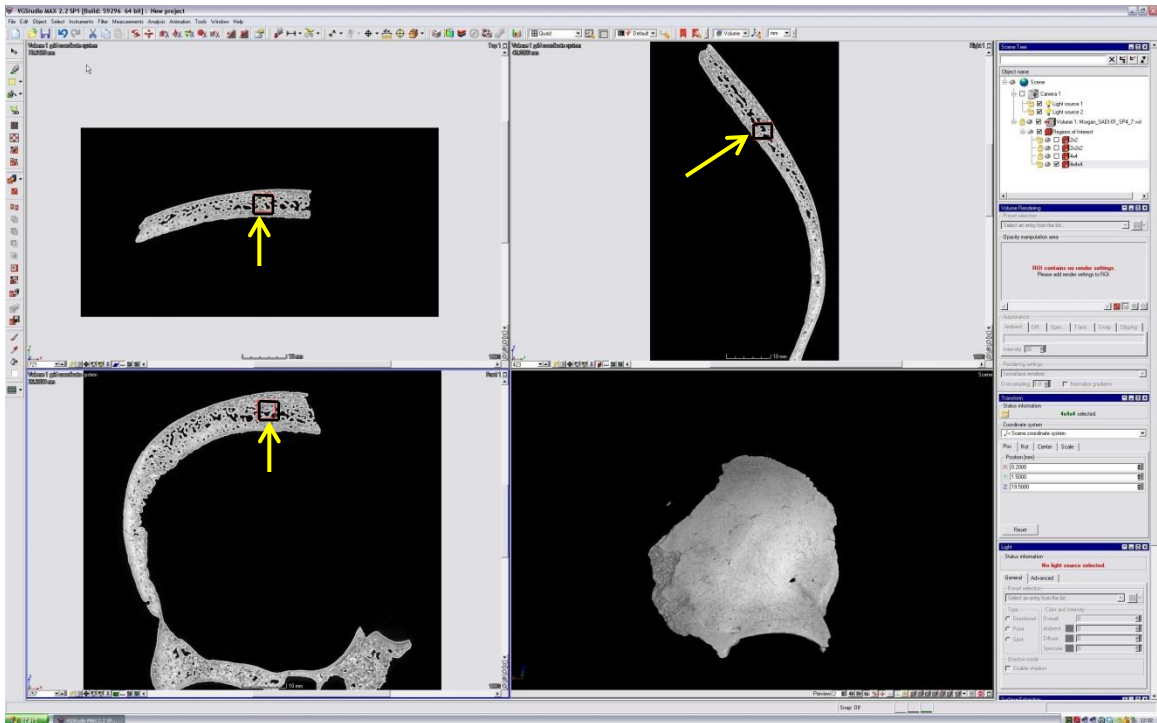
Top right: X-plane illustrating the cubic 2.5 x 2.5 x 2.5 mm^3 3D VOI; Top left: extension of the 3D VOI in the Y-plane; Bottom left: extension of the 3D VOI in the Z-plane; Bottom right: 3D reconstruction

Figure 5-9: Creating the 3D Custom VOI in VGStudio Max
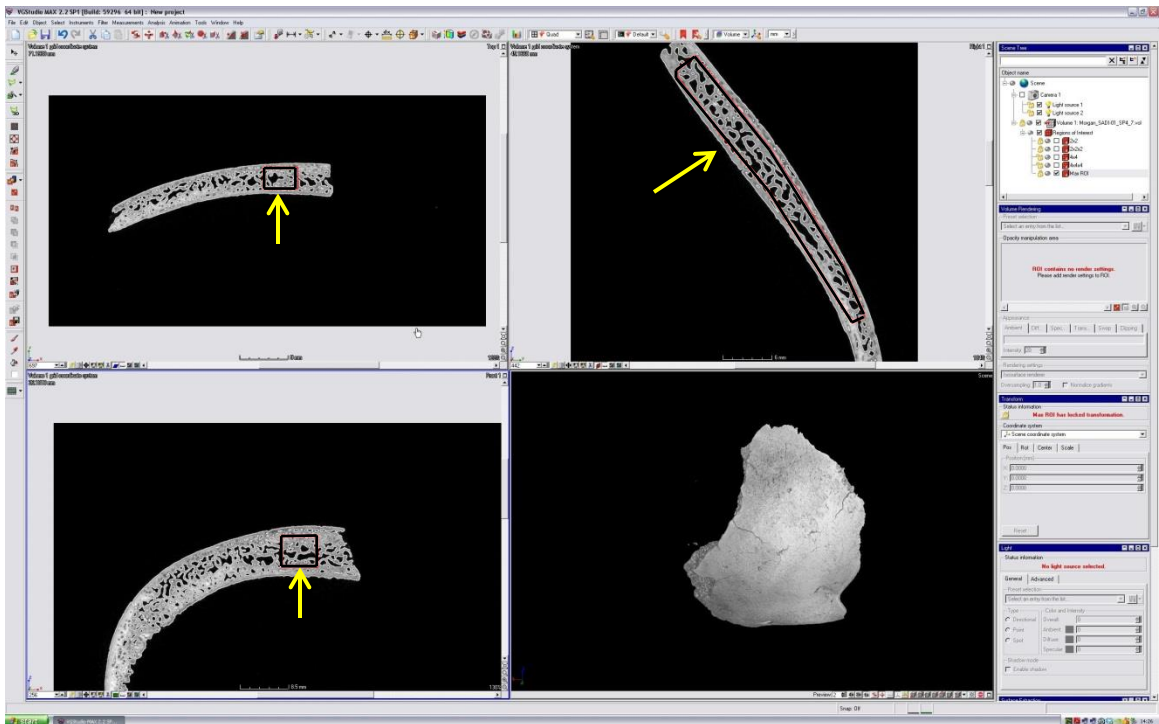
Top right: X-plane illustrating the 3D custom VOI; Top left: extension of the 3D VOI in the Y-plane; Bottom left: extension of the 3D VOI in the Z-plane; Bottom right: 3D reconstruction

Once the 2D and 3D standard VOIs were saved and exported from VGStudio, their specific placement on the micro-CT cross sections was determined based on the standard locations for the occurrence of porotic hyperostosis listed in Table 5.1 above and included within the orbits, adjacent to cranial sutures, near bosses, and/or within the squamous portion of the occipital (Buikstra and Ubelaker 1994). Since the skeletal sample used in the current study includes samples ranging from complete skulls to small individual cranial fragments, the number of locations available for the placement of VOIs on a given sample was dependent on the size and completeness of the sample. For example, a set of VOIs could be placed in each of the 4 above listed locations on a complete skull or, for those individuals represented only by cranial fragments or lone eye orbits, a set of VOIs could only be placed in one or two of the listed locations depending on the cranial element represented by the fragment.

For individuals with no evident pathological lesions, the process of VOI location selection was straight forward and followed the method described. For individuals with porotic hyperostosis, although the process followed VOI placement in the listed locations, two sets of VOIs were generally included for each location present (as listed in Table 5.1). With the exception of eye orbits, which were too small for the inclusion of two sets of VOIs, one set of VOIs was placed within the trabecular mass affected by the lesion(s), and a second set was placed in an area outside of the lesion, but still within the present listed standard locations. This was done in an attempt to capture the full range of potential trabecular variation in individuals with porotic lesions. The location and extent of a lesion was determined according to visualized porosity and/or resorption of the outer lamina in the micro-CT cross sections.

For each scanned sample, once the micro-CT cross section that best represented a standard location from Table 5.1 was located, the 2D standard VOI was imported into the dataset. This VOI was then manually positioned within the diplöe to fit between the inner and outer laminae. This manual positioning was achieved by using the "Transform" menu located in the workspace scene tree (Figure 5.10). This menu provides the specific X,Y,Z coordinates for any selected VOI, as well as the option to move a selected VOI to any specific desired location within the dataset. Once the positioning of the 2D standard VOI was determined, the coordinates of that position were saved and used to place the 3D standard VOI in the same position. The 3D custom VOI was then custom created to encompass both the 2D and 3D standard VOIs, as well as the maximum amount of surrounding trabecular architecture. The placement of the 2D standard VOI and 3D standard VOI was kept the same and the 3D custom VOI was placed to encompass the standard VOIs within each individual dataset in order to avoid introducing variability arising from repositioning the different VOIs within the diplöe and to ensure the reliable comparability of the quantitative data obtained from each of the 2D and 3D standard VOIs.

Figure 5-10: Locating the Transform Options in VGStudio
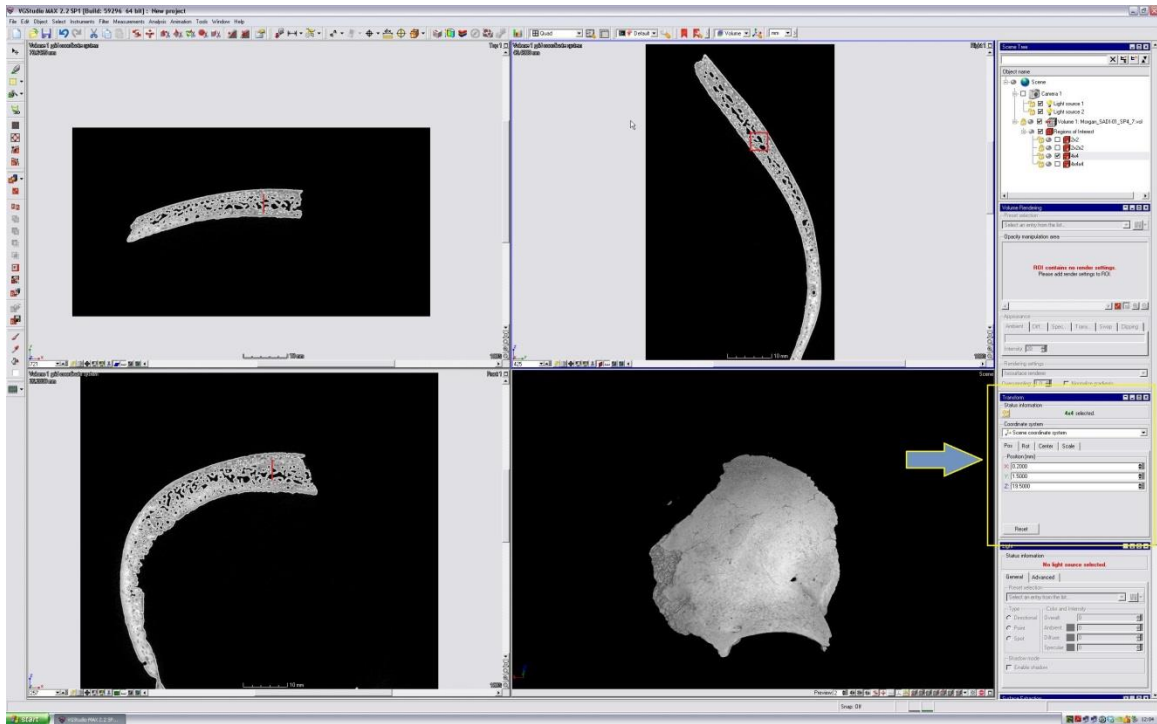
Far right: Scene tree with transform option for adjusting VOI location and placement

5.2.3   Observer Reproducibility and Reliability Testing

To address the second objective of this study, which is to investigate the reproducibility and reliability of different methods of micro-CT image data acquisition, the three defined VOI methods described above were tested for observer error. Two weeks following the completion of data collection, 10 individuals were randomly selected for the determination of intra-observer reproducibility and inter-observer reliability of the 2D and 3D methods of data collection and analysis. For testing the intra-observer reproducibility of the three different methods, the steps proceeding from section 5.2.2. were repeated for the 10 randomly selected individuals without information regarding the previously determined VOI positioning or collected quantitative data for those individuals. Following this, in order to test the inter-observer reliability of the three different methods, a colleague, Jose Sanchez (HBSc), was provided with the relevant methods sections proceeding from Section 5.2.2 of this chapter and was asked to collect and record data for the same quantitative variables. Jose Sanchez had no prior knowledge

or training on VGStudio, nor did he take part in the original micro-CT scan acquisition or data collection processes.

To statistically evaluate the reproducibility and reliability of micro-CT image analysis methods ($H3_o$) paired Pearson-R correlations were used to measure the relationship between the repeated measures made by the same observer at different points in time and by two different observers (Jamison and Zegura 1974). Coefficients of determination (R^2) were also used to further evaluate observer agreement. The coefficient of determination is used to explain how much of the variability observed in one factor can be explained by its relationship to another factor and will be applied in this study to determine the predictive relationships between repeated measures of the same variables in the assessment of observer agreement (Heathcote 1980; Ferrante and Cameriere 2009).

5.2.4   Quantitative 3D Image Analysis

After the placement of the VOIs, quantitative measures were obtained from each of the three defined VOIs using the automated tools available in VGStudio MAX in order to address the third objective outlined in the current study. Quantitative measures must be obtained from each defined VOI individually. To do this, the VOI from which quantitative measurements are desired was selected in the scene tree. From the available shortcut icons along the top of the image display, the "Properties" icon was selected and a "Properties" window was opened. From the properties window, the "Morphometrics" tab was selected and the option to "Update" the morphometrics was selected. This procedure updated a number of quantitative variables for the specific VOI that was selected from the scene tree. The VGStudio MAX software provided the current study with quantitative structural data for the following five variables:

1) BV/TV (Bone Volume Density) - the fraction of a given volume of interest (TV) that is occupied by mineralized bone (BV). This variable is used to evaluate relative changes in bone volume density (Stauber and Müller 2008). It will be used to assess how the overall amount of bone is affected by a pathological process.

2) BS/BV (Specific bone surface) – the fraction of a given volume of bone (BV) that is made up of bone surface (Stauber and Müler 2008). Like BV/TV, this measure may be used to assess how the overall amount of bone is affected by a pathological process.

3) Tb.Th (Trabecular thickness) – the mean thickness of trabecular structures within a volume of interest (Stauber and Müller 2008). This variable will be used to assess the relative amount of bone and any changes to the thickness of trabeculae due to trabecular resorption/destruction or formation in different pathological processes.

4) Tb.N (Trabecular number) – the quantification of the relative number of trabeculae within a volume of interest (Stauber and Müller 2008). This variable will be used to assess changes in the overall architecture and organization of trabeculae as well as processes of bone resorption or formation in different pathological processes.

5) Tb.Sp (Trabecular spacing) – the mean separation of trabeculae within a volume of interest (Stauber and Müler 2008). This variable will be used to assess any changes in the organization of trabeculae and changes to the size of the marrow space as a result of resorption/destruction or formation of trabeculae in different pathological processes.

The exact algorithms used to calculate these morphometric structural variables in VGStudio Max 2.1 are not known, despite several requests to VGStudio technicians, and could not be provided here. However, published algorithms for the calculation of each of these variables can be found in Hildebrand et al. (1999) and these algorithms are assumed to be comparable to those used by VGStudio Max. The morphometric variables selected for use in this study were chosen as not only are they well established in the literature, each index can be assessed in both two as well as three dimensions from micro-CT

images (e.g. Whitehouse, 1974; Aaron et al., 1987; Feldkamp et al., 1989; Compston, 1994). These indices have been used to quantitatively capture the different patterns of internal microstructural changes that occur with osteoporosis (e.g. Mittra et al. 2007; Gabet and Bab 2011) and cancer (e.g. Snoeks et al. 2011) and should be capable of quantitatively capturing trabecular changes occurring with porotic hyperostosis. Expected changes to the pattern of trabecular microarchitecture with various disease processes have been listed in Table 5.3.

Table 5-3: Expected Changes to Trabecular Microarchitecture by Disease Process

Variable	Resorptive Processes (Osteoclastic Activity) (e.g. Infection)	Formative Processes (Osteoblastic Activity) (e.g. Modification)	Mixed Processes (Mixed Cellular Activity) (e.g. Marrow Hyperplasia)
BV/TV	Decrease	Increase*	Decrease
BS/BV	Increase	Decrease*	Increase
Tb.Th.	Decrease	Increase*	Both possible
Tb.N.	Both possible	Both possible*	Both possible
Tb.Sp.	Increase	Decrease*	Increase

*Note that for some disease processes, osteoblastic activity occurs only on the periosteal surface and no trabecular changes would be expected (e.g. hemorrhage, scurvy - See Chapter 3, Section 3.7.2.1).

Once data collection was completed for all 69 individuals, the collected quantitative data were organized by location (orbits, adjacent to sutures, near bosses, squamous portion of the occipital) and further separated by individual cranial bone. The separation of data according to individual cranial bones was done to avoid the introduction of variability that may arise from normal structural differences occurring throughout the four separate bones that comprise the skull (frontal, parietal, occipital, temporal). Recent investigations of the trabecular architecture of the diplöe indicate that researchers should not assume equal conditions throughout the skull and that significant growth and development-related structural differences between the frontal, parietal, occipital, and temporal bones have been documented (Larsson et al. 2011, 2014). Based on these findings, the data available for quantitative analysis are derived from 33 orbits (15 pathological, 18 normal), 13 frontal bones adjacent to the coronal suture (3 pathological, 10 normal), 30 parietal bosses (10 pathological, 20 normal), 27 parietal bones adjacent to

the lambdoid suture (16 pathological, 11 normal), and 21 occipital bones within the squamous portion (14 pathological, 7 normal).

Prior to analysis, the distribution of data was considered and it was determined that the data collected from the 13 frontal bones adjacent to the coronal suture would not be used in the current study as the sample size for affected individuals is too small for statistical analysis (N=3). Additionally, since two of these locations - the parietal boss and the parietal bone adjacent to the lambdoid suture - occur within the same individual cranial bone, these data were combined to increase the sample size available for the analysis of porotic hyperostosis. For those individuals with data for both of these parietal bone locations, only the data for the parietal boss were considered in the analysis in order to avoid duplicated data. After these adjustments, the final sample used for statistical analysis included 33 orbits (15 pathological, 18 normal), 55 parietal bones (24 pathological, 31 normal), and 21 occipital bones (14 pathological, 7 normal) derived from a total of 66 individuals (37 pathological, 29 normal). Paired samples t tests will be used to determine if structural differences do in fact exist between the various bones of the cranial vault used in this study and whether or not these bones must be independently evaluated for the assessment of disease pathogenesis.

For the evaluation of 3D trabecular architecture, the statistical analyses will include Levene's tests of variance to evaluate the equality of variances for each of the five structural variables to determine the validity of an analysis of variance (ANOVA). If no statistically significant differences in variance are found, then an ANOVA will be used to assess any potential differences in trabecular bone microarchitecture between the visually assessed scales of lesion severity ($H4_o$) and activity ($H5_o$) in the evaluation of disease pathogenesis. If significant differences in variance are noted, then independent samples t tests will be used to compare the means for each of the structural variables. Independent samples t tests provide significance levels for variables with unequal variances. These statistical tests were selected as they are used to compare means between two or more samples and will provide data on any significant changes that may be occurring to trabecular bone during the process of lesion development.

Chapter 6

6   Results

This chapter presents the results of the macroscopic assessment of lesion severity and activity, the evaluation of observer reproducibility and reliability, and the quantitative analysis of trabecular bone micro-structures. First, for the macroscopic assessment of lesion severity and activity, tests for dependence on factors such as age or sex of the individual are presented to identify any palaeoepidemiological trends this sample may exhibit. Second, tests for the evaluation of observer reproducibility and reliability are provided to identify the most reliable methods of image analysis for the application of micro-CT methods to palaeopathological research. Finally, the quantitative analyses of the five variables used to evaluate trabecular bone micro-structure are presented and analyzed to determine: 1) the possibility of a relationship between the presence and absence of orbital and cranial porotic hyperostosis, and 2) the possibility of a relationship between the different categories of severity and/or the activity of orbital and cranial porotic hyperostosis.

6.1   Macroscopic Assessment

This section presents the results of the visual assessment of both orbital and cranial porotic hyperostosis in order to examine the palaeoepidemiological nature of this condition in the study sample. It should be noted that in most cases a complete skull was not available for analysis and the macroscopic examination of porotic hyperostosis was only possible for those cranial fragments that were present and available. In an attempt to ascertain the palaeoepidemiological pattern of porotic hyperostosis in the study sample, various comparisons were undertaken and included age and lesion severity, sex and lesion severity, age and lesion activity, and sex and lesion activity.

As noted in Chapter 5, Section 5.2, orbital and cranial porotic hyperostosis were assessed using the modified Nathan and Haas (1966) scoring system proposed by Stuart-Macadam (1985) which identifies three categories of lesion severity: light (porotic type), medium (cribrotic type), and severe (trabecular type). The macroscopic evaluation of orbital and cranial porotic hyperostosis also included the assessment of lesion activity at the time of

death using the standards recommended by Buikstra and Ubelaker (1994) and the descriptions provided by Mensforth et al. (1978) and Mittler and Van Gerven (1994) as noted in Section 5.2 of Chapter 5. Three categories of lesion activity were used in this assessment including active, healing, and mixed (evidence of active disease process and healing).

Appendices E, F, and G present the results for the macroscopic data collected from the orbits, parietal bones, and occipital squama, respectively. In cases where a specific age range could not be determined due to poor preservation, the terms "sub-adult" and "adult" are used to replace numerical age ranges in the column labelled "Age". "Sub-adult" is used to describe individuals who were estimated to be less than 18 years of age at the time of death, and "adult" is used to describe individuals estimated to be older than 18 years of age at the time of death; each of these estimates are based on available skeletal fragments.

6.1.1   Age, Sex, and Lesion Severity

The raw data from Appendices E through G are condensed into Tables 6.1 through 6.3 to demonstrate the age distribution of the different levels of severity for orbital and cranial porotic hyperostosis and include only those 37 individuals with evidence of pathological lesions out of the total sample size of 66 individuals. Table 6.1 includes those individuals with orbital porotic hyperostosis, Table 6.2 subsumes all of the individuals with cranial porotic hyperostosis located on the parietal bones and the occipital squama, and Table 6.3 summarizes all of the individuals with evidence of both orbital and cranial porotic hyperostosis.

Table 6-1: Age Distribution and Lesion Severity for Orbital Porotic Hyperostosis

	Severity			
Age	**Light**	**Medium**	**Severe**	**Total**
6 mos-3yrs	1	0	0	1
4-12	1	2	1	4
Sub-Adult (<18)*	1	0	0	1
Adult (18+)	6	3	0	9
Total	9	5	1	**15**

Table 6-2: Age Distribution and Lesion Severity for Cranial Porotic Hyperostosis

	Severity			
Age	Light	Medium	Severe	Total
6 mos-3yrs	0	0	0	0
4-12	2	1	3	6
Sub-Adult (<18)*	0	1	1	2
Adult (18+)	8	8	1	17
Total	10	10	5	**25**

Table 6-3: Age Distribution and Lesion Severity for Combined Porotic

Hyperostosis

	Severity			
Age	Light	Medium	Severe	Total
6 mos-3yrs	1	0	0	1
4-12	3	2	4	9
Sub-Adult (<18)*	1	1	1	3
Adult (18+)	13	10	1	24
Total	18	13	6	**37**

*age <18 years, but specific age range not determined

Due to small sample sizes, the combined data from Table 6.3, which includes all individuals with evidence of lesions (N=37), were evaluated and both the age and severity categories were collapsed to facilitate valid statistical analysis as all cells must contain data. In Table 6.4, each of the previous three sub-adult age cohorts have been collapsed into the "Sub-adult (<18 years)" age cohort, and the medium and severe lesion severity categories have been combined to represent the later stages of lesion development. A chi-square analysis using Yates correction for continuity (used when there are cells with an expected count of less than 5) did not result in the rejection of the null hypothesis testing the relationship between lesion severity and age ($G = 0.323$, d.f. = 1, $p= 0.570$), indicating that the severity of porotic hyperostosis is not related to the age of the individual in this sample.

Table 6-4: Collapsed Age and Lesion Severity Categories

	Severity		
Age	**Light**	**Medium-Severe**	**Total**
Sub-adult (<18)*	5	8	13
Adult (18+)	13	11	24
Total	18	19	**37**

*Includes all three sub-adult age cohorts

An additional consideration for the palaeoepidemiological profile of porotic hyperostosis in this sample is the relationship between the sex of the individual and lesion severity. Is one sex üore severely affected than the other? A re-organization of the data contained in Table 6.4 is required to consider the null hypothesis that the sex of the individual is independent of the severity of porotic hyperostosis. The sample size in this case will be reduced from 37 individuals to 23 as only individuals of known sex can be included (Tables 6.5). The smaller sample size resulted in some cells (i.e., females, severe) containing a 0. In this case, a statistical analysis is not valid and necessitated the collapsing of the severity categories as seen in Table 6.4 (Table 6.6). Again, no statistically significant relationship between the sex of the individual and the severity of the lesion is demonstrated using Yates chi-square test and the null hypothesis cannot be rejected for this sample (G = 0.349, d.f. = 1, p = 0.555).

Table 6-5: Combined Sex Distribution and Lesion Severity

	Severity			
Sex	**Light**	**Medium**	**Severe**	**Total**
Males	3	4	1	8
Females	9	6	0	15
Total	12	10	1	**23**

Table 6-6: Collapsed Sex and Lesion Severity Categories

	Severity		
Age	**Light**	**Medium/Severe**	**Total**
Males	3	5	8
Females	9	6	15
Total	12	11	**23**

6.1.2   Age and Lesion Activity

As with the evaluation of the relationship between age and lesion severity, Tables 6.7 through 6.9 summarize the age distribution for the categories of lesion activity for orbital and cranial porotic hyperostosis including active, healed, and mixed lesion activity (Buikstra and Ubelaker 1994). Again, for a statistical analysis to be valid, small sample sizes necessitated the collapsing of both the age and lesion activity categories. The "Healed" and "Mixed" activity categories were combined to represent all lesions with evidence of healing, indicating early and later stages of disease recovery (Table 6.10).

Table 6-7: Age Distribution and Lesion Activity for Orbital Porotic Hyperostosis

	Activity			
Age	**Active**	**Healed**	**Mixed**	**Total**
6 mos-3yrs	1	0	0	1
4-12	4	0	0	4
Sub-Adult (<18)	0	0	1	1
Adult (18+)	4	5	0	9
Total	9	5	1	**15**

Table 6-8: Age Distribution and Lesion Activity for Cranial Porotic Hyperostosis

	Activity			
Age	**Active**	**Healed**	**Mixed**	**Total**
6 mos-3yrs	0	0	0	0
4-12	4	1	1	6
Sub-Adult (<18)	2	0	0	2
Adult (18+)	1	13	3	17
Total	7	14	4	**25**

Table 6-9: Age Distribution and Lesion Activity for Combined Porotic Hyperostosis

	Activity			
Age	**Active**	**Healed**	**Mixed**	**Total**
6 mos-3yrs	1	0	0	1
4-12	7	1	1	9
Sub-Adult (<18)	2	0	1	3
Adult (18+)	3	17	4	24
Total	13	18	6	**37**

Table 6-10: Collapsed Age and Lesion Activity Categories

	Activity		
Age	**Active**	**Healed/Mixed**	**Total**
Sub-adult (<18)	10	3	13
Adult (18+)	3	21	24
Total	13	24	**37**

A chi-square test using Yates correction for continuity demonstrated a statistically significant relationship between the age of the individual and the activity of porotic hyperostosis (G=12.660, d.f. = 1, p = 0.000). Therefore the null hypothesis is rejected indicating that the activity of the lesion is dependent upon the age of the individual in the study sample. A careful consideration of Table 6.10 illustrates that only three out of 24 adults have unhealed lesions and that the adults also account for all but three of the healed lesions. However, when referring to the expanded table (Table 6.9), the three sub-adults (<18) included in the collapsed "healed/mixed" category in Table 6.10 belong to the original "mixed" category. This means that out of the 13 sub-adults evaluated in this study, only one individual displays healed lesions.

The possibility of a relationship between lesion activity and the sex of the individual was also evaluated. As with the evaluation of lesion severity, the data contained in Table 6.10 were reorganized and similarly collapsed to test the null hypothesis that the sex of the individual is independent of the activity of porotic hyperostosis (Table 6.11). No statistically significant relationship between the sex of the individual and the activity of the lesion is demonstrated using Yates chi-square test and the null hypothesis cannot be rejected (G = 0.00, d.f. = 1, p = 1.000). Therefore, the sex of the individual seems to have no influence on the activity of porotic hyperostosis in the study sample.

Table 6-11: Collapsed Sex and Lesion Activity Categories

	Activity		
Sex	**Active**	**Healed**	**Total**
Males	1	7	8
Females	2	13	15
Total	3	20	**23**

6.2   Observer Reproducibility and Reliability

The second objective of this study was to assess the reproducibility and reliability of various methods of data collection used on micro-CT volumes of archaeological human skeletal remains. In order to address the null hypothesis that there is no difference in the reproducibility or reliability of 2D and 3D quantitative methods for the analysis of trabecular bone microarchitecture, intra-observer and inter-observer error testing were carried out on 10 randomly selected individuals. Pearson's R correlation (R) and coefficients of determination (R^2) were used to test observer agreement and address the null hypothesis for each of the five structural variables for the three chosen methods: 1) 2D standard VOI method, 2) 3D standard VOI method, and 3) 3D custom VOI method. Definitions for the three tested methods can be found in Chapter 5, Section 5.2.2.2 and detailed descriptions for the five structural variables are provided in Section 5.2.4 of the same chapter. The results for the intra-observer and inter-observer error testing are described separately in the proceeding sections. The raw data for each of the 10 evaluated individuals can be found in Appendix H.

6.2.1   Intra-Observer Reproducibility

Table 6.12 summarizes the results of the intra-observer analysis using Pearson-R correlation and Table 6.13 provides the results for the coefficients of determination (R^2). Statistically, the strength of a relationship between two variables increases the closer the coefficients are to ±1. As a general rule, coefficients between ±0.5 and ±1 are strong, ±0.3 and ±0.5 are moderate, and ±0.1 and ±0.3 are weak (Bland and Altman 1986). For the 2D standard VOI method, moderate to strong, significant correlations ($p < 0.05$) were found using Pearson-R correlation for intra-observer repeated measures of bone volume density (BV/TV), specific bone surface (BS/BV), and trabecular thickness (Tb.Th.). The values for the coefficients of determination (R^2) also indicate that there is a strong predictive relationship between the repeated measures of BV/TV (R^2=0.752) and Tb.Th. (R^2=0.697), but a weaker predictive relationship for BS/BV (R^2=0.566). Repeated measures for the remaining two variables, trabecular number (Tb.N), and trabecular spacing (Tb.Sp.), showed both weak and statistically insignificant correlations, and the

values for the coefficients of determination for these three variables also illustrate weak predictive relationships: Tb.N. ($R^2=0.239$), and Tb.Sp. ($R^2=0.096$).

For the 3D standard VOI method, strong, significant Pearson-R correlations were found for repeated measures of all five variables: BV/TV, BS/BV, Tb.Th., Tb.Sp., and Tb.N (Table 6.12). The results for the coefficients of determination (R^2), indicate that the predictive relationships for measures of BV/TV ($R^2=0.852$), BS/BV ($R^2=0.922$), and Tb.Th. ($R^2=0.787$) were strong while the predictive relationships between the repeated measures for Tb.N ($R^2=0.557$) and Tb.Sp. ($R^2=0.640$) were weaker, but still considered strong (Table 6.13).

For the 3D custom VOI method, the Pearson-R correlations for repeated measures of all five selected variables were strong and statistically significant: BV/TV, BS/BV, Tb.Th., Tb.N., Tb.Sp (Table 6.12). In addition, the values for the coefficients of determination (R^2) for repeated measures were improved over both the 2D and 3D standard VOI methods for four of the five variables including BV/TV ($R^2=0.903$), BS/BV ($R^2=0.980$), Tb.N. ($R^2=0.837$), and Tb.Sp. ($R^2=0.929$), with the weakest predictive relationship occurring in the repeated measures of Tb.Th. ($R^2=0.689$) (Table 6.13).

Table 6-12: Summary of Intra-Observer Results for Pearson-R Correlation (R)

Intra-Observer Reproducibility: Pearson-R Correlation (N=10)										
Method	**BV/TV**		**BS/BV**		**Tb.Th.**		**Tb.N.**		**Tb.Sp.**	
	R	***p***	**R**	***p***	**R**	***P***	**R**	***p***	**R**	***p***
2D Standard	0.867	0.001*	0.752	0.012*	0.835	0.003*	0.489	0.152	0.310	0.384
3D Standard	0.923	0.000*	0.960	0.000*	0.887	0.001 *	0.746	0.013*	0.800	0.000*
3D Custom	0.950	0.000 *	0.990	0.000 *	0.830	0.002 *	0.915	0.000 *	0.964	0.000 *

* Significant correlation

Table 6-13: Summary of Intra-Observer Results for Coefficient of Determination (R^2)

Intra-Observer Reproducibility: Coefficient of Determination (N=10)					
Method	BV/TV	BS/BV	Tb.Th.	Tb.N.	Tb.Sp.
2D Standard	0.752	0.566	0.697	0.239	0.096
3D Standard	0.852	0.922	0.787	0.557	0.640
3D Custom	0.903	0.980	0.689	0.837	0.929

Overall, the variables with the least amount of intra-observer agreement or reproducibility, regardless of methodology, were trabecular thickness (Tb.Th) and trabecular number (Tb.N). In summary, based on the differences demonstrated by the Pearson-R correlations and the coefficients of determination between the 2D and 3D VOI methods, it can be noted that from this experiment, there are differences in the intra-observer reproducibility of 2D and 3D methods for quantitatively evaluating trabecular bone microarchitecture, thus the null hypothesis is rejected. Of the three defined VOI methods the one with the greatest amount of agreement and intra-observer reproducibility between repeated measures of the five selected structural variables was the 3D custom VOI method, followed closely by the 3D standard VOI method.

6.2.2 Inter-Observer Reliability

Tables 6.14 and 6.15 summarize the results of the inter-observer analysis using Pearson-R correlation and coefficients of determination (R^2), respectively. For the 2D standard VOI method, strong, significant correlations were found using Pearson-R correlations for repeated measures of two out of the five variables, BV/TV and BS/BV. For the remaining three variables, correlations between repeated measures were weak to moderate and were statistically insignificant (Tb.Th., Tb.N., and Tb.Sp.) (Table 6.14). Additionally, the values for the coefficients of determination (R^2) for measures of trabecular organization were low, indicating poor predictive relationships between repeated measures of each of those three variables using the 2D standard VOI method (Table 6.15).

For the 3D standard VOI method, strong, significant Pearson-R correlations were found for repeated measures of each of the five structural variables including BV/TV, BS/BV,

Tb.Th., Tb.N., and Tb.Sp (Table 6.14). The coefficients of determination (R^2) for two of the five variables, BS/BV (R^2=0.857) and Tb.Th. (R^2=0.839), suggest that the predictive relationships and, thus, inter-observer reliability of these two variables are high. However, the predictive relationships between repeated measures of BV/TV (R^2= 0.686), Tb.N. (R^2= 0.557), and Tb.Sp. (R^2=0.640) were weaker, suggesting moderate inter-observer reliability with the 3D standard VOI method (Table 6.15).

For the 3D custom VOI method, the Pearson-R correlations for repeated measures of all five variables were strong and statistically significant: BV/TV, BS/BV, Tb.Th., Tb.N., Tb.Sp. (Table 6.14). Again, values for the coefficients of determination (R^2) for repeated measures were improved over both the 2D and 3D standard VOI methods for four of the five variables including BV/TV (R^2=0.848), BS/BV (R^2=0.931), Tb.N. (R^2= 0.745), and Tb.Sp. (R^2=0.814), with the weakest predictive relationship occurring in the repeated measures of Tb.Th. (R^2= 0.716) (Table 6.15).

Table 6-14: Summary of Inter-observer Results for Pearson-R Correlation (R)

Inter-Observer Reliability: Pearson-R Correlation (N=10)										
Method	BV/TV		BS/BV		Tb.Th.		Tb.N.		Tb.Sp.	
	R	p	R	P	R	p	R	p	R	p
2D Standard	0.890	0.005*	0.800	0.005*	0.612	0.060	0.280	0.433	0.483	0.138
3D Standard	0.828	0.003 *	0.926	0.000 *	0.916	0.000*	0.867	0.001 *	0.696	0.025*
3D Custom	0.921	0.000 *	0.965	0.000*	0.846	0.002 *	0.863	0.001 *	0.902	0.002*

Significant correlation

Table 6-15: Summary of Inter-Observer Results for Coefficients of Determination (R^2)

Inter-Observer Reliability: Coefficient of Determination (N=10)					
Method	BV/TV	BS/BV	Tb.Th.	Tb.N.	Tb.Sp.
2D Standard	0.792	0.640	0.374	0.078	0.233
3D Standard	0.686	0.857	0.839	0.752	0.484
3D Custom	0.848	0.931	0.716	0.745	0.814

Overall, the variables with the least amount of inter-observer agreement or reliability were trabecular thickness (Tb.Th.), trabecular number (Tb.N) and trabecular spacing (Tb.Sp.). However, inter-observer agreement with these three variables increased when the 3D standard and custom VOI methods were applied (Tables 6.14 and 6.15). Based on the differences demonstrated by the Pearson-R correlations and the coefficients of determination between the 2D and 3D VOI methods, it can be stated on the basis of this testing that there are differences in the inter-observer reliability of 2D and 3D methods for quantitatively evaluating trabecular bone microarchitecture and the null hypothesis can be rejected. Of the three defined methods the method with the greatest amount of agreement and inter-observer reliability between repeated measures of the five selected structural variables was the 3D custom VOI method.

6.3   Micro-CT 3D Quantitative Analyses

Based on the results of the intra-observer and inter-observer analyses, the micro-CT method with the greatest reproducibility and reliability for quantitatively assessing trabecular bone microarchitecture is the 3D custom VOI method. As such, for the remaining evaluations of 3D trabecular architecture, only those data collected using the 3D custom VOI method were used in the remaining statistical analyses. The raw data for each of the 66 individuals evaluated in the current study are shown in Appendix I.

6.3.1   Bilateral Differences in Trabecular Architecture

The sample used in the current study consists of both complete and fragmentary cranial bones. For individuals represented by paired cranial bones, including the orbits and parietal bones, both left and right sides were present for 36 individuals. The remaining individuals represented by a paired bone had only the left or right side present. In order to determine if left and right sides are interchangeable for statistical analyses, the null hypothesis that no differences in trabecular architecture between the left and right sides of paired bones occur must be tested. Paired samples t-tests were applied to the 36 individuals with both left and right orbits (N=10) and/or parietal bones (N=26). Since data were collected based on specific cranial locations outlined in Chapter 5 (Table 5.1), the data from three locations were assessed for bilateral differences: orbits (N=10),

parietal bosses (N=17), and parietal bones adjacent to the lambdoid suture (N=9). Paired-samples t-tests were conducted for all five structural variables on sub-samples consisting of all three cranial locations combined (N=36), as well as for each cranial location separately.

Paired samples t-tests demonstrated that there are no statistically significant differences ($p > 0.05$) between the left and right sides for any of the five structural variables for the sub-sample of combined cranial locations (N=36). Table 6.16 and Figure 6.1 provide summaries of the results of the paired samples t-test for each of the five structural variables for the combined sub-sample of left and right sides. When each of the three locations – eye orbits (N=10), parietal bosses (N=17), and parietal bones at the lambdoid suture (N=9) - were evaluated as individual sub-samples, paired samples t-tests indicated that there were no statistically significant differences ($p > 0.05$) between left and right sides for each of the five structural variables. Therefore, the null hypothesis cannot be rejected and there are no differences in trabecular architecture between the left and right sides of paired cranial bones.

Table 6-16: Paired Samples t-tests for Left and Right Sides

	Mean	Std. Deviation	Std. Error Mean	95% Confidence Interval		t	df	Sig. (2-tailed)
				Lower	Upper			
BV/TV	-0.0118	0.0809	0.0134	-0.0392	0.0155	-0.881	35	0.384
BS/BV	0.1828	0.9956	0.1659	-0.1540	0.5197	1.102	35	0.278
TbTh	-0.0674	0.4363	0.0727	-0.2150	0.0802	-0.927	35	0.360
TbN	0.0355	0.1941	0.0323	-0.0301	0.1012	1.098	35	0.280
TbSp	0.0023	0.0508	0.0084	-0.0148	0.0195	0.275	35	0.785

Figure 6-1: Boxplot Summary of Bilateral Differences (N=36)
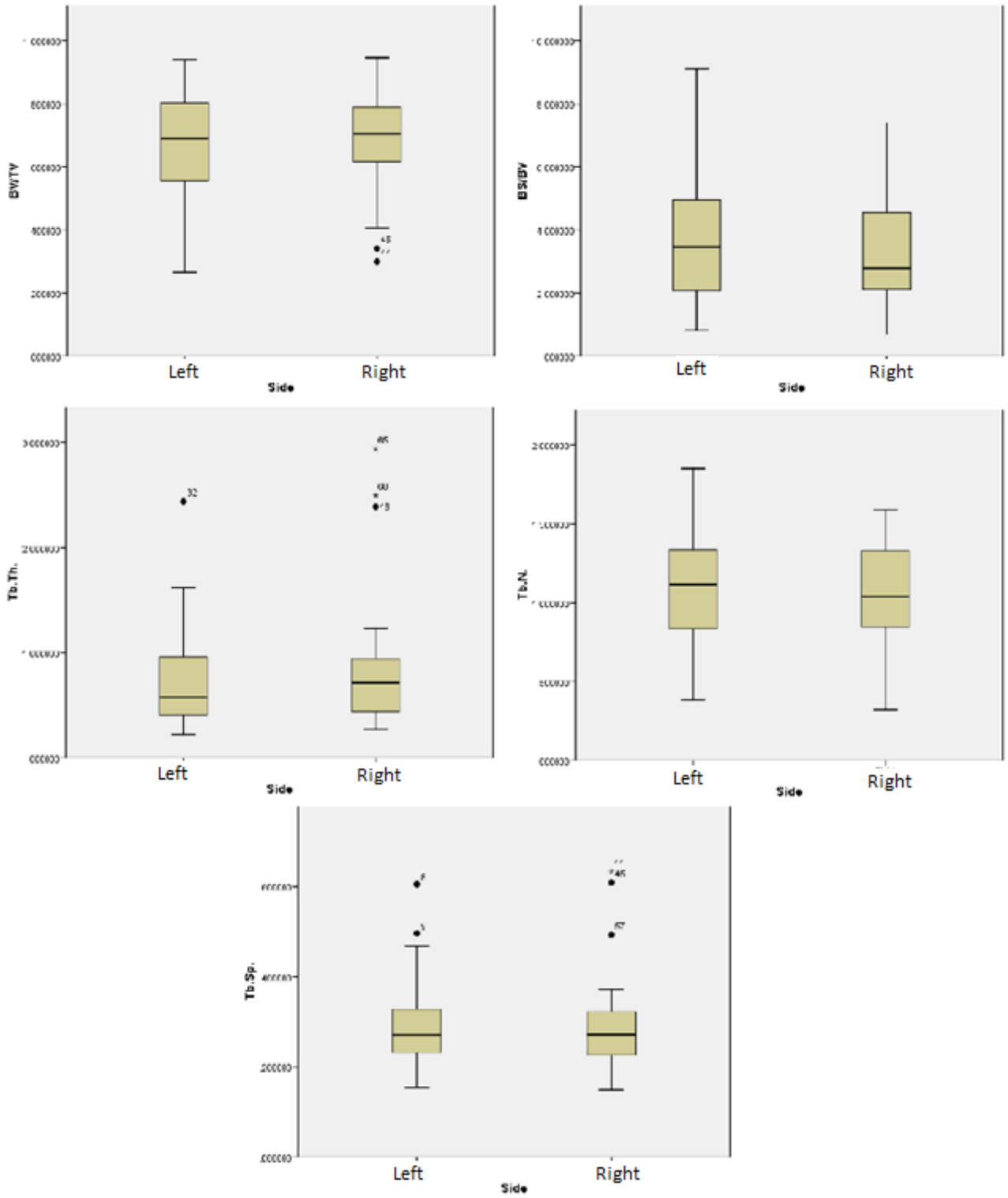
6.3.2　Evaluation of Evidence of Disease Pathogenesis

The third objective of this study is to determine if the quantification of trabecular bone microarchitecture using micro-CT image analysis methods reveals any important diagnostic information regarding the pathogenesis and/or etiology of pathological conditions that give rise to the general macroscopic appearance of porotic hyperostosis. The first consideration for evaluating this objective is to determine if the study sample demonstrates a pattern of trabecular bone microarchitecture similar to previously published results which indicate development-related structural differences throughout the skull (Larsson et al. 2011, 2014). Based on previously published findings, the study sample has been separated into three anatomical sub-samples based on the different cranial bones present for analysis and includes orbits (N=33), parietal bones (N=55), and occipital bones (N=21). In order to avoid introducing potential variability caused by pathological changes to trabecular bone microarchitecture, only those individuals with unaffected cranial bones were used in this evaluation, resulting in three sub-samples that included 18 orbits, 21 parietal bones, and 7 occipital bones. If the analysis of the study sample fails to reject the null hypothesis that no structural differences in trabecular bone microarchitecture exist between the separate cranial bones, then the three current sub-samples can be combined to increase the overall size of the sample available for later statistical analyses.

A Levene's test was used to evaluate the equality of variances (F) for each of the five structural variables to determine the validity of an analysis of variance (ANOVA) for addressing the null hypothesis. No statistically significant differences in variance were found for BV/TV (F = 0.342, p = 0.712), Tb.N. (F = 1.623, p = 0.209), or Tb.Sp (F = 0.985, p = 0.382). However, a statistically significant difference in variance was demonstrated for trabecular thickness (Tb.Th.) (F = 4.566, p = 0.016) and a value approaching significance was demonstrated for specific bone surface (BS/BV) (F = 2.461, p = 0.097). Therefore, the results of an ANOVA would not be valid for the evaluation of two of the five structural variables. As such, Independent Samples t tests, which provide significance levels for variables with unequal variances, were used to

compare the means for each of the structural variables between the three cranial bone types.

The results of the Independent Samples t tests demonstrated statistically significant differences ($p < 0.05$) between the orbits and parietal bones for each of the five structural variables (Table 6.17). It should be noted that the significance values for BS/BV and Tb.Th. are those provided assuming unequal variances (Table 6.17). For the comparison of orbit and occipital bone trabecular microarchitecture, statistically significant differences were demonstrated for four of the five variables, with Tb.Th. approaching significance ($p = 0.063$) (Table 6.18). Finally, t test results for the comparison of parietal and occipital trabecular bone microarchitecture indicated that there are no statistically significant differences ($p > 0.05$) for any of the five structural variables (Table 6.19). The demonstrated structural differences in trabecular bone microarchitecture between orbits and parietal bones and between orbits and occipital bones indicate that the null hypothesis can be rejected in these cases (Figure 6.2). However, the findings that there are no structural differences in trabecular bone microarchitecture between parietal and occipital bones mean that the null hypothesis can be accepted in this pairing (Figure 6.2). Based on these results, the data for the orbits were kept as a separate sub-sample (N=33) for the analysis of orbital porotic hyperostosis, and the data for the parietal and occipital bones were combined into a single cranial vault sub-sample (N=48) for the analysis of cranial porotic hyperostosis.

After validating the independent statistical treatment of orbital and cranial porotic hyperostosis, the next step is to determine whether the five chosen structural variables demonstrate any differences in trabecular bone microarchitecture that could reveal important diagnostic information regarding pathogenesis. In order to address the third objective, it was first necessary to investigate the possibility of an association of any of the five structural variable measures with the visually observed categories of lesion severity and activity.

Table 6-17: Independent Samples *t*-test for Orbit and Parietal Bone Differences

		Levene's Test for Equality of Variances		t-test for Equality of Means					95% Confidence Interval of the Difference	
		F	Sig.	T	Df	Sig. (2-tailed)	Mean Diff.	Std. Error Diff.	Lower	Upper
BV/TV	Equal variances	0.555	0.461	-3.62	37	0.001*	-0.178	0.049	-0.278	-0.079
	Unequal variances			-3.58	33.7	0.001	-0.178	0.049	-0.280	-0.077
BS/BV	Equal variances	3.948	0.054	3.39	37	0.002	2.358	0.693	0.951	3.764
	Unequal variances			3.27	26.6	0.003*	2.358	0.721	0.877	3.838
Tb.Th	Equal variances	6.487	0.015	-2.89	37	0.006	-0.335	0.115	-0.569	-0.100
	Unequal variances			-3.02	31.9	0.005*	-0.335	0.110	-0.561	-0.109
Tb.N.	Equal variances	2.443	0.127	2.42	37	0.020*	0.210	0.086	0.034	0.385
	Unequal variances			2.50	35.0	0.017	0.210	0.084	0.039	0.380
Tb.Sp	Equal variances	1.177	0.285	3.31	37	0.002*	0.096	0.029	0.037	0.155
	Unequal variances			3.24	30.6	0.003	0.096	0.029	0.035	0.157

Significant difference

Table 6-18: Independent Samples *t*-test for Orbit and Occipital Bone Differences

		Levene's Test for Equality of Variances		t-test for Equality of Means					95% Confidence Interval of the Difference	
		F	Sig.	T	df	Sig. (2-tailed)	Mean Diff.	Std. Error Diff.	Lower	Upper
BV/TV	Equal variances	0.341	0.565	-3.07	23	0.005*	-0.220	0.072	-0.369	-0.072
	Unequal variances			-3.3	12.5	0.006	-0.220	0.068	-0.367	-0.074
BS/BV	Equal variances	1.782	0.195	2.5	23.0	0.019*	2.751	1.091	0.493	5.008
	Unequal variances			3.1	18.5	0.006	2.751	0.876	0.914	4.587
Tb.Th.	Equal variances	8.542	0.008	-3.0	23.0	0.006	-0.468	0.154	-0.786	-0.150
	Unequal variances			-2.2	6.9	0.063	-0.468	0.212	-0.970	0.034

		Levene's Test for Equality of Variances		t-test for Equality of Means						95% Confidence Interval of the Difference	
		F	Sig.	T	df	Sig. (2-tailed)	Mean Diff.	Std. Error Diff.	Lower	Upper	
Tb.N.	Equal variances	2.933	0.100	2.5	23.0	0.018*	0.285	0.112	0.053	0.516	
	Unequal variances			2.0	7.8	0.076	0.285	0.139	-0.038	0.607	
Tb.Sp.	Equal variances	1.14	0.297	2.9	23.0	0.008*	0.124	0.043	0.036	0.212	
	Unequal variances			3.6	18.5	0.002	0.124	0.034	0.052	0.196	

Significant difference

Table 6-19: Independent Samples *t*-test for Parietal and Occipital Bone Differences

		Levene's Test for Equality of Variances		t-test for Equality of Means						95% Confidence Interval of the Difference	
		F	Sig.	T	df	Sig. (2-tailed)	Mean Diff.	Std. Error Diff.	Lower	Upper	
BV/TV	Equal variances	0.006	0.940	-0.664	26	0.513	-0.041	0.062	-0.170	0.087	
	Unequal variances			-0.656	10.1	0.527	-0.041	0.063	-0.182	0.099	
BS/BV	Equal variances	0.015	0.905	0.568	26	0.575	0.393	0.692	-1.030	1.816	
	Unequal variances			0.564	10.2	0.585	0.393	0.697	-1.155	1.941	
Tb.Th.	Equal variances	0.543	0.468	-0.658	26	0.517	-0.133	0.202	-0.548	0.282	
	Unequal variances			-0.589	8.7	0.571	-0.133	0.225	-0.645	0.379	
Tb.N.	Equal variances	0.106	0.748	0.532	26	0.599	0.074	0.140	-0.213	0.361	
	Unequal variances			0.506	9.5	0.625	0.074	0.147	-0.255	0.404	
Tb.Sp.	Equal variances	0.217	0.645	0.849	26	0.404	0.027	0.032	-0.039	0.093	
	Unequal variances			0.943	12.5	0.364	0.027	0.029	-0.035	0.090	

Figure 6-2: Boxplot Summary of Cranial Bone Differences (N=48)
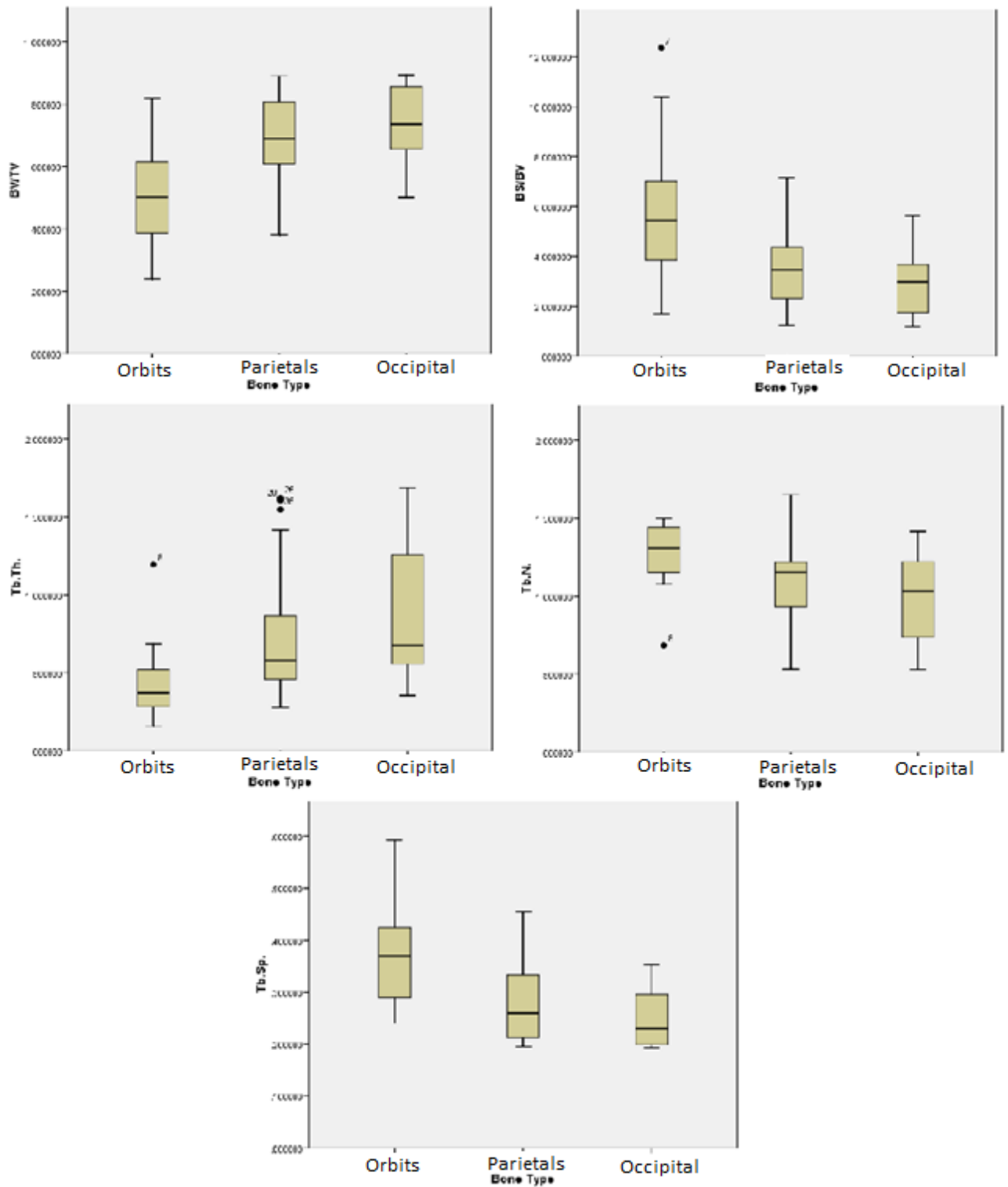
6.3.2.1   Lesion Severity and Trabecular Microarchitecture

My intitial hypothesis evaluated disease pathogenesis with the null hypothesis being that no significant differences exist in trabecular bone microarchitecture between unaffected individuals and affected individuals based on the visually observed categories of lesion severity (light, medium, severe) (H4$_o$). This hypothesis tested both orbital porotic hyperostosis (N=33) and cranial porotic hyperostosis (N=48) separately. For the sub-sample of orbits, only one individual with evidence of lesions was scored in the "severe" lesion category. Additionally, for the sub-sample of cranial vault bones, only four individuals with lesions were scored in the "severe" category. To facilitate proper statistical analysis and increase comparative sample sizes, individuals from the "medium" and "severe" lesion categories were combined to represent the later stages of disease pathogenesis.

For the analysis of orbital porotic hyperostosis (N = 33), Levene's test was used to evaluate the equality of variances (F) between the three lesion severity categories (unaffected, light, medium-severe) for each of the five structural variables to determine the validity of an analysis of variance (ANOVA) for addressing the null hypothesis. No statistically significant differences ($p > 0.05$) in variance were found for any of the five structural variables and an ANOVA can be considered a valid test of the null hypothesis. Boxplot summaries for each of the structural variables organized by lesion severity category are provided in Figure 6.3. The overall results of the ANOVA for the sub-sample of orbits demonstrated a statistically significant difference between the lesion severity categories for BS/BV ($p = 0.013$) and values approaching significance for BV/TV, Tb.Th., and Tb.N. No statistically significant difference was found between lesion severity categories for Tb.N. (Table 6.20).

Post-Hoc analyses were conducted to further explore and compare the means of each of the three lesion severity categories using Fisher's Least Significant Difference (LSD) test, which corrects for small sample sizes. Fisher's LSD test demonstrated no statistically significant differences ($p > 0.05$) between unaffected individuals and individuals with lesions scored in the "light" category for any of the five structural variables (Table 6.21). Therefore, no statistical differences in orbital trabecular microarchitecture between

unaffected individuals and individuals with evidence of light orbital porotic hyperostosis were found. The null hypothesis was accepted.

Figure 6-3: Boxplot Summary for Orbital Lesion Severity (N=33)
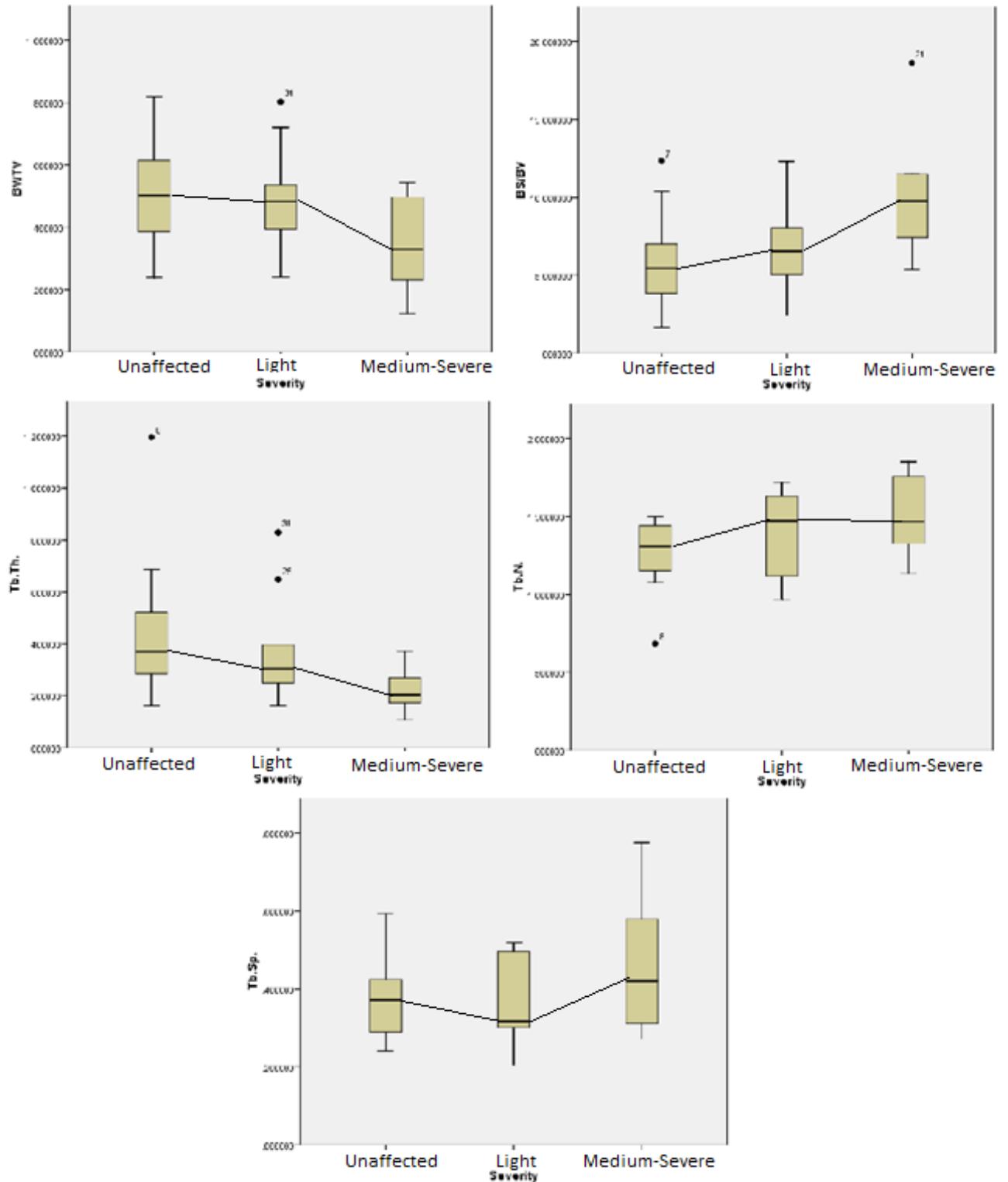
Fisher's LSD tests of unaffected individuals compared to individuals with lesions scored in the "medium-severe" category demonstrated statistically significant differences ($p <$ 0.05) for four of the five structural variables. The directionality of the mean differences for these variables is illustrated in Figure 6.3. No statistically significant differences were demonstrated for Tb.Sp. ($p = 0.156$) (Table 6.21). From these results, there are differences in orbital trabecular microarchitecture for four of the five structural variables between unaffected individuals and individuals with evidence of medium-severe orbital porotic hyperostosis. Therefore, for this comparison, the null hypothesis can be rejected when considering four of the five structural variables.

Table 6-20: ANOVA for Orbital Lesion Severity and Measures of Trabecular Structure (N=33)

		Sum of Squares	Df	Mean Square	F	Sig.
					ANOVA	
BV/TV	Between Groups	0.139	2	0.069	2.444	0.104
	Within Groups	0.85	30	0.028		
	Total	0.989	32			
BS/BV	Between Groups	100.987	2	50.493	5.079	0.013*
	Within Groups	298.22	30	9.941		
	Total	399.207	32			
Tb.Th.	Between Groups	0.212	2	0.106	2.269	0.121
	Within Groups	1.401	30	0.047		
	Total	1.613	32			
Tb.N.	Between Groups	0.264	2	0.132	2.344	0.113
	Within Groups	1.689	30	0.056		
	Total	1.954	32			
Tb.Sp.	Between Groups	0.042	2	0.021	1.317	0.283
	Within Groups	0.481	30	0.016		
	Total	0.523	32			

Significant Difference

Finally, Fisher's LSD tests of individuals with lesions scored in the "light" category compared to those with lesions scored in the "medium-severe" category, demonstrated a statistically significant difference for BS/BV ($p = 0.026$). *P*-values approaching significance were demonstrated for BV/TV ($p = 0.098$). No statistically significant differences ($p > 0.05$) between "light" and "medium-severe" lesions were demonstrated

for Tb.Th., Tb.N., or Tb.Sp. (Table 6.21). Overall, there appears to be some small differences in orbital trabecular microarchitecture, particularly with the bone surface to volume ratio (BS/BV) and bone volume density (BV/TV), between individuals with light orbital porotic hyperostosis and individuals with medium-severe orbital porotic hyperostosis. Based on these results, the null hypothesis is rejected for the analysis of specific bone surface (BS/BV) and accepted for the remaining four trabecular structure variables.

Table 6-21: Fisher's LSD Test for Post-Hoc Analysis of Orbital Lesion Severity (N=33)

Fisher's LSD							
Dependent Variable	**(I) Severity**	**(J) Severity**	**Mean Difference**	**Std. Error**	**Sig.**	**95% Confidence Interval**	
						Lower	**Upper**
BV/TV	Unaffected	Light	0.022	0.0687	0.751	-0.1183	0.1624
		Med-Severe	0.1735	0.0794	0.037*	0.0114	0.3356
	Light	Med-Severe	0.1515	0.0887	0.098	-0.0296	0.3327
		Unaffected	-0.022	0.0687	0.751	-0.1624	0.1183
	Medium-Severe	Light	-0.1515	0.0887	0.098	-0.3327	0.0296
		Unaffected	-0.1735	0.0794	0.037*	-0.3356	-0.0114
BS/BV	Unaffected	Light	-0.8212	1.2872	0.528	-3.4498	1.8075
		Med-Severe	-4.72E+00	1.4863	0.003*	-7.7528	-1.6821
	Light	Med-Severe	-3.90E+00	1.6617	0.026*	-7.29	-0.5026
		Unaffected	0.8212	1.2872	0.528	-1.8075	3.4498
	Medium-Severe	Light	3.8963	1.6617	0.026*	0.5026	7.29
		Unaffected	4.7175	1.4863	0.003*	1.6821	7.7528
Tb.Th.	Unaffected	Light	0.0539	0.0882	0.546	-0.1262	0.2341
		Med-Severe	0.217	0.1019	0.041*	0.0089	0.425
	Light	Med-Severe	0.163	0.1139	0.163	-0.0695	0.3957
		Unaffected	-0.0539	0.0882	0.546	-0.2341	0.1262
	Medium-Severe	Light	-0.163	0.1139	0.163	-0.3957	0.0695
		Unaffected	-0.217	0.1019	0.041*	-0.425	-0.0089
Tb.N.	Unaffected	Light	-0.1199	0.0969	0.225	-0.3177	0.0779
		Med-Severe	-0.2302	0.1119	0.048*	-0.4587	-0.0017

Fisher's LSD							
Dependent Variable	(I) Severity	(J) Severity	Mean Difference	Std. Error	Sig.	95% Confidence Interval Lower	Upper
	Light	Med-Severe	-0.1103	0.1251	0.385	-0.3657	0.1451
		Unaffected	0.1199	0.0969	0.225	-0.0779	0.3177
	Medium-Severe	Light	0.1103	0.1251	0.385	-0.1451	0.3657
		Unaffected	0.2302	0.1119	0.048*	0.0017	0.4587
Tb.Sp.	Unaffected	Light	0.01402	0.0517	0.788	-0.0915	0.1195
		Med-Severe	-0.0867	0.0597	0.156	-0.2086	0.0351
	Light	Med-Severe	-0.1007	0.0667	0.141	-0.237	0.0354
		Unaffected	-0.014	0.0517	0.788	-0.1195	0.0915
	Medium-Severe	Light	0.1007	0.0667	0.141	-0.0354	0.237
		Unaffected	0.0867	0.0597	0.156	-0.0351	0.2086

Significant difference

For the analysis of cranial porotic hyperostosis ($N = 48$), Levene's test was used to evaluate the equality of variances (F) between the three lesion severity categories for each of the five structural variables to determine the validity of an analysis of variance (ANOVA) for addressing the null hypothesis. No statistically significant differences ($p > 0.05$) in variance were found for any of the five structural variables and an ANOVA can be used as a valid test of the null hypothesis for the cranial vault sub-sample. Boxplot summaries for each of the structural variables organized by lesion severity category are provided in Figure 6.4. The overall results of the ANOVA demonstrated that differences between the categories of lesion severity are approaching levels of significance for BV/TV, BS/BV, and Tb.N. No statistically significant differences were found for Tb.Th. ($p = 0.177$) and Tb.Sp. ($p = 0.229$) (Table 6.22).

Figure 6-4: Boxplot Summary for Cranial Lesion Severity (N=48)
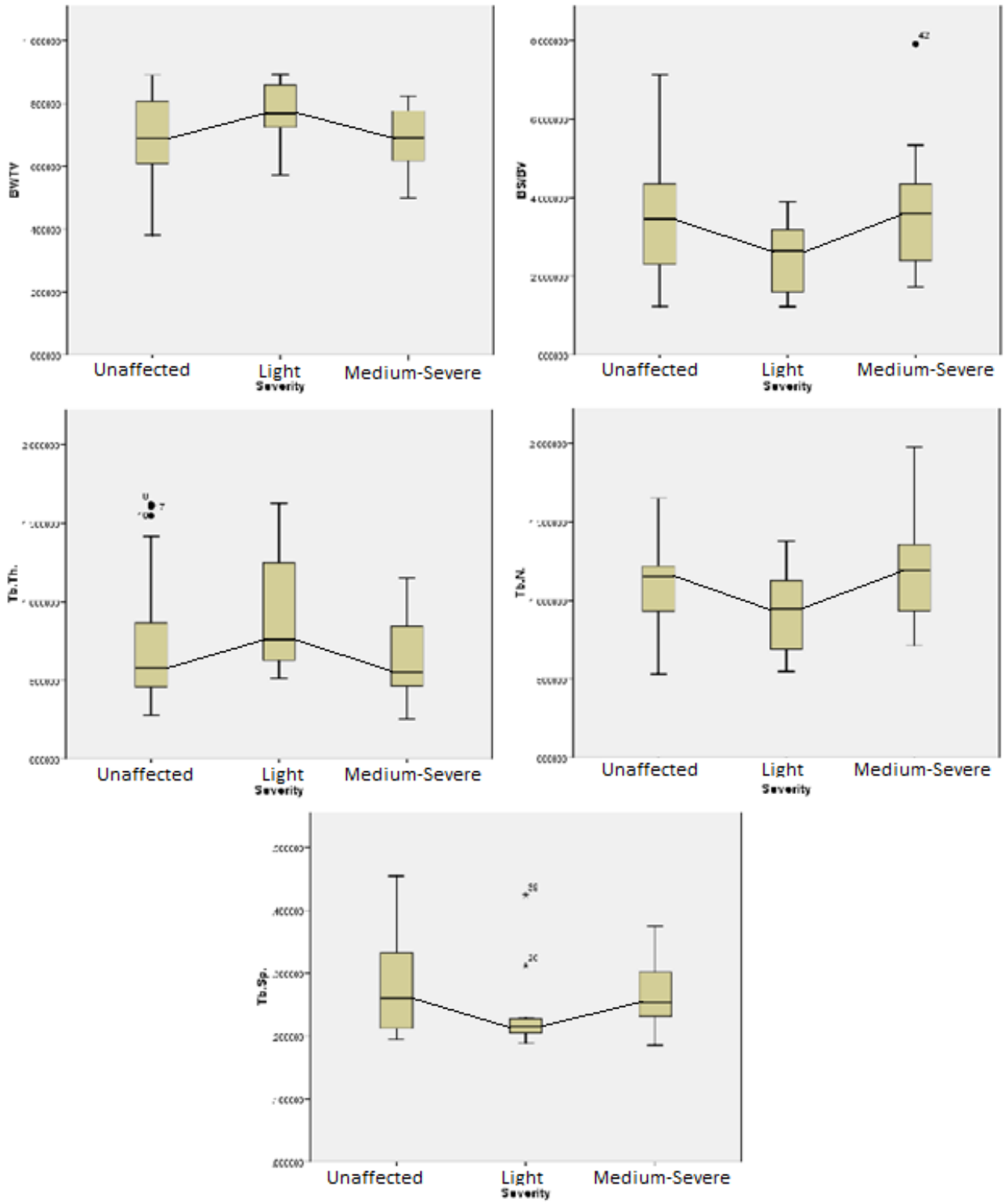
Table 6-22: ANOVA for Cranial Vault Lesion Severity and Measures of Trabecular Structure (N=48)

		Sum of Squares	df	Mean Square	F	Sig.
				ANOVA		
BV/TV	Between Groups	0.065	2	0.033	2.237	0.119
	Within Groups	0.656	45	0.015		
	Total	0.721	47			
BS/BV	Between Groups	9.513	2	4.757	2.226	0.120
	Within Groups	96.177	45	2.137		
	Total	105.691	47			
Tb.Th.	Between Groups	0.510	2	0.255	1.797	0.177
	Within Groups	6.387	45	0.142		
	Total	6.897	47			
Tb.N.	Between Groups	0.417	2	0.208	2.175	0.125
	Within Groups	4.313	45	0.096		
	Total	4.729	47			
Tb.Sp.	Between Groups	0.014	2	0.007	1.524	0.229
	Within Groups	0.205	45	0.005		
	Total	0.219	47			

Post-hoc analyses were conducted to further explore and compare the means of each of the three lesion severity categories using Fisher's Least Significant Difference (LSD) test. Fisher's LSD test demonstrated no statistically significant differences ($p > 0.05$) between unaffected individuals and individuals with lesions scored in the "light" category for Tb.Th. and Tb.N. However, differences approaching significance were found for BV/TV ($p = 0.066$), BS/BV ($p = 0.112$), and Tb.Sp. ($p = 0.088$) (Table 6.23). There appear to be some differences in cranial vault trabecular microarchitecture between unaffected individuals and individuals with evidence of light cranial porotic hyperostosis. However, based only on the demonstrated p-values, the null hypothesis was accepted for this comparison.

Fisher's LSD test of unaffected individuals and individuals with lesions scored in the "medium-severe" category demonstrated no statistically significant differences ($p > 0.05$) for any of the five structural variables (Table 6.23). These results indicate that there are no statistical differences in cranial vault trabecular bone microarchitecture between

unaffected individuals and individuals with evidence of medium-severe cranial porotic hyperostosis. Therefore, the null hypothesis was accepted for this comparison.

When comparing individuals with lesions scored in the "light" category and those with lesions scored in the "medium-severe" category, Fisher's LSD tests demonstrated a statistically significant difference for BS/BV ($p = 0.046$) and Tb.N. (0.043).   Mean differences closely approaching significance were demonstrated for BV/TV ($p = 0.064$) and Tb.Th. (0.064). No statistically significant difference ($p > 0.05$) between "light" and "moderate-severe" lesions was demonstrated for Tb.Sp. (Table 6.23). The general changes in mean directionality for all of these variables for each category of lesion severity are illustrated in Figure 6.4. Overall, there appear to be some differences in cranial vault trabecular bone microarchitecture between individuals with evidence of light cranial porotic hyperostosis and individuals with evidence of medium-severe cranial porotic hyperostosis. Therefore, the null hypothesis is rejected in the analysis of specific bone surface (BS/BV) and trabecular thickness (Tb.Th.), but was accepted for the analysis of the remaining three variables.

Table 6-23:   Fisher's LSD Test for Post-Hoc Analysis of Cranial Vault Lesion Severity (N=48)

Fisher's LSD							
Dependent Variable	(I) Severity	(J) Severity	Mean Difference (I-J)	Std. Error	Sig.	95% Confidence Interval	
						Lower	Upper
BV/TV	Unaffected	Light	-0.08217	0.0437	.066†	-0.1702	0.0058
		Med-Severe	0.00649	0.0408	0.874	-0.0757	0.0887
	Light	Med-Severe	0.08866	0.0468	.064†	-0.0055	0.1828
		Unaffected	0.08217	0.0437	.066†	-0.0058	0.1702
	Medium-Severe	Light	-0.08866	0.0468	.064†	-0.1828	0.0055
		Unaffected	-0.00649	0.0408	0.874	-0.0887	0.0757
BS/BV	Unaffected	Light	0.8581	0.529	0.112	-0.2075	1.9236
		Med-Severe	-0.3022	0.4942	0.544	-1.2976	0.6932
	Light	Med-Severe	-1.1603	0.5662	.046*	-2.3007	-0.0199
		Unaffected	-0.8581	0.529	0.112	-1.9236	0.2075
	Medium-	Light	1.16	0.5662	.046*	0.0199	2.3007

Fisher's LSD							
Dependent Variable	**(I) Severity**	**(J) Severity**	**Mean Difference (I-J)**	**Std. Error**	**Sig.**	**95% Confidence Interval**	
						Lower	**Upper**
	Severe	Unaffected	0.3022	0.4942	0.544	-0.6932	1.2976
Tb.Th.	Unaffected	Light	-0.1536	0.1363	0.266	-0.4282	0.121
		Med-Severe	0.123	0.1274	0.339	-0.1335	0.3795
	Light	Med-Severe	0.2766	0.1459	.064†	-0.0173	0.5705
		Unaffected	0.1536	0.1363	0.266	-0.121	0.4282
	Medium-Severe	Light	-0.2766	0.1459	.064†	-0.5705	0.0173
		Unaffected	-0.123	0.1274	0.339	-0.3795	0.1335
Tb.N.	Unaffected	Light	0.1295	0.112	0.254	-0.0961	0.3551
		Med-Severe	-0.1202	0.1047	0.257	-0.331	0.0906
	Light	Med-Severe	-0.2497	0.1199	.043*	-0.4912	-0.0083
		Unaffected	-0.1295	0.112	0.254	-0.3551	0.0961
	Medium-Severe	Light	0.2497	0.1199	.043*	0.0083	0.4912
		Unaffected	0.1202	0.1047	0.257	-0.0906	0.331
Tb.Sp.	Unaffected	Light	0.0426	0.0244	.088†	-0.0066	0.0918
		Med-Severe	0.0152	0.0228	0.509	-0.0308	0.0611
	Light	Med-Severe	-0.0274	0.0261	0.299	-0.0801	0.0252
		Unaffected	-0.0426	0.0244	.088†	-0.0918	0.0066
	Medium-Severe	Light	0.0274	0.0261	0.299	-0.0252	0.0801
		Unaffected	-0.0152	0.0228	0.509	-0.0611	0.0308

* *Significant Difference;* †*Approaching significance*

6.3.2.2 Lesion Activity and Trabecular Architecture

The second hypothesis evaluated disease pathogenesis with the null hypothesis being that no significant differences exist in trabecular bone microarchitecture between unaffected individuals and affected individuals based on the observed categories of lesion activity (active, healed, mixed) (H5$_o$). As with the evaluation of lesion severity, this hypothesis tested orbital and cranial porotic hyperostosis separately. For orbital porotic hyperostosis (N = 33), only two individuals with evidence of porotic lesions were scored in the

"mixed" lesion activity category. Additionally, for cranial porotic hyperostosis (N = 48), only four individuals with lesions were scored in the "mixed" activity category. To facilitate proper statistical analysis and increase comparative sample sizes, individuals from the "healed" and "mixed" lesion categories were combined to represent the healing stages of disease pathogenesis.

For the analysis of orbital porotic hyperostosis, Levene's test was used to evaluate the equality of variances (F) between the three lesion activity categories (unaffected, active, healed) for each of the five structural variables to determine the validity of an analysis of variance (ANOVA) for addressing the null hypothesis. No statistically significant differences ($p > 0.05$) in variance were found for any of the five structural variables and an ANOVA can be considered a valid test of the null hypothesis for the sub-sample of orbits. Boxplot summaries for each of the structural variables organized by lesion severity category are provided in Figure 6.5. The overall results of the ANOVA demonstrated a statistically significant difference between the categories of lesion activity for BS/BV ($p = 0.052$). No significant differences ($p > 0.05$) in lesion activity were found for BV/TV, Tb.Th., Tb. N., and Tb.Sp. (Table 6.24).

Post-hoc analyses were conducted to further explore and compare the means of the three lesion activity categories using Fisher's Least Significant Difference (LSD) test. Fisher's LSD tests demonstrated statistically significant differences ($p < 0.05$) for four of the five structural variables for the mean comparisons between unaffected individuals and individuals with lesions scored in the "active" lesion category (Table 6.25). No statistically significant difference was demonstrated for Tb.Sp. ($p = 0.187$). These results indicate that there are differences in orbital trabecular bone microarchitecture between unaffected individuals and individuals with lesions scored in the "active" lesion category. Therefore, the null hypothesis is rejected for the comparison of unaffected individuals and individuals with active orbital porotic hyperostosis for four of the five structural variables.

Figure 6-5: Boxplot Summary for Orbital Lesion Activity (N=33)
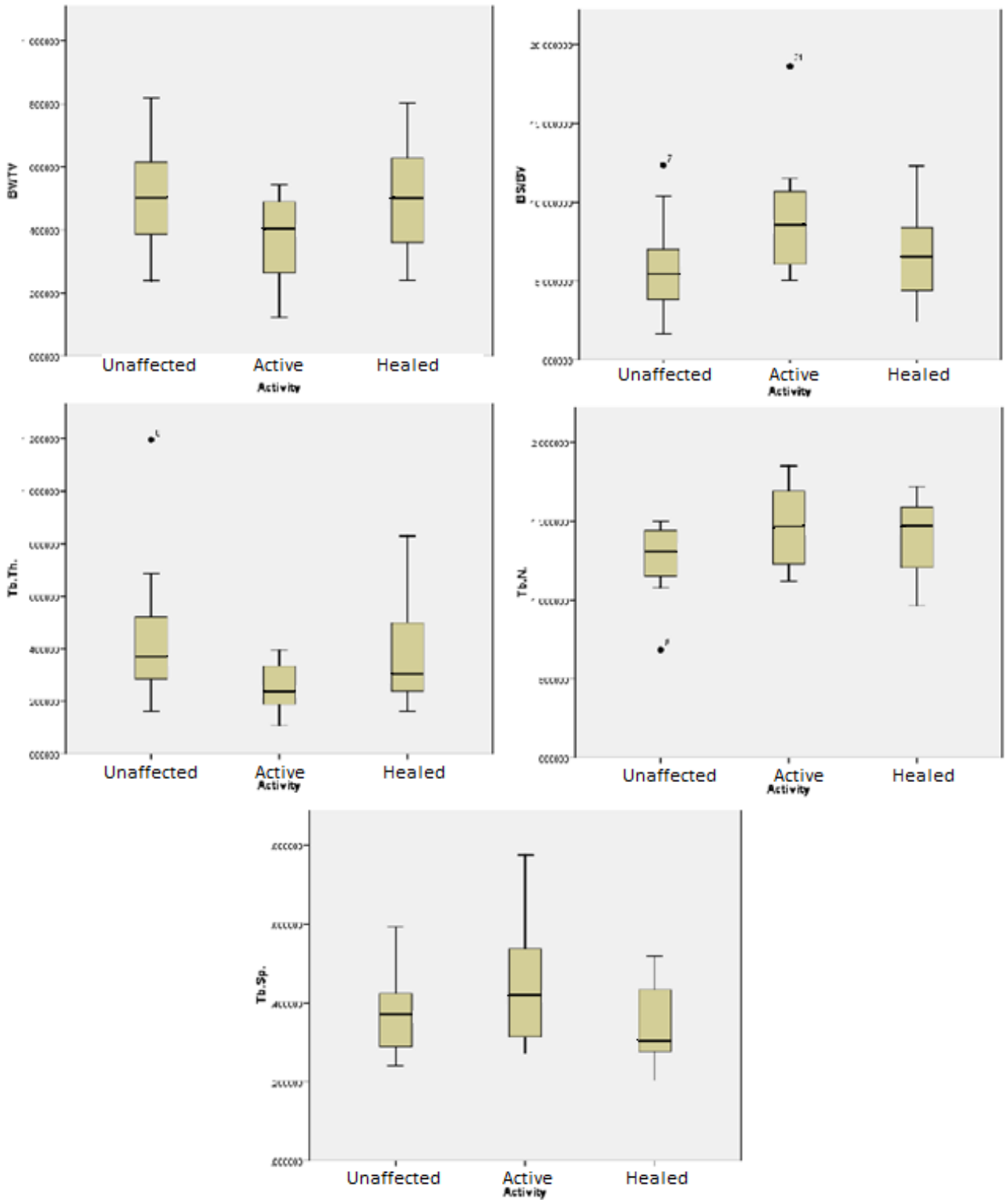
Table 6-24: ANOVA for Orbital Lesion Activity and Measures of Trabecular Structure (N=33)

		Sum of Squares	df	Mean Square	F	Sig.
		ANOVA				
BV/TV	Between Groups	0.119	2	0.059	2.048	0.147
	Within Groups	0.870	30	0.029		
	Total	0.989	32			
BS/BV	Between Groups	71.319	2	35.660	3.263	0.052*
	Within Groups	327.888	30	10.930		
	Total	399.207	32			
Tb.Th.	Between Groups	0.192	2	0.096	2.029	0.149
	Within Groups	1.421	30	0.047		
	Total	1.613	32			
Tb.N.	Between Groups	0.241	2	0.120	2.111	0.139
	Within Groups	1.713	30	0.057		
	Total	1.954	32			
Tb.Sp.	Between Groups	0.043	2	0.021	1.328	0.280
	Within Groups	0.480	30	0.016		
	Total	0.523	32			

Significant difference

Fisher's LSD comparisons between unaffected individuals and individuals with lesions scored in the "healed" activity category demonstrated no statistically significant differences ($p > 0.05$) for any of the five structural variables (Table 6.25). These results demonstrate that there are no structural differences in orbital trabecular bone microarchitecture between unaffected individuals and individuals with healing/healed orbital porotic hyperostosis. Therefore, the null hypothesis was accepted for this comparison.

When comparing individuals with lesions scored in the "active" category and those with lesions scored in the "healed" category, Fisher's LSD tests demonstrated no statistically significant differences ($p > 0.05$) for any of the five structural variables (Table 6.25). This suggests that there are no structural differences in orbital trabecular bone microarchitecture between individuals with active porotic hyperostosis and individuals with healing/healed orbital porotic hyperostosis. Therefore, the null hypothesis was accepted for this comparison.

Table 6-25: Fisher's LSD Test for Post-Hoc Analysis of Orbital Lesion Activity (N=33)

Dependent Variable	(I) Activity	(J) Activity	Mean Difference (I-J)	Std. Error	Sig.	95% Confidence Interval Lower Bound	95% Confidence Interval Upper Bound
	Active	Healed	-0.1298	0.0881	0.151	-0.3098	0.0502
		Unaffected	-0.1432	0.0724	0.057*	-0.2910	0.0046
BV/TV	Healed	Active	0.1298	0.0881	0.151	-0.0502	0.3098
		Unaffected	-0.0134	0.0759	0.861	-0.1684	0.1415
	Unaffected	Active	0.1432	0.0724	0.057*	-0.0046	0.2910
		Healed	0.0134	0.0759	0.861	-0.1415	0.1684
	Active	Healed	2.5870	1.7110	0.141	-0.9073	6.0814
		Unaffected	3.5869	1.4048	0.016*	0.7180	6.4559
BS/BV	Healed	Active	-2.5870	1.7110	0.141	-6.0814	0.9073
		Unaffected	1.0000	1.4726	0.502	-2.0075	4.0074
	Unaffected	Active	-3.5870	1.4048	0.016*	-6.4559	-0.7180
		Healed	-1.0000	1.4726	0.502	-4.0074	2.0075
	Active	Healed	-0.1427	0.1126	0.215	-0.3728	0.0873
		Unaffected	-0.1858	0.0925	0.054*	-0.3746	0.0031
Tb.Th.	Healed	Active	0.1427	0.1126	0.215	-0.0873	0.3728
		Unaffected	-0.0431	0.0969	0.660	-0.2410	0.1549
	Unaffected	Active	0.1858	0.0925	0.054*	-0.0031	0.3746
		Healed	0.0431	0.0969	0.660	-0.1549	0.2410
	Active	Healed	0.0746	0.1237	0.551	-0.1779	0.3271
		Unaffected	0.1989	0.1015	0.059*	-0.0085	0.4062
Tb.N.	Healed	Active	-0.0746	0.1237	0.551	-0.3271	0.1779
		Unaffected	0.1243	0.1064	0.252	-0.0931	0.3416
	Unaffected	Active	-0.1989	0.1015	0.059*	-0.4062	0.0085
		Healed	-0.1243	0.1064	0.252	-0.3416	0.0931
	Active	Healed	0.0994	0.0655	0.140	-0.0344	0.2331
		Unaffected	0.0727	0.0538	0.187	-0.0371	0.1825
Tb.Sp.	Healed	Active	-0.0994	0.0655	0.140	-0.2331	0.0344
		Unaffected	-0.0267	0.0564	0.639	-0.1418	0.0884
	Unaffected	Active	-0.0727	0.0538	0.187	-0.1825	0.0371
		Healed	0.0267	0.0564	0.639	-0.0884	0.1418

*Significant difference

For the analysis of cranial porotic hyperostosis (N=48), Levene's test was used to evaluate the equality of variances (F) between the three lesion activity categories (unaffected, active, healed) for each of the five structural variables to determine the validity of an analysis of variance (ANOVA) for addressing the null hypothesis. No statistically significant differences in variance ($p > 0.05$) were found for any of the five structural variables and an ANOVA can be considered a valid test of the null hypothesis for the cranial vault sub-sample. Boxplot summaries for each of the structural variables organized by lesion severity category are provided in Figure 6.6.

The overall results of the ANOVA demonstrated no statistically significant differences ($p > 0.05$) between the categories of lesion activity for any of the five structural variables (Table 6.26). Post-hoc analyses were not conducted based on the results from the ANOVA. These results demonstrate that there are no differences in cranial vault trabecular microarchitecture between unaffected individuals and individuals with lesions scored in the "active" lesion category. Therefore, the null hypothesis was accepted for the comparison of unaffected individuals and individuals with active cranial porotic hyperostosis.

Figure 6-6: Boxplot Summary for Cranial Lesion Activity (N=48)
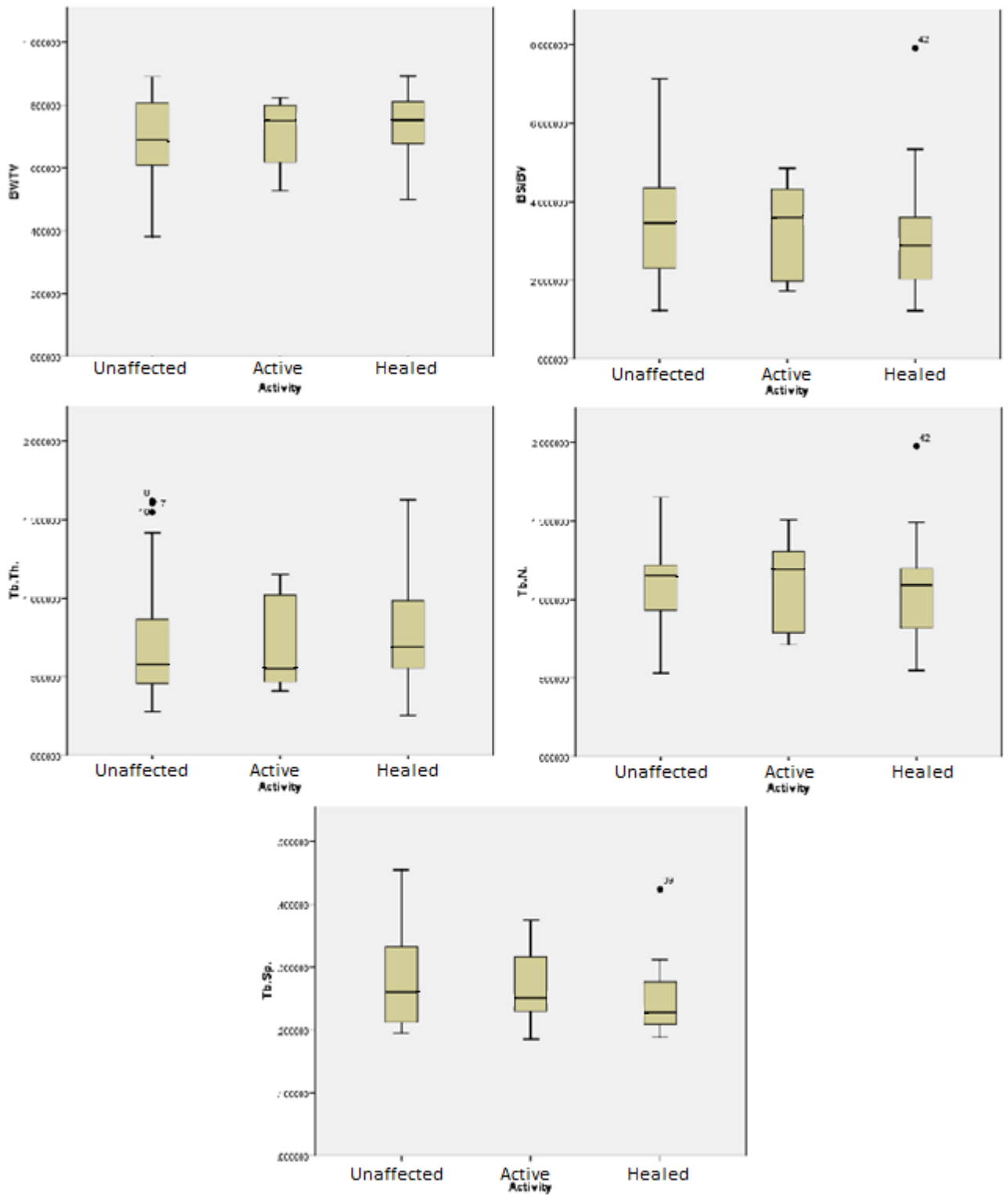
Table 6-26: ANOVA for Cranial Lesion Activity and Measures of Trabecular Structure (N=48)

		Sum of Squares	df	Mean Square	F	Sig.
ANOVA						
BV/TV	Between Groups	0.018	2	0.009	0.571	0.569
	Within Groups	0.703	45	0.016		
	Total	0.721	47			
BS/BV	Between Groups	0.704	2	0.352	0.151	0.860
	Within Groups	104.987	45	2.333		
	Total	105.691	47			
Tb.Th.	Between Groups	0.020	2	0.010	0.066	0.936
	Within Groups	6.877	45	0.153		
	Total	6.897	47			
Tb.N.	Between Groups	0.004	2	0.002	0.019	0.982
	Within Groups	4.725	45	0.105		
	Total	4.729	47			
Tb.Sp.	Between Groups	0.012	2	0.006	1.361	0.267
	Within Groups	0.206	45	0.005		
	Total	0.219	47			

6.4   Summary

This chapter presented the results of the macroscopic assessment of lesion severity and activity, the evaluation of observer reproducibility and reliability, and the evaluation of disease pathogenesis using quantitative analyses of trabecular bone microarchitecture. For the macroscopic assessment of lesion severity and activity in the evaluation of the first objective, Yates chi-square tests for dependence on age and sex of the individual were conducted to identify palaeoepidemiological trends that the current study sample may exhibit. The severity of porotic hyperostosis is neither related to the age nor the sex of the individual. Likewise, the activity of these lesions is not related to the sex of the individual. However, lesion activity is related to an individual's age at death. More specifically, of the sub-adult skeletal remains with evidence of porotic hyperostosis, the majority of individuals exhibited "active" lesions, whereas the majority of the adult skeletal remains with evidence of porotic hyperostosis exhibited "healed" lesions.

Statistical tests for the evaluation of observer reproducibility and reliability included Pearson-R correlation and Coefficients of Determination (R^2). These tests addressed the second objective of the current research study and indicated that the most reproducible and reliable methods of micro-CT image analysis are 3D volume of interest (VOI) methods and, particularly, the 3D custom VOI method described in Chapter 5, Section 5.2.2.2. For intra-observer reproducibility, the 3D custom VOI method provided the highest predictive relationships between repeated measures for four out of the five structural variables. The 3D standard VOI method provided a slightly higher predictive relationship for repeated measures of trabecular thickness (Tb.Th.) versus the 3D custom VOI method. For inter-observer reliability, the 3D custom VOI method provided the highest predictive relationships between repeated measures for three out of the five structural variables. The 3D standard VOI method provided only slightly higher predictive relationships for repeated measures of trabecular thickness (Tb.Th.) and trabecular number (Tb.N.) versus the 3D custom VOI method.

Finally, quantitative analyses of the five structural variables described in Chapter 5, Section 5.2.4 were presented and analyzed to determine if there are any patterns or associations between visually observed categories of lesion severity and activity and trabecular bone microarchitecture. These tests were conducted to address the third objective of the current research study which was to evaluate the possibility of quantitatively identifying information regarding disease pathogenesis. Based on previous findings published by Larsson et al. (2011), a statistical analysis to eliminate normal structural variation throughout the skull as a confounding variable was necessary prior to the evaluation of porotic hyperostosis. The results of independent samples *t* tests revealed that there are significant structural differences in trabecular microarchitecture between the orbits and the bones of the cranial vault, but not between the parietal and occipital bones. Based on these results, independent statistical tests were applied to orbital and cranial porotic hyperostosis. The analyses of orbital porotic hyperostosis revealed a number of significant differences in trabecular microarchitecture between the visually observed categories of lesion severity as well as the categories of lesion activity. The analysis of cranial porotic hyperostosis revealed some significant differences in

trabecular microarchitecture between the visually observed categories of lesion severity, but not to the same extent or in the same pattern as was exhibited with orbital lesions.

Additionally, unlike orbital lesions, no significant differences in trabecular microarchitecture were demonstrated between the observed categories of lesion activity for cranial porotic hyperostosis. Therefore, several measures of trabecular microarchitecture can be associated with visually observed categories of lesion severity and activity, specifically for the analysis of orbital porotic hyperostosis. These results suggest that information regarding the pathogenesis of orbital and cranial porotic hyperostosis can be quantitatively identified using published measures of trabecular microarchitecture obtained from micro-CT images. A more thorough discussion and consideration of these results and the meaning of these data are provided in Chapter 7.

Chapter 7

7 Discussion of Findings and Conclusions

Before a discussion of the quantitative micro-CT results is undertaken, the first objective, regarding porotic hyperostosis in the context of the study sample, will be evaluated. The paleoepidemiological pattern, determined in the previous results chapter, will be compared to those of the populations that make up the study sample as well as other populations reported in the bioarchaeological literature. Having explored these palaeoepidemiological patterns, the development of porotic hyperostosis in this sample will be discussed. Following these palaeoepidemiological considerations, the second and third objectives of the current research study will be addressed through a thorough discussion of the results of the micro-CT evaluation of trabecular bone microarchitecture. The standardization of methods for the collection of quantitative data from micro-CT images will be addressed through a consideration of the results for observer reproducibility and reliability, and the application of micro-CT methods to the palaeopathological study of the pathogenesis of orbital and cranial porotic hyperostosis will be discussed through an examination of the relationships between trabecular bone microarchitecture and macroscopically observable cranial lesions. Finally, future research possibilities and directions will be suggested.

7.1   Palaeoepidemiological Patterns and Context

A great number of studies exploring the prevalence and palaeoepidemiological patterns of orbital and cranial porotic hyperostosis exist in the bioarchaeological literature, many of which have developed palaeoepidemiological models in attempts to explain the development and distribution of this common skeletal condition (e.g. Wright and White 1996; Fairgrieve and Molto 2000; Papathaniasou 2005; Sullivan 2005; Keenleyside and Panayotova 2006). These palaeoepidemiological models consider factors such as age of onset, sex specific patterns, diet and nutrition, living environment, and the severity and activity of lesions which may potentially provide insight into the etiology and dynamics of disease within a population (Palkovich 1987). Unfortunately, due to the nature of this study and the specific objectives of this research, it is not possible to accurately assess the

population prevalence of orbital and cranial porotic hyperostosis for the selected study sample. This is because the study sample is not representative of a specific population, but rather a combined representation of several populations including three Maya and one Greek colonial population(s). Complete skeletal collections were not examined and the selection of individuals from each of the four larger collections was based on the presence of porotic hyperostosis as well as age- and sex-matched individuals without evidence of pathological lesions. Although population prevalence cannot be assessed, age- and sex-specific prevalence patterns were considered and will be compared to previously published data. Additionally, a discussion of published population prevalence rates of these lesions in both Maya and Greek skeletal collections will provide the necessary context for the development of porotic hyperostosis in the current study sample.

The palaeoepidemiological pattern identified in the study sample indicates that a significant age-related trend exists with regard to the development of porotic hyperostosis and the activity of porotic lesions. Of the thirteen sub-adults (<18 years) with evidence of porotic hyperostosis, all but three demonstrated active lesions, while two had lesions with mixed activity (partial healing) and one had completely healed lesions. Of the twenty four adults (> 18 years) with porotic hyperostosis, only three individuals showed evidence of active lesions while the remaining showed evidence of complete or partial healing (Chapter 6, Table 6.9). Overall, the results of this study suggest that the younger the individual is, the more likely they are to demonstrate a lesion in an active state at the time of death. This finding is consistent with other studies which indicate that porotic hyperostosis has its onset in childhood, or is a condition of childhood (e.g. Stuart-Macadam 1985, 1987a; Wright and Chew 1999; Fairgrieve and Molto 2000). More importantly, this palaeoepidemiological pattern in the development of porotic hyperostosis is also consistent with the patterns observed in the larger skeletal collections from which the study sample is derived, including the collection from the Greek colony of Apollonia and the Maya skeletal series.

The overall age distribution of orbital porotic hyperostosis in the sample from the Greek colony of Apollonia indicates that a significantly greater proportion of sub-adults (<18

years) were affected than adults. All thirteen of the sub-adults with orbital porotic hyperostosis had active lesions, while all but one affected adult (>18 years) had lesions that were partially or completely healed (Keenleyside and Panayotova 2006). Studies of orbital and cranial porotic hyperostosis in Italy during Imperial and Medieval times also note similar trends in decreasing prevalence of lesions with increasing age, as well as progressive healing with age. Individuals in older age cohorts tend to show lesions with evidence of healing more often than younger individuals (Salvadei et al. 2001). A study of several populations from Africa, including Kulubnarti, Sudan and the Dakleh Oasis, Egypt, also indicate that active lesions were more prevalent in younger individuals with a gradual decline in older cohorts (Mittler and Van Gerven 1994; Fairgrieve and Molto 2000). When further considering the findings of the study sample in relation to the results from Italy and at the Dakleh Oasis cemeteries, additional similarities in lesion activity status become evident. For example, two of the three sub-adults with evidence of healing who could be assigned to a specific age range in the study sample were subsumed under the 4-12 year cohort (Chapter 6, Table 6.9). Evidence of partial or complete healing in this specific age cohort corresponds with an increase in observed healed porotic hyperostosis in the 6-12 year cohort in both Imperial and Medieval populations from Italy, as well as the 4-12 year cohort in the Kellis 2 cemetery population from Egypt (Fairgrieve and Molto 2000: 326; Salvadei et al. 2001: 713-714). Although the samples from Italy and Kulubnarti indicate that 100% of lesions observed in adults appear to be completely healed, the finding that there are still a small number of active lesions in the adult cohort for the study sample was also consistent with the prevalence data reported for the Apollonia sample as well as both of the Dakleh cemetery populations (Fairgrieve and Molto 2000: 325).

The same palaeoepidemiological pattern of an increase in healed lesions in adults has also been noted in skeletal collections from the New World. Saul (1972) documented an abundance of healed porotic hyperostosis in adults (89.3%) at Altar de Sacrificios during the Classic Maya period. This pattern of a high prevalence of healed porotic hyperostosis in adult crania has been reported for a number of Maya skeletal collections, potentially supporting the argument that porotic hyperostosis is indicative of a childhood condition (Stuart-Macadam 1985). For example, at Classic Period inland sites such as Copán

(Whittington 1989) and Pasión (Wright 1994), 60-90% of adult crania have healed lesions. The majority of porotic lesions evaluated in adult crania at Lamanai during the Postclassic and Historic Periods were also healed (White 1988). It is important to note that Maya skeletal samples are typically small as preservation in the Maya area is notoriously poor due mainly to a humid environment and acidic soils. White (1988) noted that at Lamanai, poor preservation of sub-adults precluded an adequate study of porotic hyperostosis in children. A similar issue was encountered with the Pasión skeletal series where differential preservation meant that porotic hyperostosis could only be scored on adult crania and the age of onset of the condition could not be evaluated (Wright 1997). The issue of cranial preservation in the three Maya samples used in the current study also contributed to the small sample size, particularly with regard to sub-adults (Wright and White 1996; Wright 1997). However, the finding that the majority of lesions observed in adults are healed in Maya collections is consistent with the findings for the study sample, and is also comparable to other New World skeletal samples where sub-adult preservation is improved. In a study of a Late Woodland ossuary from Ohio, Mensforth et al. (1978: 28-29) found that the prevalence of active ("unremodelled") lesions declined significantly in sub-adults from the ages of 3 to 10, which also corresponds to the age-specific prevalence results for the study sample as well as for the Old World samples discussed above. Although the age of onset of porotic hyperostosis has been explored in a number of studies in the New World (e.g. El-Najjar et al. 1975; Lallo et al. 1977; White 1988; Wright 1997), and the patterns observed correspond to the results for the combined Old and New World study sample, a limited number of these studies discriminate between active and healed lesions. This issue may obscure important age-related trends in the palaeoepidemiology and development of porotic hyperostosis in New World populations.

Additional palaeoepidemiological considerations include the relationship between age at death and the level of lesion severity. In the comparison of lesion severity, regardless of age, the majority of individuals with porotic hyperostosis in the study sample were scored in the "light" and "medium" lesion severity categories and no significant relationship between age and lesion severity was demonstrated. Similarly, there does not appear to be an age-related trend with the level of lesion severity in the Apollonia sample, with the

majority of individuals also being scored in the light ("mild") to medium ("moderate") lesion categories (Keenleyside and Panayotova 2006). Although this is consistent with the results for the combined population study sample, these findings do not agree with those demonstrated in other Old World archaeological collections. In Italy, the most severe lesions appear to occur in the sub-adult cohorts (Salvadei et al. 2001) and in Egypt, a significant relationship between age and the level of lesion severity was demonstrated in both of the Dakleh Oasis cemetery populations (Fairgrieve and Molto 2000). A synthesis of data from the analysis of 752 individuals from Poundbury Camp, a Romano-British site, noted that more severe lesions are present exclusively in sub-adults up to the age of 14 years and that light and medium lesions were common across all affected age cohorts (Stuart-Macadam 1985). The data from these studies support the hypothesis that porotic hyperostosis is representative of a childhood condition and, therefore, the results from the study sample were expected to follow this palaeoepidemiological pattern. A failure to reject the null hypothesis in the evaluation of age and lesion severity led to the closer analysis of the study sample data. Upon further evaluation of the sub-adults, five out of thirteen affected individuals had lesions scored in the severe category, while only one affected adult out of a total of twenty four had lesions scored in the same category (Chapter 6, Table 6.3). As such, it is possible that a relationship exists between age and lesion severity in the study sample, but is concealed by the small sample size and/or by the method of lesion scoring, which considers lesion activity and severity separately.

There is a significant amount of literature on the prevalence of orbital and cranial porotic hyperostosis in the Maya skeletal series, as well as many of the skeletal collections from North America. However, very few publications consider palaeoepidemiological trends regarding age and lesion severity. Although a more detailed comparison of the palaeoepidemiological patterns of orbital and cranial porotic hyperostosis in the study sample with those of other Greek and Maya skeletal populations would be ideal, these comparisons are complicated by the lack of systematic and detailed studies of porotic hyperostosis in Greek and Maya samples (Keenleyside and Panayotova 2006). Reported prevalence rates for porotic hyperostosis for a number of Greek and Maya skeletal samples can be found in the literature (Angel 1966, 1971; Wright and White 1996;

Wright and Chew 1999; Papathanasiou 2005). However, a focus on overall prevalence without consideration of age- and sex-specific distribution obscures any potential palaeoepidemiological patterns that may be present.

Based on these results, it appears that the most consistent palaeoepidemiological trend with respect to orbital and cranial porotic hyperostosis in archaeological skeletal collections is the relationship between age and lesion activity. This supports the argument that the onset of porotic hyperostosis occurs during early childhood and is lessened or resolved in adulthood (Stuart Macadam 1985). Although less consistent in the published literature, evidence of a relationship between age and lesion severity has also been documented in archaeological collections and may in fact be a trend in the study sample upon closer scrutiny of the raw data.

The relationship between sex and the state of lesions, however, remains unclear. The determination of lesion severity and/or activity being dependent or independent of an individual's sex can help in the process of differential diagnosis. Stuart-Macadam (1985) has noted that the clinical literature clearly indicates that both children and women are at a greater risk of developing porotic hyperostosis than males. A number of studies have found significantly higher frequencies of porotic hyperostosis in females compared with males. In a study of orbital porotic hyperostosis in Italy, Guidotti (1984) reported that significantly more females were affected than males. Similar findings were demonstrated in early historic native population along the British Columbia Coast, which were attributed to iron loss due to menstruation and the physiological demands of pregnancy and lactation (Cybulski 1977). In contrast, other studies, including those discussed previously, have found no significant sex differences (e.g. El-Najjar 1976; Fairgrieve and Molto 2000; Keenleyside and Panayotova 2006). Similarly, there were no significant relationships demonstrated between the sexes and lesion activity or severity in this study sample.

Overall, it is important to note that there is considerable variation in prevalence rates between archaeological collections from across the world. This variation may be reflective of true differences that can be detected through systematic investigations of

palaeoepidemiological trends, or could simply be the result of a lack of consistency in subjective scoring systems. Regardless, future studies should focus on standardizing subjective scoring systems and thoroughly investigating epidemiological trends that may aid in elucidating the possible underlying etiology of porotic hyperostosis in different populations.

7.1.1 Etiology of Porotic Hyperostosis in the Old World

Now that the palaeoepidemiological trends noted in the study sample have been discussed and contextualized, possible explanations for the development and presence of porotic hyperostosis in this sample will be considered. Since the study sample represents individuals from both the Old World (Apollonia) and the New World (Maya), the development of porotic hyperostosis in both of these geographic areas will be considered.

The explanation given for the presence of orbital and cranial porotic hyperostosis on crania in many Old World populations is often a genetic anaemia, specifically thalassemia in the Mediterranean, or sickle cell anaemia in Africa (Angel 1967; Kent 1986; Hershkovitz et al. 1991; Keenleyside and Panayotova 2006). This explanation is rationalized as the geographic distribution of these conditions has been found to be closely correlated with that of endemic malaria (Steinbock 1976; Tayles 1996; Keenleyside and Panayotova 2006). Prevalence rates for porotic hyperostosis vary considerably in Greek samples and range from as high as 62% at Nea Nikomedeia in the Early Neolithic to as low as 8.1% at Kephala in the Late Neolithic and 9.1% at Bamboula in the Early Bronze Age (Keenleyside and Panayotova 2006). Angel (1966) attributed many of the prevalence rates in Greek skeletal remains from the eastern Mediterranean to thalassemia. Angel (1966) also argued that the decline in porotic hyperostosis from the Neolithic to the Classical period was due, in part, to a transition to agriculture which resulted in the draining of swamps, reducing the population of mosquito vectors and thereby reducing malaria.

Palaeoenvironmental investigations at Metaponto, a Greek colony from Italy, revealed evidence of marshy conditions supporting the argument for the spread of malaria-carrying mosquitos (Henneberg and Henneberg 1998). Thalassemia has also been implicated in

the development and prevalence of porotic hyperostosis in other Greek colonial skeletal series from Italy including Heraclea (Ascenzi and Balisteri 1977), Pithekoussai (Becker 1995), and Spina (Benassi and Toti 1958). Much like iron-deficiency anaemia, porotic hyperostosis in the Mediterranean region seemed to become synonymous with genetic anaemia. However, this assumption was criticized by Musgrave (1980) who argued that malaria was not endemic throughout the Mediterranean and that not all lesions of porotic hyperostosis could be attributed to a genetic anaemia. An examination of remains from a Neolithic ossuary from Alepotrypa Cave in Greece indicates that orbital and cranial porotic hyperostosis most likely reflects an acquired iron-deficiency anaemia rather than a genetic condition (Papathanasiou et al. 2000). As a result of criticism and conflicting evidence for the genetic anaemia theories, Stravapodi (2004) has suggested a reassessment of the etiology of porotic hyperostosis in Greek skeletal samples.

The composition of the combined population study sample includes individuals from the Greek colonial sample at Apollonia in Bulgaria. Unfortunately, full skeletal examinations were not possible as only a select number of eye orbits were available for study. However, all of the remains in the Apollonia sample were previously examined by Keenleyside and Panayotova (2006). This examination revealed that none of the individuals in this sample displayed evidence of lesions characteristic of thalassemia, particularly associated lesions of the infracranial skeleton. A lack of severe lesions, typically noted in individuals with thalassemia, accompanied by a decrease in lesion prevalence and activity in older age cohorts more likely indicates the presence of acquired iron-deficiency anaemia (Keenleyside and Panayotova 2006). For a description of skeletal lesions characteristic of thalassemia, see Chapter 3, Section 3.7.1.3.

Evidence supporting the hypothesis that iron-deficiency anaemia is responsible for the prevalence of porotic hyperostosis in the Mediterranean, and particularly among the Greek colonies, comes from several sources of primary, historical, and archaeological evidence. A stable isotope analysis of the remains of 54 individuals from Apollonia revealed that the population had a mixed diet of terrestrial and marine foods with a heavy reliance on C_3 plants including wheat and barley (Keenleyside et al. 2006). While wheat and barley contain adequate quantities of iron, these cereal staples are known to inhibit

the intestinal absorption of iron (Sullivan 2005; Keenleyside and Panayotova 2006). The dietary absorption of iron is regulated by the body's physiological controls and the biochemical properties of foods that are consumed (Mensforth et al., 1978; Larsen, 1997; Sullivan, 2005). In humans, iron is absorbed via the gastrointestinal tract and must be digested in a soluble state, in sufficient quantities, and for an adequate amount of time in order to meet nutritional requirements (Mensforth et al., 1978). There are two forms of dietary iron, each of which is differentially absorbed by the body. The first, non-haem iron, is derived from plant sources such as cereals, and is poorly absorbed by the body. The second is haem iron, which is more easily absorbed by the intestines and comes from red meats (Murphy et al., 2002; Roberts & Manchester, 2005). Additionally, staple cereal crops such as wheat, barley, maize, rice, nuts, and legumes, contain compounds called phytates, which are known to inhibit iron absorption in the intestines (Palkovich, 1987, Larsen, 1997; Keenleyside and Panayotova 2006). In addition to poor iron absorption, literary sources indicate that Greek colonies along the Black Sea coast suffered from periodic food shortages and malnutrition due to crop failure, warfare, and political instability (Garnsey 1999; Keenleyside and Panayotova 2006).

Other causal agents, including parasitic infections and infectious disease may also account for the prevalence of porotic hyperostosis among Greek colonists. The population of the Apollonia colony is estimated to have numbered approximately 3000 individuals during the 5th and 4th centuries BC with a sedentary settlement pattern consistent with high density occupation (Keenleyside and Panayotova 2006). The ramifications of high density, sedentary occupation include increased bacterial, viral, and parasitic infection and infestation due to poor sanitary conditions and increased contact with hosts who carry infection (Kent 1986; Roberts and Manchester 2005; Beňuš et al. 2010). Although little evidence of chronic infection was observed in the skeletal remains, this does not preclude the presence of acute and repeated episodes of infection, particularly in the sub-adult age cohorts. Infants and children from six months to around 3 years of age are not only highly susceptible to unstable nutrition, but are also prone to develop respiratory and gastrointestinal infections (Mensforth et al. 1978). Hookworm infection is also common in agricultural populations in tropical and sub-tropical regions and has been detected in modern day populations in Turkey along the coast of the Black

Sea. Fish-borne parasites may have also contributed to an acquired anaemia in Apollonia as a result of the isotopically documented consumption of marine resources (Keenleyside and Panayotova 2006; Keenleyside et al. 2006). The ability of an individual to adequately absorb iron from foods can be reduced if bacterially, virally, or parasitically induced diarrhea prevents the body from accessing ingested iron, or if blood loss through parasitism creates a chronic net loss of iron (Mensforth et al., 1978; Holland & O'Brien, 1997; Sullivan, 2005).

Additional factors that may have contributed to iron deficiency anaemia and other acquired anaemic conditions, such as megaloblastic anaemia, in Greece include early weaning and/or prolonged breast feeding periods and weanling diarrhea (Walker 1986; Keenleyside and Panayotova 2006). Greek literary sources indicate that weaning foods among the ancient Greeks consisted of gruels made from a mixture of goat or sheep's milk, honey, and domesticated cereal staples including barley (Brothwell 1969; Holt 2009). Zooarchaeological evidence indicates that goat and sheep were present at Apollonia, and stable isotopic evidence suggests that weaning onto nutritionally deficient cereal gruels began around six months of age with a few individuals with evidence of weaning as early as three months of age (Fildes 1986; Keenleyside and Panayotova 2006; Holt 2009). The early introduction of both goat's milk and honey can have dire consequences in infants less than six months of age and can adversely affect infants up until twelve months of age (Becroft and Holland 1966; Fairgrieve and Molto 2000). Fetal stores of folate are exhausted after three months and infants become dependent on dietary sources alone after this point. Infants that are weaned onto goat's milk, which is low in cobalamin and folate compared to human milk, develop a severe megaloblastic anaemia due to folic acid deficiency (Fairgrieve and Molto 2000). Honey is a confirmed source of *Clostridium botulinum* and, when fed to infants, can lead to botulism (Arnon et al. 1979; Fairgrieve and Molto 2000). If weaning practices roughly followed those outlined in early Greek texts, and some infants were weaned from human breast milk before the age of six months, it may be possible that some infants were affected by botulism as well as megaloblastic anaemia. It should also be noted that prolonged breastfeeding beyond six months may also put infants at risk for the development of iron-deficiency anaemia if there is insufficient supplementation of the diet with iron bearing foods (White et al.

2006). Isotopic data also demonstrate that breastfeeding for some infants continued up until one to three years of age (Holt 2009). It is difficult to say exactly what etiological factors may have led to the development of porotic hyperostosis in this population and there is no way to skeletally differentiate between the acquired anaemias as the bone response is the same regardless of the physiological response leading up to the anaemia.

Clearly, the determination of the etiology of orbital and cranial porotic hyperostosis in Old World populations remains a challenge. Although thalassemia cannot be completely ruled out in the Greek colony at Apollonia, the skeletal and archaeological evidence is more consistent with an acquired anaemia such as iron-deficiency or megaloblastic anaemia. Exposure to parasites and infectious disease as a result of high density occupation at Apollonia also likely played a role in the development of these lesions.

7.1.2   Etiology of Porotic Hyperostosis in the New World

In general, since there is little to no evidence for the presence of genetic hemolytic anaemias in the New World, the prevalence of porotic hyperostosis in prehistoric Maya and North American populations is typically attributed to iron deficiency anaemia and is often linked to an increased dependency on maize agriculture (Hooton 1940; Carlson et al. 1974; Saul 1977; El-Najjar 1977; Kent 1986; Wright and White 1996; Wright and Chew 1999). Virchow (1887) and Boas (1890) were the first to describe porotic cranial lesions in archaeological skeletal remains from Yucatan. Several decades later, Hooton (1940) described similar lesions, which he referred to as "osteoporosis symmetrica" in the crania of Maya children from the Post-Classic period at Cenote of Sacrifice at Chichen Itzá (Wright and White 1996; Wright and Chew 1999). Although the etiology of these porotic lesions was not firmly identified at that time, Hooton speculated that these lesions might be scorbutic and that they may have been the result of nutritional insufficiencies due to ancient Maya reliance on a diet consisting predominantly of maize (1940: 276). He also noted that, based on the high prevalence of porotic hyperostosis in this population (77.8% in sub-adults and 52.9% in adults), nutritional disease may have contributed to the collapse of the Maya civilization.

Support for this dietary interpretation has come from a number of New World studies that have indicated an increase in the prevalence of porotic hyperostosis with the transition from a foraging subsistence to one focused on agriculture (El-Najjar 1977; Cohen and Armelagos 1984). Typically, an agricultural diet tends to be dominated by one or a few plants, such as rice in Asia, wheat in temperate Asia and Europe, millet in Africa, and maize in the New World. The nutritional value of many of these agricultural domesticates is marginal, or poor. Maize, specifically, is deficient in essential amino acids lysine, isoleucine, and tryptophan and also contains very little bioavailable iron. Thus, the combination of cereal-dependent diets and the reduction in wild meat consumption have been widely cited as the primary factors which promoted iron-deficiency anaemia in prehistoric populations undergoing subsistence transitions (Palkovich, 1987, Larsen, 1997). Additionally, just as in Old World populations, parasitic infestation and non-specific infectious diseases have also been implicated as contributing etiological factors for porotic hyperostosis in the New World (Walker 1986; Palkovich 1987; Ubelaker 1992; Wright and Chew 1999). It has been proposed that the aggregation of people in combination with increased sedentism at the transition to agriculture is responsible for the increased frequency of anaemia in many parts of the world (Mensforth et al., 1978; Kent, 1986; Palkovich, 1987; Larsen, 1995, 1997; Sullivan, 2005).

The prevalence of porotic hyperostosis among the Maya skeletal series is high, reaching as high as 77% in subadults from Chichen Itzá Cenote (Hooton 1940) and 65% (healed) in adults from Pasión (Wright 1994). In comparison with other maize growing agricultural populations in North America, such as Woodland and Mississippian populations, these data are not out of place and support the implication of a dietary iron insufficiency as a significant palaeoepidemiological factor (Lallo et al. 1977; Mensforth et al. 1978). Additionally, these data are also comparable to archaeological skeletal populations from Coastal California, where the prevalence of porotic hyperostosis has been attributed to parasitism rather than dietary insufficiency (Walker 1986). Based on these palaeoepidemiological patterns, palaeopathologists working in the Americas and with Maya skeletal collections have emphasized a synergistic relationship between low dietary intake of iron, parasitism, and infectious disease in the etiology of iron-deficiency

anaemia and the prevalence of porotic hyperostosis (Cohen and Armelagos 1984; El-Najjar et al. 1986; Walker 1986; Reinhard 1992; Holland and O'Brien 1997; Wright and Chew 1999).

At Lamanai, the prevalence of porotic hyperostosis shows an increase from the Classic Period to the Postclassic Period (White 1988). This increase in prevalence has been linked to an isotopically documented increase in maize consumption (White 1988; White et al. 1994). Based on a consideration of isotopic, archaeological, and palaeo-environmental evidence it is likely that cultural and ecological factors combined with the low iron content of maize acted synergistically in the development of porotic hyperostosis among the Maya at Lamanai. An analysis of ceramics from the Postclassic Period revealed evidence for alkali processing of maize using lime, which improves the balance of amino acids and the yield of nutrients. However, when lime is consumed, it has an alkaline effect in the stomach and reduces the amount of acid in the gut, thereby improving the survival rate of intestinal parasites. The tropical lagoon environment of Lamanai suggests that helminthic and insect-borne parasites may have been a major contributing factor in the etiology of porotic hyperostosis (White 1988). A second, and significant increase in lesion prevalence is also noted at Lamanai during the Historic Period (67%), which could not be explained by the consumption and processing of maize alone as there was no corresponding increase in consumption. It has been suggested that this increase may have been related to the introduction of Spanish-borne infectious and parasitic diseases (White 1988; White et al. 1994; Wright and White 1996).

At San Pedro and Marco Gonzalez during the Postclassic and Historic Periods, the combined prevalence of porotic hyperostosis was 12%, which is much lower than the prevalence rates reported at other Maya sites during the same time periods (Wright and White 1996; White et al. 2006). Isotopic evidence confirmed a predominantly marine-based diet, which does not support the dietary hypothesis for iron-deficiency anaemia that fits most other Maya populations and may explain the lower prevalence rate. Since San Pedro and Marco Gonzalez are coastal sites, it is expected that the diet at both sites would be dominated by marine foods, which are rich in iron and should be able to meet dietary requirements (Sizer and Whitney 2000; White et al. 2006). As with other coastal

populations in North America, it is possible that the prevalence of porotic hyperostosis at San Pedro and Marco Gonzalez may be the result of parasitic infection, particularly from fish-borne parasites, rather than dietary insufficiencies (Walker 1986).

Other etiological factors that have been explored at San Pedro and Marco Gonzalez include prolonged breastfeeding and weanling gastrointestinal infection (White et al. 2006). An isotopic study by Williams et al. (2005) reported that the majority of children at these sites relied mainly on breast milk until the ages of three to four years. It is possible that the insufficient supplementation of iron rich foods and inability to maintain nutritional balance during peak growth periods predisposed young children to iron-deficiency anaemia. Prolonged breastfeeding has also been implicated in the development of iron-deficiency anaemia in North American populations along the British Columbia Coast (Cybulski 1977). Additionally, a reconstruction of the commencement of weaning using isotopic data at San Pedro and Marco Gonzalez showed a relationship between the introduction of weaning and the peak frequencies of linear enamel hypoplasias (White et al. 2006). Linear enamel hypoplasia is used as a skeletal indicator of non-specific stress events and is commonly associated with weanling stress, such as diarrheal diseases and infection which often occur in infants during weaning (Larsen 1997; Katzenberg et al. 1996; White et al. 2006). Based on these results, it is more likely that the prevalence of porotic hyperostosis at San Pedro and Marco Gonzalez can be attributed to prolonged breastfeeding, weanling stress, and parasitism and infection (White et al. 2006). A high combined prevalence of periostitis (71%) in these skeletal series may support the hypothesis that infection was a major contributing cause of acquired anaemia and resultant lesions of porotic hyperostosis (Maxwell 2003; White et al. 2006).

It has been reported that the populations at San Pedro and Marco Gonzalez also had high frequencies of scurvy (58%) (White et al. 2006). However, not only do marine resources provide adequate levels of both iron and vitamin C to meet dietary requirements (Aufderheide and Rodriguez-Martin 1998), the diverse tropical environment of the geographic area where these two sites are located is also rich in plant sources of vitamin C (Wright and White 1996; Sizer and Whitney 2000; White et al. 2006). Based on the

bioavailability and evidence of consumption of vitamin C rich resources, it is questionable and unlikely that the prevalence of porotic hyperostosis in these populations is explained by scurvy (Wright and White 1996). Many of the scorbutic lesions described elsewhere in the Maya area have been documented in adults in the form of sub-periosteal hematomas (Saul 1972; Kennedy 1983). Also, the presence of sub-periosteal hematomas and abnormal porosity are not pathognomonic for scurvy, particularly when lesions are isolated and not symmetrical (Aufderheide and Rodriguez-Martin 1998). If skeletal lesions support a diagnosis of scurvy in environments where vitamin C is readily available and consumed, it may be possible that, like iron, vitamin C deficiencies were exacerbated by prolonged diarrhea, parasitism, infection, or a co-occurrence with anaemia (White et al. 2006; Bourbou 2014), but it is an unlikely explanation for the prevalence of porotic hyperostosis based on the isotopic and palaeoenvironmental evidence for this geographic area.

7.1.3　Etiology of Porotic Hyperostosis in the Study Sample

Although several conditions have been purported to result in orbital and cranial porotic hyperostosis in the Old and New Worlds, key characteristics attributed to several of these conditions are missing in the study sample. Thalassemia does not seem to be a viable option in the differential diagnosis of porotic hyperostosis in this sample even though part of the sample is comprised of individuals from of Mediterranean origin, where thalassemia is common. There is no evidence of thalassemia or sickle cell anaemia in the Pre-Columbian New World and, thus, these genetic conditions would not be expected among Maya populations. The examination of the skeletal remains from Apollonia by Keenleyside and Panayotova (2006) and palaeopathological analyses of the remains from Lamanai, San Pedro, and Marco Gonzalez gave negative results for the presence of thalassemia and sickle cell anaemia (see Chapter 3, Section 3.7.1.3 for a description of bone changes in the genetic anaemias).

In addition to the previously discussed genetic anaemias, a genetic hemolytic anaemia without past or present geographic restrictions has not yet been considered. Hereditary spherocytosis is an autosomal dominant genetic condition involving a mutation that alters the protein spectrin, which is responsible for the normal production of the red blood cell

membrane (Cybulski 1977; Aufderheide and Rodriguez-Martin 1998). This alteration causes red blood cells to change their shape from a normal biconcave disc to that of a rigid sphere (spherocyte). The normal spleen, which is responsible for the recognition and removal of deformed red blood cells, recognizes the spherocytes as abnormal and destroys them, even if they are no more than a few days old. This premature destruction of red blood cells causes the body to react in the same way as with other anaemic conditions, resulting in a generalized expansion of the marrow spaces (Aufderheide and Rodriguez-Martin 1998). This genetic disorder cannot be completely ruled out as a factor in the etiology of porotic hyperostosis in genetically homogenous populations where documented prevalence is low, but it is not likely to be a factor in populations with high prevalence rates. This anaemia is also variable in age of onset, and bone changes can occur at any time in infancy and toward adolescence (Edeiken and Hodes 1973; Cybulski 1977), which does not correspond to the increasing prevalence of healed lesions in early childhood noted not only in the study sample, but also in the larger skeletal collections from which the study sample was derived.

Deficiencies in folic acid, iron, and vitamin C have all been implicated as potential etiological factors in the Apollonia and Maya skeletal collections and all share an interconnected nutritional significance (Brickley and Ives 2008; Bourbou 2014). When one of these nutrients is lacking, it directly affects the physiological status of the other two. Vitamin C plays an important role in the metabolism of folate and iron (White et al. 2006; Brickley and Ives 2008). Similarly, a folic acid deficiency may lead to deficiencies in both iron and vitamin C. In the Greek colony at Apollonia, it is more likely that deficiencies in iron and/or folic acid were present rather than a deficiency in vitamin C. Evidence that infants were being weaned onto goat's milk in Greece supports this argument as goat's milk is high in vitamin C (ascorbic acid) (Fairgrieve and Molto 2000), but low in cobalamin and folate. Stable isotopic evidence indicates that weaning for the majority of individuals at Apollonia occured after the age of six months, which more likely led to a deficiency in iron with the introduction of iron poor weaning foods. Evidence of early weaning (prior to three months) does not appear to have been documented in the literature for the Maya skeletal series, likely due to poor infant and sub-adult skeletal preservation. Therefore, evidence for folate deficiencies cannot be

evaluated in these collections. It is unclear as to whether any infants younger than six months of age demonstrated porotic lesions in the Apollonia sample, which may have supported an interpretation of folate deficiency. No individuals from Apollonia or any of the three Maya samples younger than six months of age were included in this study sample.

Bone lesions possibly indicative of vitamin C deficiency are generally rare in the Mediterranean due to the temperate climate that encourages the cultivation of vitamin-C rich fruits and vegetables, and the availability of fresh seafood along the coast (Bourbou 2014). However, possible evidence of scorbutic lesions has been noted in Minoan skeletal remains (McGeorge 1988), in Early and Middle Byzantine skeletons from Greece (Bourbou 2003, 2014), and the Kalfata necropolis at Apollonia (Keenleyside 2010). It has been proposed that cases of scurvy in these Greek populations are likely associated with weaning and the introduction of foods lacking in vitamin C after the cessation of breastfeeding (Bourbou 2014). Although this argument is plausible, the total exclusion of ascorbic acid from human diets is very rare, particularly when this vitamin is found in a wide range of foods including vegetables, fruits, milk, organ meat, and fish (Brickley and Ives 2008). Keenleyside and Panayotova (2006) found no evidence of bone changes associated with scurvy in the Apollonia sample. Additionally, a visual assessment of orbital porotic hyperostosis in the Apollonia sub-sample using micro-CT cross-sections in this study confirmed the presence of cortical resorption and marrow expansion, which is not consistent with the bone changes observed with scorbutic lesions, as discussed in Chapter 3, Section 3.7.2.1.

In several archaeological collections from North America and Peru, Ortner et al. (1999, 2001) and Klaus (2013) have argued that orbital porotic hyperostosis, in the absence of marrow hyperplasia, may be a manifestation of scurvy. Possible evidence of scurvy has also been documented in Maya collections (Saul 1972; Kennedy 1983), including San Pedro and Marco Gonzalez (Maxwell 2003; White et al. 2006). Again, given the tropical climate and stable isotopic evidence supporting the exploitation of marine resources, it is unlikely that a complete exclusion of vitamin C from the diet was occurring, particularly in San Pedro and Marco Gonzalez. It is possible that the presence of a severe anaemic

condition may have contributed to or exacerbated a vitamin C deficiency. However, it is important to note that the porotic lesions that have been associated with scurvy are not pathognomonic, but rather a bony response to non-specific inflammation of the periosteum. In the study sample, one individual with severe orbital and cranial porotic hyperostosis that was selected from the San Pedro collection (SP11-2/1) also had notable porosity on the greater wings of the sphenoid bones and some light porosity along the roof of the palate. A re-examination of the infracranial skeleton of this individual also revealed fine porosity on the anterior surface of the left and right ilia and along the metaphyseal ends of many of the long bones, but no sub-periosteal hematomas were noted and no antemortem tooth loss or porotic changes to the alveolar surface were found (e.g. Ortner et al. 2003). Ortner et al. (2001) have identified the pattern of porosity on the greater wing of the sphenoid as a characteristic feature of scurvy, but it is a non-specific reaction and not pathognomonic. These lesions suggest only the presence of non-specific inflammation and cannot be attributed to a specific disease process. It is possible that this individual experienced a co-morbid condition that included anaemia as well as scurvy, but more evidence is needed to support this diagnosis. The palaeopathological re-analysis of the individuals selected from Lamanai revealed that one individual with evidence of orbital and cranial porotic hyperostosis, an adult female (N12-11/3), had evidence of an isolated subperiosteal hematoma on the anterior mid-shaft of the left tibia. No further evidence of sub-periosteal hematomas was noted on any of the remaining skeletal fragments and, given the location of this lesion, its isolated nature, and the proximity of the tibial diaphysis to the skin, it is more likely that this lesion is attributable to an isolated trauma to the anterior portion of the lower leg rather than scurvy. Upon the visual assessment of orbital and cranial porotic hyperostosis from the micro-CT images of both of these individuals, it was determined that these lesions were the result of cortical resorption and marrow expansion (Figure 7.1), rather than the patterns of bone change that would be expected with scorbutic lesions. Scurvy would affect the outer table through a process of bone apposition, but would not affect the diplöe. These lesions also do not appear to be caused by rickets or inflammation. Rickets would not result in the resorption of the outer table, but rather would alter its structure and result in a splintered appearance. Marrow expansion would not be expected with non-specific

inflammation/infection as these processes completely destroy and resorb the outer table as well as any surrounding trabeculae. For more details on the specific bone changes that occur with anaemia, scurvy, rickets, and inflammation, see Chapter 3, Section 3.7. None of the remaining individuals selected from the Maya collections demonstrated bone changes that could be associated with scurvy during the palaeopathological analysis and during the visual assessment of micro-CT cross-sections.

Figure 7-1: Micro-CT Sagittal Cross-Section of Orbital Porotic Hyperostosis
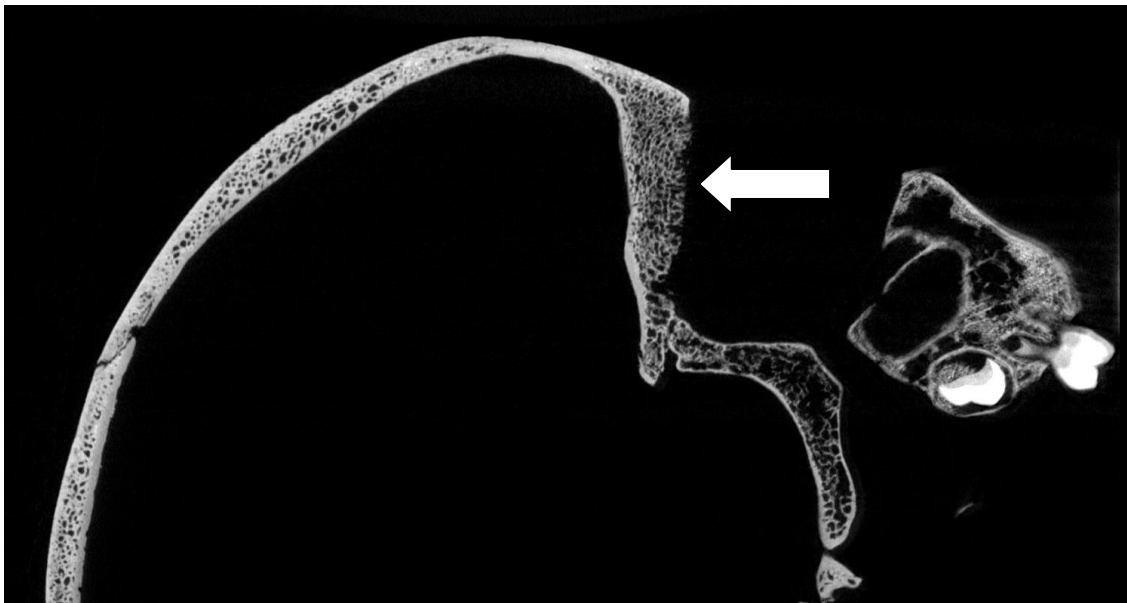
Individual # SP11-2/1: Note the complete resorption of the outer table, expansion of the trabeculae beyond the outer orbital table, and the "hair-on-end" phenomenon.

Upon a review of the skeletal, archaeological, isotopic, and documentary evidence associated with the Apollonia sample and the three Maya samples from which the study sample is derived, the occurrence of orbital and cranial porotic hyperostosis is most likely associated with acquired iron-deficiency anaemia. This would seem to be supported in the study sample by the identification of age-related trends in lesion activity and severity which suggest that active lesions are almost entirely restricted to the skeletons of sub-adults while healed lesions are typical in adults (Stuart-Macadam 1985; Walker et al. 2009). This ameliorative quality in older age cohorts is indicative of a relationship to bone marrow and the changing distribution of red blood cell production sites during growth and development. As the individual ages, the demand for increased

erythropoiesis during growth and development is decreased and shifts from the cranial vault to different regions of the axial skeleton (Loevner et al. 2002; Walker et al. 2009).

The pattern of iron deficiency anaemia being accompanied by a higher prevalence of infection as reported by Mensforth et al. (1978) is not supported by skeletal evidence in the Apollonia sample, but this does not preclude the possibility of infectious disease, and particularly weanling diarrheal diseases, from contributing to or exacerbating an anaemic condition. Sedentism and high density occupation at Apollonia make it possible to hypothesize that the population may have been exposed to an increasing number of viral, bacterial, and parasitic infections that are associated with crowded living conditions. The consumption of marine resources may have also exposed the population to fish-borne parasites (Keenleyside and Panayotova 2006). It is not possible to completely rule out folic acid deficiency in the Apollonia sample based on the finding that weaning diets were significantly low in folate and cobalamin and that a small number of infants may have been weaned prior to the age of six months (Holt 2009). Careful examinations of infants in the birth to six month cohort may clarify the potential role of folate deficiency and megaloblastic anaemia in this population. The high prevalence (71%) of infection (periostitis) in the San Pedro and Marco Gonzalez collections, and the likelihood of high levels of parasitic infection and Spanish-borne infectious disease in Lamanai supports a pattern of synergism between infectious disease and iron-deficiency anaemia.

I conclude that, based on the identified palaeoepidemiological trends, the archaeological and palaeoepidemiological context of this sample, and the results of the visual structural analysis of lesions, orbital and cranial porotic hyperostosis observed in the current study is the result of an acquired anaemia and, possibly a chronic iron-deficiency. The source of this deficiency is unclear and may either be dietary, infectious, parasitic, or the synergistic interaction of two or more of these sources. Evidence of genetic anaemia is not present in this sample nor does scurvy appear to be a contributing factor based on a lack of infracranial evidence and the visual confirmation of cortical resorption and marrow hyperplasia, rather than bone apposition, from the micro-CT cross sections of each of the 39 individuals with evidence of porotic hyperostosis. The results of the

quantitative micro-CT analysis also do not support a diagnosis of scurvy and will be discussed in Section 7.3.3 of this chapter.

7.2   Observer Reliability and Reproducibility

After providing the palaeoepidemiological context for this sample, the second major objective of this study was to assess the reproducibility and reliability of various methods of morphometric data collection used on micro-CT volumes of archaeological human skeletal remains. The assessment of observer error has become a common procedure in many disciplines and, although the importance of the evaluation of measurement accuracy and precision was stressed by Molto (1979) over three decades ago, studies of observer error in the development and application of new methodological techniques have still only received periodic attention in physical anthropology. For the field of palaeopathology, this lack of consideration for observer error cannot only result in biased subjective observations, but also in misleading or biased quantitative observations. Errors as a result of bias or unstandardized methods of data collection in palaeopathology can lead to incorrect diagnoses and unreliable interpretations of health and the presence and effects of disease in archaeological human populations.

Although technological developments, such as micro-CT, have much to offer palaeopathology, the use of new methods and technologies without first considering and addressing the limitations and potential sources of error that may be inherent with these technologies can do more harm than good, particularly when it comes to making interpretations of collected data. The current palaeopathological literature is largely lacking in discussions of the assessment of measurement error and the reliability (accuracy) and reproducibility (precision) of methods that include clinical CT and micro-CT in the process of differential diagnosis. In all research fields, measurement inconsistencies and observer error have the potential to introduce enough variation between two or more sets of data so as to produce statistical relationships that may not, in fact, be real. Significant variations that do exist can also be masked or obscured by observer error. Relationships produced in error can then lead to incorrect and unreliable interpretations of data (Molto 1979). For these reasons, it is important to investigate the potential sources of measurement error with respect to data acquisition and analysis using

micro-CT methods for the evaluation of the three-dimensional (3D) structural properties of trabecular bone, with relevance to the field of palaeopathology. Before applying methods developed from a technology that is new to the field of palaeopathology, research must first be done to determine which methods produce the most accurate and reliable results. Only after such research will palaeopathologists gain a better understanding of the value and the limitations of micro-CT to palaeopathological diagnosis and interpretation.

The selection of a region or volume of interest (VOI) is the starting point of any morphometric analysis. There are typically two different VOI methods that can be employed to obtain quantitative structural data from micro-CT volumes for the assessment of trabecular bone microstructures. Since micro-CT volumes can be viewed as two-dimensional (2D) sections in all three anatomical planes or as 3D reconstructions, data can be collected from a 2D region of interest in a micro-CT cross-section in a single anatomical plane, or from 3D volumes of interest, which can include structural information obtained from a few to several thousand micro-CT cross-sections measured in all three anatomical directions (X,Y,Z). Based on specific research objectives and goals, clinical studies, as well as a limited number of anthropological and palaeopathological research studies, have employed either of these 2D or 3D methods for the structural analysis of trabecular bone microarchitecture using micro-CT (e.g. Kuhn et al. 2007; Rühli et al. 2007; Particelli et al. 2011). However, the evaluation of the reproducibility and reliability of these different 2D and 3D methods is significantly lacking in the current literature. Therefore, research that explores which of these data collection methods provides the most accurate representation of structural properties of trabecular bone is needed.

To assess the impact of changing the dimensions and size of a VOI on the reproducibility and reliability of measures of trabecular bone microarchitecture, an evaluation of observer correlations and agreement between the 2D and 3D image analysis methods described in Chapter 5, Section 5.2.2.2 was undertaken. Of interest for the evaluation of the null hypothesis was the assessment of the amount of observer agreement in each methodology; thus, statistical analyses of the distribution of the data for the three

evaluated methods, such as skewness and kurtosis, were not considered here. Rather, paired Pearson-R correlations were used to measure the degree and direction of the linear relationship between repeated measures made by the same observer at different points in time and by two different observers. Since the correlation is being applied to the same variables collected at different times and by different individuals, we know that the variables being compared are related and that we are testing a correlation of the same phenomenon. As such, the Pearson-R correlation values are a valid test of the association between the observed variables and there is true meaning to these results (Jamison and Zegura 1974). Additionally, since we know that we are testing the association between related variables, and that Pearson-R values are valid, we can also confidently calculate the coefficient of determination (R^2) to further evaluate observer agreement (Heathcote 1980; Ferrante and Cameriere 2009). The coefficient of determination is a statistical goodness-of-fit test (how well data points fit a line) that is used to explain how much of the variability observed in one factor can be explained by its relationship to another factor. In other words, Pearson-R correlations provide information regarding the association between two variables, while the coefficient of determination (R^2) is a predictor of that association (Heathcote 1980; Ferrante and Cameriere 2009). Therefore, coefficients of determination were calculated in this study to determine the predictive relationships between repeated measures of the same variables in the assessment of observer agreement.

Using Pearson-R correlations and coefficients of determination, the null hypothesis that there is no difference in the reproducibility or reliability of 2D and 3D quantitative methods for the analysis of trabecular bone microarchitecture was rejected. Measures of trabecular microarchitecture were affected by both the dimensions and size of the volume of interest, particularly when measures were obtained from the 2D standard VOI. The R^2 values for the 2D standard VOI indicated poor observer agreement particularly for the measures of trabecular organization, including trabecular spacing (Tb.Sp.), and number (Tb.N.). These findings were not unexpected given that this particular method is capable only of providing a 2D representation of inherently 3D structures. As was expected, when the 3D standard VOI was used, observer agreement was slightly improved for measures of trabecular thickness, spacing, and number over the 2D standard method.

However, the predictive relationships both within and between observers, particularly for trabecular number (Tb.N.) and trabecular spacing (Tb.Sp.), were lower than expected since this volumetric sampling method followed those used in clinical studies of the biomechanical properties of trabecular bone. Many of these studies characteristically sample 3D VOIs of uniform size (e.g. Müller et al. 1998 used 4 x 4 x 4 mm^3). Finally, when the 3D custom VOI was evaluated, significant improvements in both intra- and inter-observer agreement were demonstrated over both the 2D and 3D standard methods for all of the variables with the exception of trabecular thickness (Tb.Th.), which did not improve over the 3D standard VOI method either within or between observers. This finding of improvement over the other two methods was not surprising given the characteristic three-dimensional structure and anisotropic nature of trabecular bone that is observed throughout the skeleton (Fajardo and Müller 2001; Stock 2009; Larsson et al. 2011; Lazenby et al. 2011).

In the evaluation of the effect of changing the dimensions and size of the VOI on the reproducibility and reliability of quantitative measures from micro-CT images the first step was to carefully consider the observer agreement results for the 2D standard VOI method. For the repeated measures of bone volume density (BV/TV) and specific bone surface (BS/BV), which are used to evaluate the relative amount of trabecular bone, intra- and inter-observer agreement was moderate to high (see Chapter 6, Tables 6.13 and 6.15). However, for the results for the three measures of trabecular organization (Tb.Th., Tb.N., Tb.Sp.), the effects of applying 2D methods of analysis on observer agreement are particularly evident. For the 2D standard VOI method, intra-observer agreement was moderate for trabecular thickness ($R^2 = 0.697$), but very low for trabecular number ($R^2 = 0.239$) and spacing ($R^2 = 0.096$) (Chapter 6, Table 6.13). Inter-observer agreement was low for all three of these variables and included R^2 values of 0.078 for trabecular number (Tb.N.), 0.233 for trabecular spacing (Tb.Sp.), and 0.374 for trabecular thickness (Tb.Th.) (Chapter 6, Table 6.15). These findings suggest that if 2D methods of micro-CT data collection are used, or if they are the only methodological option available, measures of the relative amount of bone - BV/TV, BS/BV, and in some cases Tb.Th. - may be considered moderately reliable. However, measures of trabecular number (Tb.N) and spacing (Tb.Sp) are not accurately captured using 2D methods of analysis because of

regional differences in trabecular number and spacing throughout the trabecular volume. To briefly illustrate the differences in observer agreement between measures of the amount of trabecular bone and measures of trabecular organization, Figure 7.2 provides a comparison of the intra-observer results for the R^2 goodness of fit test for bone volume density (BV/TV) and trabecular spacing (Tb.Sp.).

Figure 7-2: R^2 Goodness of Fit Line for Intra-Observer Results (2D standard VOI): A Comparison of BV/TV and Tb.Sp.
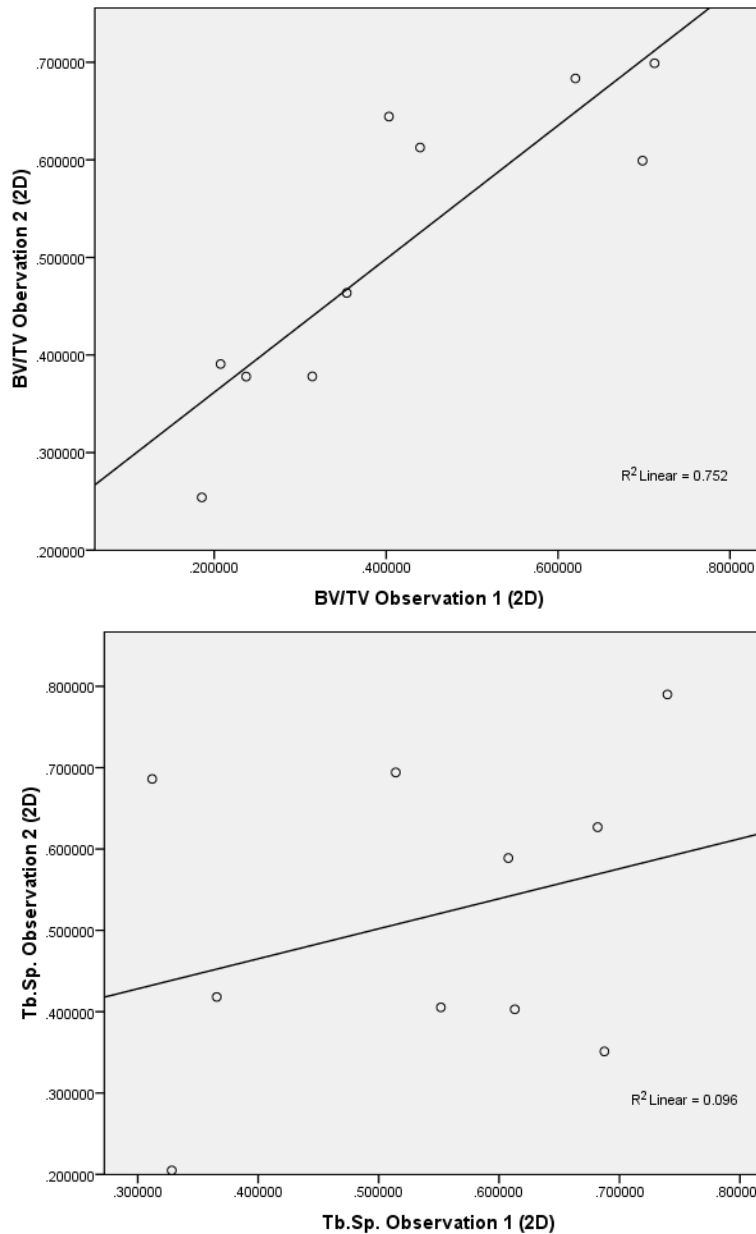
Given that trabecular structures are inherently 3D and have been shown to significantly vary in shape, orientation, and number over very small distances in human bone (Whitehouse and Dyson 1974; Fajardo and Müller 2001), it is not surprising that the 2D standard VOI method produces poor results for observer agreement between repeated measures of trabecular number and spacing. Since the 2D standard VOI method provides a 2D representation of inherently 3D structures, small or subtle changes in 3D trabecular variables can easily be overlooked or completely missed in a 2D VOI (Stout et al. 1999; Snoeks et al. 2011). As such, the data collected using this method may misrepresent the true variability of trabecular microarchitecture within the cranial diplöe and measures of the spacing and number of 3D structures will be biased as a result of under-sampling. Under-sampling has the serious potential to increase the rate of Type I error (i.e. declaring significant differences when none in fact exist) in statistical analyses of the data. Since normal trabecular bone structures within the cranial diplöe and orbital bone are fairly homogenous, it is not unexpected to find moderate to high observer agreement in the structural variables that measure the amount of bone using the 2D standard method. However, despite the homogenous nature of trabecular bone within the diplöe, measures of trabecular organization still performed poorly. Therefore, the issue of increasing rates of Type I error may be exacerbated when this method is applied to the trabecular analysis of more structurally and directionally heterogeneous sites such as load bearing bones or bones that have been altered by abnormal or pathological processes. This issue is particularly relevant for the current palaeopathological study, and future studies, focused on the use of micro-CT images in the analysis and interpretation of changes to trabecular microarchitecture in archaeological skeletal remains. Finding significant differences in trabecular bone microarchitecture where none exist can affect the analysis and interpretation of disease presence and differential diagnosis not only in palaeopathology, but also in clinical research (Lazenby et al. 2011). Differential diagnoses may be supported or refuted based on statistical results that are made in error. Overall, the 2D standard VOI method is not a reliable or reproducible method for palaeopathological investigations of trabecular microarchitecture in archaeological bone, particularly for measures of trabecular number and spacing. This also suggests that histomorphometric

methods using thin-ground sections may not produce reliable results for the study of disease processes in bone and further research on the error rates of histomorphology must be considered.

Once it was determined that the 2D standard VOI method was not reproducible or reliable for the evaluation of variables reflecting trabecular organization, the next step was to assess the reproducibility and reliability of the 3D volumetric sampling methods. For the 3D standard VOI method, a notable improvement in intra- and inter-observer agreement was demonstrated for the majority of the structural variables and, particularly for the variables reflective of trabecular organization. This finding further supports the argument that 2D methods do not accurately capture the true morphological variation present in 3D trabecular microarchitecture. However, the strength of the agreement between repeated measures of trabecular spacing and trabecular number both within and between observers was only moderate when considering overall observer agreement for the 3D standard VOI method. These results may be explained by the sensitivity of measures of trabecular organization to the size and location of standardized uniform 3D VOIs. Fajardo and Müller (2001) cautioned that the size and location of 3D VOIs must be considered carefully prior to the comparative analysis of trabecular microarchitecture in order to avoid biased results. This note of caution arose after comparisons of trabecular architecture in inter- and intra-species primate studies identified methodological challenges that had not arisen in traditional clinical studies. It was argued that using a VOI of uniform size across a study sample risks biasing results from the over- or under-sampling of trabecular microarchitecture in skeletal elements when there is variation in body size (Fajardo and Müller 2001; Lazenby et al. 2011). Accordingly, subsequent studies have scaled VOIs to specific bone size in order to avoid introducing Type I and Type II errors (Ryan and Ketcham 2005; Maga et al. 2006; Fajardo et al. 2007; Griffin 2008; Scherf 2008; Lazenby et al. 2011). In this study, the 3D standard method involved a standardized VOI of uniform size ($2.5 \times 2.5 \times 2.5$ mm^3) that was applied to cranial diplöe across the study sample. Although inter-species body size differences were not a concern in this study, differences in cranial size were observed between individuals as the study sample was comprised of both sub-adults of varying ages as well as adults. As such, the uniform VOI used in this study was small compared

to previous clinical studies (e.g. 4 x 4 x 4 mm^3 by Müller et al. 1998) as it was designed to fit within the smallest and thinnest of the cranial elements, which belonged to the sub-adults. This restriction in VOI size was likely a contributing source of observer error. A small uniform 3D VOI may have been adequate for quantifying trabecular microarchitecture in the diplöe of the sub-adults, but likely resulted in under-sampling in the adults. This is especially pertinent given that the diplöe is a primary site for erythropoiesis in childhood but not in adulthood, and that there is an increase in diplöic thickness with age, both of which more than likely have a significant effect on trabecular morphology (Hatipaglu et al. 2008; Walker et al. 2009). Although the use of the 3D standard VOI method improved intra- and inter-observer agreement over the 2D standard method, the possibility of introducing Type I error, particularly in the adult age cohorts, is increased when using a small 3D VOI of uniform size.

Additionally, since the original locations for each of the 3D standard VOIs were unknown and not provided during the re-collection of measurements, it is also possible that differences in intra- and inter-observer agreement for the 3D standard VOI method may be the result of differences in the selection of the location of the 3D VOI. It has already been demonstrated that trabecular architecture can vary over short distances in the human skeleton (Whitehouse and Dyson 1974; Whitehouse 1975; Nägele et al. 2004). In the 3D analysis of human lumbar vertebrae and long bone epiphyses, a repositioning of a uniform VOI in the same individual by 4 mm in another direction significantly altered values for trabecular thickness (Tb.Th.), number (Tb.N.), and spacing (Tb.Sp.) (Nägele et al. 2004). In studies of the trabecular architecture of the human diplöe, Larsson et al. (2011) found that measures of trabecular thickness (Tb.Th.) and bone volume density (BV/TV) were influenced by the location of the uniform 3D VOI. Larsson et al.'s study suggested that more reliable results may be obtained by determining the mean of morphometric variables of interest from measures taken from several VOIs within the same cranial bone (Larsson et al. 2011). In the sub-sample of individuals with porotic hyperostosis in my study, a small shift in the location of the VOI within a lesion may have significantly altered quantitative values, particularly if some trabeculae that are completely included in the VOI in one location were truncated or removed from the VOI when it was moved even slightly in another direction. These differences have the

potential to increase the rate of Type I or Type II errors. The sensitivity of measures of trabecular organization to variation in VOI size and location is not trivial, particularly for clinical studies and especially for palaeopathological investigations of pathologically altered bone. For example, a loss of trabecular connectivity, thickness, and number are significant predictors of mechanical integrity and structural failure in studies of osteoporosis (Riggs et al. 2008; Recker et al. 2009). Three-dimensional VOIs that are improperly scaled or placed in locations that do not represent the full extent of a pathologically altered portion of bone can significantly affect results and may not yield diagnostically informative values. The use of a single uniform 3D VOI for quantifying trabecular microarchitecture may produce biased and unreliable results if size and location are not considered carefully and in the context of palaeopathological research goals. This is also important to note when referring back to 2D methods which would, presumably, magnify issues of VOI location and placement.

In an attempt to overcome some of the limitations and potential biases of using a restrictive uniform 3D VOI size across the sample, the third method evaluated in this study was the 3D custom VOI method which involved a process similar to the scaling of 3D VOIs as recommended by Lazenby et al. (2011) and Kivell et al. (2011). However, the 3D custom VOIs were not scaled based on average sizes of sub-adult and adult cranial diplöe, but were manipulated and sized to fit the unique size and shape of each individual cranium and/or cranial fragment. The reasoning behind using individually sized VOIs was to reduce the potential for an increase in the Type I error rate. Although the size of the 3D custom VOIs varied between each of the individuals included in this study, and varied both within and between observers for repeated measures of the trabecular structural variables, intra- and inter-observer agreement was improved significantly over the 2D method for all five of the measured structural variables.

When compared to the 3D standard VOI method, intra-observer agreement improved for all variables with the exception of trabecular thickness (Tb.Th.) for which the level of agreement did not change (Chapter 6, Table 6.13). Inter-observer agreement improved for three of the five variables with the exception of trabecular thickness (Tb.Th.) and trabecular number (Tb.N.) which maintained the R^2 values achieved with the 3D standard

VOI (Chapter 6, Table 6.15). However, overall, the R^2 values suggested moderate to high observer agreement for all variables when using the 3D custom VOI method. It is important to note that the size of each of the 3D custom VOIs was based on a careful evaluation of how much data were needed to accurately represent the trabecular microarchitecture of individuals with evidence of porotic hyperostosis and those without. For those individuals without evidence of porotic lesions, VOIs were sized to include as much trabecular microarchitecture as was possible in an attempt to obtain values that most accurately reflected the true nature of normal trabecular structures.

Just as uniform 3D VOIs have the potential to under-sample in some contexts, individually sized, larger 3D VOIs have the potential to over-sample. In a study of the 3D quantification of osteolytic lesions in metastatic bone disease, Snoeks et al. (2011) demonstrated that subtle changes to tibial trabecular microarchitecture and bone volume were not detected when the entire tibial volume was included in the 3D VOI. It was determined that pathological changes in bone volume and microarchitecture occurred mainly in the proximal half of the tibia, which is the actual area where a tumor develops. When the 3D VOI was reduced in size and limited to the proximal half of the tibia to fit within the affected area, the sensitivity of the quantitative measurements to detect changes in bone volume and microarchitecture increased (Snoeks et al. 2011). This is an example of how over-sampling can conceal pathological changes occurring in bone microarchitecture and can potentially increase the rate of Type II error. The 3D custom VOIs for the sub-sample of individuals with porotic hyperostosis were sized to fit entirely within the observed lesions. Based on the results of the assessment of observer agreement for the 3D custom VOI method, and the results of previous clinical research (e.g. Snoeks et al. 2011), it would appear that maximizing 3D VOIs to specific lesion size improves the level of observer agreement in micro-CT image analysis and, thus, generates more reliable data for the evaluation of trabecular bone microarchitecture in archaeological skeletal remains.

Overall, the results of the intra- and inter-observer reproducibility and reliability testing indicate that measures of trabecular organization, including trabecular thickness (Tb.Th.), trabecular spacing (Tb.Sp.), and trabecular number (Tb.N) are most sensitive to variation

in VOI dimensions and size regardless of the methodology used. Therefore, palaeopathologists interested in quantifying trabecular architecture in pathologically altered skeletal remains must be careful to consider the sources of observer error inherent in all methods of data collection. It is clear that 2D methods generally fail to detect subtle changes in 3D trabecular structures and are therefore not robust enough to accurately capture changes in trabecular microarchitecture. Trabecular bone exists and remodels in 3D and in order to achieve an accurate and full understanding of its architecture, 3D analyses are required (Stout et al. 1999). As such, methods involving 2D VOIs are not recommended for the quantitative analysis of trabecular changes to archaeological bone in palaeopathology. This also questions the utility of histomorphometry in palaeopathology if serial sectioning methods are not applied. On the other hand, the use of three-dimensional methods that sample uniform VOIs is supported, but should only be used with careful consideration of the individual goals of the research and the potential sources of observer and measurement error. Overall, it is recommended that future palaeopathological studies that employ micro-CT image analysis use 3D methods that maximize the size of the VOI in order to reduce the potential for biased and misleading results as well as the occurrence of Type I and II errors.

7.3   Micro-CT Quantitative Image Analysis

The third, and final, objective of this research study was to determine if the quantification of trabecular bone microarchitecture reveals any important diagnostic information regarding the pathogenesis of pathological conditions that give rise to the general macroscopic appearance of porotic hyperostosis. It was expected that this analysis would provide important information regarding the types of bone processes occurring at the trabecular structural level that, when combined with additional lines of evidence (e.g. macroscopic, palaeoecological, archaeological), may help to improve our understandings of the processes of lesion development and, thereby, improve the reliability of the differential diagnosis of porotic hyperostosis in palaeopathology. The primary goals of this objective were to establish a link between subjective visual scales of assessment and reliable, objective methods of quantitative evaluation, and to provide a technological

means for more carefully examining the pathogenesis and possible etiological avenues of porotic hyperostosis.

After determining that the 3D custom VOI method produced the most reproducible and reliable results for quantifying trabecular bone microarchitecture from micro-CT images, this specific method was applied to the quantitative analysis of orbital and cranial porotic hyperostosis. As was mentioned in Chapter 5, the collected quantitative data were organized into sub-samples by individual cranial bone. This was done based on recent investigations of the trabecular architecture of the diplöe that suggested that researchers should not assume equal conditions throughout the skull where significant growth and development-related structural differences were demonstrated in trabecular microarchitecture between the frontal, parietal, and occipital bones (Larsson et al. 2011). The separation of the data by cranial bone type resulted in three smaller sub-samples consisting of 33 orbits (15 pathological, 18 normal), 55 parietal bones (24 pathological, 31 normal), and 21 occipital bones (14 pathological, 7 normal). Due to the reduction in sample size, tests were completed to evaluate whether or not there were differences in trabecular microarchitecture between paired cranial bones and between the different cranial bones that make up the skull vault in the current study sample. These tests were applied in an attempt to maximize sample size for the evaluation of disease pathogenesis.

7.3.1   Maximizing Sample Size

First, tests for bilateral differences in the paired frontal (orbits) and parietal bones were conducted to determine whether or not left and right paired cranial bones could be used interchangeably in the analysis of disease pathogenesis. The poor preservation and fragmentary nature of the study sample meant that although left and right sides of the cranial vault were available for a few individuals, many of the individuals represented by paired cranial bones had only the left or right side available. Tests of the normal, paired cranial bones indicated that bilateral variation was negligible. Therefore, in the analysis of disease pathogenesis, left orbits and/or parietals were used when both sides were present in a given individual, and the right side was used when only right orbits or parietals were present.

The second step for maximizing sample sizes was to determine if the study sample demonstrated patterns of trabecular bone microarchitecture similar to the previously published results which indicated development-related structural differences throughout the skull (Larsson et al. 2011). The obtained results revealed that the parietal and occipital sub-samples could be grouped together since no differences in the five variables reflecting trabecular microarchitecture were found. However, the sub-sample of orbits could not be grouped with the parietal and occipital bones as there were significant differences in all five structural variables between the orbits and both the parietal and occipital bones. These structural differences are likely attributable to differences in the development of the orbits during the process of intramembranous ossification in the cranial vault bones. The frontal bone is the first of the cranial bones to begin the process of ossification. After the appearance of the primary centres, usually around 6-7 weeks gestation, ossification continues in a radial pattern and occurs more rapidly in the flatter, more uniform areas of the frontal bone (pars frontalis) than in the more complexly shaped orbits (pars orbitalis) (Inman and Saunders 1937; Scheuer and Black 2000; Morriss-Kay and Wikkie 2005; Russell 2010). Small islands of bone in the ossification centres of the pars frontalis fuse to form a series of primary radiating trabeculae. Secondary trabeculae then rapidly appear and serve to link the primary trabeculae, expanding the trabecular network and connecting the two primary centres (Inman and Saunders 1937; Scheuer and Black 2000). This process works in a similar way for the parietal bones (two centres of ossification) as well as the occipital bones (four centres of ossification). In the orbits, however, the progress of ossification is much less rapid. Early literature suggests that radiating trabeculae in the orbits are much smaller than the characteristic trabeculae found in the diplöe of the pars frontalis, parietal, and occipital bones (Inman and Saunders 1937). This is partially supported by the results of this study which found that although there were a significantly greater number of trabeculae in the orbits (Tb.N.) than in the parietal and occipital bones, the thickness of the orbital trabeculae was significantly lower. Correspondingly, orbital trabecular spacing (Tb.Sp.) and specific bone surface values increased, while total bone volume density (BV/TV) decreased when compared to parietal and occipital bones. Together, these values suggest that orbital trabecular microarchitecture is characterized by a greater number of thin, rod-like trabeculae when

compared to other bones of the cranial vault. Based on the statistical analyses of cranial bone differences in the current study, it was necessary to evaluate orbital and cranial porotic hyperostosis separately in the analyses of disease pathogenesis.

7.3.2   Evaluation of Evidence of Disease Pathogenesis

The next step in the evaluation of the third objective was to investigate the possibility of an association of any of the five structural variables with the visually observed categories of lesion severity and activity. This was done to determine whether a link could be established between visual scales of lesion assessment and quantitative measures of trabecular microarchitecture. The pathological changes observed in the trabecular microarchitecture of the orbits and cranial vault bones in this study will be considered within the context of disease pathogenesis and a discussion of what these results mean for the differential diagnosis of porotic hyperostosis in palaeopathology will be provided.

7.3.2.1   Orbital Porotic Hyperostosis

The results for the quantitative analysis of orbital porotic hyperostosis demonstrated statistically significant changes in several measures of trabecular bone microarchitecture with increasing lesion severity and with changes in lesion activity. Mean values for the measures of bone volume (BV/TV) and trabecular thickness (Tb.Th.) decreased as lesions progressed in severity from unaffected to medium-severe. The decrease in the means of these two variables was significant when unaffected orbits were compared to medium-severe orbital lesions ($p = 0.041$). No significant decreases in these variables were demonstrated between the remaining categories of lesion severity (unaffected vs light; light vs medium-severe). Although no significant decreases in bone volume or trabecular thickness were found between light and medium-severe lesions ($p = 0.098$), the mean difference was noted to be closely approaching levels of significance (Chapter 6, Figure 6.3), further supporting the finding that trabecular microarchitecture is significantly altered with the progression to later stages of lesion severity. A corresponding pattern in the mean decrease of bone volume and trabecular thickness was also demonstrated in the evaluation of lesion activity. A significant decrease in the mean values for both of these variables was found between the "unaffected" and "active" categories ($p = 0.057$), but not

between the remaining categories of lesion activity (unaffected vs healed; healed vs active) (Chapter 6, Figure 6.5).

Unlike the findings for bone volume (BV/TV) and trabecular thickness (Tb.Th.), the analysis of specific bone surface (BS/BV), trabecular number (Tb.N.), and trabecular spacing (Tb.Sp.), demonstrated that mean values increased as lesions progressed in severity (Chapter 6, Figure 6.1). Significant increases in specific bone surface (BS/BV) were found between the "unaffected" and "medium-severe" categories ($p = 0.003$) as well as the "light" and "medium-severe" categories ($p = 0.026$). Mean values for trabecular number (Tb.N.) also significantly increased with lesion severity, but only for the mean comparison of unaffected orbits with medium-severe orbital lesions ($p = 0.048$). The mean values for trabecular spacing (Tb.Sp.) do appear to increase, but only for the later stages of lesion severity represented by the "medium-severe" category. However, this increase was not significant. In the analysis of lesion activity, specific bone surface (BS/BV) and trabecular number (Tb.N.) significantly increased in active orbital lesions when compared to unaffected orbits ($p = 0.016$ and 0.059, respectively). As with the analysis of lesion severity, although mean values for trabecular spacing (Tb.Sp.) increase in active lesions, this increase was not significant (Chapter 6, Figure 6.5).

A parallel relationship between bone volume (BV/TV) and trabecular thickness (Tb.Th.) is expected and understandable given the close relationship between bone volume and trabecular geometry. The thickness and overall shape of trabeculae are directly related to the amount of bone present. Normal trabeculae are characterized by both thick and thin trabeculae that create a trabecular mass with a mixed plate-rod structure (Laib et al. 2000). A decrease in bone volume will be associated with thinner and more rod-shaped trabeculae. On the other hand, an increase in bone volume will be associated with thicker trabeculae that become more plate-like in shape (Mittra et al. 2007; Gabet and Bab 2011). Additionally, in clinical studies of osteoporosis, trabecular bone loss has been defined not only by a decrease in bone volume (BV/TV), but by a corresponding increase in specific bone surface (BS/BV) (e.g. Laib et al. 2000). Specific bone surface (BS/BV) is a measure of the proportion of bone volume that is represented by the surface of bone (Hildebrand et al. 1999). Given the relationship of this variable to bone volume density

(BV/TV), a finding of a decrease in bone volume density and increase in the proportion of bone surface in this study was not unexpected. An increase in trabecular number (Tb.N.), however, was initially surprising given the observed reduction in bone volume (BV/TV) and trabecular thickness (Tb.Th.). This finding may be explained by the fenestration of thick plate-like trabeculae that occurs during abnormal remodelling, which has been documented in studies of early stage osteoporosis. Openings in the plate-like trabeculae are remodelled and result in the formation of several thinner rods from a single plate, thereby increasing the number of trabecular elements without increasing bone volume (Laib et al. 2000). It should be noted that with later stage osteoporosis, these elements are later rapidly resorbed and trabecular number (Tb.N.) is subsequently decreased (Laib et al. 2000; Gabet and Bab 2011). This may also be explained by the co-occurrence of bone resorption and bone formation that is characteristic of marrow hyperplasia. While trabeculae are being thinned by increased osteoclastic activity, osteoblasts work simultaneously to replace the resorbed outer table of the cranium with more trabeculae that radiate outwards in a pattern known as "hair-on-end" trabeculation (Williams 1929; Stuart-Macadam1987b), increasing the overall number of trabeculae.

Overall, the results of the quantitative analysis of orbital porotic hyperostosis reveal that trabecular shape, thickness, and number are significantly affected in the medium to severe stages of active disease pathogenesis, but not during early lesion development. Furthermore, by the later stages of healing, trabecular structures begin to return to normal. Medium-severe lesions in an active state are characterized by a significant decrease in bone volume density as a result of an increase in the number of thin, rod-shaped trabeculae. These changes may be attributed to higher than normal rates of osteoclastic activity given the findings of bone resorption and overall bone loss (localized demineralization). This corresponds with the expected results for both resorptive and mixed disease processes in Table 5.3 (Chapter 5). The trabecular microarchitecture of individuals with light and/or healed orbital porotic hyperostosis does not appear to be significantly changed from the trabecular microarchitecture of individuals with unaffected orbits. This would suggest that lesions in the early stages of development or in the later stages of healing cannot be quantitatively distinguished from normal bone microarchitecture using 3D micro-CT data.

During the early stages of the disease process, only the external lamina becomes porotic, presumably in response to increased vascularization, and the expansion of the diplöe is minimal. Thin-ground sections have shown that while the external lamina is being resorbed, there are only very few slightly enlarged marrow spaces (Schultz 2001). It is possible that small changes that may be occurring during the initial stages of disease pathogenesis (light stage, active lesions) may have been too subtle to detect quantitatively in such a small sample (Type II error). However, it is also possible that trabecular structures are altered only when the marrow becomes severely hyperplastic with increased red blood cell production. It is recommended that future micro-CT studies include large samples comprised of individuals representative of all lesion severity and activity categories in order to clarify whether or not early stage disease pathogenesis can be quantitatively captured in measures of trabecular microarchitecture from 3D micro-CT images.

7.3.2.2 Cranial Porotic Hyperostosis

The results for the quantitative analysis of cranial porotic hyperostosis also demonstrated statistically significant changes in several measures of trabecular bone microarchitecture. However, these results were inconsistent with the findings for orbital porotic hyperostosis and with the findings that were expected from this study, particularly for individuals scored in the "light" lesion category. Like the results for orbital porotic hyperostosis, the mean values for bone volume (BV/TV) and trabecular thickness (Tb.Th.) decrease when unaffected cranial vault bones are compared to those with evidence of medium-severe lesions (Chapter 6, Figure 6.4), which corresponds with the expectations for resorptive and mixed disease processes in Table 5.3 (Chapter 5). However, the decrease in these two variables was not statistically significant. Unlike orbital porotic hyperostosis, individuals with lesions scored in the "light" severity category demonstrated a mean increase, rather than a decrease, in bone volume (BV/TV) that closely approaches significance when compared to unaffected individuals ($p = 0.066$) and when compared to individuals scored in the "medium-severe" category ($p = 0.064$). A similar pattern of a mean increase approaching significance ($p = 0.064$) was also noted between individuals in the "light" and "medium-severe" categories for trabecular thickness (Tb.Th.). In the

analysis of lesion activity, no significant differences were found for these two structural variables.

The results for the remaining three variables, specific bone surface (BS/BV), trabecular number (Tb.N.), and trabecular spacing (Tb.Sp.) showed increases in all of the mean values when the "unaffected" category was compared to the "medium-severe" lesion category, but no significant increases were noted (Chapter 6, Figure 6.4). Again, conflicting results were found for these three variables only in the "light" lesion category. When the "unaffected" category was compared to "light" lesion category, a mean decrease approaching statistical significance was noted for trabecular spacing (Tb.Sp.) ($p = 0.088$). When the "light" lesion category was compared to the "medium-severe" category, specific bone surface (BS/BV) and trabecular number (Tb.N.) significantly decreased ($p = 0.046$ and 0.043, respectively). Again, in the analysis of lesion activity, no significant differences were found for any of these structural variables.

Overall, the results of the quantitative analysis of cranial porotic hyperostosis reveal that trabecular shape, thickness and number are significantly affected only in the light stages of lesion pathogenesis regardless of lesion activity. Light lesions are characterized by an increase in bone volume which is reflected by fewer and more closely spaced trabeculae that are significantly thicker. These changes may be attributed to higher than normal rates of osteoblastic activity given the findings of an increase in bone volume. However, this pattern does not correspond with the pattern demonstrated for orbital lesions, nor does this pattern fit with the expectations of this study. These findings more closely fit with the expectations for formative (osteoblastic) disease processes (Chapter 5, Table 5.3). These results are also not supported by the published clinical or anthropological literature on porotic hyperostosis which also illustrates that cranial bones that show a greater severity of bone changes macroscopically have more significant changes to bone structure in the examination of histologic thin-sections (e.g. Williams 1929; Nathan and Haas 1966; El-Najjar and Robertson 1976; Stuart-Macadam 1987b). It is germane to note that the mean values for medium-severe lesions in an active state do appear to decrease for measures of bone volume (BV/TV) and trabecular thickness (Tb.Th.), and increase in measures of specific bone surface (BS/BV), trabecular number (Tb.N.), and

trabecular spacing when compared to unaffected bone (Tb.Sp.) (Chapter 6, Figures 6.4 and 6.6). These data suggest that changes to the mean values for all five of the structural variables in the "medium-severe" lesion categories, although not significant, are consistent with the observed orbital results (Chapter 6, Figure 6.3) and the expected patterns for resorptive and mixed disease processes (Chapter 5, Table 5.3). Therefore, it is clear that the presence of one or several factor(s) in the "light" and/or "healed" lesion categories, that are not present in the "unaffected" or "medium-severe" categories, are contributing to conflicting and inconsistent results in the analysis of lesion severity in the cranial vault. A discussion of the possible factors contributing to these conflicting data will be considered.

First, it is possible that structural changes caused by artificial cranial modification are responsible for the observations made in this study. A total of eight out of 27 individuals with cranial porotic hyperostosis had documented evidence of artificial fronto-occipital modification (bilobed parietal expansion) (Note: six out of the 21 unaffected individuals also had evidence of cranial modification). This form of cranial modification is commonly noted in pre-Columbian coastal populations in Peru, among Maya populations in Belize, and many other archaeological populations (Cheverud et al. 1992; White 1996). Fronto-occipital modification causes bilobed expansion by artificial fronto-occipital compression using boards or pads (Allison et al. 1984; Cheverud et al. 1992). These forms of compression would have restricted growth antero-posteriorly and resulted in two distinct lobes formed in the parietal region on either side of the sagittal suture with a clear depression along the line of the suture (Cheverud et al. 1992). Dimensionally the parietal bones are affected most strongly by this type of modification (White 1996).

Cranial restraining devices applied during growth and development will produce localized areas of external compression and can alter the normal internal tensile forces created by the growing brain (Anton et al. 1992). Almost all tissues, including skeletal tissues, are sensitive to such mechanical forces and loading. They respond to and resist forces such as compression and tension by adding, differentiating, or taking away tissue (LeVeau and Bernhardt 1984). According to Wolff's Law, any change in the amount of force or load that produces stress within bone will produce a demonstrable change in the

internal architecture of the bone (Wolff 1986; LeVeau and Bernhardt 1984). Compression and tensile loads appear to be the major contributing forces to the development of trabeculae and, if there is a continual stimulus from these forces, the remodelling process attempts to maintain maximum bone density in areas of loading (LeVeau and Bernhardt 1984). Therefore, it would be expected that trabecular microarchitecture in the diplöe of artificially modified crania are likely to have increased values for bone volume density (BV/TV) and trabecular thickness (Tb.Th) with a corresponding decrease in specific bone surface (BS/BV), trabecular number (Tb.N), and trabecular spacing (Tb.Sp.). Although the published literature lacks research on the specific effects of artificial cranial modification on trabecular bone microarchitecture, based on our knowledge of bone biology and bone response to mechanical loading, it is reasonable to assume that artificial cranial modification may have had some effect on the results of this study. When the mean values for all individuals with artificially modified crania are compared to those without evidence of modification (N = 27), there is a mean increase in bone volume density (BV/TV) and trabecular thickness (Tb.Th) with an associated decrease in specific bone surface (BS/BV) and trabecular number (Tb.N) (Figure 7.3).

Additionally, of the eight modified crania with evidence of porotic hyperostosis, five were scored in the "light" lesion category. Therefore, it is possible that the quantitative structural values for individuals in the "light" lesion category were affected by structural differences caused by cranial modification, resulting in Type I error. It is also possible that the porotic lesions observed on these individuals were the result of a different pathological process unrelated to that which affected the orbits, such as pressure atrophy or bone necrosis (Gerszten 1993; Ayer et al. 2010). These types of porotic changes have been documented macroscopically in several studies (e.g. Gerszten 1993; Ayer et al. 2010; Boston 2012), but have yet to be evaluated at the microarchitectural level. Further research with larger sample sizes is needed to clarify the specific effects of artificial cranial modification on trabecular microarchitecture and on the appearance of porotic hyperostosis in order to better understand how this variable can affect quantitative analyses of pathological change in palaeopathological research.

Figure 7-3: Mean Comparisons for Cranial Modification versus Unmodified Crania
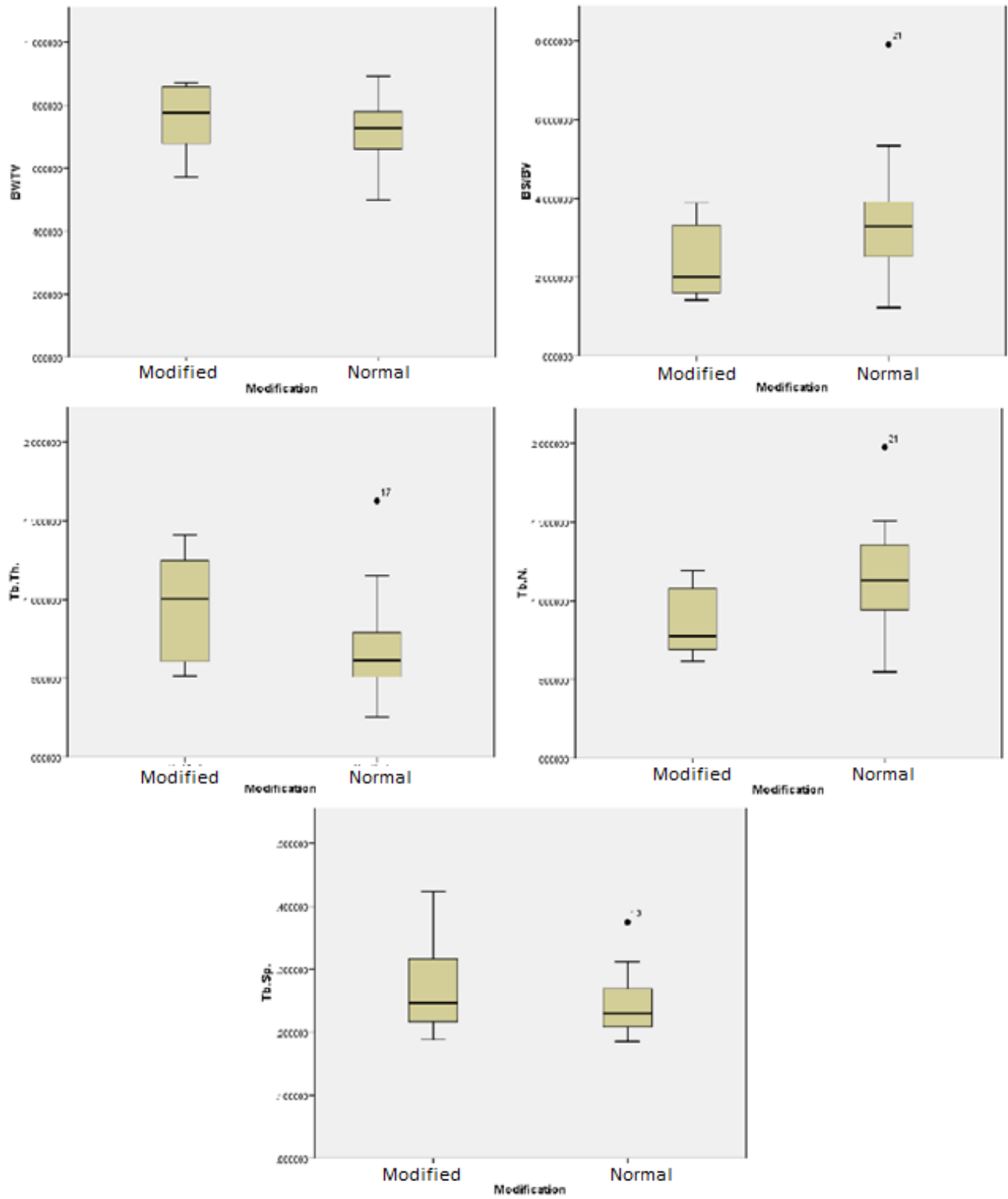
Finally, in addition to cranial modification, it is also possible that methodological error caused by over-sampling of cranial vault lesions contributed to Type II error in the evaluation of medium-severe lesions. Tests of observer error revealed that the 3D custom VOI method improved observer reproducibility and reliability, but this does not completely preclude the possibility of over-sampling. This is particularly relevant when considering the macroscopically observable limits of healing or healed cranial vault lesions. Healing lesions are characterized by the in-filling of pores along the periphery of the lesion which gradually progresses to the centre (Mensforth et al. 1978). A 3D custom VOI that includes the entirety of a healing lesion will average the trabecular architecture from the centre, which is likely more representative of an active lesion, and the periphery, which is likely more representative of a healed lesion. Since healed lesions are not significantly different from unaffected bone in either orbital or cranial porotic hyperostosis, this method may result in an averaging of trabecular microarchitecture that could obscure differences that are occurring across healing lesions. It is recommended that future studies focus on the evaluation of changes both within and across lesions, particularly with reference to healing lesions of cranial porotic hyperostosis. An evaluation of how trabecular microarchitecture changes from the periphery to the centre of a lesion may reveal additional information regarding disease pathogenesis and the mechanism of healing in porotic lesions of the skull.

7.3.3   Contributions to Differential Diagnosis

Now that the results of the quantitative analysis of trabecular microarchitecture have been thoroughly discussed, the question remains: is the differential diagnosis of orbital and cranial porotic hyperostosis aided by the visual and quantitative micro-CT analysis of trabecular microarchitecture? The quantitative analysis of orbital porotic hyperostosis suggests that porotic lesions of the orbit are the result of a primarily resorptive process with increased osteoclastic activity leading to generalized bone loss. The volume of trabecular bone is significantly reduced and trabecular shape, thickness, and number are significantly affected in active lesions during the medium to severe stages of disease pathogenesis. Trabecular spacing increases in medium to severe active lesions, but not to a significant degree. A similar pattern in mean value directionality was observed during

early lesion development and the later stages of healing, but significant changes to trabecular microarchitecture were not demonstrated. When cranial porotic hyperostosis is considered, a similar pattern of increased bone resorption and generalized bone loss is also observed in the "medium-severe" and "active" lesion categories. However, these findings were not significant. A significant increase in trabecular bone was noted in the "light" and "healed" stages of disease pathogenesis which may be related to differential effects of the disease process on the orbits versus the cranial vault. Overall, the quantitative analysis of cranial porotic hyperostosis requires further research.

When these quantitative data are considered alone, they do conform to the expected patterns for resorptive and mixed disease processes in Table 5.3 (Chapter 5), but do not contribute much to the process of differential diagnosis other than to confirm the presence of overall trabecular bone loss and localized demineralization in the advanced stages of disease. These quantitative findings may refute a diagnosis of scurvy, but do not exclude differential diagnoses of anaemia, rickets, or inflammatory processes (Schultz 2001; Roberts and Manchester 2005; Brickley et al. 2007; Waldron 2009). On the other hand, the visual appearance of porotic hyperostosis on micro-CT cross-sections does aid in differentiating cortical resorption and marrow expansion from the processes of bone apposition observed in scurvy, splintering of the outer table as observed in rickets, and the complete destruction of the outer table as well as diplöic trabeculae as observed in inflammatory processes (Chapter 3, Section 3.7). Additionally, when placing the quantitative data within the clinical, archaeological, and palaeoecological contexts of the populations that comprise the study sample, a differential diagnosis of an anaemic condition can be supported. First, despite the inconsistent results for cranial porotic hyperostosis, the quantitative findings from this study are consistent with radiographic and histologic examinations of clinical and archaeological cases of anaemia. Radiographs have revealed that in many of the anaemias (e.g. acquired anaemias, sickle cell disease, and thalassemia) there is diminished bone mass due to a widening of the marrow cavity. Diminished bone mass relative to bone volume has been reported and attributed to a loss of trabecular bone and thinning and diminution of thicker plate-like trabeculae (Garn 1970, 1992). Thin-ground sections have demonstrated that advanced stages of marrow hyperplasia are characterized by parallel, long, and considerably

thinned, or gracile, trabeculae with an increase in marrow space. These changes were noted more significantly with increasing lesion severity (e.g. Whipple and Bradford 1932; Middlemiss 1961; Nathan and Haas 1966; Schultz 2001).

Second, the palaeoepidemiological pattern of these lesions supports a condition that has its onset in early childhood and tends to be resolved in adolescence and adulthood (e.g. Stuart-Macadam 1985). The quantitative analysis of trabecular microarchitecture and its relationship to lesion severity and activity also support this palaeoepidemiological pattern. Trabecular structures are significantly affected in the active and more severe stages of disease pathogenesis that are characteristic of the sub-adults, but these changes appear to be reversed in the healing stages for the adults. These quantitative differences in lesion severity and activity are, therefore, reflective of a pathological condition that is more physiologically demanding in childhood than in adulthood. It is also possible that these differences are reflective of changes in the activity of erythropoeitic marrow from the cranium in childhood to the infracranial skeleton in adulthood (Loevner et al. 2002; Walker et al. 2009). Together, the combination of a decreased physiological demand for nutrients (e.g. iron and folate), and the modification of erythropoetic marrow with increasing age could explain the palaeoepidemiological trends and patterns of quantitative changes observed in this sample.

Although the specific cause of the anaemic condition cannot be determined, based on the multiple lines of evidence considered in this study, it is likely that an acquired anaemia caused by a synergistic relationship between dietary insufficiency, infectious disease, and parasitic infestation is responsible for the prevalence of porotic hyperostosis in these archaeological samples. The age-related pattern of lesion activity and healing is not consistent with scurvy or inflammatory processes (e.g. periostitis and osteomyelitis), nor is it consistent with a diagnosis of osteoporosis. This is because scorbutic lesions and inflammatory processes can be active at any age, and osteoporosis occurs with increasing age (cf. Schultz 2001; Roberts and Manchester 2005; Brickley et al. 2007; Waldron 2009).

7.4 Methodological Challenges and Research Limitations

The most significant challenge encountered in this study was one that is common among all research that involves archaeological skeletal collections. Poor preservation and small sample sizes made it difficult to uncover the complete picture of the pathogenesis and potential etiologies of porotic hyperostosis. The poor preservation of the Maya series made it difficult to accurately age and sex several individuals. Specific age ranges for some adults and sub-adults could not be provided nor could the evaluation of sex be completed for some adults. Preservation issues also meant that complete crania were not available for analysis in the majority of individuals and many individuals were only represented by a single cranial bone or small cranial fragments. It was, therefore, impossible to accurately evaluate the functional relationship between orbital and cranial porotic hyperostosis in the assessment of epidemiological patterning. However, the finding that orbital trabecular microarchitecture is significantly affected whereas cranial vault bones are not may support the hypothesis that orbital lesions are the earliest bony alterations in anaemia (e.g. Caffey 1937; Middlemiss 1961; Steinbock 1976; Stuart Macadam 1989). Future palaeopathological investigations of porotic hyperostosis should include samples with higher rates of cranial and infracranial preservation, such as the skeletal collections from the Dakleh Oasis, Egypt (e.g. Fairgrieve and Molto 2000). A sample such as this would not only allow for the evaluation of the functional relationship between orbital and porotic hyperostosis, but would also provide larger sample sizes for improving the validity and robusticity of statistical testing.

One of the limitations of this study was the inability of micro-CT to provide information related to several histological aspects of bone dynamics relevant to palaeopathology. Although the micro-CT method used in this study offers a reliable and efficient means of quantifying 3D parameters related to trabecular bone microarchitecture, it could not differentiate between resorbing, forming, or resting bone surfaces, nor could it provide information regarding the orientation of collagen fibres (woven versus lamellar bone) (Uchiyama et al. 1997; Müller et al. 1998; Kuhn et al. 2007; Rühli et al. 2007). Further improvement in scan resolution may allow for the identification of these additional

pathological details. However, it is important to note that as spatial resolution increases, the field of view decreases and a compromise between scan resolution, the size of the volume of interest, and the desired structural parameters is necessary (Peyrin et al. 2000). The 3D structural parameters available for lower resolution scans appear to be sufficient for the analysis of later stages of active disease pathogenesis, but not for the early or healed stages of porotic hyperostosis. Higher resolution scans may reveal valuable information regarding resorption and formation at the cellular level, as well as the orientation of collagen fibres in early and healed stages of disease pathogenesis (Cooper et al. 2003, 2007). It is recommended that future palaeopathological research on porotic hyperostosis, as well as other pathological conditions, explore and establish the relationships between data from varying levels of resolution.

A second limitation of this research was the inability to evaluate trabecular anisotropy in VGStudio Max. Anisotropy characterizes the degree of directional organization of a material and provides data on trabecular orientation (Chappard et al. 2005; Mittra et al. 2007). An option for the automated calculation of anisotropy was available in VGStudio MAX, but the restricted size of many of the smaller and medium sized 3D custom VOIs did not provide sufficient data for the calculation of this structural parameter. This was particularly disappointing given the phenomenon of "hair-on-end" trabeculation that is so characteristic of the genetic and acquired anaemias. The orientation of normal circumferentially laid down trabeculae is altered by the increased demand for marrow space and trabeculae become radially oriented at 90° angles to the inner and outer tables (Stuart Macadam 1987b, 1989; Schultz 2001). Given that the quantitative findings in this study support trabecular changes that are expected in anaemic conditions, future studies using more intact and better preserved samples should further evaluate if any significant quantitative changes to trabecular anisotropy are characteristic of porotic hyperostosis.

Finally, it is germane to discuss the challenges that were encountered with micro-CT equipment operation and scan acquisition. The micro-CT volumes obtained for this study were acquired, reconstructed, and analyzed by myself after a total of 36 hours of training on micro-CT scan set-up, acquisition software use (X-Tek), and analytical software applications (VGStudio MAX). Based on minimal experience with optimizing micro-CT

scan parameters, it is possible that image quality and resolution settings may not have been as good as they could have been had a more fully trained technician or radiologist been involved in scan acquisition. In addition, file sizes were extremely large and ranged from 8GB to 36GB per scan depending on the size of the sample. These large file sizes precluded viewing in other micro-CT capable programs. It is likely that these file sizes could have been managed more efficiently with more experience and knowledge of micro-CT volume file manipulation and the process of exporting large micro-CT datasets. With the increasing availability of equipment and facilities for non-medical research, these issues must be addressed and strategies for improving training and knowledge on optimal micro-CT scan settings for anthropological applications will be essential. Continued collaboration with imaging physicists is essential to the success of micro-CT image analysis research in anthropology and palaeopathology.

7.5   Conclusions

The purpose of this dissertation research was to assess the reliability and value of micro-CT methods to the differential diagnosis of porotic hyperostosis in palaeopathology, a common lesion observed in many archaeological skeletal collections. To date, the use of micro-CT in palaeopathology has largely been limited to subjective qualitative assessments of bone lesions with little exploration into the value of objective quantitative data to the process of differential diagnosis (e.g. Kuhn et al. 2007; Rühli et al. 2007). This research explored the value of micro-CT for the objective quantitative analysis of porotic hyperostosis in an attempt to link subjective scales of visual assessment with objective and reliable quantitative measures of trabecular bone microarchitecture.

In order to place the results of the micro-CT image analysis within the archaeological and palaeoepidemiological contexts of the skeletal populations used in this study, and to provide as accurate a differential diagnosis of porotic hyperostosis as possible, it was first necessary to consider the overall palaeoepidemiological pattern of porotic hyperostosis ($H1_o$ and $H2_o$). After exploring the palaeoepidemiological context of this study, the remaining objectives of this research were evaluated. The second objective was to evaluate the reproducibility and reliability of 2D and 3D methods of data collection for the quantitative analysis of bone micro-architecture from micro-CT images. The third,

and final, objective was to apply reliable micro-CT image analysis methods to the evaluation of orbital and cranial porotic hyperostosis to determine the value of such methods for understanding disease pathogenesis and improving the differential diagnosis of these lesions in palaeopathology.

Sixty-six individuals obtained from four skeletal collections were assessed both visually and quantitatively in order to discern the process of lesion development and the potential etiologies of porotic hyperostosis. For the evaluation of the first objective, an age-related trend in the prevalence of porotic hyperostosis was noted in this sample and supported the hypothesis that these lesions have an onset during childhood (e.g. Stuart-Macadam 1985). The goals of the second objective were met and the null hypothesis that there are no differences in the reproducibility or reliability of 2D and 3D quantitative methods was rejected. Two-dimensional methods of data collection did not provide reliable or reproducible representations of trabecular microarchitecture, and 3D VOIs of uniform size should only be used after careful consideration of the potential for introducing Type I and II error as a result of under- or over-sampling. Based on the results of this study, palaeopathologists interested in applying micro-CT methods to the study of archaeological disease should consider the use of the 3D standard and 3D custom VOI methods described in Chapter 5 (Section 5.2.2.2). The choice of 3D method will depend on the size and shape of the skeletal elements of interest as well as the types of lesions and disease processes under investigation. The 3D standard VOI method may be ideal for the investigation of systemic disease processes that affect the structures of entire skeletal elements, whereas the 3D custom VOI method may be better suited to disease processes that preferentially affect only specific locations on different skeletal elements. Future research that compares the use of different 3D VOI methods for different types of disease processes will be necessary to clarify the best use of 3D VOI methods in palaeopathology.

After addressing the first and second objectives, the 3D custom VOI method was applied to the micro-CT images to address the third objective. The null hypotheses used to meet the goals of objective three stated that no significant differences exist in trabecular bone microarchitecture between unaffected individuals and affected individuals based on the

visually observed categories of lesion *severity* (light, medium, severe) and *activity* (active, healed, mixed). The results for orbital porotic hyperostosis rejected the null hypothesis and demonstrated that 3D quantitative micro-CT methods provide valuable information regarding disease pathogenesis when porotic lesions are active and in the more severe stages of lesion development at the time of death. Therefore, subjective visual scales of assessment can be linked to objective quantitative data only when lesions are in this particular stage of lesion development. Orbital porotic hyperostosis that is in the early or healing stages of pathogenesis is not quantitatively differentiated from unaffected bone using the methods applied in this study. Additional research designed to achieve higher resolution 3D micro-CT volumes are needed to determine whether or not early stage disease pathogenesis can be quantitatively captured through the analysis of cellular level change.

As with most studies, more questions seem to have been generated than answered. The results for cranial porotic hyperostosis were inconsistent with the results for orbital porotic hyperostosis when individuals with artificially modified crania were included in the analysis of cranial vault lesions. A reconsideration of mean values and directionality indicated that changes in trabecular microarchitecture in cranial porotic hyperostosis follow a similar pattern as in orbital porotic hyperostosis, but not to the same extent. Orbits appear to be more significantly affected than the cranial vault possibly due to developmental structural differences. Future research with increased sample sizes and the inclusion of individuals representing all categories of lesion severity and activity is needed to shed light on the extent and degree of trabecular changes occurring with cranial porotic hyperostosis.

Not only are 3D micro-CT methods non-destructive and efficient, they also provide reliable 3D information that is not typically accessible through 2D histologic thin-sectioning. Future research studies in palaeopathology should, therefore, also apply 3D micro-CT methods to clinical and historically documented samples with known causes of death with the aim to evaluate previous specific histological diagnoses of porotic hyperostosis and other pathological conditions (e.g. Schultz 2001). Schultz (2001) concluded that histological analyses can reveal patterns of features in bone

microstructures which are unique to different disease processes. It is doubtful, however, based on the results of this study, that patterns of bone microarchitecture unique to specific diseases can be identified for a large majority of non-specific pathological lesions. This is because bone is limited in the number of ways that it can respond to disease, even at the micro-level. In order to support this non-specificity hypothesis, planned future 3D micro-CT evaluations of porotic hyperostosis will include clinical and archaeological individuals with evidence of diagnosed leukemia. Although these cranial lesions have been associated with leukemic bone changes (e.g. Rothschilde 1997), they are more likely a non-specific response to a secondary anaemia that often develops in clinical cases with this form of cancer. In this assessment, findings similar to the results of this study will support the hypothesis that bone changes with porotic hyperostosis are non-specific, even at the micro-level. This would also indicate that, in future palaeopathological research, the inclusion of archaeological, clinical, and palaeoecological evidence in addition to primary 3D quantitative data will be necessary in the process of differential diagnosis. Despite the limitations of non-specificity, 3D micro-CT methods are capable of providing valuable information regarding the pathogenesis of disease, leading to more reliable differential diagnoses.

This study represents a pioneering effort at developing reliable methods of 3D micro-CT quantitative data collection in a palaeopathological context and is, therefore, a significant methodological contribution to the field of palaeopathology. To the best of my knowledge, this is one of the first palaeopathological studies to use 3D micro-CT image analysis methods for the quantitative evaluation of porotic hyperostosis in an attempt to elucidate disease process and etiology. It has been demonstrated previously that this analytical tool is capable of clarifying how different disease processes affect bone microarchitecture for a variety of pathological conditions in clinical research, specifically osteoporosis (e.g. Hildebrand et al. 1999; Mittra et al. 2007). I conclude that the applications of 3D micro-CT methods of image analysis appear to be of high value in clarifying the process of disease pathogenesis and supporting current differential diagnoses of porotic hyperostosis in palaeopathology. Patterns of micro-level bone change can be quantitatively defined, compared, and contrasted not only within and between different skeletal lesions, but also within and between different archaeological

human populations. Although this method is not capable of providing specific diagnoses, it can be used in combination with archaeological, historical, and/or palaeoecological evidence to support or refute current differential diagnoses, thereby contributing to a better understanding of disease pathogenesis and epidemiology, and informing current interpretations of the health and disease of past populations.

The reliability of diagnoses plays a significant role in answering analytical questions not only regarding the population, but also the individual. At the population level, the prevalence of physically debilitating diseases such as anaemia may have meant that working capacity and productivity was adversely affected. This hypothesis has been explored as part of the ecological model for the Classis Maya collapse (White 1988; Wright and White 1996). At the individual level, a number of questions can be reliably addressed, including: what were the different physiological symptoms experienced by the individual? How might have illness affected an individual's role and/or identity in society? How might society have responded to affected individuals differently? Visible signs of disease or illness may have affected an individual's social identity and their relationship, whether positively or negatively, with other members of society (Fay, 2006). The ethnographic record illustrates that societies often take extreme positions regarding people who are different, including those with physical deformities or disabilities. In some societies, deformed and/or disabled individuals were treated poorly, whereas in others they may have been revered (Dettwyler, 1991). Without a correct diagnosis, we cannot confidently answer questions regarding individual social identity and the individual experience of disease in ancient populations.

Palaeopathologists continue to strive for new and innovative research methods that go beyond simply achieving a diagnosis. Overall, the role of this research within the broader discipline of anthropology was to provide a standardized, non-destructive method for collecting accurate primary evidence for the state of health of past human populations in order to allow for the reliable reconstruction of the dynamic interactions between the environment, culture, and disease in archaeological populations in future studies. Reliable differential diagnoses are vital for establishing these links and for correctly interpreting disease prevalence, population health, and the biocultural factors that may

have contributed to health, illness, and the spread of disease in the past. Therefore, methods of improving the process of differential diagnosis in palaeopathology have evolved to include new techniques, such as micro-CT, that provide additional diagnostic information on the pathogenesis and potential etiologies of disease. With the continued development of standardized, reliable methods, researchers will not only be able to achieve more reliable diagnoses, but will also gain a better understanding of the diseases that were present in past populations and how they may have affected population dynamics at the individual social level as well as at the population level.

Bibliography

Aksoy M., Camli N., Erdem S. (1966) Roentgenographic bone changes in chronic iron deficiency anemia: A study in twelve patients. *Blood*, 27, 677-686.

Alesan, A., Malgosa, A., Simo, C. (1999). Looking into the demography of an Iron Age population in the Western Mediterranean. I. Mortality. *American Journal of Physical Anthropology*, 110(3), 285-301.

Allison, M.J. (1984). Paleopathology in Peruvian and Chilean populations. In M.N. Cohen and G.J. Armelagos (Eds.), *Paleopathology at the Origins of Agriculture* (pp. 515-527). Orlando, Florida: Academic Press Inc.

Alt, K.W. and Buitrago-Téllez, C H. (2004). Dental paleoradiology: applications in paleoanthropology and paleopathology. *Canadian Association of Radiologists journal*, 55(4), 258-263.

Ambrose, S. H. (1993). Isotopic analysis of paleodiets: methodological and interpretive considerations. *Food and Nutrition in History and Anthropology*, 10.

Ameen, S., Staub, L., Ulrich, S., Vock, P., Ballmer, F., Anderson, S.E. (2005). Harris lines of the tibia across centuries: A comparison of two populations, medieval and contemporary in Central Europe. *Skeletal radiology*, 34(5), 279-284.

Andersen, J. G., and Manchester, K. (1992). The rhinomaxillary syndrome in leprosy: a clinical, radiological and palaeopathological study. *International Journal of Osteoarchaeology*, 2(2), 121-129.

Anderson, T., Wakely, J., Carter, A. (1992). Medieval example of metastatic carcinoma: A dry bone, radiological, and SEM study. *American Journal of Physical Anthropology*, 89(3), 309-323.

Angel, J. L. (1964). Osteoporosis: thalassemia?. *American Journal of Physical Anthropology*, 22(3), 369-373.

(1966). Porotic hyperostosis, anemias, malarias, and marshes in the prehistoric eastern Mediterranean. *Science*, 153(3737), 760-763.

(1971). *The People of Lerna: Analysis of a Prehistoric Aegean Population*. Washington, DC: Smithsonian Institution Press.

(1978). Porotic hyperostosis in the eastern Mediterranean. In El-Najjar, M. and Allison, M. (Eds.), *Paleoepidemiology* (pp. 10-16). Medical College of Virginia, Quarterly, 14.

Anton, S.C., Jaslow, C.R., Swartz, S.M. (1992). Sutural complexity in artificially deformed human (Homo sapiens) crania. *Journal of Morphology*, 214(3), 321-332.

Arlot, M. E., Jiang, Y., Genant, H. K., Zhao, J., Burt-Pichat, B., Roux, J. P., ... Meunier, P. J. (2008). Histomorphometric and μCT analysis of bone biopsies from postmenopausal osteoporotic women treated with strontium ranelate. *Journal of Bone and Mineral Research*, 23(2), 215-222.

Armelagos, G.J. (2003). Bioarchaeology as Anthropology. *Archeological Papers of the American Anthropological Association*, 13(1), 27-40.

Armelagos, G.J. and Van Gerven, D.P. (2003). A century of skeletal biology and palaeopathology: Contrasts, contradictions, and conflicts. *American Anthropologist*, 105(1), 53-64.

Arnon, S.S., Midura, T F., Damus, K., Thompson, B., Wood, R. M., Chin, J. (1979). Honey and other environmental risk factors for infant botulism. *The Journal of Pediatrics*, 94(2), 331-336.

Ascenzi, A. (1969). Microscopy and prehistoric bone. In Brothwell, D. and Higgs, E. (Eds.), *Science in Archaeology: A Survey of Progress and Research* (pp. 526-538). Thames and Hudson.

Ascenzi, A. and Balistreri, P. (1977). Porotic hyperostosis and the problem of origin of thalassemia in Italy. *Journal of Human Evolution*, 6(7), 595-604.

Assis, S.S.D. (2013). *Beyond the Visible World: Bridging macroscopic and paleohistopathological techniques in the study of periosteal new bone formation in human skeletal remains.* Doctoral Dissertation, Department of Life Sciences, University of Coimbra, Portugal.

Aufderheide, A. C. (1989). Chemical analysis of skeletal remains. *Reconstruction of Life from the Skeleton*, 237-260.

Aufderheide, A.C., Rodrıguez-Martın, C. (1998). *The Cambridge Encyclopedia of Human Paleopathology*. Cambridge and NewYork: Cambridge University Press.

Ayer, A., Campbell, A., Appelboom, G., Hwang, B.Y., McDowell, M., Piazza, M., ... Anderson, R.C. (2010). The sociopolitical history and physiological underpinnings of skull deformation. *Neurosurgical Focus*, 29(6), E1.

Baker, J., and Pearson, O.M. (2006). Statistical methods for bioarchaeology: applications of age-adjustment and logistic regression to comparisons of skeletal populations with differing age-structures. *Journal of Archaeological Science*, 33(2), 218-226.

Balto, K., Müller, R., Carrington, D. C., Dobeck, J., Stashenko, P. (2000). Quantification of periapical bone destruction in mice by micro-computed tomography. *Journal of Dental Research*, 79(1), 35-40.

Barbier, A., Martel, C., De Vernejoul, M. C., Tirode, F., Nys, M., Mocaer, G., ... Lacheretz, F. (1999). The visualization and evaluation of bone architecture in the rat using three-dimensional X-ray microcomputed tomography. *Journal of Bone and Mineral Metabolism*, 17(1), 37-44.

Barnes, I., and M.G. Thomas. (2006). Evaluating bacterial pathogen DNA preservation in museum osteological collections. *Proceedings of the Royal Society: Biological Sciences*, 273, 645-653

Bartl, R., and Frisch, B. (2009). *Osteoporosis: Diagnosis, Prevention, Therapy*. Berlin: Springer.

Beckett, R.G. and Conlogue, G.J. (2010). *Paleoimaging: Field Applications for Cultural Remains and Artifacts*. Boca Raton: Taylor and Francis Group.

Becker, M. J. (1995). Human skeletal remains from the pre-colonial Greek emporium of Pithekoussai on Ischia: Culture contact in the early VIII to the II century BC. *Oxbow Monograph* 273-282.

Becroft, D.M. and Holland, J.T. (1966). Goat's milk and megaloblastic anaemia of infancy: A report of three cases and a survey of the folic acid activity of some New Zealand milks. *The New Zealand Medical Journal*, 65(405), 303-307.

Benassi, E. and Toti, A. (1958). Notes on the bones found in the excavations of the cemeteries of Spina; confirmations of the Greek racial origin of thalassemia. *La Rassegna di Clinica, Terapia e Scienze Affini*, 57(1), 16.

Beňuš, R., Obertová, Z. and Masnicová, S. (2010). Demographic, temporal and environmental effects on the frequency of cribra orbitalia in three early Medieval populations from western Slovakia. *Journal of Comparative Human Biology*, 61, 178-190.

Berry, J., Davies, M. and Mee, A. (2002). Vitamin D metabolism, rickets and osteomalacia. *Seminars in Musculoskeletal Radiology*, 6, 173-181.

Bland JM, Altman DG. (1986). Statistical methods for assessing agreement between two methods of clinical measurement. *Lancet*; i:307-10

Blom, D.E. (2005). Embodying borders: human body modification and diversity in Tiwanaku society. *Journal of Anthropological Archaeology*, *24*(1), 1-24.

Bloom, D.W. and Fawcett, A. (1994). *A Textbook of Histology (12ᵗʰ edition).* New York: Chapman and Hall.

Boldsen, J.L. and Milner, G.R. (2012). An epidemiological approach to paleopathology. In Grauer A.L. (Ed.), *A Companion to Paleopathology* (pp. 114-132). West Sussex: Blackwell Publishing Ltd.

Böni T, Rühli FJ, Chhem RK. 2004. History of paleoradiology: early published literature, 1896-1921. *Canadian Association of Radiologists Journal,* 55, 203-210.

Bosch, X. (2000). Look to the bones for clues to human disease. *Lancet,* 355,1248.

Boston, C. (2012). *Investigations of the biological consequences and cultural motivations of artificial cranial modification among Northern Chilean populations.* Doctoral dissertation, Department of Anthropology. Western University.

Bothwell, T.H. (1995). Overview and mechanisms of iron regulation. *Nutrition Reviews*, 53(9), 237-245.

Bourbou, C. (2003). Health patterns of proto-Byzantine populations (6th–7th centuries AD) in south Greece: the cases of Eleutherna (Crete) and Messene (Peloponnese). *International Journal of Osteoarchaeology*, *13*(5), 303-313.

(2014). Evidence of childhood scurvy in a Middle Byzantine Greek population from Crete, Greece (11ᵗʰ-12ᵗʰ centuries A.D.). *International Journal of Paleopathology*. In Press. (http://www.sciencedirect.com/science/article/pii/S1879981714000023).

Boyd, S.K., Müller, R., Leonard, T., Herzog, W. (2005). Long-term periarticular bone adaptation in a feline knee injury model for post-traumatic experimental osteoarthritis. *Osteoarthritis and Cartilage*, 13(3), 235-242.

Brickley, M. and Ives, R. (2006). Skeletal manifestations of infantile scurvy. *American Journal of Physical Anthropology*, 129, 163-172.

(2010). *The Bioarchaeology of Metabolic Bone Disease*. Oxford: Academic Press.

Brickley, M., & McKinley, J. (2004). Guidance to standards for recording human skeletal remains. *University of Reading: Institute of Field Archaeologists/British Association of Biological Anthropology and Osteoarchaeology*.

Brickley, M., Mays, S. Ives, R. (2005). Skeletal manifestations of vitamin D deficiency osteomalacia in documented skeletal collections. *International Journal of Osteoarchaeology*, 15, 389-403.

(2007). An investigation of skeletal indicators of vitamin D deficiency in adults: Effective markers for interpreting past living conditions and pollution levels in 18ᵗʰ and

19th century Birmingham, England. *American Journal of Physical Anthropology*, 132, 67-79.

Britton, H.A., Canby, J.P., Kohler, C. M. (1960). Iron deficiency anemia producing evidence of marrow hyperplasia in the calvarium. *Pediatrics*, 25(4), 621-628.

Brothwell, D. R. (1969). *Food in antiquity: A Survey of the Diet of Early Peoples*. JHU Press.

Brothwell and Sandison (1967). *Diseases in Antiquity.* Springfield: CC Thomas

Brugnara, C. (2003). Iron deficiency and erythropoiesis: New diagnostic approaches. *Clinical Chemistry*, 49(10), 1573-1578.

Buikstra, J.E. and Cook, D.C. (1980). Palaeopathology: An American account. *Annual Review of Anthropology*, 9, 433-470.

Buikstra, J.E. and Ubelaker, D.L. (1994). Standards for data collection from human skeletal remains. *Arkansas Archeological Survey research series no. 44*. Fayetteville: Arkansas Archeological Survey.

Burgener, F.A. and Kormano, M. (1996). *Differential Diagnosis in Computed Tomography*. New York: Thieme Medical Publishers, Inc.

Burr, D.B. (2002). Targeted and nontargeted remodeling. *Bone*, 30(1), 2-4.

Burr, D.B., and Martin, R.B. (1989). Errors in bone remodeling: toward a unified theory of metabolic bone disease. *American Journal of Anatomy*, *186*(2), 186-216.

Bushberg, J.T., Seibert, A.S, Leidholdt, E.M. Jr., Boone, J.M. (2011). *The Essential Physics of Medical Imaging, third edition*. Lippincott, Williams, and Wilkins.

Bushong, S.C. (2008). *Radiologic Science for Technologists*, *ninth edition*. St. Louis: Elsevier Mosby.

Buzon, M.R. (2012). The bioarchaeological approach to palaeaopathology. In. Grauer A.L. (Ed.), *A Companion to Paleopathology* (pp. 58-75). West Sussex: Blackwell Publishing Ltd.

Byers, S.N. and Roberts, C.A. (2003). Bayes' Theorem in paleopathological diagnosis. *American Journal of Physical Anthropology*, 121, 1-9

Caffey, J. 1937. The skeletal changes in the chronic hemolytic anemias. *American Journal of Roentgenology, Radium Therapy and Nuclear Medicine,* 37(3): 293-324.

Caillé, A. (1906). *Differential Diagnosis and Treatment of Disease: A Textbook for Practitioners and Advanced Students.* New York: D. Appleton and Company.

Carli-Thiele, P., & Schultz, M. (1997). Microscopic differential diagnosis of so called cribra orbitalia—a contribution to the etiology of orbital porotic hyperostosis. *American Journal of Physical Anthropology* [Suppl], 24, 88.

Carlson, D., Armelagos, G., Van Gerven, D. (1974). Factors influencing the etiology of cribra orbitalia in prehistoric Nubia. *Journal of Human Evolution*, 3, 405-410.

Carlton, R.R., and Adler, A.M. (2001). *Principles of Radiographic Imaging*. Albany, NY.

Caropreso, S., Bondioli, L., Capannolo, D., Cerroni, L., Macchiarelli, S., Condo, G. (2000). Thin sections for hard tissue histology: a new procedure. *Journal of Microscopy*, 199, 244-247.

Cerutti, N., A. Marin, E. Rabino Massa. (2007). Plague in ancient remains: an immunological approach. In Signoli, M., Chevé, D., Adalian, P., Boesch, G. and Dutour, O. (Eds.), *Plague: Epidemics and Societies* (pp. 238-241). Florence: Firenze University Press.

Cesarani, F., Martina, M. C., Ferraris, A., Grilletto, R., Boano, R., Marochetti, E. F., Gandini, G. (2003). Whole-body three-dimensional multidetector CT of 13 Egyptian human mummies. *American Journal of Roentgenology*, 180(3), 597-606.

Chamberlain, A. (2001). Palaeodemography. In Brothwell, D. and Pollard, A.M. (Eds.), *Handbook of Archaeological Science* (pp. 259-268). Chichester: John Wiley and Sons Ltd.

Chan, S.S., Elias, J.P., Hysell, M.E. Hallowell, M. J. (2008). CT of a Ptolemaic Period Mummy from the Ancient Egyptian City of Akhmim1. *Radiographics*, 28(7), 2023-2032.

Chanarin, I., O'Hea, A.M., Malkowska, V., Rinsler, M.G., Price, A.B. (1985). Megaloblastic anaemia in a vegetarian Hindu community. *The Lancet*, 326(8465), 1168-1172.

Chappard, D., Guggenbuhl, P., Legrand, E., Basle, M.F., and Audran, M. (2005). Texture analysis of X-ray radiographs is correlated with bone histomorphometry. *Journal of Bone Mineralization and Metabolism*, 23, 24–29.

Chavassieux, P.M., Arlot, M.E., Reda, C., Wei, L., Yates, A.J., Meunier, P.J. (1997). Histomorphometric assessment of the long-term effects of alendronate on bone quality and remodeling in patients with osteoporosis. *Journal of Clinical Investigation*, *100*(6), 1475.

Cheverud, J.M., Kohn, L.A., Konigsberg, L.W., and Leigh, S.R. (1992). Effects of fronto-occipital artificial cranial vault modification on the cranial base and face. *American Journal of Physical Anthropology*, 88(3), 323-345.

Chhem, R. (2008). Paleoradiology: History and new developments. In Chhem, R. and Brothwell, D.R. (Eds.). *Paleoradiology: Imaging Mummies and Fossils*. New York: Springer.

Chhem, R. and Brothwell, D.R. (2008). *Paleoradiology: Imaging Mummies and Fossils*. New York: Springer.

Chhem, R. Saab, G., and Brothwell, D.R. (2008). Diagnostic Paleoradiology for paleopathologists. In Chhem, R. and Brothwell, D.R. (Eds.). *Paleoradiology: Imaging mummies and fossils* (pp.73-116). New York: Springer.

Cho, H. (2012). The histology laboratory and principles of microscope instrumentation. In Crowder, C. and Stout, S. (Eds.), *Bone histology: An Anthropological Perspective*. Boca Raton: CRC Press.

Cho, H. and Stout, S. D. (2003). Bone remodeling and age-associated bone loss in the past: a histomorphometric analysis of the Imperial Roman skeletal population of Isola Sacra. In *Bone Loss and Osteoporosis* (pp. 207-228). Springer US.

Cohen, M.N. and Armelagos, G.J. (1984). Paleopathology at the origins of agriculture: Editors' summation. In M.N. Cohen and G.J. Armelagos (Eds.), *Paleopathology at the Origins of Agriculture* (pp. 585-599). Orlando: Academic Press Inc.

Conlogue, G., Beckett, R., Posh, J. (2010). Computer-based imaging. In Beckett, R. and Conlogue, G. (Eds.), *Paleoimaging: Field Applications for Cultural Remains and Artifacts* (pp. 123-184). Boca Raton: Taylor and Francis Group.

Cook, D. and Powell, M. (2006). The evolution of American paleopathology. In Buikstra, J. and Beck, L. (Eds.), *Bioarchaeology: The Contextual Analysis of Human Remains* (pp. 281-323). Amsterdam: Academic Press.

Cook, S.D., Barrack, R.L., Thomas, K.A., Haddad Jr, R.J. (1988). Quantitative analysis of tissue growth into human porous total hip components. *The Journal of Arthroplasty*, 3(3), 249-262.

Cooley, T.B., Witwer, E.R., Lee, P. 1927. Anemia in children with splenomegaly and peculiar changes in the bones – Report of cases. *American Journal of Diseases of Children*. 34: 347-363.

Cooper, D.M.L., Turinsky, A.L., Sensen, C.W., Hallgrimsson, B. (2003). Quantitative 3D analysis of the canal network in cortical bone by micro-computed tomography. *The Anatomical Record* (Part B: New Anat), 274B, 169–179.

(2007). Effect of voxel size on 3D micro-CT analysis of cortical bone porosity. *Calcified Tissue International*, *80*(3), 211-219.

Cowin, S. C., Hart, R. T., Balser, J. R., Kohn, D. H. (1985). Functional adaptation in long bones: Establishing in vivo values for surface remodeling rate coefficients. *Journal of Biomechanics*, *18*(9), 665-684.

Curry, T.S., Dowdey, J.E., Murry, R.C. (1990). *Christensen's Physics of Diagnostic Radiology*. Philadelphia: Lippincott Williams and Wilkins.

Cushing, F.R., and Bone, H.G. (2002). Radiographic diagnosis and laboratory evaluation of Paget's disease of bone. *Clinical Reviews in Bone and Mineral Metabolism*, 1(2), 115-134.

Cybulski, J.S. (1977). Cribra orbitalia: A possible sign of anemia in early historic native populations of the British Columbia coast. *American Journal of Physical Anthropology*, 47, 31-40.

Davenport, J. (1996). Macrocytic anemia. *American Family Physician*, 53(1), 155-162.

De Boer, H.H., Van der Merwe, A.E., Maat, G.J.R. (2013). The diagnostic value of microscopy in dry bone palaeopathology: A review. *International Journal of Paleopathology*. In Press.

Del Fattore, A., Cappariello, A., Teti, A. (2008). Genetics, pathogenesis and complications of osteopetrosis: Review. *Bone*, 42(1), 19-29.

De Souza, S.M., Carvalho, D. M.D., and Lessa, A. (2003). Paleoepidemiology: is there a case to answer?. *Memórias do Instituto Oswaldo Cruz*, 98, 21-27.

Dettwyler, K.A. (1991). Can palaeopathology provide evidence for "compassion"? *American Journal of Physical Anthropology*, 84, 375-384

Dittmann, K., and Grupe, G. (2000). Biochemical and palaeopathological investigations on weaning and infant mortality in the early Middle Ages. *Anthropologischer Anzeiger; Bericht uber die biologisch-anthropologische Literatur*, 58(4), 345-355.

Donnelly, S., Donnelly, C., Murphy, E., Donnell, C. (1999). The forgotten dead: The cilliní and disused burial grounds of Ballintoy, County Antrim. *Ulster Journal of Archaeology*, 109-113.

Donoghue, H.D., Spigelman, M., Zias, J., Gernaey-Child, A.M., Minnikin, D.E. (1998). Mycobacterium tuberculosis complex DNA in calcified pleura from remains 1400 years old. *Letters in Applied Microbiology*, 27(5), 265-269.

Donoghue, H.D. (2008). Molecular paleopathology of human infectious disease. In S. Mays and R. Pinhasi (Eds.), *Advances in Human Palaeopathology* (pp. 147-176). West Sussex: John Wiley and Sons Ltd.

Downey, P.A., and Siegel, M.I. (2006). Bone biology and the clinical implications for osteoporosis. *Physical Therapy*, 86(1), 77-91.

Drancourt, M., and Raoult, D. (2005). Palaeomicrobiology: current issues and perspectives. *Nature Reviews Microbiology*, 3(1), 23-35.

Drancourt, M., Signoli, M., La Vu Dang, B.B., Roux, V., Tzortzis, S., Raoult, D. (2007). Yersinia pestis Orientalis in remains of ancient plague patients. *Emerging Infectious Diseases*, 13(2), 332.

Ducy, P., Desbois, C., Boyce, B., Pinero, G., Story, B., Dunstan, C., ... Karsenty, G. (1996). Increased bone formation in osteocalcin-deficient mice. *Letters to Nature*, 382, 448-452.

Elliott, J. C. and Dover, S. D. (1982). X-ray microtomography. *Journal of Microscopy*, 126(2), 211-213.

El-Najjar, M. and Robertson, A. L. (1976). Spongy bones in prehistoric America. *Science*, *193*(4248), 141-143.

El-Najjar, M.Y., Lozoff, B., Ryan, D.J. (1975). The paleoepidemiology of porotic hyperostosis in the American southwest: Radiological and ecological considerations. *American Journal of Roentgenology*, 125, 918-924.

El-Najjar, M.Y., Ryan, D.J., Turner, C.G.II, Lozoff, B. (1976). The etiology of porotic hyperostosis among the prehistoric and historic Anasazi Indians of the Southwestern U.S. *American Journal of Physical Anthropology*, 44, 447-488.

Enlow, D.H. and Brown, S.O. (1958). A comparative histological study of fossil and recent bone tissues. Part III. *The Texas Journal of Science*, *10*(2), 187-230.

(1957). A comparative histological study of fossil and recent bone tissues. Part II. *The Texas Journal of Science*, *9*(2), 186-204.

Ericksen, M.F. (1976). Cortical bone loss with age in three native American populations. *American Journal of Physical Anthropology*, *45*(3), 443-452.

Exner, S., Bogusch, G., Sokiranski, R. 2004. Cribra orbitalia visualized in computed tomography. *Annals of Anatomy* 186: 169-172.

Fairgreive, S.I. (1993). *Amino acid residue analysis of Type I collagen in human hard tissue: An assessment of cribra orbitalia in an ancient skeletal sample from Tomb 31, Site*

31/435-D5-2, Dakleh Oasis, Egypt. Doctoral Dissertation, Department of Anthropology. University of Toronto.

Fairgrieve, S.I. and Molto, J.E. (2000). Cribra orbitalia in two temporally disjunct population samples from the Dakleh Oasis, Egypt. *American Journal of Physical Anthropology*, 111, 319-331.

Fajardo, R.J. and Müller, R. (2001). Three-dimensional analysis of nonhuman primate trabecular architecture using microcomputed tomography. *American Journal of Physical Anthropology*, 115, 327-336.

Fandrey, J. (2004). Oxygen dependent and tissue-specific regulation of erythropoietin gene expression. *American Journal of Physiology: Regulatory, Integrative and Comparative Physiology*, 286, R977-988.

Fay, I. (2006). Text, space and the evidence of human remains in English Late Medieval and Tudor disease culture: Some problems and possibilities. In R. Gowland and C.J. Knüsel (Eds.), *Social Archaeology of Funerary Remains* (pp. 190-208). Oxford: Alden Press.

Feingold, B.F. (1933). Roentgenologic skull changes in the anemias of childhood. Report of a case: a few notes on similar findings among the skulls of Peruvian Indians. *American Journal of Roentgenology*, 29, 194-202.

Feldkamp, L.A., Goldstein, S.A., Parfitt, A.M. et al. (1989). The direct examination of bone architecture in vitro by computed tomography. *Bone*, 4, 3-11.

Feng, X., and McDonald, J. M. (2011). Disorders of bone remodeling. *Annual Review of Pathology*, 6, 121.

Ferrante, L., and Cameriere, R. (2009). Statistical methods to assess the reliability of measurements in the procedures for forensic age estimation. *International Journal of Legal Medicine*, 123(4), 277-283.

Fildes, V. (1995). The culture and biology of breastfeeding: an historical review of Western Europe. *Breastfeeding: Biocultural Perspectives*, 101-126.

Frost, H.M., and Wu, K. (1967). Histological measurement of bone formation rates in unlabelled contemporary, archeological and paleontological compact bone. In Wade, W.D. (Ed.), *Miscellaneous Papers in Paleopathology* (pp. 9-22), Flagstaff: Museum of Northern Arizona.

Gabet, Y. and Bab, I. (2011). Microarchitectural changes in the aging skeleton. *Current Osteoporosis Reports*, 9(4), 177-183.

Galea, J.C. (2013). *Analysing the microarchitecture of cribra orbitalia via micro-computed tomography in post-medieval remains from the Bristol Royal Infirmary.* MPhil Thesis, University of Bristol, England.

Gardner, J.C., Garvin, G., Nelson, A.J., Vascotto, G., Conlogue, G. (2004). Paleoradiology in mummy studies: the Sulman mummy project. *Canadian Association of Radiologists Journal*, 55(4), 228.

Garnsey, P. (1999). *Food and Society in Classical Antiquity*. Cambridge: Cambridge University Press.

Gartner, L.P. and Hiatt, J.L. (2007). *Color Textbook of Histology*. Philadelphia: Saunders Elsevier.

Gedgaudas-McClees, R. K., and Torres, W. E. (1990). *Essentials of Body Computed Tomography*. Philadelphia: WB Saunders.

Genant, H.K., Wilson, J.S., Bovill, E.G., Brunelle, F.O., Murray, W.R., Rodrigo, J.J. (1980). Computed tomography of the musculoskeletal system. *Journal of Bone and Joint Surgery*, 62A, 1088-1101.

Gerszten, P.C. (1993). An investigation into the practice of cranial deformation among the Pre-Columbian peoples of northern Chile. *International Journal of Osteoarchaeology*, 3(2), 87-98.

Goldman, L.W. (2007). Principles of CT: radiation dose and image quality. *Journal of Nuclear Medicine Technology*, 35(4), 213-225.

Goldstein, S.A., Goulet, R., McCubbrey, D. (1993). Measurement and significance of three-dimensional architecture to the mechanical integrity of trabecular bone. *Calcified Tissue International*, 53(1), S127-S133.

Goodman, A.H. and Armelagos, G.J. (1989). Infant and childhood morbidity and mortality risks in archaeological populations. *World Archaeology*, 21(2), 225-243.

Gordis L. 2000. *Epidemiology* (2nd edition). Philadelphia: WB Saunders.

Gordon, C. C., and Buikstra, J. E. (1981). Soil pH, bone preservation, and sampling bias at mortuary sites. *American Antiquity*, 566-571.

Goulet, R.W., Goldstein, S.A., Ciarelli, M J., Kuhn, J.L., Brown, M.B.,Feldkamp, L.A. (1994). The relationship between the structural and orthogonal compressive properties of trabecular bone. *Journal of Biomechanics*, 27(4), 375-389.

Graham, E. (2000). Collapse, conquest and Maya survival at Lamanai, Belize. *Archaeology International*, 4, 52-56.

Grauer, A.L. (2008). Macroscopic analysis and data collection in paleopathology. In S. Mays and R. Pinhasi (Eds.), *Advances in Human Palaeopathology* (pp. 57-76). West Sussex: John Wiley and Sons Ltd.

(2012) Introduction: The scope of paleopathology. In. Grauer A.L. (Ed.), *A Companion to Paleopathology* (pp.1-14). West Sussex: Blackwell Publishing Ltd.

Grauer, A. L., and Stuart-Macadam, P. (1998) *Sex and Gender in Paleopathological Perspective.* Cambridge: Cambridge University Press.

Greenfield, G.B., (1986). *Radiology of Bone Diseases, fourth edition*. Philadelphia: JB Lippincott.

Griffin, N. (2008). Bone architecture of the hominin second proximal pedal phalanx: a preliminary investigation. *Journal of Human Evolution*, 54, 162–168.

Guidotti A. (1984). Frequencies of cribra orbitalia in central Italy (19th century) under special consideration of their degrees of expression. *Anthropologische Anzeiger,* 42, 11–16.

Haas, C.J., Zink, A., Pálfi, G., Szeimies, U., Nerlich, A.G. (2000). Detection of leprosy in ancient human skeletal remains by molecular identification of Mycobacterium leprae. *American Journal of Clinical Pathology*, 114(3), 428-436.

Hackett, C. J. (1976). *Diagnostic Criteria of Syphilis, Yaws and Treponarid (treponematoses) and of some other Diseases in Dry Bones (for use in osteo-archaeology).* Berlin: Springer-Verlag

Hadjidakis, D.J., and Androulakis, I.I. (2006). Bone remodeling. *Annals of the New York Academy of Sciences*, 1092(1), 385-396.

Haduch, E., Szczepanek, A., Skrzat, J., Środek, R. and Brzegowy (2009). Residual rickets or osteomalacia: A case dating from the 16th – 18th centuries from Krosno Odrzańskie, Poland. *International Journal of Osteoarchaeology*, 19, 593-612

Halvorsen, S. and Bechensteen, A.G. (2002). Physiology of erythropoietin during mammalian development. *Acta Paedeatrica Supplement*, 91,17-26

Harper, K.N., Zuckerman, M.K., Harper, M.L., Kingston, J.D. Armelagos, G.J. (2011). The origin and antiquity of syphilis revisited: An Appraisal of Old World pre-Columbian evidence for treponemal infection. *American Journal of Physical Anthropology*, 146(S53), 99-133.

Harwood-Nash, D.C. (1979). Computed tomography of ancient Egyptian mummies. *Journal of Computer Assisted Tomography,* 3(6), 768-773.

Hatipoglu, H. G., Ozcan, H. N., Hatipoglu, U. S., Yuksel, E. (2008). Age, sex and body mass index in relation to calvarial diploe thickness and craniometric data on MRI. *Forensic Science International*, 182(1), 46-51.

Heaney, R P. (2002). Ethnicity, bone status, and the calcium requirement. *Nutrition Research*, 22(1), 153-178.

Heathcote, G.M. (1980). Exploratory craniometry on western Arctic skeletal groups. MS. No. 1703, in files of the *Archaeological Survey of Canada*, Bells Corners, Ontario.

Henneberg, M. and Henneberg, R.J. (1998) Biological characteristics of the population based on analysis of skeletal remains. In Carter, J.C., Morter, J. and Toxey, A.P. (Eds.) *The Chora of Metaponto: The Necropolis*, Vol. 2 (pp. 503-562). Austin: University of Texas Press.

Hershkovitz, I., Ring, B., Speirs, M., Galili, E., Kislev, M., Edelson, G., Hershkovitz, A. (1991). Possible congenital hemolytic anemia in prehistoric coastal inhabitants of Israel. *American Journal of Physical Anthropology*, 85(1), 7-13.

Hildebrand, T., Müller, R., Laib, A., Dequeker, J., Rüegsegger, P. (1999). Direct three-dimensional morphometric analysis of human cancellous bone: microstructural data from spine, femur, iliac crest, and calcaneus. *Journal of Bone Mineral Research*, 14, 1167-1174.

Holdsworth, D.W. and Thornton, M.W. (2002). Micro-CT in small animal and specimen imaging. *Trends in Biotechnology*, 20: s1-s6.

Holick, M.F. (2006). Resurrection of vitamin D deficiency and rickets. *The Journal of Clinical Investigation*, 116(8), 2062-2072.

Holland, T.D. and O'Brien, M.J. (1997). Parasites, porotic hyperostosis, and the implications of changing perspectives. *American Antiquity*, 62(2), 183-193.

Holt, S. (2009). *Individuals and Variation: Stable Isotope Analysis of Weaning Using Dental Serial Sections*. MA Thesis, Department of Anthropology. McMaster University.

Hooton, E.A. (1930). *The Indians of Pecos Pueblo: A Study of their Skeletal Remains.* New Haven: Yale University Press.

Hooton, E.A. (1940). Skeletons from the cenote of sacrifice at Chichen Itzá. In C.L. Hay (Ed.), *The Maya and their Neighbors*, (pp. 272-280). New York: Appleton-Century.

Hoppa, R.D. (2002). Paleodemography: Looking back and thinking ahead. In Hoppa, R.D. and Vaupel, J.W. (Eds.), *Paleodemography: Age Distributions from Skeletal Samples.* (pp. 9-23) Cambridge: Cambridge University Press.

Hounsfield, G. N. (1973). Computerized transverse axial scanning (tomography): Part I. Description of system. In Adrian, M.K., Thomas, A.K., Banerjee, Busch, U. (Eds.), *Classic papers in Modern Diagnostic Radiology* (pp. 1016-1022). New York: Springer.

Hrdlička, A. (1941). Lower jaw: double condyles. *American Journal of Physical Anthropology*, 28(1), 75-89.

Hui-Fang, N. (2006). Automatic threshold for defect detection. *Pattern Recognition Letters*. In Press. doi:10.1016/j.patrec.2006.03.009

Inman, V.T. and Saunders, J.B. (1937). The ossification of the human frontal bone: with special reference to its presumed pre-and post-frontal elements. *Journal of Anatomy*, 71(Pt 3), 383.

Jaffe, H.L. (1972). *Metabolic, Degenerative, and Inflammatory Diseases of Bones and Joints*. Philadelphia: Lea and Febiger.

Jamison, P.L. and Zegura, S.L. (1974). A univariate and multivariate examination of measurement error in anthropometry. *American Journal of Physical Anthropology*, 40, 197-204.

Jarcho, S. (1966). The development and present condition of paleopathology in the United States. In Jarcho, S. (Ed.), *Human Paleopathology* (pp. 3-30). New Haven: Yale University Press.

Jiang, Y., Zhao, J., White, D.L., Genant, H.K. (2000). Micro CT and micro-MR imaging of 3D architecture of animal skeleton. *Journal of Musculoskeletal and Neuronal Interactions*, 1, 45-51.

Katzenberg, M. A., Herring, D., Saunders, S. R. (1996). Weaning and infant mortality: evaluating the skeletal evidence. *American Journal of Physical Anthropology*, 101(S23), 177-199.

Katzenberg, M.A. (2000). Stable isotope analysis: A tool for studying past diet, demography, and life history. In M.A. Katzenberg and S.R. Saunders (Eds.), *Biological Anthropology of the Human Skeleton* (pp. 305-327). New York: Wiley-Liss.

Keenleyside, A. (2010). A Bioarchaeological Study of the Kalfata Necropolis. In: Apollonia Du Pont (Sozopol). La nécropole de Kalfata (Ve-IIIe s. av. J.-C.). *Fouilles franco-bulgares (2002-2004),* edited by A. Hermary. Bibliothèque d'Archéologie Méditerranéenne et Africaine – 5. Editions Errance, Centre Camille Jullian, Aix-en-Provence, pp. 83-135.pp. 267-282.

Keenleyside, A. and Lazenby, R. (2011). *A Human Voyage: Exploring Biological Anthropology*. Toronto: Nelson Education.

Keenleyside, A. and Panayotova, K. (2006). Cribra orbitalia and porotic hyperostosis in a Greek Colonial population (5th to 3rd Centuries BC) from the Black Sea. *International Journal of Osteoarchaeology*, 16, 373-384.

Keenleyside, A., Schwarcz, H., Panayotova, K. (2006). Stable isotopic evidence of diet in a Greek colonial population from the Black Sea. *Journal of Archaeological Science*, 33(9), 1205-1215.

Kempe, D. S., Lang, P. A., Duranton, C., Akel, A., Lang, K. S., Huber, S. M., ... Lang, F. (2006). Enhanced programmed cell death of iron-deficient erythrocytes. *The FASEB Journal*, 20(2), 368-370.

Kent, S. (1986). The influence of sedentism and aggregation on porotic hyperostosis and anaemia: A case study. *Man*, 21, 605-636.

Kerley ER, Bass WM. 1967. Paleopathology: meeting ground for many disciplines. *Science* 157: 638-644.

Ketcham, R.A. and Carlson, W.D., 2001. Acquisition, optimization and interpretation of X-ray computed tomographic imagery: Applications to the geosciences. *Computers and Geosciences*, 27, 381-400

Kindblom, L.G., Walaas, L., Widehn, S. (1986). Ultrastructural studies in the preoperative cytologic diagnosis of soft tissue tumors. *Seminars in Diagnostic Pathology*, (3)4:, 317-344.

Kinney, J.H., Lane, N.E., Haupt, D.L. (1995). In vivo, three-dimensional microscopy of trabecular bone. *Journal of Bone and Mineral Research*, 10(2), 264-270.

Kivell, T.L., Skinner, M.M., Lazenby, R., Hublin, J.J. (2011). Methodological considerations for analyzing trabecular architecture: an example from the primate hand. *Journal of Anatomy*, 218, 209-225.

Klaus, H. (2013). Sub-adult scurvy in Andean South America: Evidence of vitamin C deficiency in the late Pre-Hispanic and colonial Lambayeque Valley, Peru. *International Journal of Paleopathology.* In Press. (http://dx.doi.org/10.1016/j.ijpp.2013.09.002)

Kolman, C. J., Centurion-Lara, A., Lukehart, S. A., Owsley, D. W., Tuross, N. (1999). Identification of Treponema pallidum subspecies pallidum in a 200-year-old skeletal specimen. *Journal of Infectious Diseases*, 180(6), 2060-2063.

Koury, M. J., Price, J. O., & Hicks, G. G. (2000). Apoptosis in megaloblastic anemia occurs during DNA synthesis by a p53-independent, nucleoside-reversible mechanism. *Blood*, 96(9), 3249-3255.

Kuhn, G., Schultz, M., Müller, R., Rühli, F.J. (2007). Diagnostic value of micro-CT in comparison with histology in the qualitative assessment of historical human postcranial bone pathologies. *Journal of Comparative Human Biology*, 58, 97-115.

Kurth, A.A., and Müller, R. (2001). The effect of an osteolytic tumor on the three-dimensional trabecular bone morphology in an animal model. *Skeletal Radiology*, 30(2), 94-98.

Laib, A., Barou, I.O., Vico, L., Lafage-Proust, M.H., Alexandre, C., Rüegsegger, P. (2000). 3D micro-computed tomography of trabecular and cortical bone architecture with application to a rat model of immobilisation osteoporosis. *Medical and Biological Engineering and Computing*, 38, 326-332.

Lambert, J.B., Vlasak, S.M., Thometz, A.C., and Buikstra, J.E. (1982). A comparative study of the chemical analysis of ribs and femurs in Woodland populations. *American Journal of Physical Anthropology*, 59(3), 289-294.

Lanzkowsky P. (1968). Radiological features of iron-deficiency anemia. *American Journal of Diseases of Children* 116:16–29.

Lagia, A., Eliopoulos, C., Manolis, S. (2007). Thalassemia: macroscopic and radiological study of a case. *International Journal of Osteoarchaeology*, *17*(3), 269-285.

Lallo, J.W., Armelagos, G.J., Mensforth, R.P. (1977). The role of diet, disease, and physiology in the origin of porotic hyperostosis. *Human Biology*, 49(3), 471-483.

Larsen, C.S. (1995). Biological changes in human populations with agriculture. *Annual Review of Anthropology*, 24, 185-213.

(1997). *Bioarchaeology: Interpreting Behaviour from the Human Skeleton*. Cambridge: Cambridge University Press.

Larsson, E., Brun, F., Tromba, G., Cataldi, P., Uvdal, K., Accardo, A. (2011). Quantification of Structural Differences in the Human Calvarium Diploe by Means of X-ray Computed Microtomography Image Analysis: A Case Study. In *5th European Conference of the International Federation for Medical and Biological Engineering* (pp. 599-602). Springer Berlin Heidelberg.

Larsson, E, Brun, F., Tromba, G., Cataldi, P., Uvdal, K., and Accardo, A. (2014). Morphological Characterization of the Human Calvarium in Relation to the Diploic and Cranial Thickness Utilizing X-Ray Computed Microtomography. *XIII Mediterranean Conference on Medical and Biological Engineering and Computing 2013,* IFMBE Proceedings Volume 41, 2014, pp 194-197

Lazenby, R.A., Skinner, M.M., Kivell, T.L., Hublin, J.J. (2011). Scaling VOI size in 3D µCT studies of trabecular bone: a test of the over-sampling hypothesis. *American Journal of Physical Anthropology*, 144, 196-203.

Lemann Jr, J., and Favus, M.J. (1999). The intestinal absorption of calcium, magnesium, and phosphate. In Favus MJ (ed), *Primer on the Metabolic Bone Diseases and Disorders of Mineral Metabolism* (pp. 63-67). Philadelphia, Lippincott, Williams and Wilkins,

LeVeau, B.F. and Bernhardt, D.B. (1984). Developmental biomechanics effect of forces on the growth, development, and maintenance of the human body. *Physical Therapy*, 64(12), 1874-1882.

Lewin, P.K. and Harwood-Nash, D.C.F. (1977). Computerized axial tomography in medical archeology, *Paleopathology Newsletter* 17, 8-9.

Lewin, P. K., Trogadis, J. E., Stevens, J. K. (1990). Three-dimensional reconstructions from serial X-ray tomography of an Egyptian mummified head. *Clinical Anatomy*, 3(3), 215-218.

Lilienfeld, D.E. and Stolley, P.D. 1994. *Foundations of Epidemiology*, *third edition*. Oxford University Press: New York.

Livingstone, F. B. (1958). Anthropological Implications of Sickle Cell Gene Distribution in West Africa 1. *American Anthropologist*, 60(3), 533-562.

Lynnerup, N. (2008). Computed tomography scanning and three-dimesional visualization of mummies and bog bodies. In S. Mays and R. Pinhasi (Eds.), *Advances in Human Palaeopathology* (pp. 101-120). West Sussex: John Wiley and Sons Ltd.

Loevner, L.A., Tobey, J.D., Yousem, D.M., Sonners, A.I., Hsu, W.C. (2002). MR Imaging characteristics of cranial bone marrow in adult patients with underlying systemic disorders compared with healthy control subjects. *American Journal of Neuroradiology*, 23, 248-254.

Lovell, N. (2000). Paleopathological description and diagnosis. In M.A. Katzenberg and S.R. Saunders (Eds.), *Biological Anthropology of the Human Skeleton* (pp. 217-248). New York: Wiley-Liss.

Maat, G.J., Van Den Bos, R.P., Aarents, M.J. (2001). Manual preparation of ground sections for the microscopy of natural bone tissue: update and modification of Frost's 'rapid manual method'. *International Journal of Osteoarchaeology*, 11(5), 366-374.

Maga, M., Kappelman, J., Ryan, T., Ketcham, R. (2006). Preliminary observations on the calcaneal trabecular microarchitecture of extant large-bodied hominoids. *American Journal of Physical Anthropology*, 129, 410–417.

Marks, M.K. and Hamilton, M.D. (2007). Metastatic carcinoma: palaeopathology and differential diagnosis. *International Journal of Osteoarchaeology*, *17*(3), 217-234.

Martin, D.L., and Armelagos, G.J. (1985). Skeletal remodeling and mineralization as indicators of health: an example from prehistoric Sudanese Nubia. *Journal of Human Evolution*, 14(5), 527-537.

Maxwell, J. (2003). *Evaluating Morbidity and Mortality in Skeletal Remains: An Analysis of Paleopathology at the Maya Sites of Marco Gonzalez and San Pedro, Belize,* MSc Thesis, Department of Anthropology. Western University.

Mays, S. (1995). The relationship between Harris lines and other aspects of skeletal development in adults and juveniles. *Journal of Archaeological Science*, 22(4), 511-520.

(2006). The osteology of monasticism in Medieval England. In R. Gowland and C.J. Knüsel (Eds.), *Social Archaeology of Funerary Remains* (pp. 179-189). Oxford: Alden Press.

(2008a). Radiography and allied techniques in the palaeopathology of skeletal remains. In S. Mays and R. Pinhasi (Eds.), *Advances in Human Palaeopathology* (pp. 77-100). West Sussex, England: John Wiley and Sons Ltd.

(2008b). Metabolic bone disease. In S. Mays and R. Pinhasi (Eds.), *Advances in Human Palaeopathology* (pp. 215-252). West Sussex: John Wiley and Sons Ltd.

(2012). The relationship between paleopathology and the clinical sciences. In. Grauer A.L. (Ed.), *A Companion to Paleopathology* (pp. 286-309). West Sussex: Blackwell Publishing Ltd.

Mays, S., Brickley, M., Ives, R. (2006). Skeletal manifestations of rickets in infants and young children in a historic population from England. *American Journal of Physical Anthropology*, 129(3), 362-374.

Mays, S., Crane-Kramer, G., Bayliss, A. (2003). Two probable cases of treponemal disease of Medieval date from England. *American Journal of Physical Anthropology*, 120(2), 133-143.

McCarthy, E.F. and Frassica, F.J. (1998). *Pathology of Bone and Joint Disorders with Clinical and Radiographic Correlation*. Philadelphia: W.B. Saunders Company.

McErlain, D.D., Chemm, R.K., Bohay, R.N., Holdsworth D.W. (2004). Micro-computed tomography of a 500-year-old tooth: technical note. *Canadian Association of Radiologists Journal*, 55: 242-245.

McGeorge, P.J.P. (1988). Health and diet in Minoan times. In Jones, R.E. and Catling, H.W. (Eds). *New Aspects of Archaeological Science in Greece* (pp. 47–54). British School at Athens Occasional Paper No.3 of the Fitch Laboratory.

Melcher, A.H., Holowka, S., Pharoah, M., Lewin, P.K. (1997). Non-invasive computed tomography and three-dimensional reconstruction of the dentition of a 2,800-year-old Egyptian mummy exhibiting extensive disease. *American Journal of Physical Anthropology*, 103: 329-340.

Melikian, M. (2006). A case of metastatic carcinoma from 18th century London. *International Journal of Osteoarchaeology*, 16(2), 138-144.

Mendonça de Souza, S.M., Reinhard, K. J., Lessa, A. (2008). Deformación craneana como causa de muerte de un niño del Valle de Chillón, Perú. *Chungará (Arica)*, 40(1), 41-53.

Mensforth, R.P., Lovejoy, C.O., Lallo, J.W. and Armelagos, G.J. (1978). The role of constitutional factors, diet, and infectious disease in the etiology of porotic hyperostosis and periosteal reactions in prehistoric infants and children. *Medical Anthropology* 2(1), 1-57.

Merrill, R.M. and Timmreck, T.C. (2006). *Introduction to Epidemiology, fourth edition.* Sudbury, MA: Jones and Bartlett Publishers

Middlemiss, H. (1961). *Tropical Radiology.* London: William Heinmann Medical Books.

Miller, E., Ragsdale, B.D., Ortner, D.J. (1996). Accuracy in dry bone diagnosis: A comment on palaeopathological methods. *International Journal of Osteoarchaeology*, 6, 221-229.

Mittler, D.M. and Van Gerven, D.P. (1994). Developmental, diachronic, and demographic analysis of cribra orbitalia in the Medieval Christian populations of Kulubnarti. *American Journal of Physical Anthropology*, 93, 287-297

Mittra, E., Rubin, C., Gruber, B., Qin, Y. (2007). Evaluation of trabecular mechanical and microstructural properties in human calcaneal bone of advanced age using mechanical testing, mCT, and DXA. *Journal of Biomechanics*. In Press.

Moon Jr, K.L., Genant, H.K., Helms, C.A., Chafetz, N.I., Crooks, L.E., Kaufman, L. (1983). Musculoskeletal applications of nuclear magnetic resonance. *Radiology*, 147(1), 161-171.

Moore, S. (1929). The bone changes in sickle cell anemia with note on similar changes observed in skulls of ancient Mayan Indians. *J. Missouri MA*, 26, 561.

Morris-Kay, G.M., and Wikkie, A.M. (2005). Growth of the normal skull vault and its alteration in craniosynostosis: Insights from human genetics and experimental studies. *Journal of Anatomy*, 207(5):637-653.

Moseley, J.E. (1974). Skeletal changes in the anemias. *Seminars in Roentgenology*, 9(3), 169-184.

Müller R. (2003). Bone microarchitecture assessment – current and future trends. *Osteoporosis International*, 14, 89–99.

Müller, R., Koller, B., Hildebrand, T., Laib, A., Gianolini, S., and Rüegsegger, P. (1996). Resolution dependency of microstructural properties of cancellous bone based on three-dimensional mu-tomography. *Technology and Health Care: Official Journal of the European Society for Engineering and Medicine*, 4(1), 113-119.

Müller, R., Van Campenhout, H., Van Damme, B., Van der Perre, G., Dequeker, J., Hildebrand, T., Rüegsegger, P. (1998). Morphometric analysis of human bone biopsies: a quantitative structural comparison of histological sections and micro-computed tomography. *Bone*, 23(1), 59-66.

Musgrave, J.H. (1980). The human remains from the cemeteries. In Popham, M.R., Sackett, L.H., Themelis, P.G. (Eds.), *Lefkandi I , The Iron Age. The Cemeteries*. (pp. 429–446). London: Thames and Hudson.

Nägele, E., Kuhn, V., Vogt, H., Link, T.M., Müller, R., Lochmüller, E.M., Eckstein, F. (2004). Technical considerations for microstructural analysis of human trabecular bone from specimens excised from various skeletal sites. *Calcified Tissue International*, 75(1), 15-22.

Nathan, H. and Haas, N. (1966). "Cribra Orbitalia" A bone condition of the orbit of unknown nature. *Israel Journal of Medical Science* 2, 171-191.

Nather, A., Ong, H.J.C., Aziz, Z. (2005). *Structure of Bone*. World Scientific Publishing Co. Pte. Ltd.

Nicholson, R.A. (2001). Taphonomic investigations. In Pollard, M.A. and Brothwell, D (Eds.), *Handbook of Archaeological Science* (pp. 179-190). Chichester: Wiley.

Norr, L. (1984). Prehistoric subsistence and health status of coastal peoples from the Panamanian Isthmus of lower Central America. In M.N. Cohen and G.J. Armelagos (Eds.), *Paleopathology at the Origins of Agriculture* (pp. 463-485). Orlando: Academic Press Inc.

Odgaard, A., Andersen, K., Ullerup, R., Frich, L. H., Melsen, F. (1994). Three-dimensional reconstruction of entire vertebral bodies. *Bone*, 15(3), 335-342.

Ortner, D.J. (1991). Theoretical and methodological issues in paleopathology. In D.J. Ortner and A.C. Aufderheide (Eds.), *Human Paleopathology: Current Syntheses and Future Options* (pp. 5-12). Washington: Smithsonian Insitution.

(1992). Skeletal paleopathology: probabilities, possibilities and impossibilities. In J.W. Verano and D.H. Ubelaker (Eds.), *Disease and Demography in the Americas* (pp. 5-15). Washington: Smithsonian Insititution.

(1994). Descriptive methodology in paleopathology. In D.W. Owsley and R.J. Jantz (Eds.), *Skeletal Biology in the Great Plains* (pp. 73-80). Washington: Smithsonian Institution.

(2003). *Identification of Pathological Conditions in Human Skeletal Remains* (pp. 37-44). London: Academic Press.

(2007). Forward. In R. Chhem, R. and Brothwell (Eds.), *Paleoradiology: Imaging Mummies and Fossils* (pp. I-X). New York: Springer.

(2012). Differential diagnosis and issues in disease classification. In. Grauer A.L. (Ed.), *A Companion to Paleopathology* (pp. 250-267). West Sussex: Blackwell Publishing Ltd.

Ortner, D.J. and Aufderheide, A.C. (1991). *Human Paleopathology*. Washington, DC: Smithsonian Inst. Press.

Ortner, D.J., Butler, W., Cafarella, J. and Milligan, L. (2001). Evidence of probable scurvy in subadults from archeological sites in North America. *American Journal of Physical Anthropology*, 114, 343-351.

Ortner, D.J. and Eriksen, M.F. (1997). Bone changes in the human skull probably resulting from scurvy in infancy and childhood. *International Journal of Osteoarchaeology*, 7, 212-220.

Ortner, D.J., Kimmerle, E.H. and Diez, M. (1999). Probable evidence of scurvy in subadults from archeological sites in Peru. *American Journal of Physical Anthropology*, 108, 321-331.

Ortner, D.J. and Putschar, W.G. J. (1981). *Identification of Pathological Conditions in Human Skeletal Remains.* Washington DC: Smithsonian Institution Press.

Otsu, N. (1979). A threshold selection method from gray-level histograms. *IEEE Transactions on Systems, Man, and Cybernetics*, 9(1): 62-66.

Palkovich, A.M. (1987). Endemic disease patterns in palaeopathology: Porotic hyperostosis. *American Journal of Physical Anthropology*, 74, 527-537.

Parker-Pearson, M. (1999). *The Archaeology of Death and Burial.* Stroud: Sutton.

Papathanasiou, A. (2005). Health status of the Neolithic population of Alepotrypa Cave, Greece. *American Journal of Physical Anthropology*, 126, 377-390.

Papathanasiou, A., Spencer Larsen, C., Norr, L. (2000). Bioarchaeological inferences from a Neolithic ossuary from Alepotrypa cave, Diros, Greece. *International Journal of Osteoarchaeology*, 10(3), 210-228.

Parfitt, A.M. (2003). Misconceptions (3): calcium leaves bone only by resorption and enters only by formation. *Bone*, 33(3), 259-263.

Parfitt, A.M., Mathews, C.H., Villanueva, A.R., Kleerekoper, M., Frame, B., Rao, D.S. (1983). Relationships between surface, volume, and thickness of iliac trabecular bone in aging and in osteoporosis. Implications for the microanatomic and cellular mechanisms of bone loss. *Journal of Clinical Investigation*, 72(4), 1396.

Particelli, F., Mecozzi, L., Beraudi, A., Montesi, M., Baruffaldi, F., Viceconti, M. (2012). A comparison between micro-CT and histology for the evaluation of cortical bone: effect of polymethylmethacrylate embedding on structural parameters. *Journal of Microscopy*, 245(3), 302-310.

Passmore R, Eastwood MA. 1986. *Davidson and Passmore's Human Nutrition and Dietetics.* Edinburgh: Churchill Livingstone.

Pearce N. 2005. *A Short Introduction to Epidemiology* (2nd edition). Occasional Report Series No. 2, Centre for Public Health Research. Massey University: Wellington.

Peyrin, F., Salome, M., Nuzzo, S., Cloetens, P., Laval-Jeantet, A.M., Baruchel, J. (2000). Perspectives in three-dimensional analysis of bone samples using synchrotron radiation microtomography. *Cellular and Molecular Biology (Noisy-le-Grand, France)*, 46(6), 1089-1102.

Pinhasi, R. and Bourbou, C. (2008). How representative are human skeletal assemblages for population analysis? In S. Mays and R. Pinhasi (Eds.), *Advances in Human Palaeopathology* (pp. 31-44). West Sussex: John Wiley and Sons Ltd.

Pinhasi, R. and Turner, K. (2008). Epidemiological approaches in paleopathology. In S. Mays and R. Pinhasi (Eds.), *Advances in Human Palaeopathology* (pp. 45-56). West Sussex: John Wiley and Sons Ltd.

Ponec, D.J., and Resnick, D. (1984). On the etiology and pathogenesis of porotic hyperostosis of the skull. *Investigative Radiology*, 19(4), 313-317.

Ragsdale, B.D. and Lehmer, L.M. (2012). A knowledge of bone at the cellular (histological) level is essential to paleopathology. In. Grauer A.L. (Ed.), *A Companion to Paleopathology* (pp. 227-249). West Sussex: Blackwell Publishing Ltd.

Recker, R. R., Weinstein, R. S., Chesnut III, C. H., Schimmer, R. C., Mahoney, P., Hughes, C., ... Meunier, P. J. (2004). Histomorphometric evaluation of daily and intermittent oral ibandronate in women with postmenopausal osteoporosis: results from the BONE study. *Osteoporosis International*, 15(3), 231-237.

Recheis, W., Weber, G.W., Schafer, K., Knapp, R., Seidler, H., zur Nedden, D. (1999). Virtual reality and anthropology. *European Journal of Radiology*, 31:88–96.

Reimann, F., Talasli, U., Gökmen, E. (1976). [Radiological determination of skull thickness and skull thickness increase in patients with severe blood dyscrasias and hyperplasia of the red marrow (author's transl)]. *RoFo: Fortschritte auf dem Gebiete der Rontgenstrahlen und der Nuklearmedizin*, 125(6), 540-545.

Reinhard, K. (1990). Archeoparasitology in North America. *American Journal of Physical Anthropology*, 82, 145-163.

Resnick, D. (1995). Hemoglobinopathies and other anemias. In D. Resnick (Ed.), *Diagnosis of Bone and Joint Disorders (3rd ed)* (pp. 2107-2146). London: W.B. Saunders.

Resnick, D. and Niwayama, G. (1995). Osteomyelitis, septic arthritis, and soft tissue infection: mechanisms and situations. In D. Resnick (Ed.), *Diagnosis of Bone and Joint Disorders (3rd ed)* (pp. 2325-2418). London: W.B. Saunders.

Resnick, D., and Pettersson, H. (1992). *Skeletal Radiology*. London: Merit Communications.

Ridley, D.S. and Jopling, W.H. (1966). Classification of leprosy according to immunity. A five group system. *International Journal of Leprosy*, 34, 255.

Riggs, B.L., Melton, L.J., Robb, R.A., Camp, J.J., Atkinson, E.J., McDaniel, L., Amin, S., Rouleau, P.A., Khosla, S. (2008). A population-based assessment of rates of bone loss at multiple skeletal sites: evidence for substantial trabecular bone loss in young adult women and men. *Journal of Bone Mineral Research*, 23, 205–214.

Ritman, E.L. (2004). Micro-computed tomography – Current status and developments. *Annual Review of Biomedical Engineering*, 6, 185-208.

Robb, R. A., & Morin, R. L. (1991). Principles and instrumentation for dynamic x-ray computed tomography. In Marcus, M.L., Schelbert, H.R., Skorton, D.J., Wolf, G.L. (Eds.)*, Cardiac imaging: A Companion to Braunwald's Heart Disease* (pp. 634-668). Philadelphia: WB Saunders Company.

Roberts, C. and Manchester, K. (2005). *The Archaeology of Disease* (3rd ed.). New York: Cornell University Press.

Roberts, C.A., Lewis, M.E., Manchester, K. (2002). *The Past and Present of Leprosy.* British Archaeological Reports International Series S1054. Oxford: Archaeopress.

Rosai, J. (2011). *Rosai and Ackerman's Surgical Pathology*. Edinburgh London: Mosby Co.

Ross, P. and Logan, W. (1969). Roentgen findings in extramedullary hematopoiesis. *American Journal of Roentgenology, Radium Therapy and Nuclear Medicine*, 106, 604-613.

Rothman, K.J. (2002). *Epidemiology: An Introduction*. New York: Oxford University Press.

Rüegsegger, P., Koller, B., Müller, R. (1996). A microtomographic system for the nondestructive evaluation of bone architecture. *Calcified Tissue International*, 58, 24–29.

Rühli, F.J., Hodler, J., Böni, T. (2002a). CT-guided biopsy: a new diagnostic method for paleopathological research: technical note. *American Journal of Physical Anthropology*. 117, 272-275.

Rühli, F.J., Kuhn, G., Evison, R., Müller, R., and Schultz, M. (2007). Diagnostic value of micro-CT in comparison with histology in the qualitative assessment of historical human skull bone pathologies. *American Journal of Physical Anthropology*, 133, 1099-1111.

Rühli, F.J., Lanz, C., Ulrich-Bochsler, S., Alt, K.W. (2002b). State-of-the-art imaging in palaeopathology: the value of multi-slice computed tomography in visualizing doubtful cranial lesions. *International Journal of Osteoarchaeology*, 12, 372-379.

Russell, D.J. (2010). *Human Cranial Growth and Shape Change: Are Fetal Rates and Morphologies Extended throughout the First Year of Life?* MA Thesis, Department of Anthropology. Georgia State University.

Russell, R.G., Graveley, R., Skjodt, H. (1993). The effects of cyclosporin A on bone and cartilage. *British Journal of Rheumatology*, 32, 42-46.

Ryan, T.M. and Ketcham, R. (2005). Angular orientation of trabecular bone in the femoral head and its relationship to hip joint loads in leaping primates. *Journal of Morphology*, 265, 249–263.

Saab, G., Chhem, R., Bohay, R. N. (2008). Paleoradiologic techniques. In Chhem, R. and Brothwell, D.R. (Eds.). *Paleoradiology: Imaging Mummies and Fossils* (pp.15-54). New York: Springer.

Saiki, R. K., Chang, C. A., Levenson, C. H., Warren, T. C., Boehm, C. D., Kazazian Jr, H. H., Erlich, H. A. (1988). Diagnosis of sickle cell anemia and β-thalassemia with enzymatically amplified DNA and nonradioactive allele-specific oligonucleotide probes. *New England Journal of Medicine*, 319(9), 537-541.

Sakamoto, Y., and Takano, Y. (2002). Morphological influence of ascorbic acid deficiency on endochondral ossification in osteogenic disorder Shionogi rat. *The Anatomical Record*, 268(2), 93-104.

Salvadei, L., Ricci, F. and Manzi, G. (2001). Porotic hyperostosis as a marker of health and nutritional conditions during childhood: Studies at the transition between Imperial Rome and the early Middle Ages. *American Journal of Human Biology*, 13, 709-717.

Salvolini, L., Bichi Secchi, E., Costarelli, L., De Nicola, M. (2000). Clinical applications of 2D and 3D CT imaging of the airways—a review. *European Journal of Radiology*, 34(1), 9-25.

Sandison, A.T. (1967). Sir Marc Armand Ruffer (1859-1917) pioneer of palaeopathology. *Medical History*, 11(2), 150.

Sandison, A.T. and Tapp, E. (1998). Disease in ancient Egypt. In A. Cockburn, E. Cockburn and T.A. Reyman (Eds.), *Mummies, Disease and Ancient Cultures* (pp. 38-58). Cambridge: Cambridge University press.

Sankur, B. and Sezgin, M. (2004). Image thresholding techniques: A survey over categories. *Journal of Electronic Imaging*, 13(1): 1-35

Saul, F.P. (1972). *The Human Skeletal Remains of Altar de Sacrificios: An Osteobiographic Analysis.* Peabody Museum of Archaeology and Ethnology, Papers 63(2). Cambridge: Harvard University Press.

(1977). The paleopathology of anemia in Mexico and Guatemala. In Cockburn, E.(Ed.), *Porotic Hyperostosis : An Enquiry,* (pp. 10-15), Monograph No. 2, Paleopathology Association, Detroit, ML.

Saunders, S.R. (2000). Non-adult skeletons and growth related studies. In Katzenberg, M.A. and Saunders, S.R. (Eds.), *Biological Anthropology of the Human Skeleton* (pp. 135-161). New York: Wiley-Liss.

Scarfe, W. C. and Farman, A. G. (2008). What is cone-beam CT and how does it work?. *Dental Clinics of North America*, 52(4), 707-730.

Schaffer, J. R. (1889) Über den feinen bau fossilen knochen, *Akademie der Wissenschafen in Wien, Abteilung III*, 98,319–64.

Scherf, H. (2008). Locomotion-related femoral trabecular architecture in primates—high resolution computed tomographies and their implications for locomotor preferences in fossil primates. In: H. Endo and R. Frey (Eds.). *Anatomical Imaging Towards a New Morphology*. (pp. 39–60). Tokyo: Springer.

Scheuer, L., and Black, S. (2000). *Developmental Juvenile Osteology*. San Diego: Elsevier Academic Press.

Schultz, M. (1993). Initial stages of systemic bone disease. In Gruppe, G. and Garland, A.N. (Eds.), *Histology of Ancient Human Bone: Methods and Diagnosis* (pp.185-203). Berlin: Springer-Verlag.

(2001). Paleohistopathology of bone: A new approach to the study of ancient diseases. *Yearbook of Physical Anthropology* 44, 106-147.

(2012). Light microscopic analysis of macerated pathologically changed bones. In Crowder, C. and Stout, S. (Eds.), *Bone Histology: An Anthropological Perspective*. Boca Raton: CRC Press

Schwamm, H.A. and Millward, C.L. (1995). *Histological Differential Diagnosis of Skeletal Lesions*. New York: Igaku-Shoin.

Sebes, J.I., and Diggs, L.W. (1979). Radiographic changes of the skull in sickle cell anemia. *American Journal of Roentgenology*, 132(3), 373-377.

Seeram, E. (1994). *Computed Tomography: Physical Principles, Clinical Applications and Quality Control*. Philadelphia, W.B. Saunders Company.

Serjeant, G. R., Serjeant, B. E., & Milner, P. F. (1969). The irreversibly sickled cell; a determinant of haemolysis in sickle cell anaemia. *British Journal of Haematology*, 17(6), 527-533.

Shafik M, Selim, A, Eisheik E, Abdel Fattah, S., Amer H, Hawas Z, (2006). The first multidetector CT study of royal mummy: King Tutankhamen. Abstract, *Radiological Society of North America*, Nov 26-Dec1, 2006.

Sizer F, Whitney E 2000. *Nutrition: Concepts and Controversies*, eighth edition. Scarborough: Wadsworth.

Snoeks, T.J.A., Khmelinskii, A., Lelieveldt, B.P.F., Kaijzel, E.L., Löwik, C.W.G.M. (2011). Optical advances in skeletal imaging applied to bone metastases. *Bone*, 48(1), 106-114.

Spoor F, Jeffery N, Zonneveld F. 2000. Using diagnostic radiology in human evolutionary studies. *Journal of Anatomy*, 197:61–76.

Spoor, F., Stringer, C., Zonneveld, F. (1998). Rare temporal bone pathology of the Singa calvaria from Sudan. *American Journal of Physical Anthropology*, 107(1), 41-50.

Stark, R. and Garvie-Lok, S. (2011). Juvenile scurvy-a radiographic perspective. In *American Journal of Physical Anthropology*, 144, 283-283).

Stauber, M and Müller, R. (2008). Micro-computed tomography: A method for the non-destructive evaluation of the three dimensional structure of biological specimens. In J.J. Westendorf (Ed.), *Methods in Molecular Biology, Vol. 455, Osteoporosis: Methods and Protocols* (pp. 273-285). Totowa, N.J: Humana Press.

Steinbock, R.T. (1976). *Paleopathological Diagnosis and Interpretation*. Springfield, Illinois: Charles Thomas.

Stock, S.R. (2009). *Micro Computed Tomography: Methodology and Applications*. Boca Raton: CRC Press

Stodder, A.L.W. (2006). Skeletal biology: Southwest. In Sturtevant, W.C. (Ed.), *Handbook of North American Indians* (pp. 557-580). Washington: Smithsonian Institution.

Stout, S.D. (1978). Histological structure and its preservation in ancient bone. *Current Anthropology*, 601-604.

Stout, S. and Crowder, C. (2012). Bone remodeling, histomorphology, and histomorphometry. In Stout, S. and Crowder, C. (Eds.), *Bone Histology: An Anthropological Perspective.* Boca Raton: CRC Press.

Stout, S., and Simmons, D.J. (1979). Use of histology in ancient bone research. *Yearbook of Physical Anthropology*, 22, 228-249.

Stout, S.D., Brunsden, B.S., Hildebolt, C.F., Commean, P.K., Smith, K.E., Tappen, N.C. (1999). Computer-assisted 3D reconstruction of serial sections of cortical bone to determine the 3D structure of osteons. *Calcified Tissue International, 65,* 280–284

Stravopodi, E. (2004). The profile of 'porotic hyperostosis'in prehistoric societies in Greece: a re-evaluation of data, a shift in paradigms. *Poster presented at the 31st Annual Meeting of the Paleopathology Association,* April 13–14, Tampa, Florida.

Stuart-Macadam, P. (1985). Porotic hyperostosis: Representative of a childhood condition. *American Journal of Physical Anthropology*, 66, 391-398.

(1987a). A radiographic study of porotic hyperostosis. *American Journal of Physical Anthropology*, 74, 511-520.

(1987b). Porotic Hyperostosis: New evidence to support the Anemia Theory. *American Journal of Physical Anthropology*, 74, 521-526.

(1989). Porotic hyperostosis: relationship between orbital and vault lesions. *American Journal of Physical Anthropology*, 80, 187-193.

(1992). Anemia is past human populations. In P. Stuart-Macadam and S.K. Kent (Eds.), *Diet , Demography and Disease: Changing Perspectives on Anemia* (pp. 151-170). New York: Aldine De Gruyter

Sullivan, A. (2005). Prevalence and etiology of acquired anemia in Medieval York, England. *American Journal of Physical Anthropology*, 128, 252-272.

Tamada, T., Sone, T., Jo, Y., Imai, S., Kajihara, Y., Fukunaga, M. (2005). Three-dimensional trabecular bone architecture of the lumbar spine in bone metastasis from prostate cancer: comparison with degenerative sclerosis. *Skeletal Radiology*, 34(3), 149-155.

Tayles, N. (1996). Anemia, genetic diseases, and malaria in prehistoric mainland southeast Asia. *American Journal of Physical Anthropology*, 101, 11-27.

Turner-Walker, G. (2008). The chemical and microbial degradation of bones and teeth. In R. Pinhasi and S. Mays (Eds.), *Advances in Human Paleopathology* (pp. 3-30). West Sussex: John Wiley and Sons Ltd.

Turner-Walker, G and Mays, S. (2008). Histological studies on ancient bone. In R. Pinhasi and S. Mays (Eds.), *Advances in Human Paleopathology* (pp. 121-146). West Sussex: John Wiley and Sons Ltd.

Tykot, R.H., van der Merwe, N.J. and Hammond, N. (1996). Stable isotope analysis of bone collagen, bone apatite, and tooth enamel in the reconstruction of the human diet: A case study from Cuello, Belize. In M.V. Orna (Ed.), *Archaeological Chemistry: Organic, Inorganic, and Biochemical Analysis* (pp. 355-365). Washington, D.C.: American Chemical Society.

Ubelaker, D. (1982). The development of human paleopathology. In Spencer, F. (Ed.), *A History of American Physical Anthropology, 1930-1980,* volume 2 (pp.337-356). New York: Academic Press.

(1992). Porotic hyperostosis in prehistoric Ecuador. In P. Stuart-Macadam and S.K. Kent (Eds.), *Diet , Demography and Disease: Changing Perspectives on Anemia* (pp. 201-217). New York: Aldine De Gruyter.

Ulrich, D., Van Rietbergen, B., Laib, A., Ruegsegger, P. (1999). The ability of three-dimensional structural indices to reflect mechanical aspects of trabecular bone. *Bone*, 25(1), 55-60.

Van der Merwe, A.E., Steyn, M., Maat, G.J.R. (2010). Adult scurvy in skeletal remains of late 19th century mineworkers in Kimberley, South Africa. *International Journal of Osteoarchaeology*, 20(3), 307-316.

van Kaick, G. and Delorme, S. (2005). Computed tomography in various fields outside medicine. *European Radiology Supplements*, 15(4), d74-d81.

Vercellotti, G., Caramella, D., Formicola, V., Fornaciari, G., and Larsen, C. S. (2010). Porotic hyperostosis in a late upper Palaeolithic skeleton (Villabruna 1, Italy). *International Journal of Osteoarchaeology*, 20(3), 358-368.

Vigorita, V.J. (1999) In *Orthopaedic Pathology, Implant Pathology* (pp 621–639), Vigorita, V.J. and Ghelman, B. (Eds.). Philadelphia: Lippincott Williams and Wilkens.

Vogt, E. C., & Diamond, L. K. (1930). Congenital anemias, roentgenologically considered. *American Journal of Roentgenology*, 23(625), 293-310.

Von Hunnius, T. (2009). Using microscopy to improve a diagnosis: an isolated case of tuberculosis-induced hypertrophic osteopathy in archaeological dog remains. *International Journal of Osteoarchaeology*, 19(3), 397-405.

Wade, A.D., Holdsworth, D.W., and Garvin, G.J. (2009). CT and micro-CT analysis of a case of Paget's disease (*osteitis deformans*) in the Grant skeletal collection. *International Journal of Osteoarchaeology*, 21(2), 127-135.

Waldron, T. (1994). *Counting the Dead: The Epidemiology of Skeletal Populations*. New York: John Wiley and Sons.

(2007). *Palaeoepidemiology: The Measure of Disease in the Human Past*. California: Left Coast Press, Inc.

(2009). *Palaeopathology*. Cambridge: Cambridge University Press.

Walker, P.L. (1986). Porotic hyperostosis in a marine-dependent Californian Indian population. *American Journal of Physical Anthropology*, 69, 345-354.

Walker, P.L., Bathurst, R.R., Richmond, R., Gjerdrum, T. and Andrushko, V.A. (2009). The causes of porotic hyperostosis and cribra orbitalia: A re-appraisal of the iron-deficiency anemia hypothesis. *American Journal of Physical Anthropology*, 139, 109-125.

Wanek, J., Papageorgopoulou, C., Rühli, F. (2012). Fundamentals of paleoimaging techniques: Bridging the gap between physicists and paleopathologists. In. Grauer A.L. (Ed.), *A Companion to Paleopathology* (pp. 324-338). West Sussex: Blackwell Publishing Ltd.

Wapler, U., Crubézy, E. and Schultz, M. (2004). Is cribra orbitalia synonymous with anemia? Analysis and interpretation of cranial pathology in Sudan. *American Journal of Physical Anthropology*, 123, 333-339.

Weber, F. (1927). Cytoplasma-und kern-zustandsänderungen bei schließzellen. *Protoplasma*, 2(1), 305-311.

Weinstein, R. S., Simmons, D. J., and Lovejoy, C. O. (1981). Ancient bone disease in a Peruvian mummy revealed by quantitative skeletal histomorphometry. *American Journal of Physical Anthropology*, 54(3), 321-326.

Welcker, H. (1885). Die abstammung der bevolkerung von secotra. *Mittheilung im Geographentage zu Hamburg, Sitzung vom* 11. Berlin: Dietrich Reimer

Wells, C. (1963). The radiological examination of human remains. In Brothwell, D.R. and Higgs, E. (Eds.), *Science in Archaeology* (pp. 401-412), London: Thames and Hudson.

Whipple, G.H. and Bradford, W.L. 1932. Racial or familial anemia of children associated with fundamental disturbances of bone and pigment metabolism. *American Journal of Diseases of Children*, 44(2) 336-355.

White, C.D. (1988). The ancient Maya from Lamanai, Belize: Diet and health over 2,000 years. *Canadian Review of Physical Anthropology*, 6, 1-21.

White, C.D. (1997). Ancient diet at Lamanai and Pacbitun: Implications for the ecological model of collapse. In S.L. Whittington and D.M. Reed (Eds.), *Bones of the Maya: Studies of Ancient Skeletons* (pp. 171-180). Washington: Smithsonian Institution Press.

White, C., Maxwell, J., Dolphin, A., Williams, J., Longstaffe, F. (2006). Pathoecology and paleodiet in Postclassic/Historic Maya from northern coastal Belize. *Mem Inst Oswaldo Cruz,* Rio de Janeiro, 101(Suppl. II).

White, C.D., Wright, L.E., Pendergast, D.M. (1994). Biological disruption in the early Colonial period at Lamanai. In C.S. Larsen and G.R. Milner (Eds.), *In the Wake of Contact: Biological Responses to Conquest* (pp. 135-145). New York: Wiley-Liss.

Whitehouse, W.J. (1975). Scanning electron micrographs of cancellous bone from the human sternum. *Journal of Pathology*, 116, 213–224.

Whitehouse WJ, Dyson ED. 1974. Scanning electron microscope studies of trabecular bone in the proximal end of the human femur. *Journal of Anatomy*, 118,417–444.

Whittington, S.L. (1989). *Characteristics of Demography and Disease in Low Status Maya from Classic Period Copan, Honduras*. Doctoral dissertation, Pennsylvania State University.

Willey, G.R. and Shimkin, D.B. (1973). The Maya Collapse: A summary view. In Culbert,T.E (Ed.), *The Classic Maya Collapse,* (pp.457-502). Albuquerque: University of New Mexico Press

Williams, H.U. (1929). Human paleopathology with some observations on symmetrical osteoporosis of the skull. *Arch Fur Anthropology*, 7:839–902.

Williams, J.S., White, C.D., Longstaffe, F.J. (2005). Trophic level and macronutrient shift effects associated with the weaning process in the Postclassic Maya. *American Journal of Physical Anthropology*, 128(4), 781-790.

Witwer, E. R., and Lee, P. (1927). Anemia in children with splenomegaly and peculiar changes in the bones. *American Journal of Diseases of Children*, 34, 347.

Wolff, J. (1986)*. The Law of Bone Remodelling*. Berlin: Springer-Verlag.

Wood, J.M. (2005). Paleodemography. *Encyclopedia of Social Measurement,* 3, 1-5.

Wood, J.M., Milner, G.R., Harpending, H.C., Weiss, K.M. (1992). The osteological paradox: Problems of inferring prehistoric health from skeletal samples. *Current Anthropology*, 33, 343-370.

Wright, L.E. (1994) *The Sacrifice of the Earth?: Diet, Health, and Inequality in the Pasion Maya Lowlands.* Doctoral dissertation. University of Chicago.

Wright, L. E. and Chew, F. (1998). Porotic hyperostosis and paleoepidemiology: A forensic perspective on anemia among the ancient Maya. *American Anthropologist*, 100(4), 924-939.

Wright, L.E. and White, C.D. (1996). Human biology in the Classic Maya collapse: Evidence from paleopathology and paleodiet. *Journal of World Prehistory*, 10(2), 147-198

Wright, L.E., and Yoder, C.J. (2003). Recent progress in bioarchaeology: approaches to the osteological paradox. *Journal of Archaeological Research*, 11(1), 43-70.

Wu, J. S., and Hochman, M. G. (2009). Soft-tissue tumors and tumorlike lesions: a systematic imaging approach. *Radiology*, 253(2), 297.

Wu, X., and Schepartz, L.A. (2009). Application of computed tomography in paleoanthropological research. *Progress in Natural Science*, 19(8), 913-921.

Zeitz, P.S., Butler, J.C., Cheek, J.E., Samuel, M.C., Childs, J.E., Shands, L.A., ... Peters, J. (1995). A case-control study of hantavirus pulmonary syndrome during an outbreak in the southwestern United States. *Journal of Infectious Diseases*, 171(4), 864-870.

Zollikofer, C. P., & de León, M. S. P. (2005). *Virtual Reconstruction: A Primer in Computer-Assisted Paleontology and Biomedicine*. Wiley-Interscience.

Zollikofer, C.P., de León, M.S.P., Lieberman, D.E., Guy, F., Pilbeam, D., Likius, A., ... Brunet, M. (2005). Virtual cranial reconstruction of Sahelanthropus tchadensis. *Nature*, 434(7034), 755-759.

Zuckerman, M.K., Turner, B.L., Armelagos, G.J. (2012). Evolutionary thought in paleopathology and the rise of the biocultural approach. In. Grauer A.L. (Ed.), *A Companion to Paleopathology* (pp. 34-57). West Sussex: Blackwell Publishing Ltd.

Appendices

Appendix A: Age and Sex Data

Individual #	Catalogue #	Age (yrs)	Sex	Affected/Unaffected
Greek Colonial Collection (Apollonia [Ap])				
1	Ap. 457	20-25	Male	Affected
2	Ap. 5040-46	8±24mos	Undetermined	Affected
3	Ap. 5097-12	20-35	Female	Unaffected
4	Ap. 5518-10	12±36mos	Undetermined	Unaffected
5	Ap. 5518-22	35-50	Male	Unaffected
6	Ap. 5518-46	8±24mos	Undetermined	Affected
7	Ap. 5518-174	18-20	Female	Affected
8	Ap. 5536-5	20-35	Female	Affected
9	Ap. 5536-12	35+	Female	Unaffected
10	Ap. 5536-13	20-35	Female	Affected
11	Ap. 5536-17	35-50	Female	Affected
12	Ap. 5536-18	20-35	Male	Unaffected
Maya Collection (San Pedro [SP], Marco Gonzalez [MG], Lamanai [YDL, N])				
13	SP 2	4±12mos	Undetermined	Unaffected
14	SP 4	30-40	Male	Affected
15	SP 7	25-30	Female	Affected
16	SP 8	30+	Female	Unaffected
17	SP 10A	20-25	Female	Unaffected
18	SP 10E	8±24mos	Undetermined	Affected
19	SP 11-2/1	6±24mos	Undetermined	Affected
20	SP 11-2/2	8±24mos	Undetermined	Affected
21	SP 11-2/3a	35-40	Male	Unaffected
22	SP 11-2/4a	35-50	Male	Unaffected
23	SP 11-2/5	25-30	Female	Unaffected
24	SP 11-2/6	18-20	Male	Affected
25	SP 11-2/7b	12±36mos	Undetermined	Affected
26	SP 11-2/11	Adult	Male	Unaffected
27	SP 11-3/3	Adult	Male	Unaffected
28	SP 11-3/4	40+	Female	Unaffected
29	SP 11-3/5	17-19	Female	Affected
30	SP 11-8/2	sub-adult	Undetermined	Affected
31	SP 17-6/1	35-40	Male	Affected
32	SP 17-6/3	12±36mos	Undetermined	Affected
33	SP 17-6/4	3±12mos	Undetermined	Affected

Individual #	Catalogue #	Age (yrs)	Sex	Affected/Unaffected
34	SP 18-1/1a	Adult	Female	Unaffected
35	MG 11/7	25-30	Female	Affected
36	MG 12/1a	40+	Male	Unaffected
37	MG 12/2	40+	Female	Affected
38	MG 12/3	40+	Male	Unaffected
39	MG 12/6	40+	Female	Unaffected
40	MG 14/11	40+	Male	Unaffected
41	MG 14/15	25-30	Female	Unaffected
42	MG lot 77a	Adult	Undetermined	Affected
43	MG lot 199	Adult	Undetermined	Affected
44	YDL-1 85/1	Adult	Female	Affected
45	YDL-1 85/4	Adult	Female	Affected
46	YDL-1 85/6	Adult	Female	Affected
47	YDL-1 85-7	sub-adult	Undetermined	Affected
48	YDL-1 85/9	50+	Female	Unaffected
49	YDL-1 85/10	1-2.	Undetermined	Unaffected
50	YDL-1 85/14	Adult	Male	Affected
51	YDL-1 85/17	20-40	Female	Unaffected
52	YDL-1 85/21	20-30	Female	Unaffected
53	YDL-1 85/24	20-25	Female	Unaffected
54	YDL-1 85/25	Adult	Male	Affected
55	YDL-1 85/26	Adult	Undetermined	Unaffected
56	YDL-1 85/30	20-30	Male	Unaffected
57	YDL-1 85/41	Adult	Female	Affected
58	YDL-1 85-42a	5±12mos	Undetermined	Unaffected
59	YDL-1 85/50b	Adult	Undetermined	Affected
60	YDL-1 85/54	sub-adult	Undetermined	Affected
61	YDL-1 85/68	Adult	Male	Affected
62	YDL-1 85/73	Adult	Male	Affected
63	YDL-1 85-/77	6±24mos	Undetermined	Affected
64	YDL-1 85/88	Adult	Female	Unaffected
65	YDL-1 85/89	Adult	Male	Affected
66	YDL-1 85/92	Adult	Male	Affected
67	N12 11/3	40-50	Female	Affected
68	N12 11/5B	18+	Female	Affected
69	N12 11/6	Adult	Female	Unaffected

Appendix B: Example of Standard Skeletal Inventory Forms

Skeletal Inventory – Adult Remains

Date: 14-05-2012   Observer: J. Morgan   Identification: SP 11-2/6

Site: San Pedro   Age: 18-20   Sex: probable M

Skeletal Inventory
Sub-Adult Remains
Date: 14-05-2012   Observer: J. Morgan   Identification: SP 11- 2/1
Site: San Pedro   Age: 6   Sex: N/A

Appendix C: Example of Palaeopathology Recording Forms
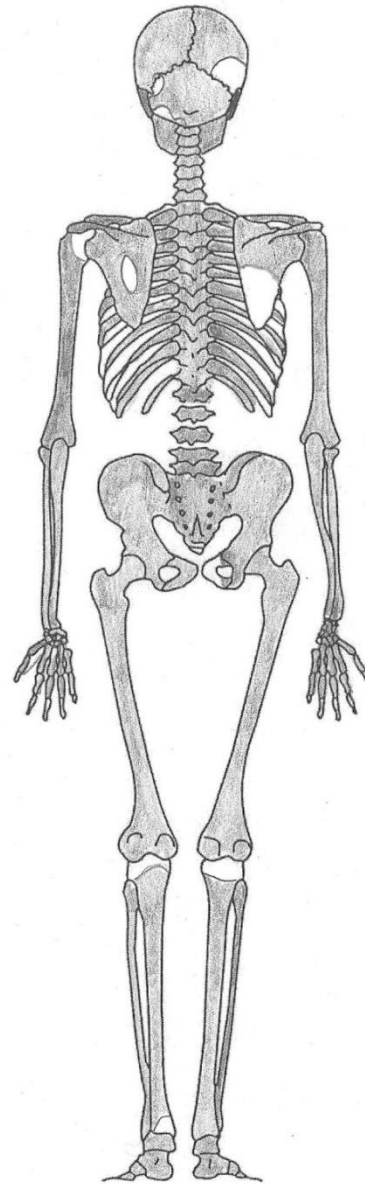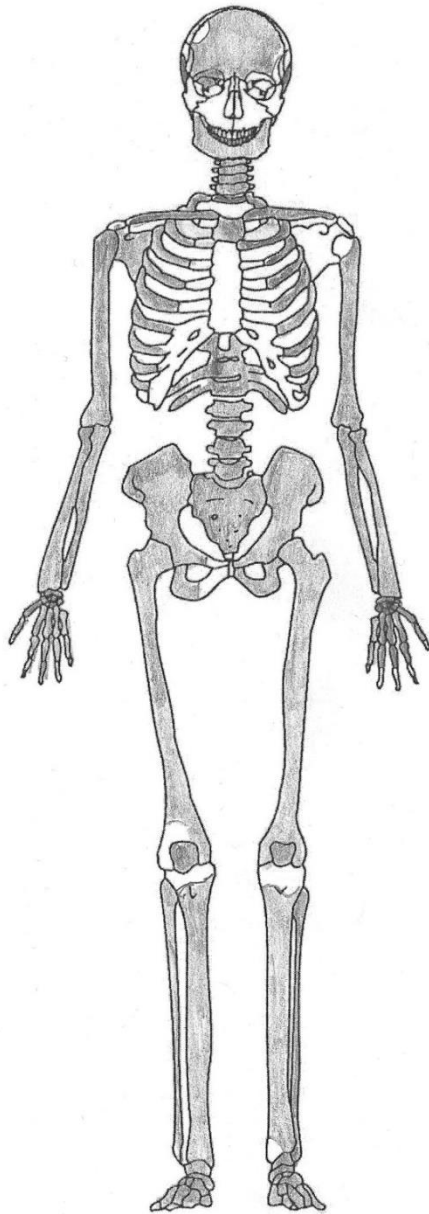
(Buiksta and Ubelaker 1994)

Cranial Pathology Summary – Location and Distribution
Adult Remains

Date: 14-05-2012   Observer: J. Morgan   Identification: SP 11-2/6
Site: San Pedro   Age: 18-20   Sex: probable M

Anterior View
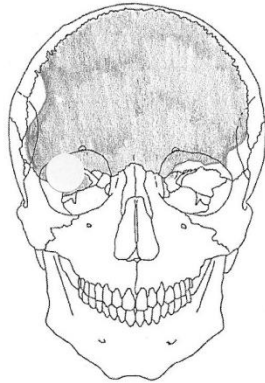
Posterior View
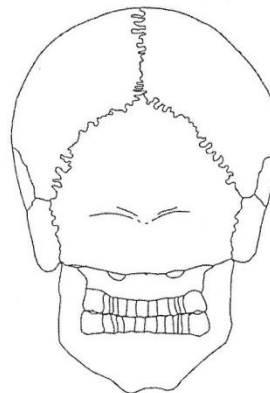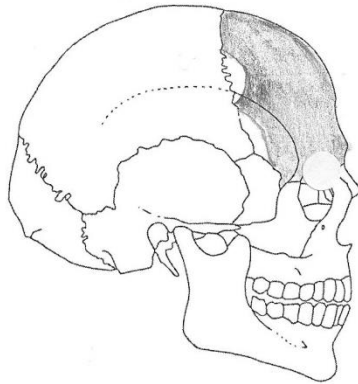
Right Lateral View
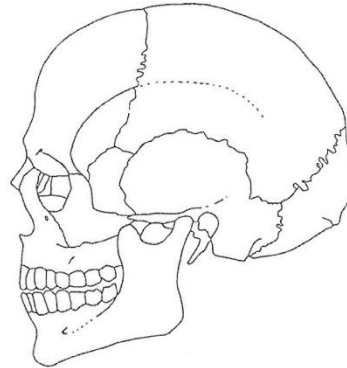
Left Lateral View
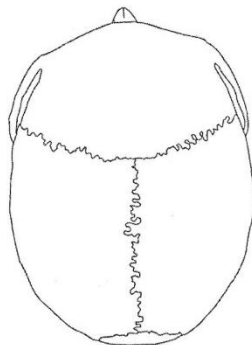
Superior View
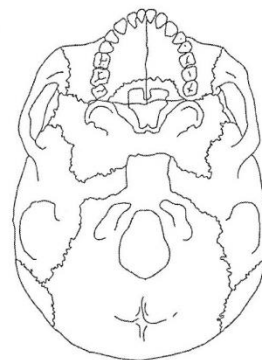
Inferior View

Cranial Pathology Summary – Location and Distribution
Sub-Adult Remains

Date: 14-05-2012   Observer: J. Morgan   Identification: SP- 11-2/1
Site: San Pedro   Age: 6   Sex: N/A

Anterior View
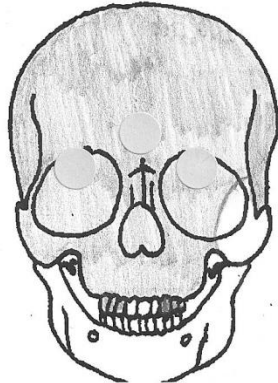
Posterior View
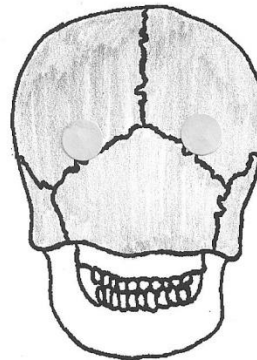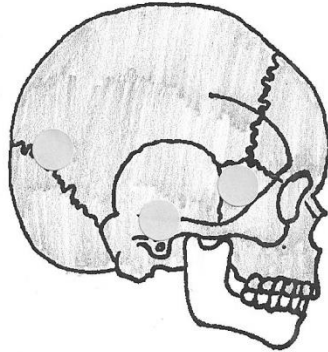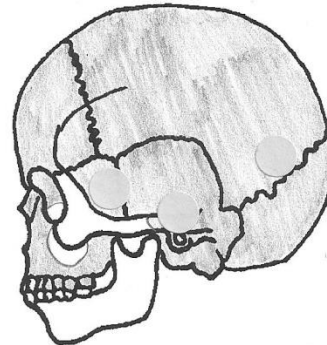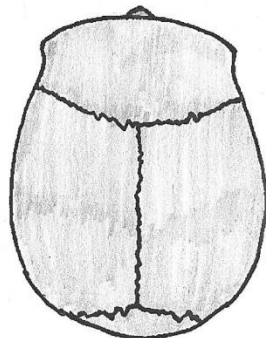
Right Lateral View

Left Lateral View

Superior View

Inferior View
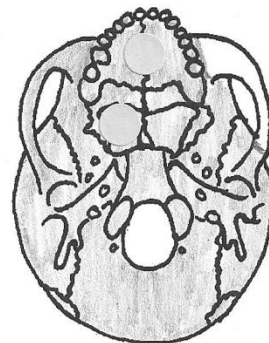
Cranial Pathology – Description

Date: 14-05-2012   Observer: J. Morgan   Identification: SP 11-2/6

Site: San Pedro   Age: 18-20   Sex: probable M

Cranial deformation - parallelo - fronto - occipital (tabular oblique)
↳ bilobate expansion

Cribra orbitalia - present
          Degree: light
          Location: orbit (right) → left is fragmentary and cannot
                    be analyzed
          Activity: healed.

Porotic hyperostosis - absent

Post-Cranial Pathology – Description

Date: 14-05-2012   Observer: J. Morgan   Identification: SP 11-2/6

Site: San Pedro   Age: 18-20   Sex: probable M

Vertebral Coloumn: N/A

Upper Limb: N/A

Lower Limb: N/A

Rib Cage: N/A

Innominates: N/A

Appendix D: MicroCT Scan Data for all Individuals

Individual. #	Sample #	kV	μA	ms	Frames	Projections	Scan Time (mins)	Res. (μm)
1	Ap. 457	135	30	500	2	1238	23	102.1
2	Ap. 5040-46	135	30	500	2	1356	28	102.1
3	Ap. 5097-12	135	30	500	2	1356	28	102.1
4	Ap. 5518-10	135	30	500	2	1356	28	102.1
5	Ap. 5518-22	130	30	500	2	1238	21	102.1
6	Ap. 5518-46	130	30	500	2	1238	21	102.1
7	Ap. 5536-5	145	50	500	2	3142	39	102.1
8	Ap. 5536-12	135	30	500	2	1238	23	102.1
9	Ap. 5536-13	145	50	500	2	3142	39	102.1
10	Ap. 5536-17	145	50	500	2	3142	39	102.1
11	Ap. 5536-18	135	30	500	2	1238	23	102.1
12	Ap. 5578-174	130	30	500	2	1238	21	102.1
13	SP 2	135	25	500	2	1687	28	102.1
14	SP 4	135	25	500	2	1633	27	102.1
15	SP 7	135	35	500	2	1686	53	102.1
16	SP 8	135	35	500	2	3142	53	102.1
17	SP 10A	140	35	500	2	3142	53	102.1
18	SP 10E	135	35	500	2	3142	53	102.1
19	SP 11-2/1	145	50	500	2	3142	53	102.1
20	SP 11-2/2_a	135	35	500	2	3142	51	102.1
20	SP 11-2/2_b	135	25	500	2	1248	21	102.1
21	SP 11-2/3a	140	35	500	2	3142	53	102.1
22	SP 11-2/4a	140	35	500	2	3142	53	102.1

Individual. #	Sample #	kV	μA	ms	Frames	Projections	Scan Time (mins)	Res. (μm)
23	SP 11-2/5	135	35	500	2	3070	51	102.1
24	SP 11-2/6	135	30	500	2	3142	53	102.1
25	SP 11-2/7b_a	135	35	500	2	2886	48	102.1
25	SP 11-2/7b_b	135	35	500	2	3142	53	102.1
26	SP 11-2/11	140	35	500	2	3142	53	102.1
27	SP 11-3/3	135	35	500	2	3121	53	102.1
28	SP 11-3/4	135	30	500	2	2654	44	102.1
29	SP 11-3/5	140	35	500	2	3142	53	102.1
30	SP 11-8/2	135	30	500	2	2030	34	102.1
31	SP 17-6/1	140	35	500	2	3142	53	102.1
32	SP 17-6/3	140	30	500	2	3142	53	102.1
33	SP 17-6/4	135	30	500	2	3142	53	102.1
34	SP 18-1/1a	135	30	500	2	3051	51	102.1
35	MG 11/7	135	30	500	2	3142	53	102.1
36	MG 12/1a	135	30	500	2	1638	27	102.1
37	MG 12/2	140	30	500	2	3142	53	102.1
38	MG 12/3	140	30	500	2	3142	53	102.1
39	MG 12/6	135	35	500	2	3142	53	102.1
40	MG 14/11	135	30	500	2	2394	40	102.1
41	MG 14/15	135	30	500	2	3142	53	102.1
42	MG lot 77a	135	35	500	2	2173	36	102.1
43	MG lot 199	135	30	500	2	2112	35	102.1
44	YDL-1 85/1	135	30	500	2	3142	53	102.1
45	YDL-1 85/4	135	30	500	2	2275	38	102.1
46	YDL-1 85/6	135	30	500	2	2395	40.3	102.1

Individual. #	Sample #	kV	μA	ms	Frames	Projections	Scan Time (mins)	Res. (μm)
47	YDL-1 85-7	135	30	500	2	2224	37	102.1
48	YDL-1 85/9	135	30	500	2	2366	40	102.1
49	YDL-1 85/10	130	30	500	2	1685	28	102.1
50	YDL-1 85/14	130	30	500	2	1092	18.5	102.1
51	YDL-1 85/17	135	30	500	2	2483	42	102.1
52	YDL-1 85/21	130	30	500	2	1511	25	102.1
53	YDL-1 85/24	130	30	500	2	2272	38	102.1
54	YDL-1 85/25	130	30	500	2	2887	48	102.1
55	YDL-1 85/26	130	30	500	2	3142	53	102.1
56	YDL-1 85/30	130	30	500	2	1329	22	102.1
57	YDL-1 85/41	130	30	500	2	1079	18	102.1
58	YDL-1 85-42a	130	30	500	2	1257	21	102.1
59	YDL-1 85/50b	130	30	500	2	1706	29	102.1
60	YDL-1 85/54	130	30	500	2	2200	37	102.1
61	YDL-1 85/68	130	30	500	2	2964	50	102.1
62	YDL-1 85/73	130	30	500	2	2559	43	102.1
63	YDL-1 85-/77	130	30	500	2	1228	20	102.1
64	YDL-1 85/88	130	30	500	2	2063	35	102.1
65	YDL-1 85/89	130	30	500	2	2633	44	102.1
66	YDL-1 85/92	130	30	500	2	2698	45	102.1
67	N12 11/3_a	130	30	500	2	1314	22	102.1
67	N12 11/3_b	130	30	500	2	3142	53	102.1
68	N12 11/5B	130	30	500	2	2751	46.5	102.1
69	N12 11/6	130	30	500	2	3076	51	102.1

Appendix E: Macroscopic Assessment of Orbits

Sex	
1= Male	
2= Female	
3= Undetermined	

Affected/Unaffected	
1= Affected	
2= Unaffected	

Activity	
1= Active	
2= Healed	
3= Mixed	
4= Unaffected	

Severity	
1= light	
2= medium/moderate	
3= severe	
4= unaffected	

Unaffected Orbits					
Sample #	**Age**	**Sex**	**Aff/Unaff**	**Activity**	**Severity**
Ap5518-10	12±36mos	3	2	4	4
SP10A	20-25	2	2	4	4
YDL85-24	20-25	2	2	4	4
Ap5536-18	20-35	1	2	4	4
Ap5097-12	20-35	2	2	4	4
MG14-15	25-30	2	2	4	4
Ap5536-12	35+	2	2	4	4
SP11-2/3a	35-40	1	2	4	4
Ap5518-22	35-50	1	2	4	4
SP11-2/4a	35-50	1	2	4	4
SP11-3/4	40+	2	2	4	4
MG14-11	40+	1	2	4	4
YDL85-9	50+	2	2	4	4
SP11-2/11	Adult	1	2	4	4
SP11-3/3	Adult	1	2	4	4
SP18-1/1a	Adult	2	2	4	4
YDL85-26	Adult	3	2	4	4
N12-11/6A	Adult	2	2	4	4
Affected Orbits					
Sample #	**Age**	**Sex**	**Aff/Unaff**	**Activity**	**Severity**

SP17-6/4	3±12mos	3	1	1	1
SP11-2/1	6± 24mos	3	1	1	3
Ap5518-46	8±24mos	3	1	1	2
Ap5040-46	8±24mos	3	1	1	1
SP11-2/7b	12±36mos	3	1	1	2
SP11-8/2	sub-adult	3	1	3	1
SP11-3/5	17-19	2	1	3	1
Ap5518-174	18-20	2	1	1	2
SP11-2/6	18-20	1	1	2	1
Ap457	20-25	1	1	2	1
Ap5536-5	20-35	2	1	2	1
Ap5536-13	20-35	2	1	1	2
SP7	25-30	2	1	2	1
Ap5536-17	35-50	2	1	2	1
N12-11/3	40-50	2	1	1	2

Appendix F: Macroscopic Assessment of Parietal Bones

Sex
1= Male
2= Female
3= Undetermined

Affected/Unaffected
1= Affected
2= Unaffected

Activity
1= Active
2= Healed
3= Mixed
4= Unaffected

Severity
1= light
2= medium/moderate
3= severe
4= unaffected

Unaffected Parietal Bones						
Sample #	Age	Sex	Side	Aff/Unaff	Activity	Severity
YDL-85/10	1-2.	3	1	2	4	4
SP 2	4±12mos	3	2	2	4	4
YDL-85/42a	5±12mos	3	2	2	4	4
SP 10A	20-25	2	1	2	4	4
YDL-85/21	20-30	2	1	2	4	4
YDL-85/30	20-30	1	1	2	4	4
YDL-85/17	20-40	2	1	2	4	4
SP 11-2/5	25-30	2	1	2	4	4
MG 14-15	25-30	2	1	2	4	4
SP 8	30+	2	1	2	4	4
SP 11-2/3a	35-40	1	2	2	4	4
SP 11-2/4a	35-50	1	1	2	4	4
MG 12-1a	40+	1	1	2	4	4
MG 12-3	40+	1	2	2	4	4
MG 12-6	40+	2	1	2	4	4
MG 14-11	40+	1	1	2	4	4
SP 11-2/11	Adult	1	1	2	4	4
SP 11-3/3	Adult	1	2	2	4	4
SP 18-1/1a	Adult	2	1	2	4	4
YDL-85/26	Adult	3	2	2	4	4
YD-L85/88	Adult	2	2	2	4	4

Affected Parietal Bones						
Sample #	**Age**	**Sex**	**Side**	**Aff/Unaff**	**Activity**	**Severity**
SP 11-2/1	6±24mos	3	1	1	1	2
SP 11-2/2	8± 24mos	3	2	1	1	3
SP 10E	8±24mos	3	2	1	2	1
SP 11-2/7b	12±36mos	3	1	1	1	3
SP 17-6/3	12±36mos	3	1	1	3	1
YDL-85/7	Sub-adult	3	2	1	1	3
YDL-85/54	Sub-adult	3	2	1	1	2
SP 11-3/5	17-19	2	1	1	2	1
N12-11/5b	18+	2	2	1	2	1
SP 7	25-30	2	1	1	2	1
MG 11-7	25-30	2	1	1	2	1
N12-11/3	40-50	2	2	1	2	2
MG 12-2	40+	2	1	1	2	2
MG lot199	Adult	3	1	1	2	1
YDL-85/1	Adult	2	1	1	2	1
YDL-85/4	Adult	2	2	1	3	2
YDL-85/6	Adult	2	2	1	2	1
YDL-85/14	Adult	1	1	1	3	2
YDL-85/25	Adult	1	1	1	3	2
YDL-85/41	Adult	2	1	1	2	2
YDL-85/68	Adult	1	1	1	1	3
YDL-85/73	Adult	1	1	1	2	2
YDL-85/89	Adult	1	2	1	2	1
YDL-85/92	Adult	1	1	1	2	2

Appendix G: Macroscopic Assessment of Occipital Bones

Sex
1= Male
2= Female
3= Undetermined

Affected/Unaffected
1= Affected
2= Unaffected

Activity
1= Active
2= Healed
3= Mixed
4= Unaffected

Severity
1= light
2= medium/moderate
3= severe
4= unaffected

Unaffected Occipital Bones					
Sample #	Age	Sex	Aff/Unaff	Activity	Severity
SP10A	20-25	2	2	4	4
SP8	30+	2	2	4	4
SP11-2/3a	35-40	1	2	4	4
SP11-2/4a	35-50	1	2	4	4
MG12-3	40+	1	2	4	4
SP11-2/11	Adult	1	2	4	4
YDL85-26	Adult	3	2	4	4
Affected Occipital Bones					
Sample #	Age	Sex	Aff/Unaff	Activity	Severity
YDL85-77	6±24mos	3	1	1	3
SP11-2/2	8± 24mos	3	1	1	3
SP17-6/3	12±36mos	3	1	2	1
YDL85-7	Sub-adult	3	1	1	3
YDL85-54	Sub-adult	3	1	1	2
N12-11/5b	18+	2	1	2	1
SP17-6/1	35-40	1	1	2	1
MG12-2	40+	2	1	2	2
YDL85-25	Adult	1	1	1	2
YDL85-50b	Adult	3	1	2	1
YDL85-68	Adult	1	1	1	2
YDL85-73	Adult	1	1	2	2

| YDL85-89 | Adult | 1 | 1 | 2 | 1 |
| YDL85-92 | Adult | 1 | 1 | 3 | 2 |

Appendix H: Intra- and Inter-Observer Error- Raw Data

2D Standard VOI Method

Intra-Observer Error- 2D Standard VOI										
Sample	BV/TV 1	BV/TV 2	BS/BV 1	BS/BV 2	Tb.Th 1	Tb.Th 2	Tb.N 1	Tb.N 2	Tb.Sp 1	Tb.Sp 2
SP11-8/2	0.620	0.683	3.732	4.521	0.536	0.442	1.157	1.545	0.328	0.205
YDL85-4	0.354	0.464	7.093	3.334	0.282	0.600	1.256	0.773	0.514	0.694
SP18-1/1a	0.237	0.378	9.438	5.252	0.212	0.381	1.119	0.992	0.682	0.627
MG12-6	0.403	0.644	4.826	2.739	0.414	0.730	0.973	0.882	0.613	0.403
YDL85-88	0.440	0.613	4.622	3.120	0.433	0.641	1.016	0.956	0.552	0.405
E-51	0.186	0.254	12.764	16.722	0.157	0.120	1.185	2.124	0.687	0.351
MG12-2	0.314	0.378	7.187	5.587	0.278	0.358	1.129	1.056	0.608	0.589
SP11-2/7b	0.698	0.599	2.770	1.950	0.722	1.025	0.967	0.584	0.312	0.686
YDL85-10	0.712	0.699	2.211	2.060	0.905	0.971	0.787	0.720	0.366	0.418
SP11-2/2	0.207	0.391	10.331	3.948	0.194	0.507	1.071	0.771	0.740	0.790
Inter-Observer Error- 2D Standard VOI										
Sample	BV/TV 1	BV/TV 2	BS/BV 1	BS/BV 2	Tb.Th 1	Tb.Th 2	Tb.N 1	Tb.N 2	Tb.Sp 1	Tb.Sp 2
SP11-8/2	0.620	0.684	3.732	2.308	0.536	0.867	1.157	0.789	0.328	0.400
YDL85-4	0.354	0.399	7.093	9.143	0.282	0.219	1.256	1.824	0.514	0.329
SP18-1/1a	0.237	0.460	9.438	3.398	0.212	0.589	1.119	0.781	0.682	0.691
MG12-6	0.403	0.683	4.826	3.442	0.414	0.581	0.973	1.176	0.613	0.269
YDL85-88	0.440	0.747	4.622	1.678	0.433	1.192	1.016	0.627	0.552	0.403
E-51	0.186	0.131	12.764	13.734	0.157	0.146	1.185	0.897	0.687	0.970
MG12-2	0.314	0.507	7.187	4.796	0.278	0.417	1.129	1.216	0.608	0.405
SP11-2/7b	0.698	0.727	2.770	2.022	0.722	0.989	0.967	0.735	0.312	0.371
YDL85-10	0.712	0.743	2.211	2.965	0.905	0.674	0.787	1.102	0.366	0.233

SP11-2/2	0.207	0.416	10.331	7.354	0.194	0.272	1.071	1.529	0.740	0.382

3D Standard VOI Method

Intra-Observer Error - 3D Standard VOI										
Sample	**BV/TV 1**	**BV/TV 2**	**BS/BV 1**	**BS/BV 2**	**Tb.Th 1**	**Tb.Th 2**	**Tb.N 1**	**Tb.N 2**	**Tb.Sp 1**	**Tb.Sp 2**
SP11-8/2	0.698	0.674	4.322	4.039	0.463	0.495	1.509	1.361	0.200	0.240
YDL85-4	0.459	0.598	8.637	5.743	0.232	0.348	1.983	1.717	0.273	0.234
SP18-1/1a	0.291	0.348	8.380	6.688	0.239	0.299	1.221	1.162	0.580	0.561
MG12-6	0.542	0.758	4.491	2.753	0.445	0.726	1.217	1.044	0.376	0.232
YDL85-88	0.581	0.662	5.024	4.302	0.398	0.465	1.459	1.424	0.287	0.237
E-51	0.163	0.220	16.816	13.316	0.119	0.150	1.373	1.467	0.609	0.532
MG12-2	0.448	0.533	5.725	6.443	0.349	0.310	1.281	1.719	0.431	0.271
SP11-2/7b	0.799	0.755	2.377	2.659	0.841	0.752	0.950	1.004	0.211	0.244
YDL85-10	0.821	0.807	2.404	2.682	0.832	0.746	0.986	1.082	0.182	0.179
SP11-2/2	0.504	0.509	5.161	5.667	0.388	0.353	1.300	1.442	0.382	0.341
Inter-Observer Error - 3D Standard VOI										
Sample	**BV/TV 1**	**BV/TV 2**	**BS/BV 1**	**BS/BV 2**	**Tb.Th 1**	**Tb.Th 2**	**Tb.N 1**	**Tb.N 2**	**Tb.Sp 1**	**Tb.Sp 2**
SP11-8/2	0.698	0.793	4.322	2.848	0.463	0.702	1.509	1.129	0.200	0.183
YDL85-4	0.459	0.473	8.637	8.982	0.232	0.223	1.983	2.122	0.273	0.249
SP18-1/1a	0.291	0.569	8.380	4.409	0.239	0.454	1.221	1.255	0.580	0.345
MG12-6	0.542	0.693	4.491	3.306	0.445	0.605	1.217	1.145	0.376	0.268
YDL85-88	0.581	0.749	5.024	1.138	0.398	0.637	1.459	1.175	0.287	0.213
E-51	0.163	0.190	16.816	15.867	0.119	0.126	1.373	1.510	0.609	0.536
MG12-2	0.448	0.676	5.725	4.213	0.349	0.475	1.281	1.423	0.431	0.228
SP11-2/7b	0.799	0.800	2.377	2.164	0.841	0.924	0.950	0.855	0.211	0.232
YDL85-10	0.821	0.849	2.404	2.194	0.832	0.912	0.986	0.932	0.182	0.162
SP11-2/2	0.504	0.363	5.161	6.373	0.388	0.314	1.300	1.156	0.382	0.551

3D Custom VOI Method

Sample	BV/TV 1	BV/TV 2	BS/BV 1	BS/BV 2	Tb.Th 1	Tb.Th 2	Tb.N 1	Tb.N 2	Tb.Sp 1	Tb.Sp 2
SP11-8/2	0.660	0.659	4.624	3.966	0.433	0.504	1.526	1.306	0.223	0.261
YDL85-4	0.500	0.533	7.907	7.242	0.253	0.276	1.975	1.928	0.253	0.242
SP18-1/1a	0.318	0.388	7.639	6.664	0.262	0.300	1.214	1.293	0.562	0.473
MG12-6	0.631	0.791	3.588	2.276	0.557	0.879	1.131	0.900	0.327	0.232
YDL85-88	0.725	0.795	2.920	2.438	0.685	0.820	1.058	0.969	0.260	0.211
E-51	0.162	0.187	14.675	13.716	0.136	0.146	1.189	1.281	0.705	0.635
MG12-2	0.738	0.720	2.635	2.811	0.759	0.711	0.972	1.012	0.270	0.276
SP11-2/7b	0.858	0.772	1.877	2.566	1.065	0.780	0.805	0.991	0.177	0.230
YDL85-10	0.650	0.706	5.072	4.197	0.394	0.477	1.649	1.482	0.212	0.198
SP11-2/2	0.615	0.653	3.877	3.347	0.516	0.598	1.193	1.093	0.323	0.317
Inter-Observer Error - 3D Custom VOI										
Sample	BV/TV 1	BV/TV 2	BS/BV 1	BS/BV 2	Tb.Th 1	Tb.Th 2	Tb.N 1	Tb.N 2	Tb.Sp 1	Tb.Sp 2
SP11-8/2	0.660	0.816	4.624	2.614	0.433	0.765	1.526	1.066	0.223	0.173
YDL85-4	0.500	0.522	7.907	7.424	0.253	0.269	1.975	1.937	0.253	0.247
SP18-1/1a	0.318	0.453	7.639	5.452	0.262	0.367	1.214	1.236	0.562	0.442
MG12-6	0.631	0.818	3.588	1.938	0.557	0.792	1.131	1.032	0.327	0.230
YDL85-88	0.725	0.789	2.920	2.576	0.685	0.776	1.058	1.016	0.260	0.208
E-51	0.162	0.095	14.675	17.396	0.136	0.115	1.189	0.825	0.705	1.097
MG12-2	0.738	0.735	2.635	2.604	0.759	0.768	0.972	0.957	0.270	0.277
SP11-2/7b	0.858	0.782	1.877	2.376	1.065	0.842	0.805	0.929	0.177	0.235
YDL85-10	0.650	0.720	5.072	4.032	0.394	0.496	1.649	1.452	0.212	0.193
SP11-2/2	0.615	0.657	3.877	3.284	0.516	0.609	1.193	1.080	0.323	0.317

Appendix I: Raw Data for Quantitative Analysis of Trabecular Microarchitecture

Unaffected Orbits					
Sample #	**MaxBV/TV**	**MaxBS/BV**	**MaxTb.Th**	**MaxTb.N**	**MaxTb.Sp**
Ap5518-10	0.450427	6.2091	0.322108	1.39837	0.393009
SP10A	0.72003	3.05912	0.653782	1.10133	0.25421
YDL85-24	0.245316	10.3888	0.192516	1.27427	0.59225
Ap5536-18	0.387302	7.46251	0.268006	1.44512	0.423976
Ap5097-12	0.450231	6.65814	0.300384	1.49885	0.366794
MG14-15	0.47876	6.21769	0.321663	1.48839	0.35023
Ap5536-12	0.239022	12.3522	0.161915	1.47622	0.515491
SP11-2/3a	0.818428	1.67288	1.19555	0.684564	0.265238
Ap5518-22	0.598445	3.5925	0.556716	1.07496	0.373555
SP11-2/4a	0.607501	3.83956	0.520894	1.16627	0.336543
SP11-3/4	0.583845	4.93773	0.405044	1.44144	0.288709
MG14-11	0.740639	2.91725	0.6856	1.08028	0.240087
YDL85-9	0.528183	4.36465	0.458227	1.15267	0.409327
SP11-2/11	0.46773	5.95785	0.335692	1.39333	0.382013
SP11-3/3	0.654574	4.32429	0.462503	1.41528	0.244068
SP18-1/1a	0.317962	7.63909	0.261811	1.21447	0.561593
YDL85-26	0.383388	7.01449	0.285124	1.34463	0.458573
N12-11/6A	0.615101	3.90133	0.512646	1.19985	0.320788

Affected Orbits					
Sample #	**MaxBV/TV**	**MaxBS/BV**	**MaxTb.Th**	**MaxTb.N**	**MaxTb.Sp**
SP17-6/4	0.444453	5.03509	0.397212	1.11893	0.496498
SP11-2/1	0.543664	5.37922	0.371801	1.46224	0.31208
Ap5518-46	0.12167	18.6118	0.107459	1.13225	0.77574
Ap5040-46	0.483108	6.74557	0.296491	1.62942	0.317225
SP11-2/7b	0.497364	7.44062	0.268795	1.85035	0.271645
SP11-8/2	0.535443	5.74708	0.348003	1.53862	0.301931
SP11-3/5	0.720483	3.08528	0.64824	1.11145	0.251489
Ap5518-174	0.298993	9.83913	0.20327	1.47091	0.476579
SP11-2/6	0.501203	6.54899	0.305391	1.64119	0.303925
Ap457	0.324258	8.04094	0.248727	1.30367	0.518339
Ap5536-5	0.23932	12.308	0.162496	1.47278	0.516494

Affected Orbits

Sample #	MaxBV/TV	MaxBS/BV	MaxTb.Th	MaxTb.N	MaxTb.Sp
Ap5536-13	0.230914	11.4909	0.174051	1.3267	0.579696
SP7	0.802305	2.41344	0.828694	0.968156	0.204197
Ap5536-17	0.39454	8.72066	0.22934	1.72032	0.351946
N12-11/3	0.361547	9.71307	0.205908	1.75587	0.363611

Unaffected Parietal Bosses

Sample #	MaxBV/TV	MaxBS/BV	MaxTb.Th	MaxTb.N	MaxTb.Sp
YDL85-10	0.650247	5.07153	0.394359	1.64887	0.212116
SP2	0.781685	2.7697	0.7221	1.08252	0.201673
SP10A	0.861863	1.61291	1.24	0.695052	0.198744
YDL85-21	0.672174	3.46914	0.576512	1.16593	0.281171
YDL85-30	0.553575	4.40768	0.453754	1.21955	0.366222
YDL85-17	0.504301	5.22988	0.382418	1.31872	0.375895
SP11-2/5	0.738319	2.61605	0.764512	0.965739	0.270964
MG14-15	0.863318	1.23405	1.62068	0.532688	0.25659
SP8	0.68846	3.81059	0.524853	1.31172	0.237505
SP11-2/3a	0.890356	1.24589	1.60527	0.554644	0.197684
SP11-2/4a	0.857627	1.41319	1.41524	0.605994	0.234942
MG12-1a	0.662868	3.6496	0.548005	1.2096	0.278713
MG12-3	0.381189	7.14059	0.280089	1.36096	0.454689
MG12-6	0.525069	5.4539	0.367959	1.42698	0.332824
MG14-11	0.608515	3.50707	0.570277	1.06705	0.366884
SP11-2/11	0.651317	3.59235	0.556738	1.16988	0.29805
SP11-3/3	0.867636	1.29237	1.54755	0.560653	0.236089
SP18-1/1a	0.528518	4.3606	0.458652	1.20686	0.409156
YDL85-26	0.806282	2.30749	0.866742	0.930244	0.208245
YDL85-88	0.724627	2.92011	0.684906	1.05799	0.260278

Affected Parietal Bosses

Sample #	MaxBV/TV	MaxBS/BV	MaxTb.Th	MaxTb.N	MaxTb.Sp
SP11-2/2	0.615258	3.87674	0.515898	1.1926	0.322609
SP11-2/7b	0.779835	1.82358	1.09675	0.711044	0.309636
SP17-6/3	0.741597	3.08708	0.647862	1.14468	0.225742
MG12-2	0.773331	2.17919	0.917774	0.842617	0.269006

Affected Parietal Bosses

Sample #	MaxBV/TV	MaxBS/BV	MaxTb.Th	MaxTb.N	MaxTb.Sp
MGlot199	0.723555	2.45131	0.81589	0.88683	0.311722
YDL85-14	0.657776	3.65494	0.547205	1.20207	0.284697
YDL85-41	0.765516	2.60969	0.766376	0.998878	0.234747
YDL85-68	0.822913	1.73508	1.15269	0.71391	0.248052
YDL85-73	0.558834	5.34187	0.374401	1.49261	0.295567
YDL85-92	0.68899	3.94471	0.507008	1.35893	0.228863

Unaffected Parietal at Lambdoid

Sample #	MaxBV/TV	MaxBS/BV	MaxTb.Th	MaxTb.N	MaxTb.Sp
SP2	0.586419	4.43424	0.451036	1.30016	0.3181
YDL85-42a	0.774871	2.97098	0.673179	1.15106	0.195584
YDL85-17	0.725443	3.18531	0.627881	1.15538	0.237633
SP11-2/5	0.871619	1.56483	1.27809	0.681967	0.188252
MG14-15	0.829811	1.54738	1.29251	0.642016	0.265085
SP8	0.801064	2.33489	0.856572	0.935197	0.212721
MG12-1a	0.669076	3.19113	0.626738	1.06755	0.309984
MG12-3	0.552459	4.93199	0.405516	1.36236	0.328504
MG12-6	0.618622	4.47748	0.44668	1.38493	0.275377
SP11-3/3	0.892584	0.849887	2.35325	0.379298	0.283196
YDL85-26	0.757815	2.99634	0.667481	1.13534	0.213316

Affected Parietal at Lambdoid

Sample #	MaxBV/TV	MaxBS/BV	MaxTb.Th	MaxTb.N	MaxTb.Sp
SP11-2/1	0.817176	2.12011	0.943347	0.866252	0.211051
SP10E	0.848572	1.63729	1.22153	0.694678	0.217983
SP11-2/2	0.636658	4.49604	0.444836	1.42122	0.253868
YDL85-7	0.528024	4.77098	0.419201	1.2596	0.374704
YDL85-54	0.748892	3.60777	0.554359	1.35092	0.18588
SP11-3/5	0.871075	1.57095	1.27311	0.684208	0.18843
N12-11/5b	0.726229	3.27824	0.610083	1.19038	0.229987
SP7	0.892958	1.23018	1.62578	0.549248	0.194888
MG11-7	0.571447	3.53834	0.565237	1.01099	0.423896
N12-11/3	0.663906	3.28087	0.609595	1.08909	0.3086
YDL85-1	0.836025	1.89706	1.05426	0.792996	0.206779
YDL85-4	0.49958	7.90683	0.252946	1.97505	0.253371

Affected Parietal at Lambdoid					
Sample #	MaxBV/TV	MaxBS/BV	MaxTb.Th	MaxTb.N	MaxTb.Sp
YDL85-6	0.76233	2.90367	0.688784	1.10678	0.214741
YDL85-25	0.785476	2.87784	0.694965	1.13024	0.189804
YDL85-89	0.775126	2.84506	0.702974	1.10264	0.203942
MGlot199	0.899885	1.13004	1.76986	0.508451	0.196901

Unaffected Occipital					
Sample #	MaxBV/TV	MaxBS/BV	MaxTb.Th	MaxTb.N	MaxTb.Sp
SP10A	0.893026	1.18466	1.68825	0.528965	0.202233
SP8	0.820054	2.26871	0.881559	0.930232	0.193442
SP11-2/3a	0.892611	1.2249	1.63278	0.54668	0.196438
SP11-2/4a	0.69661	2.95565	0.67667	1.02947	0.294706
MG12-3	0.501221	5.64232	0.354464	1.41402	0.352737
SP11-2/11	0.734498	3.14095	0.63675	1.15351	0.230169
YDL85-26	0.616184	4.1909	0.477203	1.29124	0.297124

Affected Occipital					
Sample #	MaxBV/TV	MaxBS/BV	MaxTb.Th	MaxTb.N	MaxTb.Sp
YDL85-77	0.620644	4.85699	0.411778	1.50723	0.251691
SP11-2/2	0.6792	3.64352	0.54892	1.23734	0.259266
SP17-6/3	0.87143	1.59789	1.25165	0.696222	0.184668
YDL85-7	0.662417	4.0422	0.49478	1.33881	0.252151
YDL85-54	0.635417	5.04462	0.396462	1.60272	0.227478
N12-11/5b	0.782877	2.6147	0.764905	1.02349	0.212139
SP17-6/1	0.867468	1.4173	1.41114	0.61473	0.215594
MG12-2	0.965313	0.454377	4.40163	0.219308	0.158168
YDL85-25	0.808551	2.61188	0.765733	1.05592	0.181311
YDL85-50b	0.70841	3.88989	0.514153	1.37782	0.211631
YDL85-68	0.870053	1.21241	1.64961	0.527429	0.246379
YDL85-73	0.455361	6.92301	0.288892	1.57623	0.345532
YDL85-89	0.654399	3.99656	0.500431	1.30767	0.264287
YDL85-92	0.590792	4.22009	0.473924	1.2466	0.328261

Curriculum Vitae

Name: Jennifer Morgan

Post-secondary   Trent University
Education and   Peterborough, Ontario, Canada
Degrees: 2003-2006 BSc. (Hons.)

                      The University of Manitoba
                      Winnipeg, Manitoba, Canada
                      2007-2009 M.A.

                      The University of Western Ontario
                      London, Ontario, Canada
                      2009- present Ph.D.

Honours and   Manitoba Graduate Scholarship (MGS)
Awards: 2007-2008

                      Social Science and Humanities Research Council (SSHRC)
                      CGS Master's
                      2008-2009

                      Anthropology Department Research Scholarship, Western
                      University
                      2009

                      Faculty of Social Science Dean's Scholarship, Western University
                      2009

                      Ontario Graduate Scholarship in Science and Technology
                      (OGSST)
                      2010-2011

                      Ontario Graduate Scholarship (OGS)
                      2011-2012

                      Graduate Thesis Research Award (GTRS)
                      2012

                      Western Graduate Research Scholarship (WGRS)
                      2009-2013

Related Work   Teaching Assistant
Experience   The University of Western Ontario
                         2007-2013

Publications:

Morgan, J., Lynnerup, N., and Hoppa, R.D. 2013. The Lateral Angle Revisited: A Validation Study of the Reliability of the Lateral Angle Method for Sex Determination using Computed Tomography (CT). *Journal of Forensic Sciences,* 58 (2): 443-447.

Morgan, J. 2008. Cribra Orbitalia and Porotic Hyperostosis: Perspectives on the Nutrition and Parasite Models. *Manitoba Anthropology Students' Association (MASA) Journal*, Winnipeg: Department of Anthropology, University of Manitoba.

Conference Presentations:

Morgan, J, Lynnerup, N and Hoppa, RD. 2010 Sex Determination from Head to.... Well Just the Head: A Validation of Methods Using the Petrous Portion of the Skull from CT Data. *Poster presented at the 38th annual meeting of the Canadian Association for Physical Anthropologists*. Saskatoon, SK.

Nelson, AJ, Wade, AD, Hibbert, R, MacDonald, B, Donaldson, M, Chatelain, R, Nguyen, N, Lywood, V, Gibson, G, Trumpour, M, Friedman, SN, Granton, PV, Morgan, J, Holdsworth, DW and Cunningham, IA. 2009. The UQAM Mummy – The Use of Non-Destructive Imaging to Reconstruct an Ancient Osteobiography and to Document Modern Malfeasance*. Poster presented at the 37th annual meeting of the Canadian Association for Physical Anthropologists*. Vancouver, BC, October 29, 2009.